MECHANISMS AND CONSEQUENCES OF CHIRALLY SELECTIVE PROCESSES AT MINERAL SURFACES

Thesis submitted in accordance with the requirements of the University of Liverpool for the degree of Doctor in Philosophy

By

Joe David Wilkinson

Department of Earth and Ocean Sciences
University of Liverpool

September 2010

ABSTRACT

Mechanisms and Consequences of Chirally Selective Processes at Mineral Surfaces

Joe D. Wilkinson

This work examines the adsorption of the organophosphorus pesticide acephate in solution at the surface of common, predominantly achiral minerals. The enantiomer selective properties of these minerals are assessed with particular focus on the 2:1 smectite, montmorillonite.

Initial batch sorption experiments reveal that unmodified montmorillonite K10 suspended in acetonitrile preferentially adsorbs the (−) enantiomer of acephate equating to nearly 10 % deviation from the racemic state after a 48 h equilibration period. It is also noted that in acephate solutions in acetonitrile and water a preference for the (−) and (+) enantiomers of acephate are respectively observed, highlighting the importance of the solvent in enantioselective adsorption processes. Enantioselectivity is also exhibited in adsorption studies involving a large number of surface modifications to K10 and bentonite SWy-2. For example, exchange of the interlayer cations for a selection of alternative exchangeable cations provides evidence that they are involved in the enantioselective adsorption process. Also, complexation with various enantiopure amino acids appears to enhance the enantioselective capabilities of K10 and SWy-2. Mechanisms are proposed for the mode of adsorption including partial ligand exchange between acephate enantiomers and lysine-cation complexes within the interlayer space. Also of note is that opposite enantiomers of complexed amino acids do not result in a preference for opposite enantiomers of acephate. This is important information in determining the whereabouts and extent of the chiral environment required for enantioselectivity. Additionally, variations in the pH of the suspension in a number of batch sorption experiments reveal a substantial effect on both the sorption and enantioselectivity for acephate on SWy-2. For example, an increase in pH above the pKa value for acephate results in a marked decrease in enantioselective adsorption reflecting the importance of the ionised state of acephate and thus supports ligand exchange as a mechanism for enantioselective adsorption. An important factor inferred from the majority of sorption and enantiomeric fraction plots produced is that some "enantioblind" sorption must occur in the early stages of equilibration before enantioselective adsorption begins to dominate. This implies that the orientation of the initially adsorbing enantiomers and their interaction with newly adsorbing enantiomers is fundamental to the overall extent and direction of enantioselectivity. Also of importance is that an initial enantiomeric imbalance of acephate in an aqueous solution adsorbed at the surface of unmodified montmorillonite K10 is shown to enhance enantioselectivity. The greater the initial imbalance, the greater the extent of enantioselective adsorption observed beyond that expected from an initial racemic mixture. This reiterates the importance of acephate-acephate interactions in the early stages of the equilibration process.

I certify that the work described in this thesis is my own except where otherwise stated and has not previously been submitted for any degree at this or any other University.

Joe D. Wilkinson

ACKNOWLEDGEMENTS

First of all I would like to thank my family for encouraging me to make the step from marine science as a passionate hobby to marine science as a possible career. Your further encouragement and support since then has been available on tap and is massively appreciated.

Next, I would like to thank my awesome fiancée Amelia for the complete lack of sympathy she has provided me over the course of this "PDF". Just as she knew it would, it has helped me cut down on my whingeing, focus on getting through the tough periods and endeavour to prove to her that I can be a doctor too! Seriously though, without your love, this PhD and I would have had no chance.

Of course, I'd also like to thank Martin for offering me the opportunity to take this PhD on, believing that I could achieve it and providing quality support when demanded. Many of the skills I have acquired over the last four years have been from you, particularly those involving taking things apart and putting them back together!

Despite such much appreciated help from Martin, life in the lab would not have been possible without Anu and Carmel. Both have provided me with so much support and guidance when it comes to equipment and procedures and have tolerated my clumsiness and dangerously laid-back attitude with great patience. I am also grateful for the support from other lecturers throughout the department, in particular George and Harry for their open door policy and their tolerance of how little I have remembered from our undergraduate work.

Another massive thank you must go to Paula, without whom, so many things would have gone so horribly wrong! Your skills with forms and finance, your keys, your knowledge of everything, your pep-talks, your tellings off, your practical and moral guidance and your general support has made the finishing of this PhD possible.

I'd also like to thank all my friends from before and throughout the last four years for their support and tolerance of my slightly less laid-back attitude during the tough times. And Clare, thank you for being my partner in crime and for always taking my side.

You're all very much appreciated, thank you all!

CONTENTS

LIST OF TABLES

LIST OF FIGURES

CHAPTER 1 INTRODUCTION

This project sets out to explore the mechanisms and consequences of chirally selective processes at mineral surfaces.

In simple terms, chirality refers to the specific organisation of molecular structures in the three dimensional space. It relates to the fact that some chemicals of identical composition can exhibit different properties depending on their 3-D structure. Where two possible structures exist, a mixture of equal quantities of each alternative is termed racemic.

This chapter aims to present the background required to enable understanding of the work carried out in this research and includes an introduction to chirality and chiral species found in the environment. It considers how chiral species interact with each other and with some of the chiral and achiral minerals found commonly on a global scale. Within the examination of such species significant focus will be applied to chiral organophosphorus pesticides and their global distribution and transport. Additionally, parts of the research carried out in this work will provide insight into the homochiral nature of some of the naturally occurring biologically active molecules and so a brief review of the current theories for the initiation of the homochirality of life will also be included in this chapter. Several techniques have been employed in order to obtain data throughout this project and thus a brief review will be included of how such techniques are to be utilised. Finally, the overall aim and objectives of the study will be presented.

Many synthetically produced biomolecules, such as agrochemicals and pharmaceutical drugs, are chiral and are usually produced as racemic mixtures. Despite having identical physical properties the biological properties of enantiomers of a chiral molecule may vary greatly. For this reason, of the enantiomers in a racemic mixture only one might be active and so an enantiopure form of a molecule is likely to be far more efficient for providing targeted control whether it be as an antibiotic or an agricultural pesticide. As such, there is now strong interest in finding processes or new technologies that can either separate the enantiomers to make enantiopure products or lead to the asymmetric synthesis of enantiopure molecules. Additionally, the fate and transport of chiral pollutants in the environment can be

better assessed if the abiotic/biotic adsorption or transformation of the individual enantiomers in the subsurface can be studied. These problems can be examined by interacting model mineral surfaces such as quartz and clays selectively with chiral molecules providing insight into the chemical mechanisms at work and the potential for enantiopurification processes. The study of chiral selective adsorption at mineral surfaces can also take on a more philosophical and fundamental character providing a vital part of the attempts to determine the origin of the homochirality of life which raise questions like: why are all biologically active amino acids left handed and sugars right handed? Wide ranging contemporary research continues to investigate this question in a broad interdisciplinary forum drawing from areas such as chemistry and biology, to geology, to astrobiology and physics.

1.1 Definition of Chirality

The terms chiral and chirality, both derived from the Greek χειρ (*cheir*, a hand), referring to the handedness of chiral species (Suh et al. 1997). Human hands are one of the best ways of explaining and visualising the phenomenon of chirality as they are mirror images of each other that have no internal axes or planes of symmetry and, therefore, cannot be superimposed on one another. In this macroscopic scale, there are many examples of chirality that we see every day; from left and right-handed scissors and left and right hand drive cars to cyclones that spin clockwise in the southern hemisphere and anti-clockwise in the northern hemisphere. But it is in the molecular scale that chirality becomes fascinating as we strive to scientifically explain the unusual and potentially powerful properties observed of chiral species and the way they interact with their surroundings. It is important to begin with a clear definition of chirality in respect to molecules. A chiral molecule is one that is not superimposable on its mirror image. This is a *necessary and sufficient condition* for chirality, with no exception. There is no further definition that can apply to all forms of chiral molecule but for the purpose of this work we can say that a molecule arranged in a tetrahedral form with four different groups surrounding a central atom will exist in two forms, identical in structure and physical properties but differing in the way they rotate the plane of polarised light. Such forms of a molecule are known as enantiomers.

1.2 The History of Stereochemistry

Our knowledge of stereochemistry began at the start of the nineteenth century when Haüy (1809), observed that there were right and left-handed quartz crystals. He then postulated, from crystal cleavage observations, that a crystal and each constituent molecule are images of each other in the overall shape of the crystal (Ali & Aboul-Enein 2004). But it was Jean-Batiste Biot who, in 1815, discovered that solutions of certain organic compounds had the ability to rotate the plane of polarisation of light, he termed this phenomenon *optical activity* (Drayer 2001; Suh et al. 1997). Later, Eilhard Mitscherlich (communicated by Biot 1844) noted that different sodium ammonium salts of tartaric acid caused different deviations from the plane of polarised light despite have the same chemical composition, crystalline form, specific weight and the same inclination in their optical axes. This was the precursor for Louis Pasteur's (1948) elegant experiment whereby separating mirror image crystals of sodium tartrate he revealed that crystals of this organic compound can exist in different spatial configurations. Finally, Le Bel (1874) and Van't Hoff (1874) simultaneously and independently proposed that the four valences of the carbon atom remain directed towards the vertices of an atom-centred tetrahedron. This lead to the theory of three-dimensional molecular structures of molecules by which the phenomenon of chirality and Pasteur's discovery could be explained scientifically (Ali & Aboul-Enein 2004).

1.3 Nomenclature for chiral species

The most palpable way of distinguishing between two enantiomers of a chiral molecule is by the direction in which they rotate the plane of polarised light. The signs (+) and (−) are used in this instance. A (+) notation before the enantiomer's name or formula indicates a rotation to the right (clockwise) whereas rotation to the left (anticlockwise) is designated by the (−) notation. Commonly, an enantiomer which rotates the plane of polarised light to the right is known as dextrorotatory (*d* is used in place of the (+) sign) enantiomer whereas rotation to the left is caused by the laevorotatory (*l* is used in place of the (−) sign) enantiomer. It is important to note here, the difference between the d/*l* and D/L notation which correlates the configuration of a molecule with the configuration of D/L-glyceraldehyde according to the Fischer convention (Ali & Aboul-Enein 2004). This terminology is now predominantly used for the naming of amino acids and carbohydrates but not for

pollutants. The use of (+) and (−) labels serves a purpose but is flawed in that the observer is unable to derive the number of chiral centres in the molecule. As such, in the field of pollutants and contaminants, it has largely been replaced by the Cahn-Ingold-Prelog (CIP) convention (Cahn et al. 1956), which assigns the notations R (*rectus* – Latin for 'left')or S (*sinister* – Latin for 'right') to describe the spatial arrangement of the substituents of a molecule around its asymmetrical centre. The CIP convention can be applied by applying three strict rules which are summarised as follows:

(1) The *sequence rule* demands that the four atoms around an asymmetric central atom must be ordered in a priority sequence. The higher the atomic number of each atom the higher their priority. In a case where the atomic number of more than one atom is the same then the next bonded atoms are considered. Additionally, in the case of a double bond, the atomic number of the atom on the end of the bond is considered to be double.

(2) The *conversion rule* involves drawing or visualising the molecule so that the atom with the lowest priority is directed into the plane of the paper.

(3) Now by drawing or visualising the path of an arrow through the priority constituents from highest to lowest the direction of rotation becomes apparent. The *absolute configuration label* can then be applied to the stereocentre of the molecule as *R* for clockwise movement or *S* for anticlockwise movement.

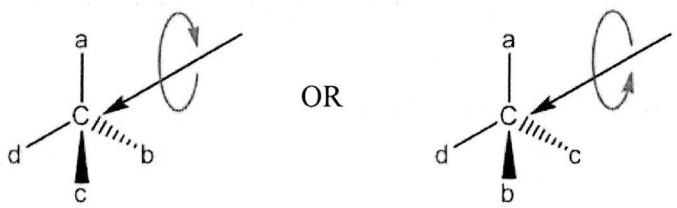

a → b → c clockwise = *R* a → b → c anticlockwise = *S*

It is also important to make clear the terminology used for different types of molecular isomers that occur in relation to the discipline of stereochemistry. *Diastereomers* (or diastereoisomers) are stereoisomers not related as mirror images

and are characterized by differences in physical properties, and by some differences in chemical behaviour towards achiral as well as chiral reagents (McNaught & Wilkinson 1997). Like enantiomers, diastereomers may have more than one optically active atom (known as a stereocentre). However, the configuration of the adjoined atoms or groups of one or more (but not all) of the stereocentres must be different. In the case where only one stereocentre shows a different configuration to its diastereomer it is referred to as an *epimer*. It can also be noted that enantiomers of a compound with more than one stereocentre are also diastereomers of the other stereoisomers of that compound that are not their mirror image. The type of chirality addressed thus far is known as *central chirality* and always involves at least one stereocentre and results in the presence of either a diastereomer or an enantiomer. However, there are some other types of chirality that do not have a stereocentre and, as such, are unable to rotate the plane of polarized light but are nonetheless chiral. *Axial chirality* is where stereoisomers of a compound contain a plane of symmetry or an 'axis of chirality'. The enantiomers of this type of chirality are labeled *meso-* and are internally compensated with respect to the rotation of plane polarized light, meaning the rotation of its two halves are of opposite sign and cancel each other out. This type of chirality includes geometric isomerism and atropisomerism (where rotation around a single bond is hindered enough to isolate conformers) but will not be discussed further here. Of course, a helix is always chiral due to its clockwise or anticlockwise 'corkscrew' structure. Helicity is a unique form of chirality that normally occurs in longer chain molecules such as proteins and polysaccharides.

1.4 Enantiomeric Relationships

Advancement in our understanding of pest biochemistry and metabolic pathways of pesticides and the subsequent increase in the molecular complexity of pesticides have lead to more frequent use of chiral agrochemicals. Now, more than 25% of all agrochemicals are chiral in nature (Williams 1996), the majority of which are produced with equal amounts of both enantiomers. This is known as a *racemic mixture*. Practically, however, it is usually only one of the enantiomers that cause the desired pesticidal effect. Receptors in the target species are generally *enantioselective* meaning they distinguish between chiral pairs leaving half of the enantiomers ineffective in that particular process. Unfortunately, the unused enantiomer may not be idle with respect to non-target species and, in fact, to any of

its further interactions, biotically or abiotically, in the environment. Consequently, deviations from the original racemic state may occur and need to be studied. Several terms have thus been used to describe the extent of deviation from the racemic composition. The enantiomeric ratio (ER) is a straight forward ratio of the two enantiomers existing as part of a chiral compound:

$$ER = \frac{[E_+]}{[E_-]} \quad or \quad \frac{[E_1]}{[E_2]} \qquad \text{(Equation 1.1)}$$

Where E_+ is the concentration of the *dextro-* (+) enantiomer and E_- the *laevo-* (−) enantiomer or where E_1 is the first eluting enantiomer and E_2 the second. The ER of a racemic mixture gives a value 1.0 while deviation from this value indicates an imbalance in the ration of the enantiomers. The enantiomeric fraction (EF) can be derived from the ER and is now thought to be superior because it provides a more meaningful representation of graphical data and is more easily employed in mathematical fate expressions (Harner et al. 2000):

$$EF = \frac{ER}{ER + 1} \quad or \quad \frac{[E_+]}{[E_+ + E_-]} \quad or \quad \frac{[E_1]}{[E_1 + E_2]} \qquad \text{(Equation 1.2)}$$

In the case of EF, a value of 0.5 is obtained if there is a racemic mixture of enantiomers. In order to determine which enantiomer is in greater abundance in a non-racemic mixture it is necessary to know the elution order of the enantiomers of an analyte separated via chromatography. For example, in the case of acephate, a chiral organophosphorus pesticide used throughout this project, the (+) enantiomer is known to elute before the (−) one (Miyazaki et al. 1988). Enantioexcess (ee) can also be used and indicates the excess of the enantiomer with higher concentration (E_h) over another that has a lower concentration (E_l):

$$ee = \frac{[E_h - E_l]}{[E_h + E_l]} \qquad \text{(Equation 1.3)}$$

1.5 Homochirality in Life

A fundamental hallmark of life's chemistry is *homochirality* (Fischer 1894; Ruch 1968; Mason 1988). It is well known that, despite an equal global mixture of both the D- and L- form of chiral amino acids (AAs), they are almost exclusively active as the L- form within living systems. L- AAs are the fundamental building blocks of

polypeptide chains which in turn make up proteins, essential for terrestrial life. This inherent homochirality finds its way up into higher-order structures such as the right-handed α-helix (secondary structure), and the fold (tertiary structure) that is unique to each different protein in its native state (Barron 2008). Likewise, only the D- form of carbohydrates are found engaged in biological structures; in fact, the homochirality of the sugar D-deoxyribose, a fundamental component of nucleic acid and thus DNA, is reflected in the right-handed B-type DNA double helix. How this phenomenon came about has been grounds for much consideration and perusal for over a century. Fischer (1894) proposed a 'lock and key' approach to optically active biochemical molecules designed to 'provide a simple solution to the enigma of natural asymmetric synthesis.' The idea holds true to this day and essentially observes that by starting with a single enantiomer or even with an enantiomeric excess in a mixture of optical isomers, synthetic reactions lead inevitably to a dominant diastereomeric product favoured by the steric congruence of the reaction intermediates (Mason 1988). This is the reason L-sugars and D-AAs cannot (with few exceptions) find a foothold in living organisms and why homochirality is fundamental in the efficiency of biochemistry. In fact, some studies (Joyce et al. 1984) imply that the homochirality of life is a prerequisite for the origin of life itself. Metabolic efficiency is also reflected as industrial and economic efficiency in the macro-world and is well demonstrated by the convention of using right-handed threads on nuts and bolts in normal circumstances. But what was the spark that provided the initial enantiomeric excess? This is a question that has puzzled scientists since the discovery of homochirality and although many theories have been proposed none are pervasively accepted. Four of the more prominent ideas pertaining to the cause of the homochirality of life are briefly explored below. For a major review of the topic see Meierhenrich (2008).

1.5.1 Polarised Light

Circular dichroism (CD) describes the way homochiral substances have different absorption intensities for left and right circularly polarised (CP) light. Since photolysis (the chemical breakdown of a substance with light) requires absorption of light, the enantiomers of such a compound would decay at different rates (enantioselectively). Of course, both enantiomers will be broken down to some extent by the CP light meaning that total homochirality cannot be accounted for by

this mechanism alone. It also appears that the right-circular component observed at sunrise and in particular at the North Pole is almost completely cancelled out by the left-circular component observed at sunset and the South Pole (Kemp et al. 1987). The net effect is of the order of one part per million (Mason 1988). Additionally, the sign of the enantioselectivity is only consistent over small frequency bands; light from the whole spectrum would cause the signs to cancel each other out resulting in no overall selectivity. It is not unthinkable, however, that a localised region may have arisen in the prebiotic Earth where the positioning and aspect of a pool of racemic amino acids could have led to enantioselective photolysis.

1.5.2 Parity Violations

Another physical theory is that of selective β-decay – governed by the *weak* force. This force has a slight handedness, called *parity violation*. The parity violation energy difference (PVED) may have been a starting point for the development of homochirality (Garay & Ahlgren-Beckendorf 1990). However, the PVED is exceptionally small (about 10^{-17} kT) (Bada 1995) and would have needed an additional factor such as autocatalysis. Autocatalysis is where a minute enantiomeric excess is rapidly and greatly enriched and was nicely demonstrated by Kondepudi (1990) who showed saturated solutions of sodium perchlorate, an achiral compound, can spontaneously crystallise, when stirred, into either pure left- or right-handed crystals. However, Kondepudi himself admitted that for autocatalytic enantiomeric amplification to take place, extremely specific, and perhaps unlikely, conditions are required.

1.5.3 Alien Source

There is some evidence to suggest that the homochirality of life on Earth was initiated as a result of the arrival of the first molecular building blocks from an extra terrestrial source. Such evidence arises predominantly from analysis of amino acids present in meteorite samples. In fact the majority of analyses have been conducted on fragments from a particular source, the Murchison meteorite, which fell to Earth in Australia in 1969. It has since been found to contain at least 89 different amino acids (Meierhenrich 2008). Many of these amino acids are chiral and several have been found to exist with small enantiomeric excesses (For example, Engel & Nagy 1982). However, the results are generally thought to be unconvincing due to the possibility of contamination from terrestrial amino acids. Cronin & Pizzarello (1997) made the

breakthrough when they showed that enantiomeric excesses existed in amino acid samples that were not known to exist terrestrially and thus were almost certainly indigenous to the meteorite. The excesses were of the L- form and provided a possible source for the origin of life on Earth as well as the initial imbalance from which homochirality developed.

1.5.4 Minerals

More than 70 years ago it was suggested that asymmetric preferential adsorption of one enantiomer of a racemate on to quartz crystals may have been responsible for the origin of the homochirality in life (Karagunis & Coumoulos 1938). Bonner et al. (1974; 1975) later confirmed their work but makes clear that it is only possible under anhydrous conditions. Additionally, it is now known that the global distribution of quartz enantiomers is racemic. Many now accept that these obstacles now render the mechanism totally implausible in any realistic prebiotic environment(Klabunovskii & Thieman 2000; Klabunovskii 2001; Bonner 1995). However, it is also notable that, locally, distribution of quartz enantiomers can be significantly non-racemic (Bonner et al. 1974; Támara 2009) signifying that preferential adsorption on the surface of quartz crystals as the trigger for the homochirality of life cannot be ruled out.

Clay minerals have also been cited as an abiotic solution to the origin of homochirality. Initially it was thought that a chiral clay mineral such as kaolinite might be capable of enantiospecific adsorption and polymerization of amino acids and several workers had managed to provide experimental in support (Jackson 1971; Degens et al. 1970; Bondy & Harrington 1979). However, others were unable to replicate or verify such experiments (Bonner & Flores 1973; McCullough & Lemmon 1974; Bonner & Flores 1975; Friebele et al. 1981; Youatt & Brown 1981) casting doubt on such a theory. A significant problem was that the two enantiomorphic forms of kaolinite, like quartz, are equal in abundance on a global scale. This means that if enantiospecific adsorption did occur in a prebiotic world it would result in the formation of an equal amount of L- and D-amino acids globally. Nevertheless, the idea was revisited by Julg et al. (1990) and thought to be viable by taking into account the theory of parity violation. This suggests that electroweak interactions on a nuclear scale are likely to undergo transformations that do not preserve parity. Experiments have shown that during radioactive β-emissions, for example, the electrons released were observed to have electron spin that

preferentially describes a left-handed helix (Cronin & Reisse 2005). Another consequence of the violation of parity that originates in the so-called electroweak interactions that result from unification of the intranuclear weak interactions and electromagnetic interactions resulting in a parity-violating energy difference (PVED) (Cronin & Reisse 2005). Julg et al. (1990)explain that as a result of the weak nuclear interaction at the mineral level there is a preferential formation of kaolinite of one enantiomorphic form. Furthermore, it is this asymmetry that causes the asymmetrical adsorption of amino acids observed in their work and thus, is likely to have played an important role in the initiation of life on Earth.

Spontaneous breaking of symmetry was first proposed as a mechanism by Frank (1953) and suggests that one enantiomer can be the catalyst for its own production while preventing the production of its opposite enantiomer. This would require random deviation from the racemic state of the enantiomers of a molecule which is, in fact, exactly how a racemic mixture of enantiomers exists (Mills 1932). The idea that a racemic mixture, at any one time, is made up of an exactly even number of opposite enantiomers is a statistical generalisation and is technically incorrect. In a classic analogy, if a coin was tossed 100 times it is by no means necessary for exactly 50 heads and 50 tails to emerge. Similarly, if synthesis of an enantiomeric mixture from a chiral starting material is repeated many times the resulting mixtures will consist of different enantiomeric compositions. Of course, a bell curve of the ERs for each mixture will peak at 1.0 with decreasing occurrences of mixtures with increasing deviations from the racemic state but nonetheless, any single racemic mixture of enantiomers might not contain exactly even numbers of opposite enantiomers. This has been demonstrated in several experiments (Havinga 1954; Calvin 1969; Bonner 1994) indicating that one of the enantiomers could work its way from a position of slight excess to the total destruction of its antipode. However, as pointed out by Bonner (1995), such a process is probably unlikely in a prebiotic world – in the case where a resolved crystalline enantiomer was produced by spontaneous resolution, it would eventually return back to its racemic state on redissolving under those conditions. Nonetheless, that this mechanism played a role is not out of the question, particularly if combined with some of the other theories reviewed in this section.

1.6 Chiral pollutants in the environment

Discussion of chirality in the field of environmental pollution is of utmost importance. If, as already stated, more than a quarter of all pollutants are chiral (Williams 1996) it is vital to examine carefully the behaviour of these chiral compounds after their application. This is especially so when we see that in many cases one enantiomer can be more toxic than its counterpart. Furthermore, after environmental application, as a pesticide moves, temporally and spatially, it can degrade enantioselectively. As such, non-racemic samples of a chiral pesticide may be found despite knowledge that the pesticide is only produced and applied as a racemic mixture. Thus, the overall toxicity of the compound in the environment cannot be accurately determined.

The difference in toxicological properties of the enantiomers stems from their chirality which enables them to interact with enantiomers of other chiral molecules independently through different biochemical mechanisms (Garrison et al. 1996). Perhaps the most pertinent example of this occurrence is the case of the Contergan sedative, given to pregnant women worldwide from 1957 until 1961to treat morning sickness. Contergan contained racemic thalidomide; the (R)-enantiomer of which had the desired therapeutic effects, whereas the (S)-enantiomer had teratogenic effects and caused severe teratogenic defects in many of the babies born (Bentley 1995). Of course, it is not just pharmacological compounds that this applies to but all bioactive compounds that are chiral, including pesticides. Williams (1996) notes that when a pesticide is chiral in nature half the product may react with a different cellular receptor and may cause unwanted, and potentially damaging, side-effects. Lin (2006) found that the toxicity of methamidophos towards *Daphnia magna* was an order of magnitude greater in the (−) enantiomer over the (+) enantiomer. Likewise, Zhou et al. (2009) found the (R) enantiomer of salithion, an organophosphorus (OP) pesticide, was five times more potent towards the same species as was the (S) enantiomer. Interestingly, Zhou et al. also noted that in terms of enantiomeric toxicity, salithion is not the sum of its parts; the potency of racemic salithion was significantly less than the combined strength of the two enantiomers acting independently. The process is known as antagonism and, in fact, occurs in the case of four other chiral OPs but to date no one has been able to propose a mechanism (Zhou

et al. 2009). This is one particularly attractive argument for the use of enantiopure chiral pesticides.

Not only is it common for the toxicity of chiral pesticide enantiomers to differ but it is also frequently reported that the degradation rates of intra-molecular enantiomers can vary (Ali & Aboul-Enein 2004). This is found in the measurement of ER or EF of chiral pesticides sampled in the environment. Deviation from the racemic state has been observed, indicating enantioselective degradation (or selective removal) of the enantiomers of the given pesticide (Kallenborn & Hühnerfuss 2001). Jantunen & Bidleman (1998) reported ER values of 0.75 for dissolved α-HCH at high latitude in the Greenland Sea and Wiberg et al. (1998) noted ER values for trans-chlordanein samples of Baltic Herring as low as 0.32 in Resolute Bay, Canada. Further reports of this kind have been made (Faller, Hühnerfuss, Konig & Ludwig 1991; Kallenborn et al. 1991; Kallenborn & Hühnerfuss 2001; Hühnerfuss et al. 1993; Ludwig et al. 1992; Qin et al. 2006; Zipper et al. 1998; Faller, Hühnerfuss, Konig, Krebber et al. 1991; Druzina & Stegu 2007; Lewis et al. 1999). Enantioselective degradation of chiral chemicals is normally attributed to microbial activity. The inherent chirality of life inevitably means that the biological metabolism of a chiral species will be enantioselective. Most workers attribute the presence of non-racemic mixtures of chiral pesticides in the environment entirely to their interaction with biologically selective organisms such as enzymes and bacteria and, in fact, use selective enantiomer degradation as a marker for biological activity (Garrison 2006). However, over the years there have been reports (Degens et al. 1970; Bondy & Harrington 1979) that interactions between chiral agrochemicals and achiral minerals can show enantioselective degradation of the chiral species. In most cases this is disputed (Bonner & Flores 1973; McCullough & Lemmon 1974; Bonner & Flores 1975; Friebele et al. 1981; Youatt & Brown 1981)but more recent investigations (Castro-Puyana et al. 2008; Wedyan & Preston 2005)have provided evidence for the possibility of enantioselectivity solely as a consequence of abiotic processes.

The differing toxicity and variable degradation rates of enantiomers of an individual species combine to powerfully indicate the dangers of treating a chiral chemical as a single entity. It is, therefore, extremely important to differentiate both enantiomers of a chiral species if distribution and fate in the environment are to be understood.

1.7 Enantiomorphism in minerals

The concept of chirality as explained so far can be applied to individual crystals and mineral surfaces. Minerals may be inherently chiral due to their morphology as whole crystals, which exhibit mirror symmetry without superimposability. As is the case with quartz, which occurs as *d*-quartz or *l*-quartz racemically on a global scale (Támara 2009). Alternatively an achiral mineral may show chirality between its individual faces, as is the case with calcite, for example. Minerals such as calcite and gypsum, although acentric, have no morphological chirality as they possess planes of symmetry through their crystal structures. This, however, means that the crystal faces must be chiral by definition as they are not superimposable on one another. An extensive review of minerals that exhibit chirality by either of these means has been carried out by Hazen (2004).

Several workers (Hazen 2004; Horvath & Gellman 2003) have outlined three scenarios in which a mineral crystal surface can exhibit chirality, whether or not the crystal or any face is inherently chiral. In the first scenario, the structure of a two-dimensional (2D) surface of a crystal face exists as a non-superimposable image of its reflection across a perpendicular mirror plane (Figure 1.1 a). The atoms making up this layer can exist as a planar sheet or may show topography. In the case of many crystal surfaces there is no chiral structure to the 2D atom arrangement. However, in the second scenario, the surface may involve a step terrace feature that will result in the face demonstrating chirality as long as the step does not run at right-angles to the perpendicular mirror plane (Figure 1.1 b). For the third scenario, if the terrace edge does run at right-angles to the mirror plane, it may still maintain asymmetry if a 'kink' is present (Figure 1.1 c). This will leave a chiral centre at the site of the kink, again revealing a potential enatiomorphic face.

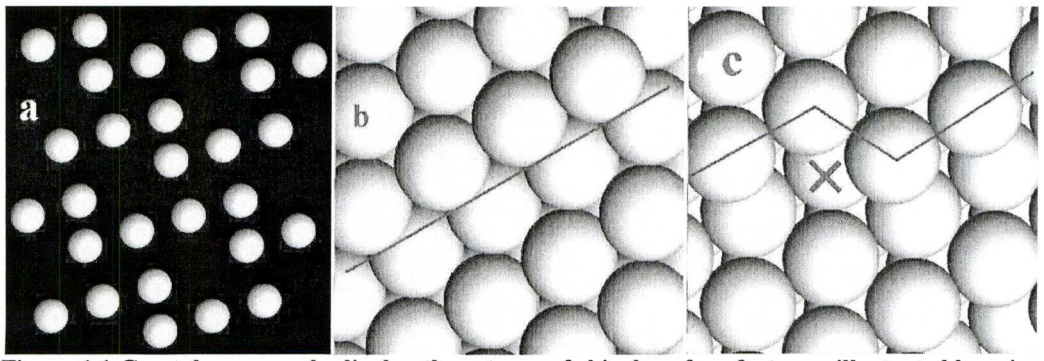

Figure 1.1 Crystals commonly display three types of chiral surface features, illustrated here in idealized drawings. (a) A periodic two -dimensional chiral arrangement of atoms in a plane; these atoms may be coplanar or they may occur at slightly different heights. (b) A terrace step that is chiral along a step edge (red line) (c) A kink site that provides a chiral center (X).

1.7.1 Rock forming minerals

Quartz is the second-most abundant mineral in the Earth's continental crust and is made up of silicon and oxygen in the formula, SiO_2. It is stable below 573°C and is the predominant mineral in most beach sand. Quartz gains its inherent chirality from its silicate framework that incorporates either right- or left-handed helices of corner-linked SiO_4 tetrahedra (Hazen 2004) (Figure 1.2) and occupies the trigonal space group $P3_121$ or $P3_221$ for *d*- and *l*-quartz crystals respectively. Quartz crystals principally exists in the form of a 6-sided prism with 6-sided pyramidal end-structures (Figure 1.3 a and Figure 1.3 b). The important chiral faces (Figure 1.3 c) are the ubiquitous (100) prism faces, *m*, the dominant (101) rhombohedral termination, *r*, and the (011) rhombohedral termination, *z*. However, it is not usually possible to determine the handedness of an individual of these common enantiomorphs. This is only possible when the rarer (111) and (511) faces (*s* and *x*, respectively) are present (Figure 1.3 a and Figure 1.3 b, respectively) as they slope to the right on a *d*-quartz crystal and left on an *l*-quartz crystal in accordance with the Weiss' convention for morphological handedness. Of course each face adheres to Biot's (1844) optical convention and so plane polarized light through a quartz slab perpendicular to the optical axis is rotated clockwise in a *d*-quartz specimen when the observer looks towards the source of the light.

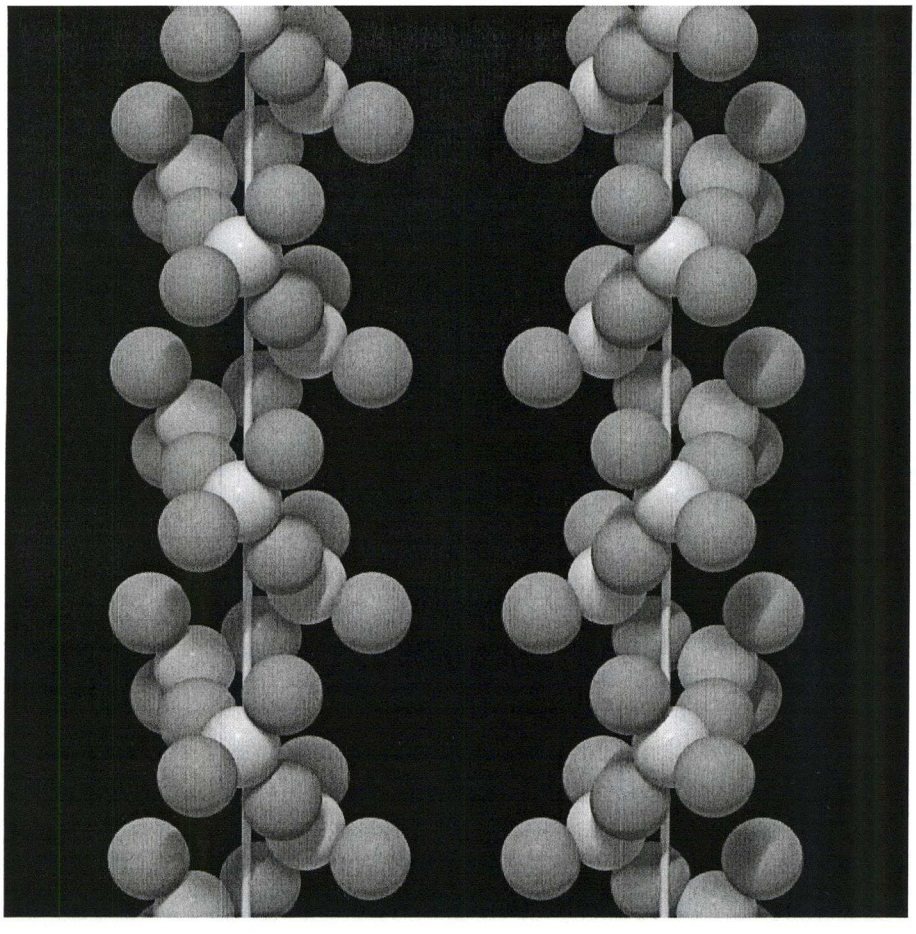

Figure 1.2 Left- and right-handed threefold helices of SiO4 molecules along the c-axis, each tetrahedron to other helices as two more points. From www.quartzpage.de

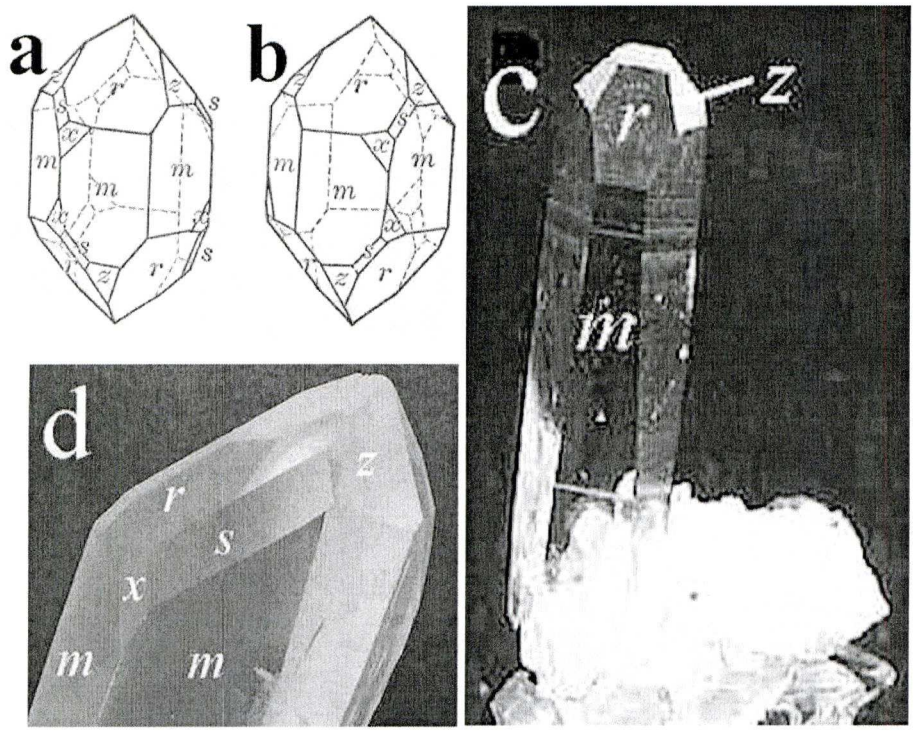

Figure 1.3 l- and d-quartz showing the left and right hand slope of the s and x faces (a and b respectively). Most crystals, such as the 3.2 –cm diameter specimen from Montgomery County, Arkansas (c), display only the m, r, and z faces. Less common specimens, suchas the 3.5 cm diameter right-handed crystal from Betroka, Madagascar (d), develop the additional forms (Hazen 2004).

As stated above, many other minerals, although not possessing intrinsic morphological chirality, do show chirality between individual faces due to mirror planes within their structure. Calcite ($CaCO_3$) is the principal mineral of limestone and marble and in recent decades has been of interest in studies of chiral selection by mineral surfaces (Didymus et al. 1994; Teng et al. 1998; Orme et al. 2001; Hazen et al. 2001; Hazen 2006; Kulp & Switzer 2007; Held & Gladys 2008; Maruyama et al. 2009). Calcite was an extremely abundant marine mineral on the early Earth and interestingly, its crystal surfaces would have been prevalent in prebiotic environments (Sumner 1997). Additionally, calcite is a common biomineral strongly bonded to proteins in the shells of many marine invertebrates. Figure 1.4 better illustrates the concept of chiral faces for calcite. The dogtooth or scalenohedral calcite form displays faces designated as *v* (214) characterized for being mirror images of each other. The potential for calcite to interact with chiral molecular species has been underscored by studies of surface growth topology, Teng et al.(1998) followed by Orme et al. (2001) suggest surface growth topography may be strongly affected by the presence of L-versus D- amino acids (Figure 1.5).

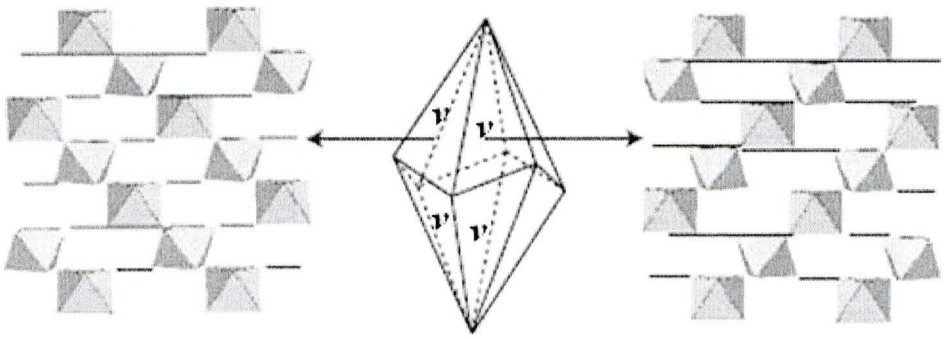

Figure 1.4 Trigonal calcite crystal. Enantiomorphic faces (v(211)) show corner linked CaO6 octahedra (yellow) crosslinked by planar CO3 groups.

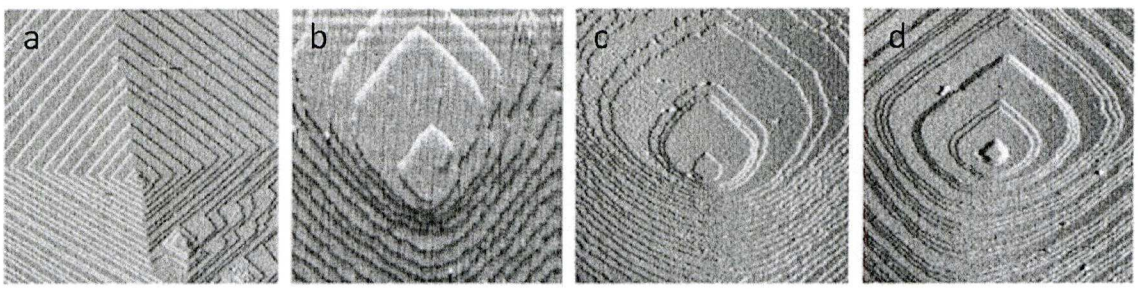

Figure 1.5 (a): a pure calcite growth hillock. (b): Growth hillocks following addition of supersaturated solutions with 0.01M glycine, an achiral amino acid. (c): 0.01M l-aspartic acid. (d): 0.01M d-aspartic acid. Images from Orme et al. (2001).

It is important to note here, particularly given the scope of this work, the comments of Hazen (2004): "crystal surfaces possess etch pits, growth steps, twin boundaries and other non-periodic features that provide numerous local chiral centres on an otherwise achiral surface environment." The extent of these sorts of chiral interactions with intrinsically achiral minerals and the variety of the minerals where they may occur is not well understood.

1.7.2 Clay minerals

Clays are a class of hydrated phyllosilicates making up the fine grained fraction of rocks, sediments and soils (Faïza Bergaya et al. 2006). Typically a phyllosilicate involves a continuous tetrahedral sheet. Each tetrahedron is made up of a cation (non-interchangeable) bound to four oxygen atoms, and linked to neighbouring tetrahedra at the corners of the three basal oxygen atoms. This results in an infinite 2D hexagonal mesh pattern along the *a*, *b* crystallographic directions. Additionally, there will be an octahedral sheet where connections between each octahedron to adjacent octahedra are made by sharing edges. This forms a sheet of hexagonal symmetry. The two sheets can align whereby the apical oxygen atoms of the tetrahedra point in the same direction and connect to the octahedral sheet to form a

common plane. A 1:1 layer clay structure involves the repetition of one tetrahedral sheet and one octahedral sheet whereas in a 2:1 layer structure one octahedral sheet is "sandwiched" between two tetrahedral sheets with their apical oxygen atoms pointing inwards. These structures are clearly illustrated in Figure 1.6. from Bergaya et al.(2006).

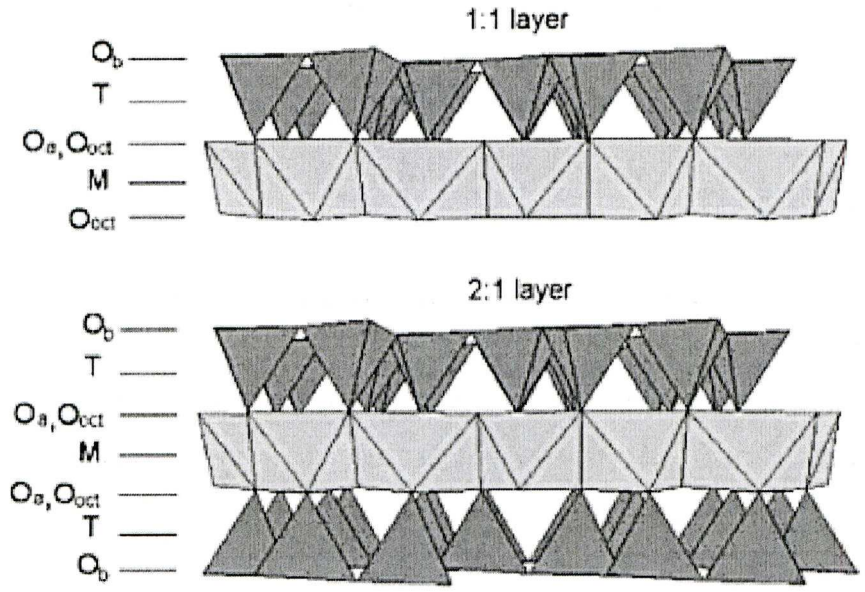

Figure 1.6 Models of a 1:1 and 2:1 layer structure, O_a, O_b and O_{oct} refer to the tetrahedral apical, tetrahedral basal and octahedral anionic position, respectively. M and T indicate the octahedral and tetrahedral cation, respectively (Faïza Bergaya et al. 2006).

The octahedral sheets in a clay can be known as trioctahedral if all six octahedral sites are occupied or dioctahedral if only four of the sites are engaged – although structure is often reported in half unit cells and so such classification is based on three octahedral site. Common tetrahedral cations are Si^{4+}, Al^{3+} and Fe^{3+} while octahedral cations are usually Al^{3+}, Fe^{3+}, Mg^{2+} and Fe^{2+}.

1.7.2.1 Kaolinite

Kaolinite is a dioctahedral 1:1 type layer clay with a general structure of $[Si_2]Al_2O_5(OH)_4$ (half unit-cell content). As a 1:1 type mineral it has a stacking sequence of repeated identical layers with a distance of ~7.2 Å from the basal oxygen atoms of the tetrahedra of one sheet to the other including the interlayer space between the units (total distance known as basal spacing). The kaolinite layer is ideally neutral but in reality is subject to some isomorphous replacement (Theng 1974). This is where an octahedral cation is replaced by another, usually of a lower

charge resulting in a permanent negative charge for the layer. It is this charge that gives kaolinite a small but measurable exchange capacity under acidic conditions. The presence of hydroxyl groups at edges of the octahedral sheets and the basal oxygen atoms of the tetrahedral sheets give rise to hydrogen bonding in the interlayer. Such bonds hold the unit layers together and must be broken in order for organic compounds to penetrate. This is difficult and such adsorption is generally confined to the external crystal surfaces (Theng 1974). In addition to hydrogen bonds in the interlayer there are more hydrogen bonds within the unit cells associated with the vacant octahedral site. Together these bonds have been suggested to be significant in the surface electrostatics that influence the formation of complexes with external organic compounds (Hobbs et al. 1997).

Many argue against the enantiomorphic properties of clay minerals (Hazen 2004; Bonner 1995; Bonner & Flores 1975; McCullough & Lemmon 1974). However, some workers have considered the dissymmetry of edge sites of dioctahedral clays (Degens et al. 1970; Jackson 1971). Such enantiomorphism derives from the arrangement of oxygen atoms, hydroxyl groups, aluminium atoms and the vacant octahedral sites (Jackson 1971). Site vacancy is of fundamental importance to the asymmetry of a clay. The three octahedral sites (half unit cells) where a vacancy might exist in a dioctahedral clay are referred to by Brigatti et al. (2006) as A, B and C vacancy sites. They also point out that the structure is chiral if the vacant site is B or C, and achiral if the vacant site is A. All naturally occurring kaolinites are thus chiral (Brigatti et al. 2006) (Figure 1.7).

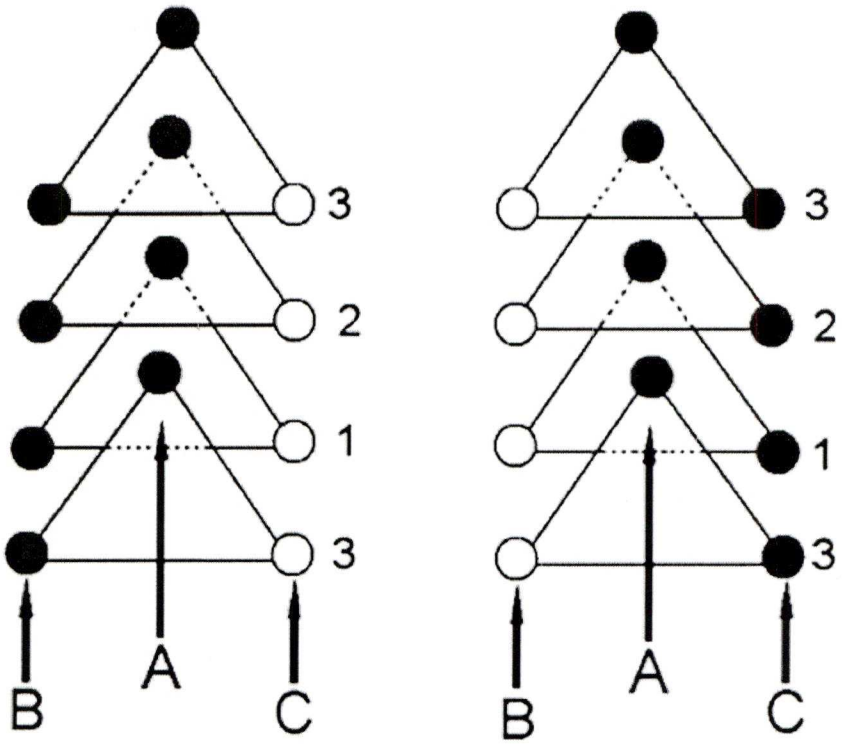

Figure 1.7 Projection on the (001) plane of the octahedral sites in kaolinite showing the possible placement of the vacant octahedral site (open circles). Closed circles represent Al3+ octahedra (Adapted from Brigatti et al. 2006).

1.7.2.2 Montmorillonite

Since montmorillonite will play a large role as a sorbent throughout the course of this project, details of its provenance as well as global prevalence are provided here. Montmorillonite is one of four dominant clay minerals found in the fine grain fraction of pelagic marine sediments. It makes up the majority of the clay mineral deposit, bentonite, formed by thermal and chemical alterations to volcanic ash deposits predominantly in subaqueous environments (Altaner et al. 1984; Christidis & Huff 2009). It is, therefore, at its most prevalent in volcanic regions particularly in marine environments. In some cases there may be inputs from the continents but normally the deposits are determined as authegenic (J.J. Griffin et al. 1968). As such, bentonite deposits are often considered indicative of volcanic regimes. The distribution of montmorillonite in the global oceans is listed in Table 1.1.

Table 1.1 Montmorillonite distribution in the global ocean expressed as a percentage of the four dominant clay minerals in the fine grain fraction; illite, chlorite, montmorillonite and kaolinite (From Griffin et al. 1968).

Ocean	Average Percentage (%)
North Atlantic	16
South Atlantic	26
North Pacific	35
South Pacific	53
Indian	41

In terms or soil composition, montmorillonite is a relatively common constituent of clay-dominated soils, particularly in close proximity to volcanic ash deposits. Furthermore, montmorillonite is the predominant component of vertisol, a soil order that is prevalent throughout North America but, in particular, dominates large areas of eastern Africa, Argentina, India and eastern Australia (Coulombe et al. 1996). Globally, vertisols make up an estimated 308 million ha of the earth's surface (USDA-SCS 1994).

Bergaya et al. (2006) provide an excellent description of the structure and chemical make-up of montmorillonite and thus, some of the more relevant information is summarised in the paragraph below.

Montmorillonite is a 2:1 type clay mineral and is a member of the smectite family. Smectite mineral particles are very small and thus, X-ray diffraction data are sometimes difficult to analyze. Some SEM micrographs of various modified and unmodified montmorillonite samples used throughout this project are included in the Appendix. As a dioctahedral smectite, the octahedral sheet is dominated by trivalent cations with one vacant octahedral site. Isomorphous substitution of the Al^{3+} cations for alternatives such as Mg^{2+} or Fe(II) will always occur if possible. Despite some internal compensation, the result will be an excess of negative layer charge. This permanent charge has important implications for the physical properties of montmorillonite including its exchange capacity and its ability to swell under hydration. Balancing of the positive charge deficiency occurs through the sorption of exchangeable cations into the interlayer structure of the crystal. Typical

exchangeable cations include Na^+, K^+, Ca^{2+} and Mg^{2+}. In addition, water molecules can readily be adsorbed in the interlayer space.

Bergaya et al. (2006) highlight three main elements of interlayer hydration: (i) hydration of interlayer cations, (ii) interaction of clay surfaces with water molecules and interlayer cations and (iii) water activity in the clay-water system. In terms of space occupation, the water enters the interlayer in integral layers and thus has a direct impact on the basal spacing of the crystal. Normally, hydrated swelling clays such as montmorillonite will have between 1 and 4 complete layers of water molecules depending largely on the nature of the exchangeable cation. As such the basal spacing can vary from 9.5 Å in its fully collapsed state to about 19 Å when fully hydrated. And in fact the interlayer may expand or even completely dissociate further if the exchangeable cations are monovalent and small (Theng 1974). An extensive list of exchangeable cations and the subsequent basal spacing for montmorillonite is presented by Norrish(1954). Once water has penetrated the montmorillonite interlayer it can form hydration complexes with the exchangeable cations. In the case where the cations bind directly to the aluminosilicate surface on one side and to water molecules on the other side, the resulting complex is known as an 'inner-sphere' complex whereas an 'outer-sphere' complex involves the interlayer cation being completely surrounded by water molecules (Faïza Bergaya et al. 2006). In the case of Na^+-exchanged montmorillonite, for example, the Na^+ cation is surrounded by five water molecules and is situated above the hexagonal cavity just over the octahedron. The cation's water ligands are involved in forming an intermolecular hydrogen bonded network. Hydrogen bonds may also bind interlayer species to the aluminosilicate sheet surface but these bonds are weak and cannot last long. Such bond strengths contribute to the high cation exchange capacity (CEC) of montmorillonite, ranging from 70 to 120mmol/100g of clay (Grim 1968) – although Meier & Nüesch(1999) actually found a lower limit of montmorillonite CEC of 65 ±2 mmol/100 g fully swellable montmorillonite. However, it is important to note that the CEC and the ability to take on water are predominantly limited by the layer charge. The layer charge of the half unit-cell content of montmorillonite can be as small as −0.2 (Faïza Bergaya et al. 2006) but may be as high as ~ −0.43 according to Theng (1974) and Shoonheydt & Johnston(2006). Negative layer charges such as these either arise from the previously mentioned substitution of Al^{3+} for a lower

charge cation in the octahedral sheet as well as via, albeit less frequently, substitution of Si (IV) for Al^{3+} in the tetrahedral sheet. Ultimately, the presence of such charges and their variability are what gives montmorillonite and other 2:1 phyllosilicates their ability to take on exchangeable cations and makes them so important across so many disciplines.

Montmorillonite is also capable of being made into a pillared clay (PILC). PILCs are prepared by first intercalation of a 2:1 layered silicate such as montmorillonite with strong polycations (J. Q. Jiang et al. 2002). The intercalation is normally followed by thermal conversion of the polycations to nanoscopic metal aggregates. These aggregates literally act as pillars supporting the structure that is the silicate layers of the clay. Consequently, the diameter of the interlayer space can be more than doubled while heating of the clay to temperatures of, in some cases, as high as 800 °C has no effect on the basal spacing (Faïza Bergaya et al. 2006). Furthermore, the surface area of the clay is greatly increased, improving its effectiveness as a catalyst or as a catalyst support material. This is the primary industrial function of PILCs but they are also commonly used as adsorbents or ion exchangers.

Akin to kaolinite, montmorillonite has been reported to be capable of enantioselective sorption of a chiral species (Bondy & Harrington 1979). Unlike kaolinite, however, montmorillonite does not and cannot display structural asymmetry and, in fact, several workers were unable to confirm Bondy and Harrington's preferential binding of either enantiomer of any sorbate (Youatt & Brown 1981; Friebele et al. 1981). Further work has continued until now (Hashizume et al. 2002; Wedyan & Preston 2005) as preferential enantioselection continues to be reported but is rarely repeated. Some suggestions have been made as to mechanisms involved but no definitive answers are even suggested let alone settled upon. Siffert and Naidja (1992) found preferential adsorption of the L forms of glutaminic and aspartic acid on Na-montmorillonite. Additionally, they provided XRD data showing that the two enantiomers of the same amino acid had different basal spacings indicating that the "stacking of the molecules in the interlayer space are different for the two amino acids enantiomers." Since, statistically, the crystal structure of montmorillonite cannot possess its own structural chirality, Siffert and Naidja (1992) suggested two hypotheses. The first is based on an idea from Ponnamperuma et al. (1982) who suggest that some form of asymmetry may come about from the way that

octahedral vacancies are arranged. As a result it may be that the distribution, randomly, of these vacancies at cation exchange sites on the tetrahedral silica sheets causes some degree of chirality. Such an asymmetric surface could favour stacking of the enantiomers in different orientations. Previously, Cairns-Smith (1975) had touched on the same idea and considered that "clay minerals which themselves are not constituted by chiral structural units should nevertheless be able to exhibit a chiral character due to the stacking of their structural units." The second hypothesis is from Yamagishi (1981; 1982; 1983; 1985; 1987) who argues that an asymmetry can be created at the interlayer surfaces by the way in which optically active ions stack onto each other. He showed, through experiment, that the assumed chirality of the montmorillonite interlayer surface on optically active molecules arises due to differences in the stacking of the metallic complexes; so in effect, structural chirality would be induced by the adsorbate (Siffert & Naidja 1992).

1.8 Chiral organophosphorus pesticides

Organophosphorus (OP) compounds have been used in many applications including lubrication, flame retardation and chemical warfare. It is as OP pesticides, however, that their use has been most widespread, in particular as a response to the banning of some toxic organochlorine pesticides (OCs) in the 1970s which impact non-target organisms and have marked ability to persist and accumulate in the environment. Now 36 % of the total world market for pesticides comes from OPs (Kanekar et al. 2004). The EPA published a list of organophosphorus pesticides totaling over 100 compounds (Reigart & Roberts 1999) although currently the EPA list 49 compounds in the re-registration review process for organophosphates in the US (US EPA 2009). OP pesticides are derivatives of phosphoric, phosphonic, phosphorothioic, or phosphonothioic acids, comprising of many chemicals with a wide range of pesticidal uses (Druzina & Stegu 2007). About 30 % of current-use OPs are chiral due to asymmetry around the phosphorus atom (Garrison 2006), although this value is constantly changing as emerging chiral pesticides are being continually developed (Wong 2006).

Chiral OP pesticides are extremely wide ranging in terms of structure and toxicological effects of target and non-target organisms. Chirality normally arises due to asymmetry around the phosphorus atom, but carbon can also be the chiral centre, as in the case of malathion, or occasionally a sulfur atom, as in the case of

fensulfothion. They may also contain halides and exist as aliphatic or aromatic compounds (Figure 1.8.).

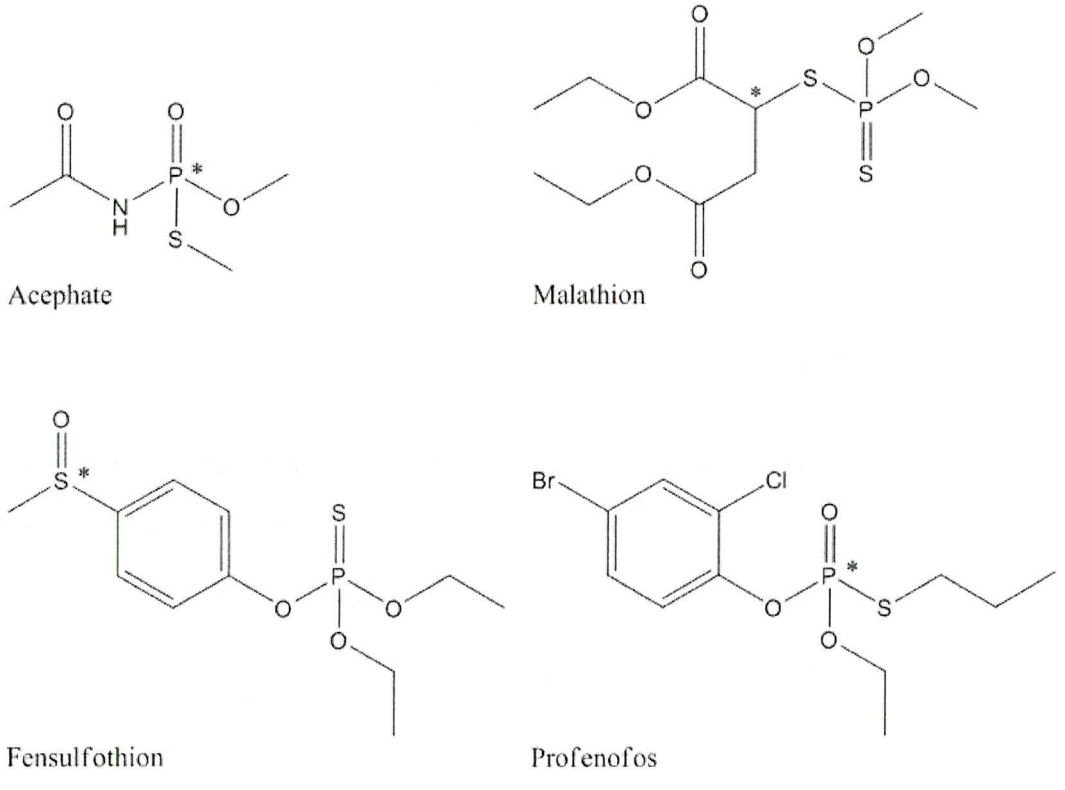

Figure 1.8 Some common OP pesticides demonstrating position of chiral centres (*) and aliphatic and aromatic forms.

To some extent, the modes and mechanisms of OP pesticide toxicity are not well known at present (Kozawa et al. 2009). However, much work has been done to clarify the biotoxic action of OPs (Costa 2006; J. E. Chambers et al. 2001; H. W. Chambers et al. 2001). Structurally, OPs can be represented by (Costa 2006):

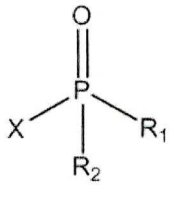

Where X represents the group that will be displaced in an animal's nervous system when the OP phosphorylates acetylcholinesterase (AChE). In this way an OP acts as a strong acetylcholinesterase (AChE) inhibitors. AChE is an enzyme that facilitates the degradation of the neurotransmitter, acetylcholine, through hydrolysis. Thus its inhibition causes a build up of acetylcholine around the cholinergic synapses where it

is released. This, along with overstimulation of the muscarinic and nicotinic receptors (Kozawa et al. 2009), results in cholinergic syndrome and possible symptoms ranging from sweating to vomiting to respiratory failure and death (Kanekar et al. 2004). Kanekar et al. also report some other modes of biotoxicological action. One example is organophosphate-induced polyneuropathy (OPIDP), the symptoms of which cause a delayed sensory loss, progressive muscle weakness and further weakness of the distal skeletal muscles (Lotti & Moretto 2005), is caused by breakdown of neuritic segments and of their myelin sheaths (Ehrich & Jortner 2001).

OP insecticides show no species preference in terms of their toxicity. Aquatic and terrestrial animals alike are at risk from AChE inhibition if sufficiently exposed. Significant *Ceriodaphnia dubia* mortality was observed in 87% of samples from a river channel in California draining an urban/agricultural watershed, while 100% mortality occurred in a nearby channel receiving direct agricultural surface furrow runoff (Hunt et al. 2003). Intuitively, species with a preference for soil habitats are particularly vulnerable to OP pesticides (De Lange et al. 2009). Of course, acute toxicity is not the only means of poisoning to non-target species; sublethal exposure may depress the brain and/or blood AChE activity, and may alter the physiology and behaviour of the species (Lambert et al. 2005).

1.9 Acephate

Acephate (O,S-dimethyl acetylphosphoramidothioate) is an important OP compound used globally as an agricultural systemic insecticide and its interaction with a variety of sorbents is the focus of this work. It consists of a phosphorus atom surrounded by four different molecular groups, making the overall structure asymmetric and therefore chiral.

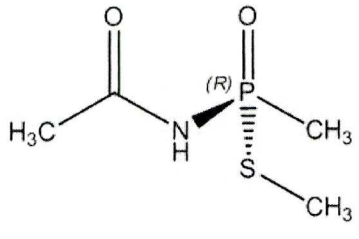

Figure 1.9 Chiral acephate molecule (R) presented as a 3D structure

Physical and chemical properties of acephate are compiled in work by Szeto et al.(1979). Some of the most relevant of these are presented in Table 1.2 below.

Table 1.2 Selected physical and chemical properties of the organophosphorus insecticide, acephate (Data from Szeto et al. 1979).

	Acephate[a]	α-HCH[b]	PCB 52[b]
Empirical Formula	$C_4H_{10}NO_3PS$	$C_6H_6Cl_6$	2,2',5,5'-$C_{l4}C_6H_3C_6H_3$
Molecular Weight	183.16	290.83	291.99
Water Solubility (mol/m^3)	3821.80	0.12	0.42
Vapour Pressure (Pa)	5.33	0.14	9.06×10^{-3}
Octanol-Water Partition, K_{OW} (25°C)	0.13	6310	1,258,925

[a] From Szeto et al. (1979)
[b]From Klecka et al. (2000)

Acephate was introduced in Taiwan in 1972to control insects damaging vegetables, cotton, tobacco, rice, and flowers (Yen et al. 2000) but is now in widespread use. Reliable production values for acephate are sparse but according to U.S. Geological survey, over 1000 tonnes of the active ingredient were applied on average annually between 1999 and 2004 (USGS 2008). More than half of this value is applied specifically to cotton crops targeting a wide range of "chewing" insects.

Acephate is soluble and adsorptive and, thus, is considered to be mobile in most soils. Fan and Walters (2002) found acephate to be hydrolytically and photolytically stable in water at pH values between 5 and7 with hydrolysis half-lives of 169-325 days and aqueous photolysis half- lives of 17.5-173 days, but they did not record a specific correlation between pH and half-life. However, such a correlation was reported by (Downing 2002) who found that the half-life of acephate was reduced at higher pH values signifying its increased stability in acidic conditions. Nonetheless, in both acidic and alkaline conditions, hydrolysation occurs by cleavage of the P-N bond (Szeto et al. 1979). A final property of note is that a decrease in temperature results in much slower rates of acephate degradation (Szeto et al. 1979; Downing

2002). This is likely to prove important when assessing the fate of acephate in the environment, particularly at the poles.

Acephate was chosen as the sorbate for batch sorption experiments throughout this work for a number of reasons, including its global significance as an OP pesticide as discussed above. Additionally, its phosphorus chiral centre and its relatively small size as an organic pollutant makes it a good option for assessing sorptive interactions within and around the interlayer spacing of a clay mineral sorbent. The strong polarity of the molecule makes it easily soluble in water as well as acetonitrile making it a straightforward candidate for analysis via GC and HPLC. Furthermore, of a variety of OP pesticides analysed using GC-ECD, acephate enantiomers proved the easiest to resolve with the shortest retention time. Finally, despite its high toxicity with an LD50 of 900 mg/kg in rats (Mahajna et al. 1997), acephate is actually one of the safer OP pesticides to handle.

The toxicity of acephate is attributed to acetylcholinesterase (AChE) inhibition, the action of which was explained in the previous section. However, the actual AChE inhibitor is methamidophos, the metabolic degradation product of acephate (Mahajna et al. 1997). The structure of methamidophos and its proposed mechanism of formation from acephate is provided in Figure 1.10.

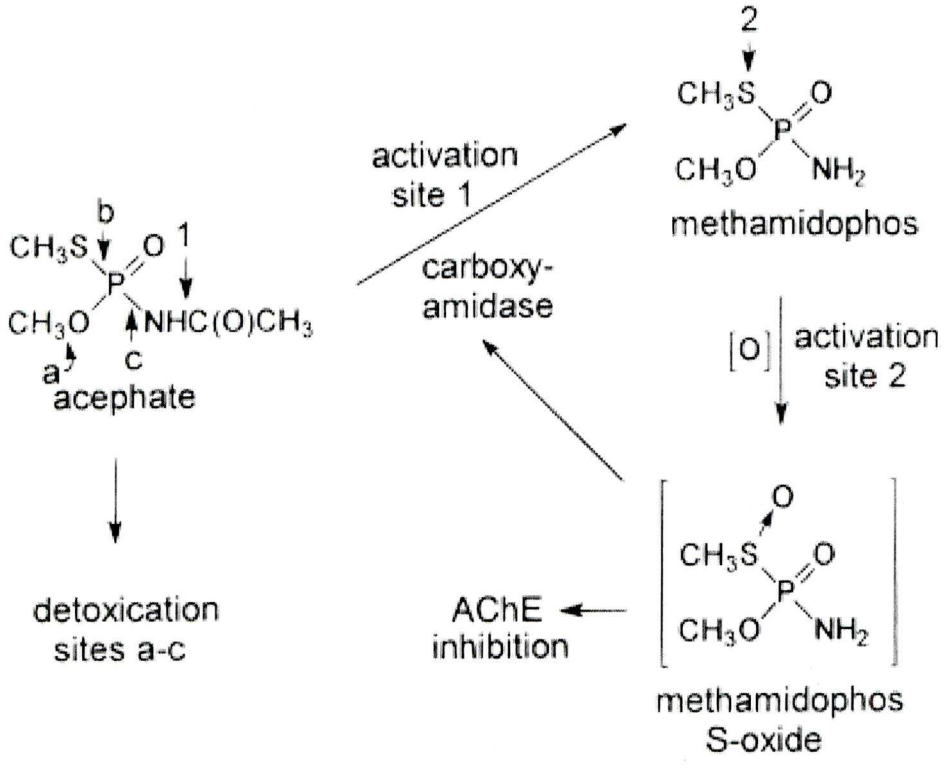

Figure 1.10 Hypothesis for the metabolic activation of acephate proposed by Mahajna et al. (1997). Methamidophos S-oxide is proposed but not established as an intermediate.

1.10 Global production, distribution, degradation and transport of organophosphorus insecticides

Chiral OP insecticides can pollute the environment from a variety of sources. Ali and Aboul-Enein (2004) categorise sources of contamination into point and nonpoint classes. Point sources include aspects of industrial and domestic activities such as lawn treatment and pest control. Nonpoint-source OPs come mainly from excess agricultural application and are caused by rainfall or snowmelt running over or leaching through the ground and can be found near or far from their original source in the world's groundwater, rivers, lakes and oceans as well as in sediment, soil and atmospheric systems (Matthies et al. 2009; Yen et al. 2000; Muir et al. 2004; Hageman et al. 2006).

Domestic, industrial and agricultural application is normally the initial pathway into the environment. This is the source of immediate contamination in the area of application. The transport of such contaminants away from the source can occur through a number of further pathways. Direct transfer from the source soil to groundwater, rivers, lakes and the ocean may occur through leaching, runoff and general flushing of waste water from agricultural land and industrial and housing

complexes. Additionally, volatilisation results in transfer of contaminants into the atmosphere where they may remain or be return to surface systems via desorption, precipitation or further air/water exchange processes.

Compartmentalisation can be applied to the global environment and be used to assess transport of pollutants in the environment. The three root compartments are generally thought to be air, water and soil (plus sediment). The state of equilibrium of partitioning between the compartments can be defined using a constant (Figure 1.11). Further compartmentalisation results in air being sub-classified into gas and aerosol components, soil into upper terrestrial soil, deep soil and groundwater and water into freshwater, the surface ocean and the deep ocean. Mackay et al. (1996) and Klecka (2000) suggest higher levels of disaggregation of the compartments that will not be discussed in full here.

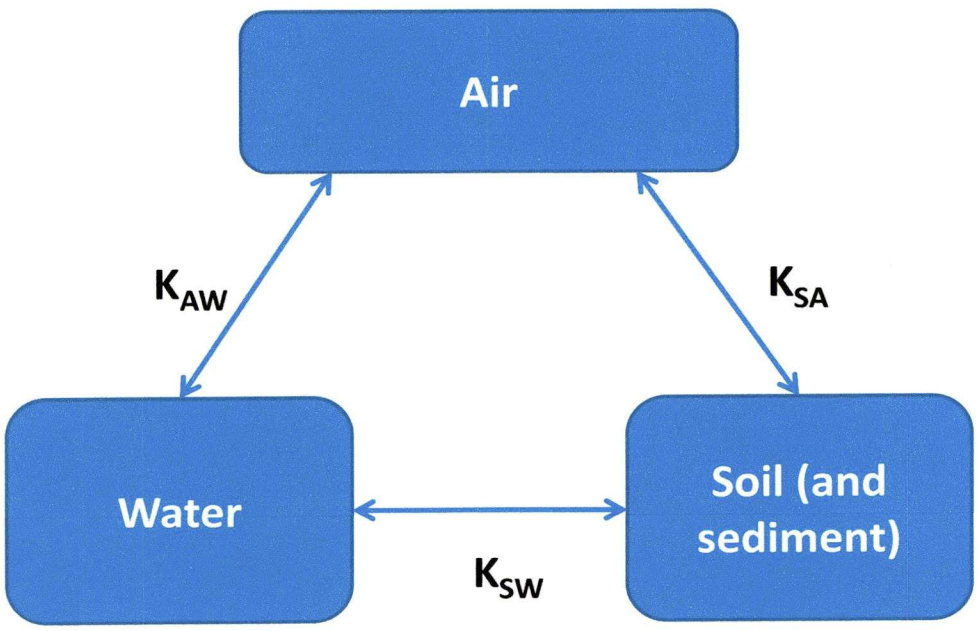

Figure 1.11 3-compartment system with equilibrium partitioning between compartments (From Klecka 2000).

The compartments in Figure 1.11 are essentially the three different phases that make up the global environment; gaseous, liquid and solid media. Here, they are referred to as the air phase, the water phase and the mineral phase. The Reversible distribution at equilibrium conditions between such phases are important for assessing insecticide distribution in the environment and can be described by the respective distribution coefficient, K_{xy}.

$$K_{xy} = \frac{C_x}{C_y} \qquad \text{(Equation 1.4)}$$

Where $C_x$and C_y are the concentrations of the compounds in phases x and y, respectively. The distribution coefficients for air-water (K_{AW}), soil-water (K_{SA}) and soil-air (K_{SW}) are thus defined by Equation 1.4.For the purposes of phase partitioning of organic pollutants, two additional phases are often considered: the octanol phase and the pure organic phase (Klecka 2000). The octanol phase represents a surrogate for environmental lipids and organic matter and is considered important in terms of specific storage for hydrophobic persistent pollutants such as many OCPs and PCBs. As such, the Octanol-water partition coefficient (K_{OW}) indicates the potential of an organic contaminant to concentrate from water into aquatic organisms. Low K_{OW} values for acephate (Table 1.2), therefore, suggest little tendency towards bioaccumulation. It is the mineral phase, however, that proves important for the storage of many OP insecticides due to their polarity and hydrophilic nature (causing interaction with specific minerals such as clays). Partition between the pure organic phase and the air and water phases respectively depends fundamentally on two physicochemical properties of the subject: the vapour pressure and the aqueous solubility.

Semi-volatile organic compounds (SVOCs) are defined as chemicals that have the capacity to partition between the gas and particle phases due to their intermediate ambient vapour pressures. In environmental science this commonly means within a range of temperatures typical of those on Earth. SVOCs, which include many OPs, may be subjected to repeated phase transformations and compartmental partition resulting in long distance transport. As discussed previously, enantiomers of chiral pollutants are found far from their source and furthermore may display ER/EF values that indicate significant deviation from the racemic state in which they were applied. Such a phenomenon is most likely made possible through long range atmospheric transfer (LRAT). This involves repeated sorption (and desorption) of an SVOC on a biological compound or mineral. In warm regions of the world SVOCs will have a tendency to evaporate to the atmosphere where they are subjected to a net poleward transfer (Wania et al. 1998). However, as they move to higher altitudes and latitudes they cool and condense (no saturation occurs but the phase of the compound will change). This may result in deposition at the surface of soils, water, sediments or

aerosols. However, changes in temperature and other climatic conditions can result in re-evaporation and a repeat of the process described above. Such cycles can happen frequently and over relatively short distances and are sometimes referred to as "the grasshopper effect" (Wania 2003). The process is described graphically in the figure below:

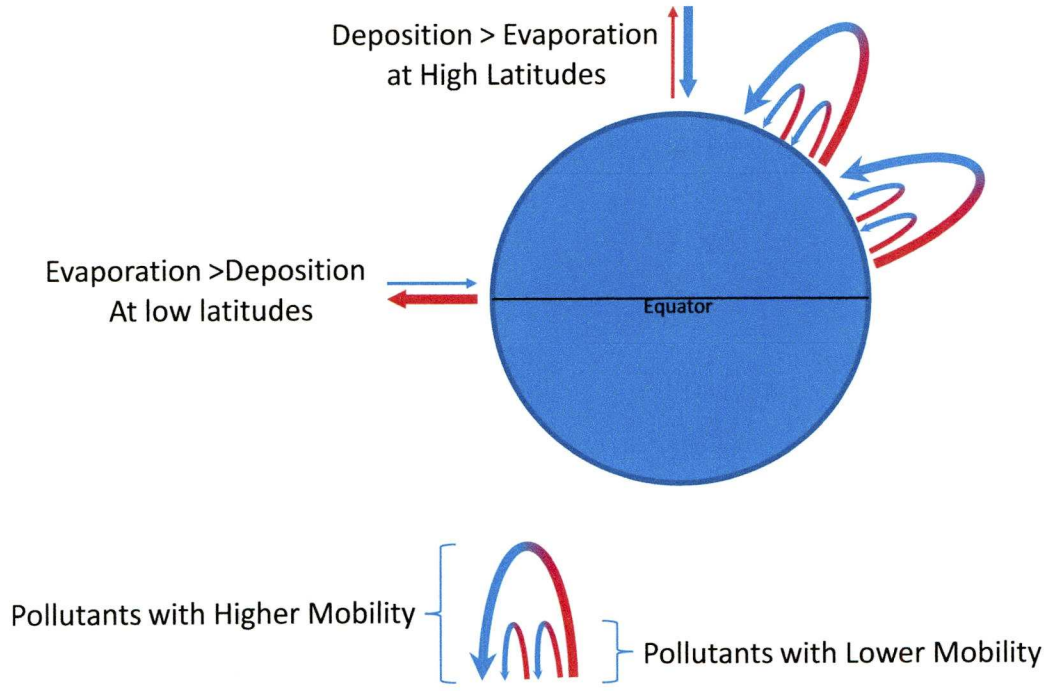

Figure 1.12 Schematic cartoon as a visual aid for explanation of the fundamental processes involved in the grasshopper effect.

Here we can see that adsorption/desorption cycles (which may, for example, represent day/night cycles or seasonal cycles) occur as the compounds are repeatedly evaporated to the atmosphere and redeposited to surface systems (Wania & Mackay 1996) The process represents a kind of fractionation whereby more volatile compounds are retained in the gaseous phase for longer and, therefore, transported polewards faster. Furthermore, the ERs of chiral compounds are altered if the enantiomer selective adsorption occurs in the adsorbed phase of the LRAT. This process is analogous to chiral separation using gas chromatography: if an enantiomer is preferentially adsorbed to the stationary phase, even if only very slightly, repeated adsorption/desorption cycles will result in greater retention and later elution of that enantiomer.

Very little data is available detailing LRAT of OPs as it is generally thought not to apply due to their high solubility in water and high vapour pressure. Assessments using US EPA methodology agrees: "US EPA methodology was used to assess degradation and immobilization of hazardous constituents in waste-soil mixtures for determination of the potential for migration of hazardous constituents to groundwater and to the atmosphere. Model output results indicated that no significant migration to groundwater or atmosphere was likely (McLean et al. 1988)." However, there is some work to the contrary on the LRAT of OPs.

Freed et al. (1979) found that certain OP pesticides, particularly those involving aromatic ring structures, were found to have surprisingly high octanol-water partition coefficients. This indicated an increased potential for storage and hence, a longer persistence and, furthermore, suggested the possibility of uptake by organisms and thus an increased opportunity for biomagnification. Later, observations and model results from Muir et al. (2004) suggest that in south-central Canada, at relatively high latitude with low precipitation rates, many current use pesticides (CUPs) are transported in the atmosphere on a regional scale and reach lakes that are a significant distance from their point of agricultural application. When assessing the LRAT potential of CUPS, including various OP pesticides, Muir et al. (2004) stress the importance of accounting for periods of minimal precipitation as well as assuring the constants employed, such as degradation rates and oxidant concentrations, are the correct ones for the region and time period of interest (Muir et al. 2004). Officially compiled lists may be guilty of overlooking such factors. Work by Hageman et al. (2006) supports this and points out that although none of the current-use pesticides that they detected were listed as persistent organic pollutants (POPs) under the 2001 Convention on POPs[1],their consistent appearance in remote ecosystems indicates they are persistent enough to enable transport over significant distances.

[1]They possess a particular combination of physical and chemical properties such that, once released into the environment, they:

- remain intact for exceptionally long periods of time (many years);
- become widely distributed throughout the environment as a result of natural processes involving soil, water and, most notably, air;
- accumulate in the fatty tissue of living organisms including humans, and are found at higher concentrations at higher levels in the food chain;
- and are toxic to both humans and wildlife.

Hermanson et al. (2005) note that many OP pesticides or their degradation products are not considered persistent and assumed not to be capable of LRAT because they are subject to oxidation. They consider that the dominant process for oxidation in the case of these pesticides is defined by hydroxyl radical reaction rates. High vapour pressure and low water solubility result in CUPs and other organic compounds existing in the gas phase under conditions of low oxidation. When the K_{AW} (often determined by the ratio of vapour pressure and water solubility) is high the compound tends to remain in the gas phase (Hermanson et al. 2005). A lack of atmospheric moisture found in arctic environments, for instance, may influence the effect of water solubility and therefore the value of K_{AW} and the compound's persistence.

Chlorpyrifos is a widely used OP insecticide that is not normally thought to have long-range atmospheric transport (LRAT) capabilities. This is due to its atmospheric lifetime being based on rapid reaction with hydroxyl radicals. However, Hermanson et al. (2005) identified its presence in the Austfonna ice cap, Norway as far back as 1972. The actual hydroxyl radical reaction rate, therefore, must be much slower than predicted from the literature because hydroxyl radical production is seasonal and often low in the Arctic. Such a departure from expected degradation rates was observed for several other OPs with traces present at least from depths relating to 1986 or earlier. The implication is that OPs can indeed be subject to LRAT.

1.11 Enantiomer Selective degradation or removal of chiral organophosphorus insecticides

Given the generally high mobility of OP insecticides in the environment and their unexpected ability to persist and be subject to LRAT, it is important to assess the means of adsorption and desorption en route and the extent of enantioselectivity in such cycles. Many such studies have been conducted for OC pesticides (Barrie et al. 1992; Jantunen & Bidleman 1998; Bidleman et al. 2002; Burkow & Kallenborn 2000; Jantunen & Bidleman 1997; Wiberg et al. 1998) due to their well know environmental persistence and are briefly discussed earlier in this chapter. However, little evidence can be found in the literature of any such studies pertaining to OP insecticides. Nonetheless, some observations of uneven proportions of enantiomers in the environment have been made and are summarised below.

Liu et al. (2005) assessed the enantioselectivity of a variety of synthetic pyrethroids (SPs) and OPs in both aquatic toxicity and degradation. They found that the (−) enantiomers of the OPs, in all cases, were dramatically more toxic to the freshwater invertebrates, *Ceriodaphnia dubia* and *Daphnia magna.* Lui et al. (2005) only measured degradation rates for the SPs, *cis*-bifenthrin and *cis*-permethrin, but found that the (−) enantiomer in both cases was preferentially removed by what they presumed was microbial action. Qin et al. (2006) also found similar results for pyrethroid under both field and laboratory conditions although the direction and degree of enantioselectivity were not always predictable. Some enantioselective degradation (or enantioselective removal) of OP enantiomers has been observed, however, by Wang et al. (2006). They found that the (+) enantiomer of fenamiphos was degraded faster than the (−) enantiomer in water over a 21day period. Elsewhere it was noted that, in Brazilian soils, a complete switch could occur from an enantiomeric imbalance with a preference for the less toxic (−) enantiomer of ruelene to an exclusively preference for the (+) enantiomer. The switch was attributed to changes in environmental conditions caused by deforestation (Lewis et al. 1999). In the same paper it was reported that a warming of Norwegian soils[2] caused about a quarter of the samples studied to switch from an enrichment of (−) ruelene to one of (+) ruelene. This final observation highlights the significance of climate change and its potential effect on the global fate of chiral pollutants.

1.12 Enantiomeric separation of chiral OP pesticides

The separation of enantiomers depends on the three-point interaction rule proposed by Dalgliesh (1952) and improved by Lochmüller & Souter (1975). The chiral recognition required for such separation can be demonstrated with a vivid model provided by Meyer and Rais (1989) using our own (and someone else's) hands. The thumb (T), forefinger (F) and middle finger (M) on the left (S) and right (R) hands are the analogy. It can be demonstrated (Figure 1.13) that with the use of two fingers only (a two-point interaction) S cannot tell the difference between S and R of another person (or molecule).

[2]Soils were heated in situ, 5°C above ambient temperatures by computer controlled cables within the soil over a period of 7 years (Lewis et al. 1999).

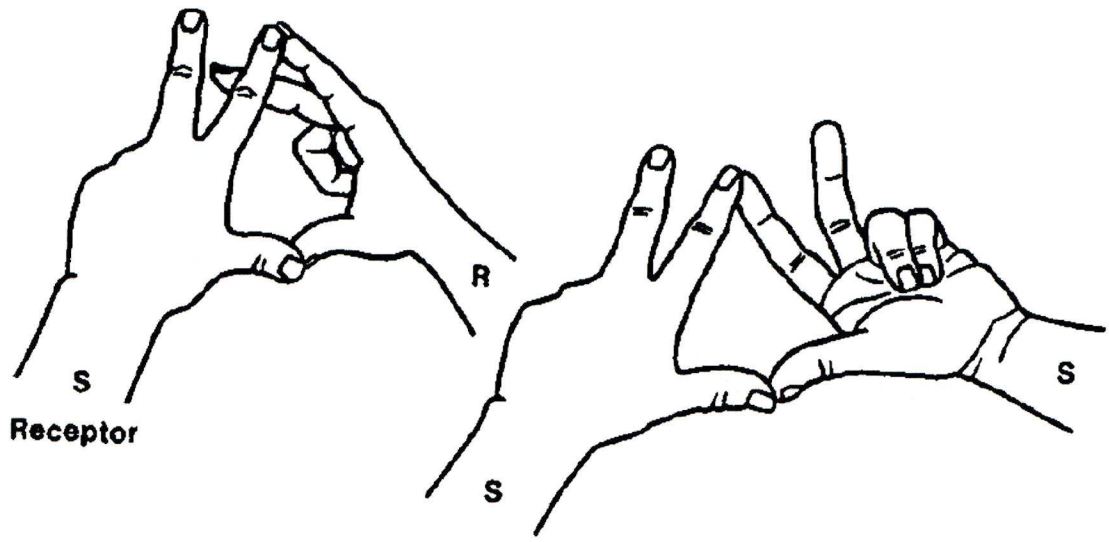

Figure 1.13 Left (S) and right (R) hands demonstrate that a two-point interaction is not sufficient for chiral recognition

In the case of a three-point interaction, however, S can combine with the R of another molecule but can only combine with that molecule's S via a two-point interaction (Figure 1.14). A three-point interaction is more stable than a two-point one and so for this example, in terms of chromatography, R will be retained longer and eluted later.

It is important to note here that the three interactions should be different in nature, e.g., a hydrogen bond, a $\pi - \pi$ interaction and a dipole interaction (Meyer & Rais 1989). Otherwise the sites may become interchanged unintentionally making chiral recognition impossible.

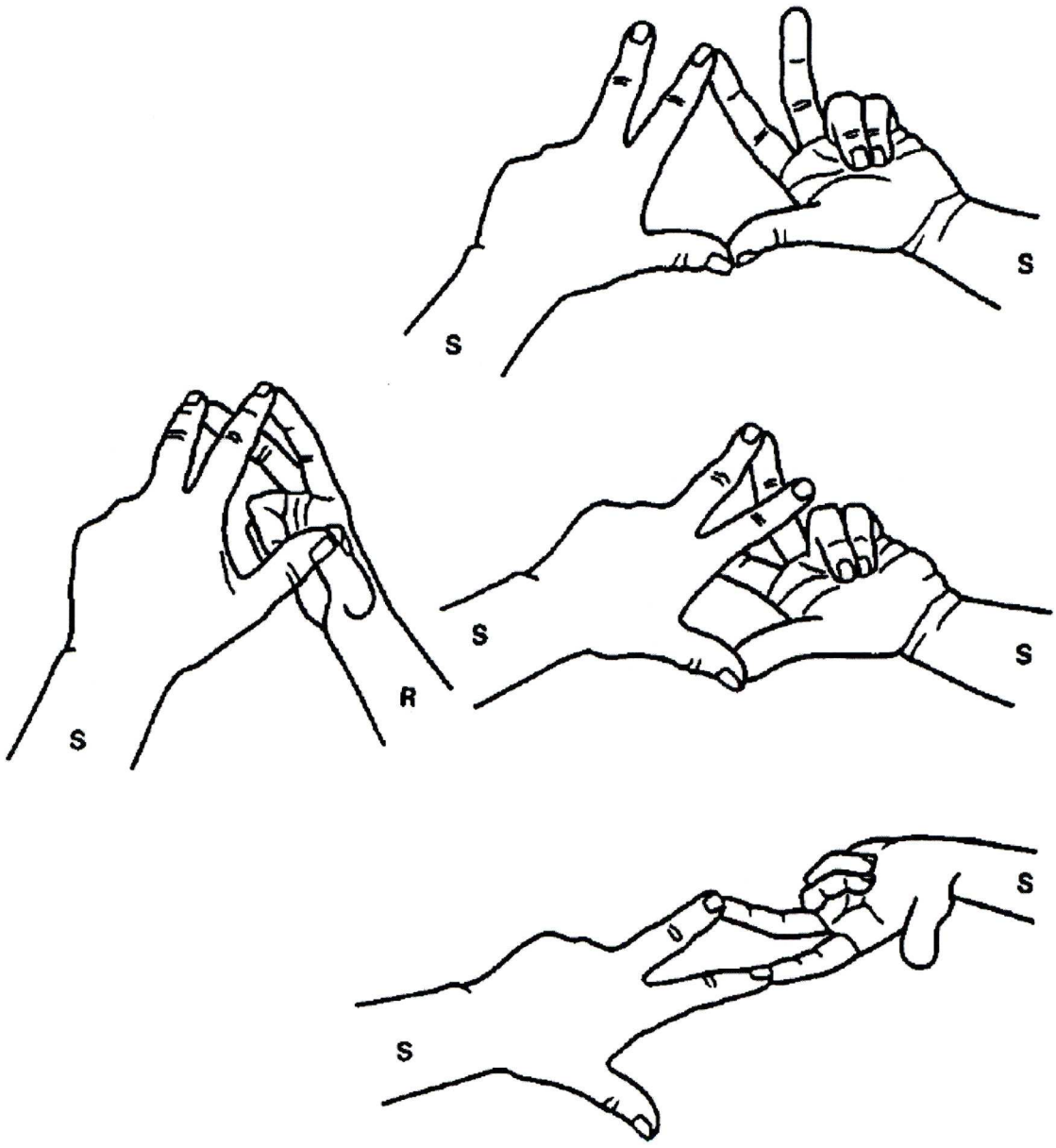

Figure 1.14 Left (S) and right (R) hands demonstrate that a Three-point interaction is sufficient for chiral recognition

Meyer and Rais also point out that one of the three interactions can be repulsive while maintaining chiral recognition. Their work should be consulted for demonstrations of such recognition using the left and right hand model.

The three-point interaction rule for chiral recognition can apply to chromatographic systems where the stationary phase must act as the chiral receptor preferentially retarding elution of one of enantiomers of the target molecule.

Separation of chiral species may also be performed using chiral auxiliary compounds and template surfaces via diastereomeric association complexes. Diastereomers are stereoisomers but are not mirror images of each other and thus do not have the same physical properties. They may occur as a result of a compound having more than one stereogenic centre. A diastereomer can be explained by the interaction of two right-hands verses that of a left-hand and a right-hand: a handshake represents an equal association whereas holding hands represents diastereomeric association. Diastereomeric association complexes can be used to separate the enantiomers of chiral species via crystallisation or chromatography. Diastereomeric complexes also play a large role in chiral recognition by biological receptors (Mannschreck et al. 2007) as well as achiral structures (Davankov et al. 1990; Davankov & Kurganov 1983).

This rule is vital for chiral recognition of enantiomers at the sorbent-sorbate interface and therefore applies to enantiomers of acephate at the surface of a mineral and will be taken into account in Chapter 3 as the adsorption mechanisms for enantioselectivity at mineral surfaces is examined.

1.13 Objectives of this research

The primary objective of this research is to examine, through rigorous experimentation, the molecular interaction between acephate and a variety of synthetic and natural minerals modified by a range of mechanisms. The primary hypothesis is that some achiral mineral surfaces are capable of chiral selection in the form of preferential enantiospecific adsorption. Confirmation of the hypothesis is hoped to be achieved, in the most part, through analysis of a series of batch sorption experiments which evolve over the course of the project based on the light of each set of new results. Furthermore, these batch sorption experiments involving sorbents with a range of modified surfaces are designed to give insight into the mechanistic properties of the adsorption process that may, or may not, lead to enantioselectivity.

Chapter 2 will present the methodology and the materials used throughout the investigation in approximately the order in which they occurred.

CHAPTER 2 MATERIALS AND METHODS

This chapter describes the materials and the experimental procedures used to assess the sorptive behaviour of selected OP pesticides at a variety of mineral surfaces. The materials and reagents are listed along with their relevant properties followed by a description of the experimental procedures carried out on this project. The operating conditions, method reproducibility and instrument calibrations for procedures detecting and separating the enantiomers of the selected pesticides using gas chromatography (GC) and high performance liquid chromatography (HPLC) are also outlined. GC was the instrument of choice for the majority of the work completed due to its sensitivity and high separation power. A major drawback to GC is that analytes need to be suitably volatile in order to be carried in the gas phase. This demands derivatization of many analytes in order to increase the vapour pressure sufficiently to facilitate vaporization. However, the vapour pressure for the chiral organophosphorus chemicals used in this work are all sufficiently high as not to require this step thus eliminating the chief disadvantage of GC analysis.

2.1 Chemicals and Materials

A list of reagents used in all experimental procedures including their chemical formula, purity and supplier is presented in Table 2.1. Milli-Q water (18.2 μΩ-cm resistivity; Milli-Q Gradient, Millipore) was used for the preparation of aqueous solutions.

Table 2.1 List of reagents used in the experimental work

Reagent	Chemical Formula	Purity	Supplier
Acetone	$(CH_3)_2CO$	HPLC-grade	Fisher Scientific (Loughborough, Leicestershire, UK)
Acetonitrile (ACN)	CH_3CN	HPLC-grade	Fisher Scientific (Loughborough, Leicestershire, UK)
Chlorotrimethylsilane (TCMS)	$(CH_3)_3SiCl$	≥99%	Sigma Aldrich (Gillingham, UK)
Cupric acetate	$Cu(CO_2CH_3)_2$	≥98.0% anhydrous	Fluka (Buchs, Switzerland)

Cupric Chloride	$CuCl_2$	97%	Sigma Aldrich (Gillingham, UK)
Cupric sulphate 5-hydrate	$CuSO_4.5H_2O$	AnalaR grade	BDH (Poole, England)
Dichloromethane (DCM)	CH_2Cl_2	HPLC-grade	Fisher Scientific (Loughborough, Leicestershire, UK)
Ethylenediamine	$C_2H_4(NH_2)_2$	99%	Fisher Scientific (Loughborough, Leicestershire, UK)
Hydrochloric acid (35.4%v/v)	HCl	AnalaR grade	BDH (Poole, England)
Methanol	CH_3OH	HPLC-grade	Fisher Scientific (Loughborough, Leicestershire, UK)
n-Hexane	C_6H_{14}	HPLC-grade	Fisher Scientific (Loughborough, Leicestershire, UK)
Sodium hydroxide	NaOH	HPLC-grade Bioreagent	Fisher Scientific (Loughborough, Leicestershire, UK)
Tetrahydrofuran (THF)	$(CH_2)_4O$	>99.5+% (HPLC)	Fisher Scientific (Loughborough, Leicestershire, UK)

2.1.1 Clays and Powdered Minerals

Silica and aluminosilicate minerals were obtained from Sigma-Aldrich with the exception of bentonite SWy-2 which was ordered from the Source Clay Repository, Indiana, USA. Silica and aluminosilicate minerals used as sorbents in all batch sorption experiments are detailed in Table 2.2.

Table 2.2 Physical chemical characteristics of powdered minerals

Mineral	Structural Formula	Surface Area (m^2/g)	Other Properties
Montmorillonite K10	$M_{0.33}^{+}(AlMg)Si_4O_{10}(OH)_2.nH_2O$ [b]	220-270	Off-white powder pH=2.5-3.5
Kaolinite	$Al_2Si_2O_5(OH)_4$	14.3 [a]	Off-white powder pH=3.5-5 (20% in water) 0.1-4μm particle size
Montmorillonite KSF (K-catalyst)	Contains 5% sulphuric acid	20-40	Off-white to beige powder. pH=1-2
Quartz Sand [c]	SiO_2	0.0563 [a]	Off-white to beige granules. ~ 50-70 mesh particle size. >6 μm
Aluminium Oxide	Al_2O_3		White granules
Bentonite SWy-2 [d]	$(Ca_{0.12}Na_{0.32}K_{0.05})$ $[Al_{3.01}Fe(III)_{0.41}Mn_{0.01}Mg_{0.54}$ $Ti_{0.02}][Si_{7.98}Al_{0.02}]O_{20}(OH)_4$ [e]	31.82 +/- 0.22 [f]	Beige to grey powder pH=8.5-9.5

[a] Surface area determined by BET analysis on a Micromeritics ASAP 2000analyzer
[b] M^+ in the natural material includes one or more cations such as Na^+, K^+, Mg^{2+}, and Ca^{2+}[c]Purchased from Sigma Aldrich and ground to 50-70 mesh particle size
[d] Purchased from the Source Clays Repository, Chantilly, Virginia
[e] Data from the Source Clays Repository, Chantilly, Virginia
[f] Surface area obtained from Source Clays Physical Data Sheet

2.1.1.1 Montmorillonite K10

Montmorillonite K10 is an acidic clay catalyst. It is prepared via the calcination and acidification of the natural montmorillonite discussed in Chapter 1. Montmorillonite K10 is a Brönsted and Lewis acidic catalyst and can be modified easily by exchanging its interlayer cations with a host of other cations including Ca, Na, Cu, Zn and even heavier metal cations such as Hg. Montmorillonite K10 can also be pillared, generally by using metal oxide complexes to increase the basal spacing between the clays platelets. These are stable at high temperatures and give the clay a greater capacity for sorption making it more efficient as a catalyst or agent for contaminant removal (Valverde et al. 2003).

The composition of the Montmorillonite K10 was determined by XRD analysis by Dr. Steve Crowley of the University of Liverpool Earth and Ocean Sciences Department:

For XRD analysis, approximately 10 g of dry K-10 was transferred to a glass beaker and hydrated for 48 h in 100 mL of distilled water. The component particles were then suspended by gentle stirring with a glass rod and separated by ultrasonic dispersion for a period of 15 min. The dispersed particles were then size separated to produce <2 μm, 2-20 μm and >20 μm fractions (equivalent spherical diameter) using standard particle size separation techniques (gravity settling and centrifugation). The resultant size fractions were suspended in distilled water and quickly frozen with liquid nitrogen prior to removal of water by freeze-drying. Once dry, each size fraction was allowed to equilibrate (24 h) at ambient temperature (~ 20°C) and humidity (~ 30 % relative humidity) and then transferred to a side-loading aluminium cavity mount to produce a randomly orientated sample. Such samples were analysed in step scan mode from 3 to 65°2θ with step increments of 0.02°2θ and a counting time of 2 seconds per step using a Siemens 500D X-ray diffractometer (fitted with a graphite monochromator, 1°divergence and anti-scatter slits, 0.15° detector slit), and Cu Kα (λ= 1.5419 Å) radiation generated at 40 kV and 30 mA.

The overall composition (%) of Montmorillonite K10, as supplied, was found to be 56.0 % smectite, 29.0 % quartz and 15.0 % muscovite.

2.1.1.2 Bentonite SWy-2

Bentonite are predominantly used in the drilling industry where it is an important component of drilling mud used to cool the drill bit and remove waste material from the well bore. However, it is also employed as a sealant for subsurface disposal systems for spent nuclear fuel, as a component of cement, in adhesives, cat litter and as an alternative medicine. Bentonite SWy-2 is an impure 2:1 layered clay made up predominantly of montmorillonite. There are several types of bentonite, named after a dominant cation such as potassium, sodium, calcium or aluminium. Swy2 is a sodium dominated bentonite (Mermut & Cano 2001) originating from the Newcastle formation in the American State of Wyoming and as such is often referred to as 'Wyoming bentonite'. The stock sample was originally collected in 1972 from which

working samples are now taken. The source clays repository lists its chemical composition (%) as follows: SiO_2: 62.9, Al_2O_3: 19.6, TiO_2: 0.090, Fe_2O_3:3.35, FeO: 0.32, MnO: 0.006, MgO: 3.05, CaO: 1.68, Na_2O: 1.53, K_2O: 0.53,F: 0.111, P_2O_5: 0.049, S: 0.05 (Mermut & Cano 2001).Its cation exchange capacity was determined by Borden and Giese (2001) and found to be 76.4 meq/100 g with the principal exchange cations being sodium and calcium. The mean layer charge was calculated by Mermut & Lagely (2001) as having a charge of ~ 0.30, the unit of which, $(Si,Al)_4O_{10}$ (eq/mol),was calculated from the charge distribution. Finally, the surface area was found to be 31.82 +/- 0.22 m^2/g (Source Clays Repository, Chantilly, Virginia).

2.1.1.3 Deep-sea sediments

Deep sea sediments were collected on research expedition JC027 in August 2008 from surface sediment at 4000-5000m depth along a North – South transect off the North-African Atlantic coast. Specific coordinates are given in Table 2.3.

Table 2.3 JC027 station numbers and geographical positions

Core number	Date - time	Latitude	Longitude	Water depth (m)
JC027-25-2	16/08/08 – 07:34	35°44.75'N	09°59.27'W	4633
JC027-43	22/08/08 – 18:10	38°21.66'N	09°59.08'W	4572
JC027-45	23/08/08 – 14:09	38°23.18'N	10°24.13'W	4835

The sediments were collected using a Mega-Corer (Figure 2.1) deployed from the side of RSS James Cook. This method retrieves a core of approximately 50 cm in depth and 15 cm in diameter by means of a number of 10 cm diameter Perspex cylinders. The mega-corer is hydraulically dampened at the sea floor so as not to disturb the surface sediments. Only surface sediments were required for contaminant analysis as sedimentation rates in the deep sea are only in the order 3 mm per thousand years (Edward D. Goldberg & John J. Griffin 1964) meaning man-made contaminants are unlikely to be found below a few millimetres. However, influences such as bioturbation can result in redistribution of material and so the upper five centimetres of each core were taken by slicing each core into 1 cm sections, using a large metal spatula. The sections were frozen (-20°C) prior to analysis.

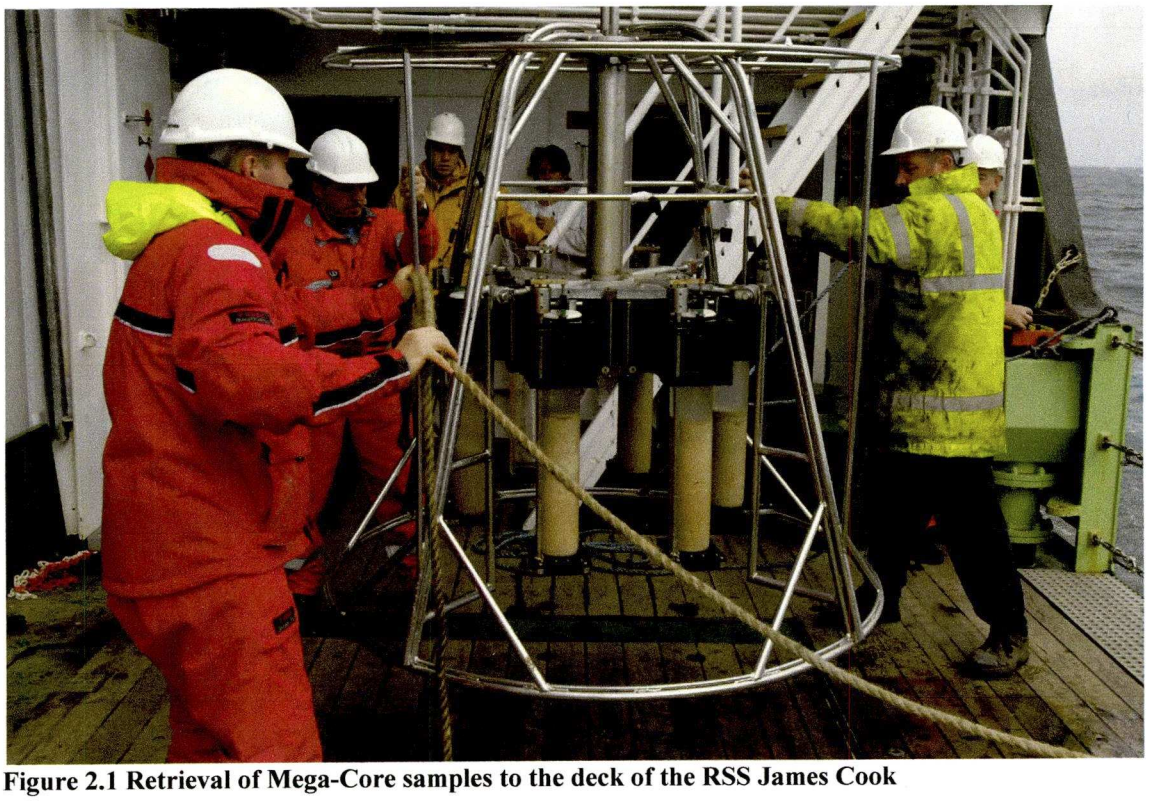

Figure 2.1 Retrieval of Mega-Core samples to the deck of the RSS James Cook

2.2 Glassware Cleaning Protocol

The majority of glassware was cleaned by soaking in the surface active cleaning agent Decon 90 (Decon Laboratories, Sussex, UK) for a minimum of 12 h before being rinsed extensively with tap water and MilliQ water respectively. The glassware was then dried in a drying oven set at 30-50 °C until all moisture had evaporated. Other glassware including Pasteur pipettes and 1.5 mL and 7 mL clear glass vials was wrapped in aluminium foil and heated to 400°C for 4 hours in a muffle furnace in order to remove unwanted organic purities. Plastic 2 mL centrifuge tubes were cleaned by immersion in methanol for 30 s, and subsequently air dried for several hours. An exhaustive list of all glassware and consumables used is presented in Table 2.4.

Table 2.4 List of glassware and consumables used throughout research with type of cleaning procedure employed

Glassware/consumable	Cleaning technique
Glass beaker (250 mL)	Washed in Decon 90 – dried at 30 – 50 °C
Volumetric flask(varying capacity)	Washed in Decon 90 – air dried
Pasteur pipette	Pyrolysed (400 °C) – one use only
Glass vial – small (2 mL)	Pyrolysed (400 °C) – one use only
Glass vial – large (7 mL)	Pyrolysed (400 °C) – one use only
Polypropylene centrifuge vials (2 mL)	Immersion in MeOH for 30 s – air dried
Polypropylene centrifuge bottles (35mL)	Washed in Decon 90 – dried at 30 – 50 °C
Syringes (50 - 500 µL)	Rinsed in DCM or ACN
Metal spatula	Washed in Decon 90 – dried at 30 – 50 °C
polypropylene petri dishes	Untreated – one use only
Aluminium foil	Pyrolysed (400 °C) – one use only

2.3 Preparation of Clays and Powdered Minerals

2.3.1 Montmorillonite K10, Kaolinite, Aluminium Oxide, Bentonite from Sigma Aldridge and Bentonite SWy-2

Each material was prepared by heating to 400°C for a period of 24h (unless otherwise stated) to ensure the lack of biotic processes such as enzyme and bacterial activities and stored separately in the dark in foil sealed glass jars. This form of pre-treatment will not, however, remove humic substances such as fulvic and humic acid. In fact, there is evidence to suggest that small changes in EF of chiral compounds can occur as a result of interaction with humic acid (Oravec et al. 2010). Nonetheless there is very little work supporting these claims at this stage and, although an interesting avenue for further work it, the idea is not considered any further in this work.

2.3.2 Separation of the 2 μm Fraction

For each of Bentonite (Sigma Aldrich), Bentonite SWy-2 and Montmorillonite K10, a <2 μm fraction counterpart was also prepared:

100 g of each were suspended in DI water and the two bentonites were sonicated for 2 h in order to achieve sufficient dispersion. The suspension was then centrifuged at 850 rpm for five minutes which, according to Stokes Law (Equation 2.1), is sufficient for particles larger than 2 μm to settle.

$$F_d = 6\pi \mu R V \qquad \text{(Equation 2.1)}$$

Where F_d is the frictional force acting on the interface between the fluid and the particle (N), μ is the fluids viscosity (kg m^{-1} s^{-1}), R is the radius of the spherical object (m) and V is the particle's velocity (m s^{-1}). The settled material was discarded and the supernatant retrieved. This procedure was repeated until the supernatant contained no visible suspension. The large amount of supernatant was extracted, pooled and forced to flocculate by the addition of 20 mL of 1M NaCl and the clear supernatant discarded (in some cases further centrifugation may be required). There was also a significant ultra-fine component in suspension that is almost impossible to settle out; this material was problematic while using GC analysis as it contaminates syringes, inlet systems and the chiral column. Subsequently, to prevent damage to the equipment and the compromising of chromatographic traces, the <0.5 μm was also

removed by centrifuging at 3200 rpm for six minutes before discarding the supernatant. The resultant material was re-suspended in fresh DI water and centrifuged several more times as a cleaning process. It is important to remember that the separation obtained is an approximation as Stoke's Law assumes spherical objects whereas clays such as these will exist in flat shards of material varying in size from one or two to a few hundred unit layers.

2.3.3 Deep-sea Sediments

The top 1 cm samples from each station were individually homogenised with a pestle and mortar before pyrolysation at 400°C to remove organic content. They were then freeze-dried in a Heto PowerDry LL3000 freeze drying unit with a Thermosarant ValuPump VLP200 ready for use in a batch sorption experiments. The same samples were also extracted for the detection of Water Soluble Organic Content (WSOC) by Oritsejolomi Etuwewe of the University of Liverpool using the following method:

Dissolution was carried out in MilliQ water before extraction by sonication for 1 h. The mixture was then ionised to pH 1 before back extraction into DCM, rotary evaporation and drying of the extract with sodium sulphate. Evaporation to dryness was then exacted under nitrogen gas. Finally, the extract was derivatised at 70°C for 45 min.

Additionally, all the samples were sent for elemental analysis (CN) by Sabena Blackbird of the University of Liverpool.

2.3.4 Copper-exchanged Montmorillonite K10

0.607g of copper (II) acetate was mixed with 1g of montmorillonite in 25 mL of MilliQ water (Ratio of components from Tsvetkov & Mingelgrin 1987a). The pH of the solution was recorded and altered to 8 (approximately that of average seawater) using acetic acid and sodium hydroxide. The same pH adjustment was applied to all subsequent montmorillonite K10 and bentonite SWy-2 modifications unless otherwise stated. The mixture was then agitated for 48 h using a rotary tumbler. After being centrifuged and washed until blue colouring of the supernatant disappeared, the remaining material was freeze dried.

2.3.5 Copper-lysine-exchanged Montmorillonite K10

Copper-lysine-exchanged montmorillonite was prepared for use in batch sorption experiments with acephate to give insight into how the presence of a chiral body at active reaction sites affects chiral recognition. The procedure used was adapted from Tsvetkov and Mingelgrin (1987b):

Cu-L-lysine solution was prepared by mixing 0.182 g of Copper (II) acetate and 0.439 g of L-lysine in 25 mL of MilliQ (40 mM $Cu(CH_3COO)_2$: 120 mM L-lysine. The Cu-L-lysine-montmorillonite complex was then prepared by suspending 1 g of pyrolysed (400°C) montmorillonite in the Cu-L-lysine complex at a 1:25 clay (g) to solution (ml) ratio. The mixture was then agitated for 48 h using a rotary tumbler. After being centrifuged and washed until the blue colouring of the supernatant was discharged the complex was freeze dried.

The same procedure was used for preparation of Cu-D-lysine-montmorillonite.

A Cu-L-lysine-montmorillonite complex was also prepared with increased amounts of Cu-L-lysine complex so as to ensure that all active reaction sites were saturated. The above procedure was followed with the same clay : solution ratio but with revised ingredient amounts;

- 1 g of Montmorillonite
- 0.607 g of copper (II) acephate
- 1.462 g of L-lysine
- 25 mL of MilliQ water

2.3.6 Silanisation of Montmorillonite K10

The montmorillonite was derivatised in order to cap hydroxyl groups and thus removing these active species from the adsorption process. The following procedure was adapted from Zhang et al. (2006):

A portion of pyrolysed montmorillonite K10 (10 g)was placed in a 500 ml three-neck round bottom flask containing 300 mL of anhydrous acetone. The mixture was further dried using 2 spatula measures of sodium sulphate and left for 12 h. The system was stirred under nitrogen gas for 20 min before the addition of a 50 mL aliquot of trimethylchlorosilane was added to the suspension and the system was gently refluxed (72 h). The product was collected by filtration, washed with acetone,

then with acetone/H_2O (50:50). After drying at 80 °C for 12 h, the silanised clay was ground to a powder. Enough material for the batch sorption experiments (described later in the chapter) was dispersed in a saturated saline solution for 24 h to remove the ammonium ions; the same process was repeated three times. It was then filtered, air-dried and ground to a powder again ready for use in batch sorption experiments.

2.3.7 Amino acid-exchanged Bentonite SWy-2

A variety of complexes were prepared with amino acids (AAs) and bentonite SWy-2 to assess the consequences of different species occupying active sites on the clay surfaces. The L and D forms of lysine and alanine were used along with the non-chiral glycine according to the following procedure:

The chosen AA and the non-exchanged, pyrolysed (400°C) bentonite SWy-2 (amounts listed in Table 2.5.) was combined with MilliQ water (25 mL) at a ratio of 1:25 clay (g) to solution (mL) ratio. The suspension was then mechanically agitated for 48 h and centrifuged at 5000 rpm for 30 min. Finally, it was washed five times to dispel excess reagent and freeze-dried for 24 h.

Table 2.5 Quantities of AAs and bentonite SWy-2 used in the preparation of the AA-exchanged bentonite SWy-2

AA	AA used (mg)	Bentonite SWy-2 used (mg)
L-lysine (or D-lysine)	365 [a]	1000
L-alanine (or D-alanine)	223 [a]	1000
Glycine	188	1000

[a]In the case of the chiral AAs, a racemic mixture was also prepared by combining the enantiomers in equal proportions up to the amount listed here.

Additionally, bentonite SWy-2 was prepared following the same procedure, but without any complexing reagents, to act as a blank for batch sorption experiments.

2.3.8 Activated Copper

Activated copper, often referred to as 'spongy copper', was prepared in order to investigate the effect on chiral recognition of copper alone. The procedure was adapted from Blumer (1957). Cupric sulphate (45g) was dissolved in MilliQ water (500mL) and acidified with the addition of 2M hydrochloric acid (20mL). Zinc slurry (15g pure zinc in 25mL MilliQ water) was then added *very* slowly over a 20 min

period with rapid stirring until precipitated copper turned from red to brown and the supernatant became colourless. The supernatant was then removed and the precipitate thoroughly washed with MilliQ until neutral pH was achieved. Further washing was then required using methanol then dichloromethane. A batch of activated copper was also prepared with the addition of L-Lysine (500 mg) at the same stage as the cupric sulphate in an attempt to form an activated L-lysine-copper complex. The precipitates were kept frozen until needed.

2.3.9 Initial pH Determination

In the case of all clays and powdered minerals, 5 g were combined in separate sterile plastic bottles with 30 mL of MilliQ water and shaken sufficiently to ensure complete hydration. These were used to determine the initial pH of each material. Table 2.6 lists these materials with their corresponding pH values.

Table 2.6 List of clays and powdered minerals used and their corresponding initial pH values (in aqueous suspension)

Clay or mineral powder	Initial pH (in aqueous suspension)
Montmorillonite K10	3-4
Kaolinite	4-5
Aluminium oxide	6-8
Quartz	2-3
Bentonite SWy-2	8-9
Deep-sea sediments	-
Cu-exchanged montmorillonite K10	3-4
Cu-lysine-exchanged montmorillonite K10	8-9
Silanised montmorillonite K10	-
Lysine-exchanged bentonite SWy-2	8-9
Alanine-exchanged bentonite SWy-2	8-9
Glycine-exchanged bentonite SWy-2	8-9

2.4 Preparation of Organophosphorus Pesticides and Aqueous Solutions

The organophosphorus pesticide, acephate, was used in all batch sorption experiments. It was purchased from Sigma Aldrich in its pure crystallized state and kept at -20°C. Typically, a stock solution of 100 mg/L was made up in the following manner. 10 mg of pure acephate was weighed on a microbalance (sensitive to 100 ng) and deposited in a clean 100 mL capacity volumetric flask. The solution was then made up to volume using freshly filtered MilliQ water and kept refrigerated ready for use. Freshly made stock solution such as this was kept for a maximum of one week and discarded if not completely used in this time so as to reduce risk of contamination and/or chemical alteration of the reagent. Internal standards were not used for fear of interaction with sorbent or sorbate, directly or indirectly.

2.5 Experimental Procedures and Apparatus

2.5.1 Cation Exchange Capacity (CEC) Determination

Montmorillonite K10 was not supplied with values for the CEC nor were they available in the literature. Thus, they were determined here using a method adapted from (F. Bergaya & Vayer 1997). The procedure consists of a single-step using copper ethylenediamine ($Cu(EDA)_2^{2+}$) releasing copper ions as the $(EDA)_2^{2+}$binds

with the undetermined cations present in the clay interlayer. The CEC can then be obtained by the difference in concentration of the copper in the initial and final solutions as determined by atomic absorption spectroscopy (AAS).

The $Cu(EDA)_2^{2+}$ complex was prepared mixing1 M copper (II) chlorideand1 M ethylenediamine at a ratio of 1:2 with a slight excess of the latter to ensure complete formation of the complex.The complex was made up to volume (25 mL) to give a concentration of 0.05 M and the pH of the intensely blue solution was measured at 6.3. In this case, known volumes (1 to 5 mL) of the 0.05 M $Cu(EDA)_2^{2+}$ solution are diluted with water to 25 mL (resulting in standards of 0.05, 0.04, 0.03, 0.02 and 0.01M). The solutions were then run on AAS to create a calibration (Figure 2.2.) plot for the determination of the $Cu(EDA)_2^{2+}$concentration in subsequent samples.

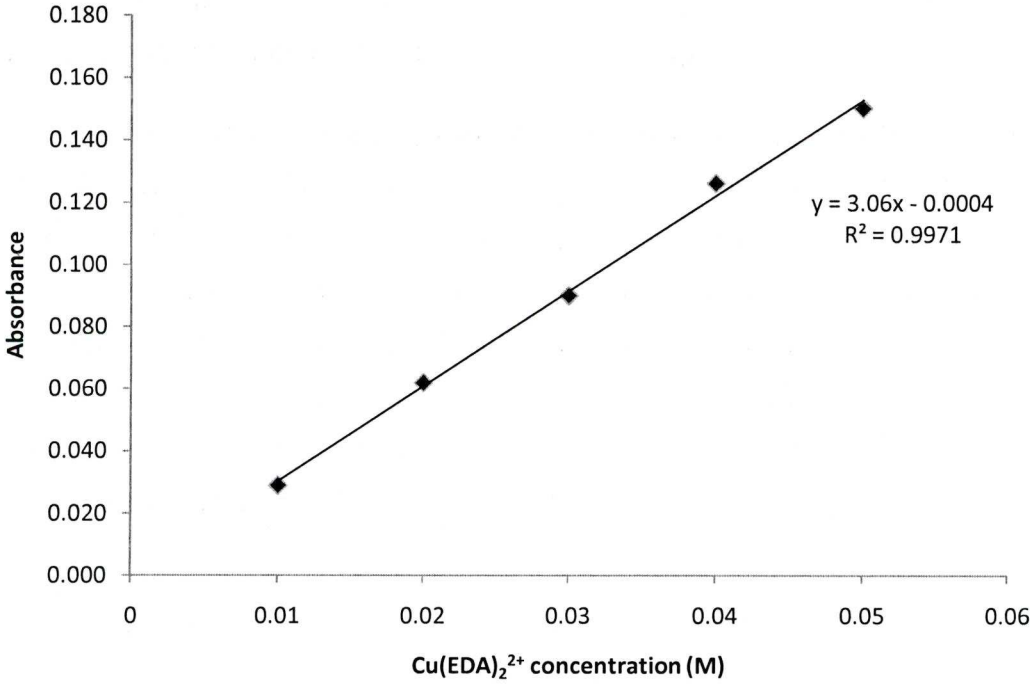

Figure 2.2 AAS calibration for the determination of $Cu(EDA)_2^{2+}$concentration

0.05 M $Cu(EDA)_2^{2+}$ was then added to 0.5 g of clay sample (with unknown CEC) in a centrifuge tube, agitated for 30 min and centrifuged allowing the concentration of the $Cu(EDA)_2^{2+}$ remaining in the supernatants to be determined. The CEC could then be determined for the clay modifications listed in Table 2.7.

Table 2.7 Clay modifications prepared for CEC determination

Abbreviation	Basic Mineral	Modification
M	Montmorillonite K10	Unheated
M105	Montmorillonite K10	Heated to 105°C
M400	Montmorillonite K10	Heated to 400°C
B	Bentonite SWy-2	Unheated
B105	Bentonite SWy-2	Heated to 105°C

2.5.2 Batch Sorption Experiments

Batch sorption experiments were used to generate the majority of data to be used in this work. A typical batch sorption experiment involved a variety of mineral amounts ranging from 5 mg to 500 mg. These were each combined with an aliquot of chiral organophosphorus compound at constant concentration and agitated by means of end-over-end shaker or a clamp shaker usually for a period of 48 h (enough for the components of the suspension to equilibrate). The samples were then centrifuged in order to isolate the supernatant, of which 100 µL was removed and prepared for GC analysis. A blank was simultaneously prepared without the presence of clay and subjected to identical conditions throughout. Table 2.8 lists the variables for batch sorption experiments adhering to the above generic recipe.

Table 2.8 Variables for selected batch sorption experiments

Sorbate	Sorbent	Conc. of sorbate (mg/L)	Vol. of sorbate (mL)	Amounts of sorbent (mg)	Solvent
Acephate	Montmorillonite K10	81.54	0.5	0, 5, 10, 20, 50	ACN
Acephate	Quartz	104.3	0.75	0, 50, 100, 200, 500	ACN
Acephate	Aluminium Oxide	104.3	0.75	0, 10, 20, 50, 100, 200	ACN
Acephate	Kaolinite	104.3	0.75	0, 10, 20, 50, 100, 200	ACN
Acephate	Copper-exchanged montmorillonite K10	100.8	0.75	0, 10, 20, 50	MilliQ
Acephate	All amino acid-modified montmorillonite K10s	100.8	0.75	0, 10, 20, 50	MilliQ
Acephate	Silanised montmorillonite K10	100.8	0.75	0, 10, 20, 50	MilliQ
acephate	Deep-sea sediments	100.3	1.00	0, 50, 100, 200	MilliQ

The following procedures align to the initial generic recipe unless otherwise stated.

2.5.2.1 Acephate and Bentonite SWy-2 at varied pH

500 mg bentonite SWy-2 (unmodified) was weighed in to five 35 mL polycarbonate centrifuge vials. 25 mL of acephate solution (100.4 mg/L) in MilliQ was then added to each vial and the pH altered to 11, 9, 7, 5 and 3 using hydrochloric acid and

sodium hydroxide solutions. Suspensions were equilibrated for 48 hr at 25°C and 700 rpm by planar agitation. They were then centrifuged at 10,000 rpm for 30 min and 200 µL of the supernatant removed in quintuplicate from each vial.

2.5.2.2 Acephate and Amino Acid-Modified Bentonite SWy-2

50 mg samples of the each complex (including a blank SWy-2 bentonite prepared identically to the rest of the complexes but with MilliQ water only) were added to 2mL solutions of racemic acephate (100.9 mg/L) in MilliQ water. A blank containing only the racemic acephate was also prepared. The resulting suspensions were equilibrated while agitating for 48 hr at 25°C then centrifuged. 200 µL of the supernatant was removed for GC analysis after 30 min of centrifugation at 10,000 rpm.

2.5.2.3 Effect of Acephate Concentration on Bentonite SWy-2 Basal Spacing

100 mg of bentonite SWy-2 (<2µm fraction) was weighed into five 12 mL plastic Sterillin vials with 10 mL acephate in MilliQ water at concentrations of 50, 100, 200, 500, 1000 mg/L. They were then equilibrated with a planar agitator and pumped through a micropore filter and dried for 30 min at 60°C. The partially dried disc of clay was then mounted onto a slide ready for XRD analysis. Such analysis was carried out by Dr. Steve Crowley of the University of Liverpool[3].

2.5.2.4 Initial enantiomeric excess experiment

A basic batch sorption experiment was set up with variations to determine whether an initial enantiomeric excess an acephate solution will affect the extent of selective sorption seen at the Montmorillonite K10 surface.100 mL of acephate in MilliQ water (500mg/L) was added to 500 mg of montmorillonite K10 and equilibrated for 48 h. The supernatant was then used as the acephate containing solution for a repeat of the same procedure. The cycle is repeated four times.

2.5.2.5 Acephate and activated copper precipitate

500 mg of the activated copper and 500 mg of the activated L-lysine-copper complex were weighed in to separate 7 mL vials with 2 mL acephate (100 mg/L) in aqueous

[3] Conditions: Step scan mode from 3 to 65°2θ with step increments of 0.02°2θ and a counting time of 2 seconds per step using a Siemens 500D X-ray diffractometer (fitted with a graphite monochromator, 1°divergence and anti-scatter slits, 0.15° detector slit), and Cu Kα (λ= 1.5419 Å) radiation generated at 40 kV and 30 mA.

solution added to each vial. A blank of aqueous acephate solution only (100 mg/L) was also prepared The batches were then equilibrated through agitation for 72 h and the supernatant removed after centrifugation for 15 min at 3000 rpm. The remaining precipitate was weighed to determine total copper content. The batches were prepared in quintuplicate.

2.5.2.6 Temperature Modifications

It has been suggested (Reddy et al. 2009) that heating of 2:1 clays to high temperatures can lead to collapse of the interlayer as the water is driven out. As well as significantly affecting the sorptive capabilities of clay it may give insight into where enantioselective sorption might be happening. Consequently, a series of simple batch sorption experiments were carried out involving acephate and clays subjected to temperatures of 400°C, 105°C and room temperature (25°C).

2.5.2.7 Determination of Vial Wall influences

In the case of pyrethroids, vial wall sorption can provide significant interference (J. L. Zhou et al. 1995). Consequently, a simple experiment was set up to determine the influences of the vial wall on sorption and enantioselectivity for acephate at the mineral surface. Acephate in aqueous solution was placed in three polypropylene vials and three glass vials. 100 µL was then removed for GC analysis immediately, after 24 h and after 48 h respectively. The experiment was carried out in quintuplicate.

2.5.3 Scanning Electron Microscope (SEM) Images and spectra

A Philips XL30 SEM was used to produce secondary (SE) images of a selection of modified montmorillonites. The modifications were all made using montmorillonite K10 and are listed in Table 2.10.

Table 2.9 List of montmorillonite K10 clays modified for SEM analysis

Montmorillonite K10 modification/treatment	Codename for analysis
Acid washed	ACID
Copper-exchanged ($CuSO_4$),	CU
Sodium-exchanged (NaCl)	NACL
Pyrolysis + sodium-exchanged (NaCl)	NAPYRO
Pyrolysis	PYRO

The samples were mounted on 12.5mm aluminium stubs and coated with gold/palladium using a sputter coater. The images were taken using a 20kV electron beam emitted from a tungsten filament. The spot size was 5.5 (beam area) with a working distance of about 13mm.

Energy dispersive x-ray spectroscopy was used to determine the elemental make up of the sample with an Oxford Instruments ISIS system.

2.6 Chromatographic Methods

2.6.1 Gas Chromatography

GC is a technique that can be used to separate organic compounds that are volatile. A gas chromatograph consists of a flowing mobile phase, an injection port, a separation column containing the stationary phase, a detector, and a data recording system. The organic compounds are separated due to differences in their partitioning behaviour between the mobile gas phase and the stationary phase in the column. Mobile phases are generally inert gases such as helium, argon, or nitrogen. The injection port consists of a rubber septum through which a syringe needle is inserted to inject the sample. The injection port is maintained at a higher temperature than the boiling point of the least volatile component in the sample mixture. Since the partitioning behaviour is dependent on temperature, the separation column is usually contained in a thermostat-controlled oven. Separating components with a wide range of boiling points is accomplished by starting at a low oven temperature and increasing the temperature over time to elute the high-boiling point components.

GC is frequently used for the chromatographic resolution of environmental pollutants and has been for half a century (Bennett et al. 1958; West et al. 1959; Levadie & Harwood 1960; Rushing 1958). Furthermore, enantiomeric resolution of chiral species on GC has been in operation for several decades (König et al. 1988; Pirkle et al. 1980; Gassmann 1981) including the first separation of enantiomers on a capillary column using gas chromatography by Emanuel Gil-Av (1966). The application to chiral environmental pollutants dates to the early 1990s (König et al. 1991; Buser & Mueller 1994; Buser & Mueller 1995; Huhnerfuss et al. 1992; Hühnerfuss & Kallenborn 1992; Hühnerfuss et al. 1993). Despite the emergence of several alternative techniques (e.g. liquid chromatography (LC) and capillary electrophoresis (CE)) for the enantiomeric resolution of chiral pollutants, GC still maintains its status in this field. GC remains useful, largely because the relative peak area of the analyte can be determined with such high precision. Additionally, Ridal et al. (1997) made the point that variations in recovery rates do not affect the determination of the enantiomeric ratio (ER) or enantiomeric fraction (EF) values whereas the precision in measuring absolute concentrations of trace organics can vary greatly. As such, GC has been used almost exclusively for the resolution and quantification of chiral organophosphorus enantiomers throughout this work.

The majority of analyses were conducted on a Hewlett-Packard HP 5980 series II gas chromatograph equipped with a capillary column with a cyclodextrin stationary phase (CYCLOSIL-B) of dimensions 25 m, 0.25 mm I.D., 0.25 μm film thickness purchased from J & W Scientific, UK. In some early analyses the GC was coupled with a flame ionisation detector (FID) but an electron capture detector (ECD) was soon found to give improved sensitivity. GC analysis throughout this work has been almost exclusively focussed on the detection of acephate in various solvents. GC-ECD is frequently used in the detection of organochlorine (OC) compounds due to its high sensitivity, excellent separation efficiency and speed of analysis (Garrido Frenich et al. 2003).With run times of less than 30 minutes and complete resolution of both enantiomers without the need for a derivatization step, as well as the ready availability of the instruments in the laboratory, GC-ECD became the method of choice for the resolution and detection of acephate.

Batch sorption experiments had largely been carried out in aqueous solution in order to give some comparability with interactions in the environmental conditions.

However, the low volatility of water and its incompatibility with a capillary column or an ECD means the analytes had to be dissolved in acetonitrile (ACN). This involved evaporating the water at an accelerated rate under nitrogen gas leaving the analyte dry and then redissolving in the same volume of ACN.

Chromatographic conditions were developed over the course of the project, with alterations being made to account for new and conditioned columns. Typical conditions for the analysis of acephate were:

1 μL of acephate solution (ACN) is injected into the capillary column through the splitless injection port. The injector was purged for 1 min after the injection is made to avoid overloading of the column. Helium was used as the carrier gas while an argon methane mixture (10% methane) was used as the make-up gas. The initial temperature of column was 80 °C which was maintained for 1 min before increasing at 10°C per min to 158°C. The temperature was then maintained isothermally for a further 21.2 min, a total run time of 30 min. The injector and ECD were set at 220°C and 250°C respectively. These conditions were developed to give the best resolution of enantiomers that could be achieved but with a retention time that was short enough to enable efficiency in overall analysis. An example of a resulting chromatogram for acephate run under these conditions is illustrated in Figure 2.3.

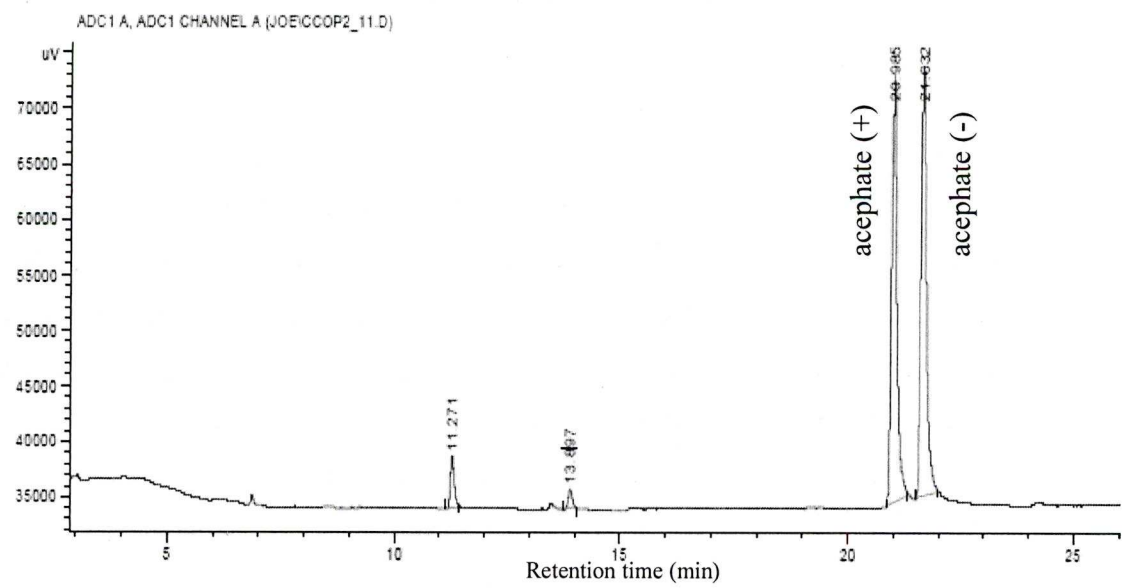

Figure 2.3 Gas chromatogram of acephate enantiomers in ACN (~100 mg/L).

2.6.2 Montmorillonite K10 as a packing material in a high performance liquid Chromatography (HPLC) customised column

As discussed in detail in the previous chapter, there is significant demand for the manufacture of enantiopure chemicals. Although some synthetic fabrication of individual enantiomers does take place in the pharmacological, flavour development and agricultural industries, the vast majority involves production in racemic mixtures. Despite understanding the environmental advantage of enantiopure chemicals, this continues to be true predominantly due to the high cost of enantiopure synthesis on industrial scales. Consequently, demand for cost reducing procedures is strong. In this work it was decided that an experiment would be set up to determine whether the apparent selective behaviour observed between acephate and montmorillonite K10 could be harnessed to begin the development of an enantiopurification technique. The aim was to manufacture an HPLC column packed with montmorillonite K10 serving as the stationary phase to pass a solution of acephate through it and quantify the enantiomeric fraction to see if the ratios had changed. An Agilent 1100 HPLC system with DAD UV-detector was used for preparation of the column and the running of samples.

The preparation of the column involved removal of the packing (silica with C18 stationary phase) in a small column (150mm x 4.6 mm I.D.) before soaking (overnight) in Decon 90. After rinsing and drying, the column was then filled with pyrolysed montmorillonite K10 using a small funnel and a ramrod (sterile copper stirring rod). Once superficially filled it was connected to the HPLC pump and ACN was passed through it. Due to the extremely small particle size of the clay, the pressure of the system could become quite high. It was allowed to rise to 200 bar before being shut off and the column removed. Under pressure the clay had compacted and more could be added. The process was repeated a number of times until, at a pressure of 200 bar the column was fully packed. The column was then sealed ready for the experiment.

1. The detectability of acephate on the DAD UV-detector was assessed by a series of repeat runs through a similar column packed with a C18 stationary phase. The acephate peak was identifiable but too broad to be quantifiable. It was isolated and prepared for GC analysis.

2. The custom made column was installed and acephate in aqueous solution (500 mg/L) was injected (1 μL) with the mobile phase consisting of a water:MeOH mixture at a ratio of 20:80. Run time was 30 min at 0.03 mL/min with a pressure of 197 bar.

3. The fraction was between 10 and 30 min taking into account tube lengths before and after the column.

4. The fraction was prepared for GC analysis and run under the identical conditions (detailed above) as previous acephate detection.

The procedure was repeated 5 times to increase reliability and between each acephate run an injection (1 μL) of water only was made under the same conditions. In addition, the needle was rinsed in the injection port for 30 s before each injection.

It is important to note here that not all the acephate was removed from the stationary phase using this method. It is for this reason that analysing a fraction on GC can yield information on enantiomer selective sorption processes. If *all* the eluent were removed, the enantiomers of acephate would, of course, prove to be present in a racemic mixture.

2.6.3 Quantification of the Analyte using GC

2.6.3.1 Calibration

For each batch sorption experiment executed, a calibration was carried out in order to quantify the analyte in question. This typically involved the preparation of at least 4 standard concentrations of the analyte run in triplicate. The concentration was then plotted against the mean peak area of the three repeat runs showing a linear relationship from which the concentration of unknown samples can be determined using the gradient of the linear trendline. A typical calibration plot is provided in Figure 2.4:

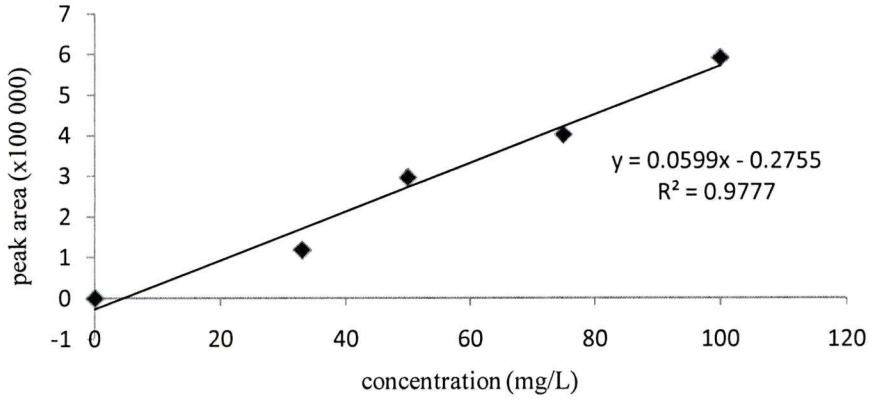

Figure 2.4 Calibration plot for D-enantiomer of acephate

Each standard was prepared in a manner mimicking the preparation of the samples. For example, the standard would be made up as an aqueous solution before being dried and redissolved in ACN ready for GC analysis. This means that any potential human error in the sample preparation is mirrored in the calibration.

2.6.3.2 Peak area integration

The software ChemStation (Agilent, UK) was used for processing the chromatograms and allowed manual and automatic peak area integration. Due to small imperfections in the chromatograms, the software was unable to automatically integrate the peak areas with any degree of reproducibility. Subsequent manual integration simply involved using the mouse to draw a line across the base of the peak and allowing the software to calculate the internal area of the peak. Although this appears to be subject to significant potential human error, in reality the process is repeated so many times that the operator can draw a line of the same length and angle from the horizontal with remarkable reproducibility.

2.6.3.3 Reproducibility

Reproducibility was ensured throughout all batch sorption experiments by running each set of samples in quintuplicate from the beginning of the experiment. The mean and standard deviation was then calculated for each data set and used to produce error bars on the final plots. This not only applies to the sorption of sorbate but also to the subsequently calculated EF. In each run, the EF was calculated, averaged over all replicates and the standard deviation determined.

It was also important to look at EF reproducibility from the same standards or samples run repeatedly. This gave an indication of the precision of the results; a factor that was fundamental to the significance of EFs determined by batch sorption experiments. The precision was calculated by repeat running (5 times) a selection of acephate standards. The range was designed to represent values that might be encountered in supernatants from a number of sorption experiments. The average EFs were calculated along with the percentage of relative standard error (%RSE) for each set of peaks (Table 2.10).

Table 2.10 % RSE for raw uncorrected EF values for a range of acephate concentrations determined by GC

Standard Concentration	Average EF	% RSE
103.4	0.4974	0.25
73.86	0.4976	0.27
51.70	0.4979	0.37
25.85	0.4989	0.22
12.93	0.4983	0.23

The % RSE was calculated using equation 2.2:

$$\%_{err} = \left[\frac{SE_{\bar{x}}}{\overline{EF}}\right].100 \qquad \text{(Equation 2.2)}$$

Where $\overline{EF}$ and $SE_{\bar{x}}$represents the mean enantiomeric fraction and the standard error of the mean, respectively. If the % RSE of a repeated standard is larger than the observed variation in EF for any particular sample in a sorption experiment then the result can be considered statistically "insignificant".

2.6.3.4 Sample correction for batch sorption experiments

In batch sorption experiments, the concentration of the analyte remaining in the supernatant was corrected relative to the standard, run for each respective experiment. The corrected values (C_{corr}) were calculated using a simple equation:

$$C_{corr} = C_{obs} \times \left[\frac{C_{st}}{C_{Sobs}}\right]$$

WhereC_{obs} represents the observed concentration of the sample, C_{st} the known concentration of the standard and C_{Sobs} the observed concentration of the standard. This allowed subsequent plots of sorption against mineral content to display sorption of exactly zero when the mineral content was also zero. Furthermore, the EFs in each batch sorption experiment were calculated from the C_{corr}values for each enantiomer.

2.7 Assessment of the extent of sorption at the vial wall surface

Simple batch sorption experiments were conducted involving no clay sorbent and a set acephate concentration to determine the ability of polypropylene and glass vials to sorb acephate and their effect on the EF. The batches were allowed to equilibrate for varying lengths of time. After 0 h, 24 h and 48 h little significant variation between the two types of vial could be seen although there was a very small reduction in the acephate present in the supernatant solution with increasing equilibration time. In terms of enantiomer selective sorption onto the vial wall, there was very little deviation from the racemic state of acephate in supernatant although the 24 h equilibrating period did appear to show a very slight deviation below an EF of 0.5.

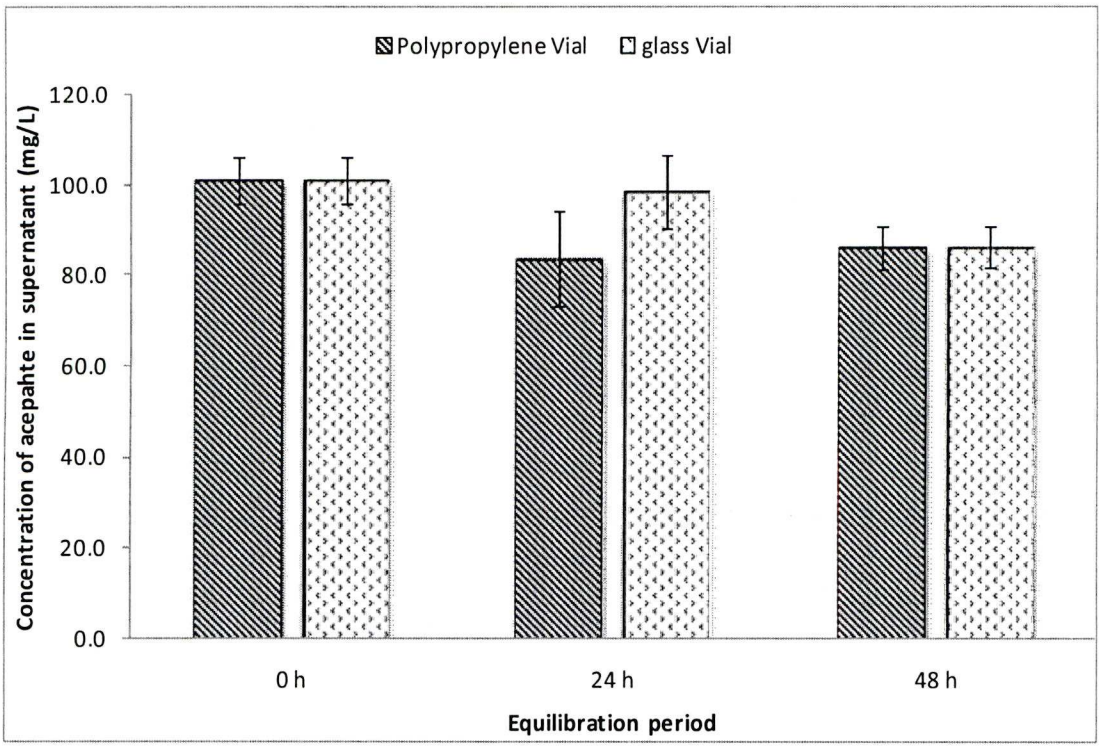

Figure 2.5 The amount of acephate in the supernatant (mg/L) after increasing equilibration times with polypropylene or glass vials

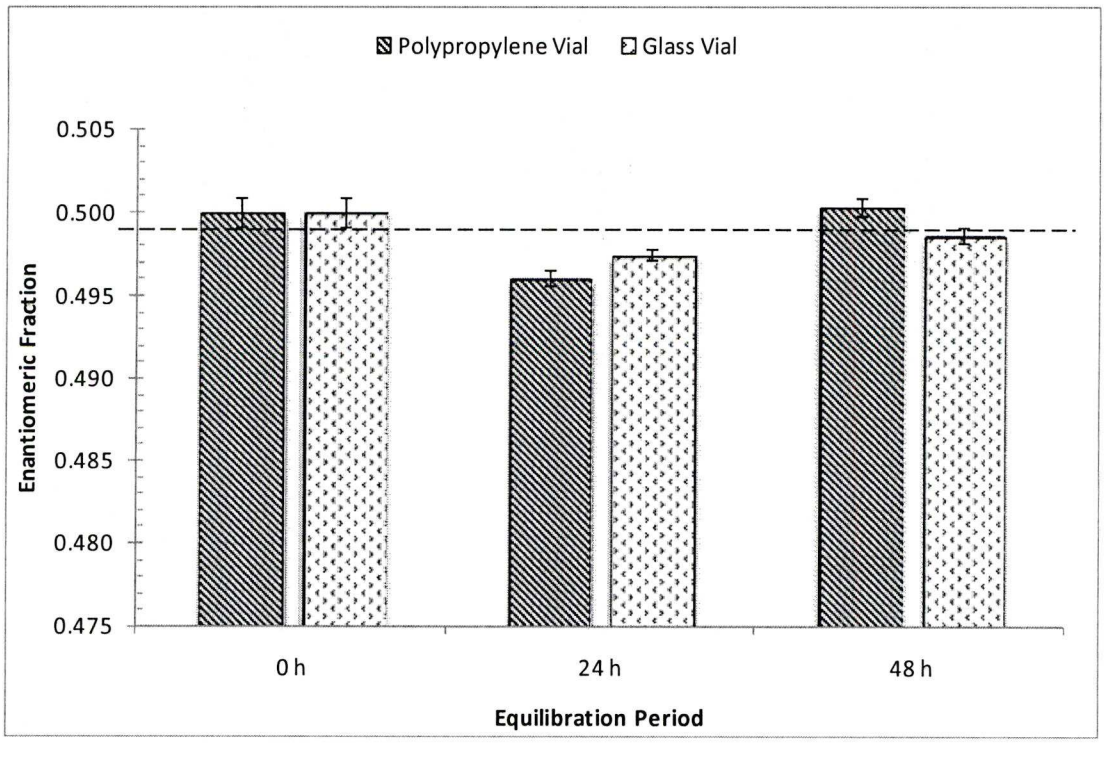

Figure 2.6 The EF values for acephate in the supernatant after increasing equilibration times with polypropylene or glass vials

2.8 Determination of the Cation Exchange Capacity (CEC)

The CEC of montmorillonite K10 and bentonite SWy-2 was calculated from experimental data in order to make comparisons to sorption experiments from other sources more reliable. Additionally, by obtaining CECs for the clays with varying temperature pre-treatments, the results can be used to complement previous experiments to investigate the effects of heat treatment on the internal structure and sorptive capabilities of the studied clays. In the case of montmorillonite K10 the CEC values correlate with the sorption results for the previous experiment. An increase in the pre-treatment temperature results in a decrease in the CEC. A reduction in CEC of ~16 % is observed between the unheated and the 400°C pre-heated montmorillonite K10 batches. Bentonite SWy-2 showed a small decrease in CEC between the unheated and 105°C pre-heated batches.

Table 2.11CEC values for a variety of K10 and SWy-2 clay temperature pre-treatments

Clay pre-treatment	CEC meq/100g
unheated	83.7
105	81.7
400	70.6
B0	77.8
B105	75.2

The results of the experiments described in this chapter and subsequent detailed discussion are presented in Chapter 3, predominantly in the chronological order in which they were conducted.

CHAPTER 3 ADSORPTION ON UNMODIFIED MINERAL SURFACES

Adsorption of the chiral organophosphorus insecticide (OP), acephate (Figure 3.1), on the surface of naturally occurring minerals has been extensively studied throughout this work. A variety of conditions and chemical modifications to the sorbent have been prepared in the laboratory in order to improve understanding of the fate of racemic acephate in the environment and the mechanisms involved in enantiomer selective adsorption where this occurs. Enantioselective degradation (or retardation – the slower adsorption of one enantiomer over the other) of chiral pesticides in the environment has been widely observed and extensively studied (Faller, Hühnerfuss, Konig & Ludwig 1991; Kallenborn et al. 1991; Kallenborn & Hühnerfuss 2001; Hühnerfuss et al. 1993; Ludwig et al. 1992; Qin et al. 2006; Zipper et al. 1998; Faller, Hühnerfuss, Konig, Krebber et al. 1991; Druzina & Stegu 2007; Wiberg et al. 1998; Jantunen & Bidleman 1998; Lewis et al. 1999). Such selection processes are widely thought to be due to biotic processes and, in fact, are often used as biological markers (Garrison 2006). However, recent evidence (Wedyan & Preston 2005; Abid 2008) has thrown some doubt on this assumption and, thus, this research investigates the possibility of abiotic enantioselectivity of an achiral mineral towards a chiral molecule. As discussed in Chapter 1, a small amount of disputed work has been conducted in this area with reference to amino acid sorbates (Degens et al. 1970; Bondy & Harrington 1979) on the surface of several clays including montmorillonite. So far, however, these investigations have not been extended to chiral OPs and the present study is the first to consider the enantioselective adsorption of an OP insecticide by sterile, achiral mineral surfaces.

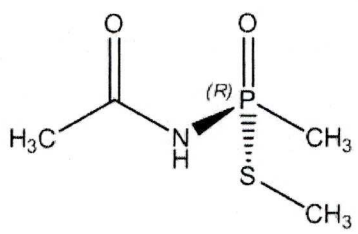

Figure 3.1 Chemical structure of acephate (*O*,S-dimethyl acetylphosphoramidothioate) with the chemical formula $C_4NH_{10}NO_3PS$

This research addresses the adsorption mechanisms for acephate onto mineral surfaces and, to some extent, its fate within the environment. More specifically, the chirality of acephate compounds and the minerals it binds to will be examined as well as the effect this characteristic has on their transport in the environment. It is hypothesised that some minerals found in soils and sediments in the environment are capable of abiotic, selective adsorption of a larger proportion of one enantiomer than the other in the chiral pesticide, acephate.

Enantioselective GC (see Chapter 2) makes it possible to separate and quantify the enantiomers of acephate enabling the calculation of an EF, which, as described in Chapter 1, is used throughout as a means of assessing the enantioselective capabilities of a variety of adsorbents.

This chapter presents the results of batch sorption experiments designed to assess the enantioselective adsorption capabilities of a number of mineral sorbents towards acephate. The implications of the results are discussed where relevant. An overview of the sequence is presented in Figure 3.2.

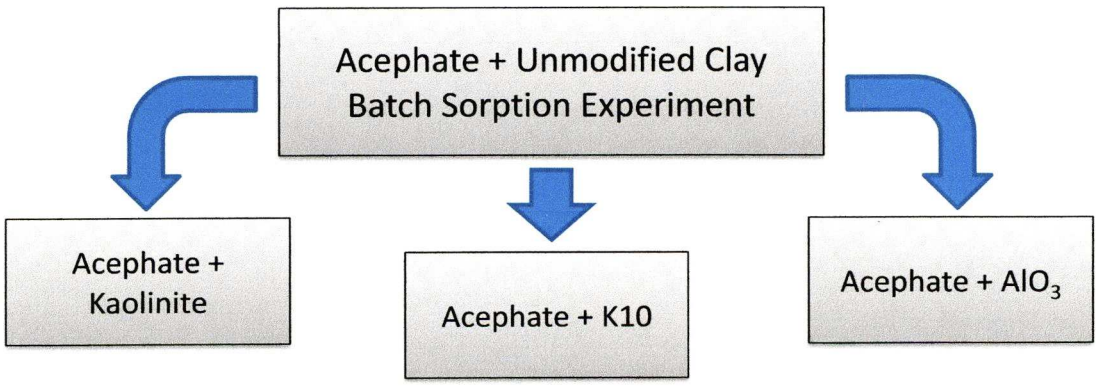

Figure 3.2 Schematic representation of key experiments throughout this chapter. See respective sections within this chapter for definitions of abbreviations.

The investigation begins with basic batch sorption experiments involving racemic acephate and the minerals montmorillonite K10 (K10), kaolinite and aluminium oxide. K10, kaolinite and aluminium oxide are known to be achiral minerals although some work suggests that kaolinite may exhibit chiral properties to a certain extent(Degens et al. 1970; Jackson 1971; Brigatti et al. 2006). The sorption experiments involve varying the amount of mineral in each batch while keeping the initial sorbate concentration constant. After equilibration, the sorbate concentration in each supernatant solution was quantified through GC analysis. The results are

presented in a format whereby the percentage (%) of the sorbate adsorbed at the surface of the mineral is plotted against the amount of mineral (mg) in each batch. Where relevant, the % sorption was also plotted against the total available mineral surface (m^2) calculated by multiplying the amount of mineral (mg) by the specific surface area of the mineral (m^2/g).

3.1 Acephate Adsorption on Montmorillonite K10

As discussed in Chapter 1, K10 is an acid treated montmorillonite used frequently for catalysing organic reactions due particularly to its high specific surface area. The structure is shown in Figure 3.3 below. Additionally, SEM micrographs and spectra showing chemical composition for various modified and unmodified K10 samples are included in Appendix 1 (Figures A1.1 – A1.5).

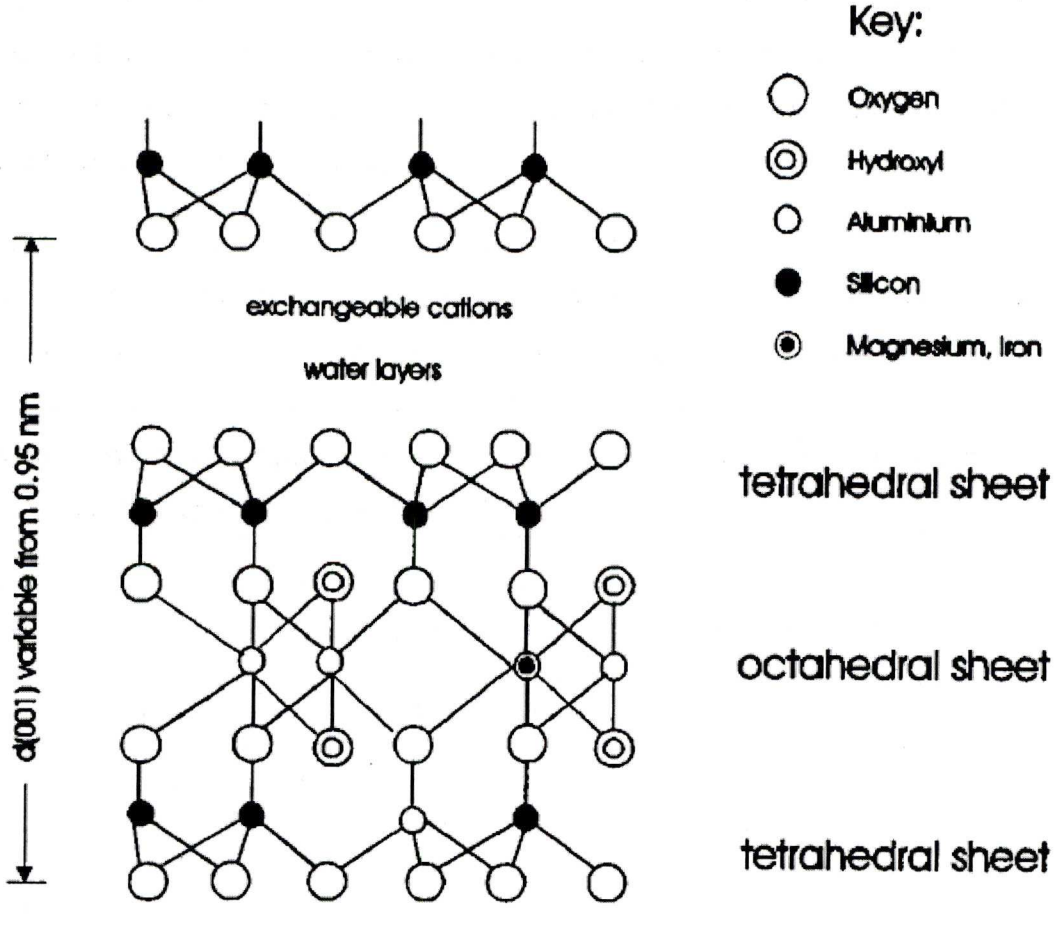

Figure 3.3 The Hofmann-Endell-Wilm-Marshall-Maegdefrau-Hendricks structure of montmorillonite layer viewed along the *a* axis (Hofmann et al. 1933). Basal spacing is given in nm units. The drawing used here is from Luckham & Rossi(1999)

Increased amounts of K10, involved in batch sorption experiments saw a decrease in the equilibrium concentration of the acephate in the aqueous supernatant (Figure 3.4). Five milligrams of the sorbent allows sorption of ~58% of the acephate present in the initial solution. One would assume that this is the sorption capacity for such an amount of K10. Doubling the amount of sorbate to 10 mg, however, only resulted in the sorption of about a further 16% of the acephate. Such a pattern continued whereby further adsorption of the sorbate occurred in reduced increments as more active sites became available with increasing mineral additions.

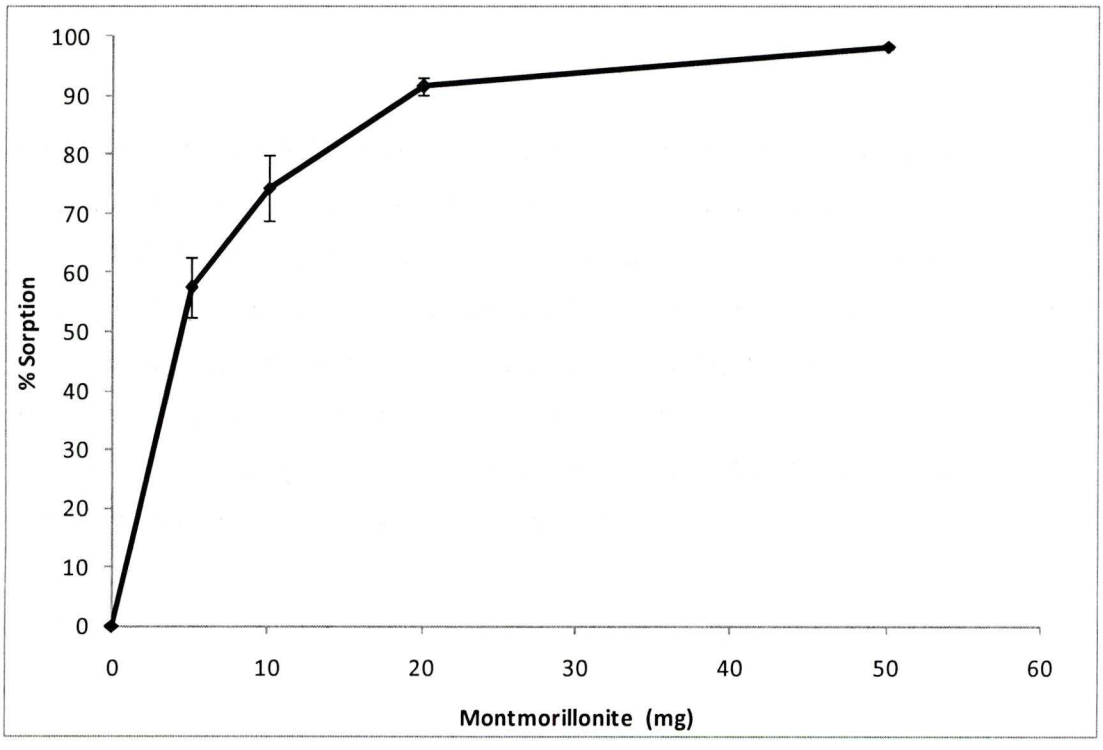

Figure 3.4 Acephate sorption (%) on the surfaces of montmorillonite K10 clay. Error bars represent the standard error calculated for each data point.

Whilst coinciding in shape, this plot is not a Langmuir isotherm as the initial concentration of the sorbate is constant throughout the experiment while the amount of mineral varies. However, all the parameters are available to enable the description of such a clay mineral adsorption experiment by the linear form of the Langmuir equation:

$$\frac{C}{\frac{x}{m}} = \frac{1}{kV_m} + \frac{C}{V_m} \qquad \text{(Equation 3.1)}$$

Where C is the equilibrium concentration, x is the amount adsorbed per unit weight m of clay while k and V_m are constants; the latter being identifiable with the monolayer capacity of the adsorbent (Theng 1974). Adsorption can be said to conform to the Langmuir equation if a straight line is observed when $C/(x/m)$ is plotted against C. The nearer the R^2 value for a data set is to 1.0 the more closely the adsorption conforms to the Langmuir equation. From Figure 3.5, showing the Langmuir conformity plot for acephate on K10, a significant conformity can be seen. This essentially means that by assuming there are a fixed number of active sites and that only one layer of molecules can form on the clay's surface, the more active sites are filled the more difficult it becomes to adsorb molecules as competitions for sites increases. Additionally, the amount of ionic adsorption cannot exceed that which is allowed by the cation exchange capacity of the clay. However, other types of interaction may occur freely. For example, molecular dipole interactions enable acephate molecules to interact with each other as well as direct binding of acephate to the clay surface. Nonetheless, observing whether adsorption conforms to the Langmuir equation in a number of batch sorption experiments allows better comparison of the mechanisms of adsorption. So, if each set of data conforms to the Langmuir equation then the type of adsorption can be ruled out as a variable that might affect the adsorption mechanism. If the data do not conform to the Langmuir equation, however, there is very little that can be inferred as other mechanisms for adsorption are possible. These include direct interaction at and even beneath the clay surface as well as dipole interactions resulting in further acephate-clay and acephate-acephate bonding processes.

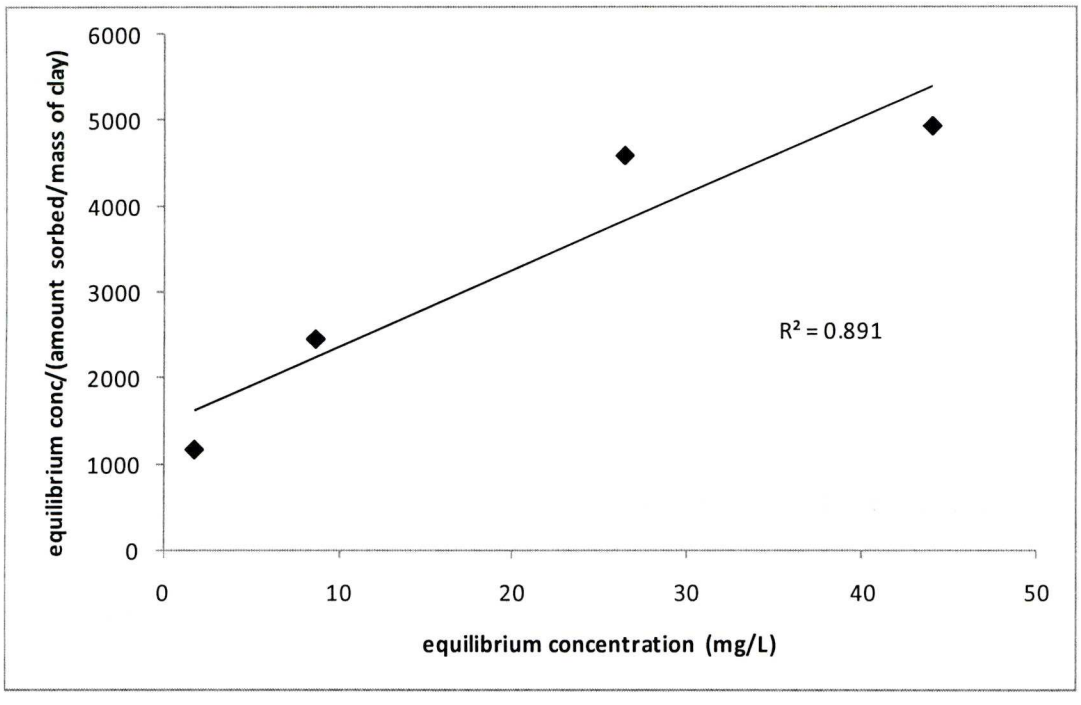

Figure 3.5 Langmuir conformity plot for acephate sorption on montmorillonite K10 clay

The enantiomeric fraction (EF) of the enantiomers of acephate in the supernatant solution was calculated for the different quantities of K10 in each batch using equation 3.2 below. The benefits of using EF to assess enantioselective adsorption are discussed in Chapter 1.

$$EF = \frac{A_1}{A_1 + A_2} \qquad \text{(Equation 3.2)}$$

The resulting plot (Figure 3.6) shows a clear trend of increasing deviation from an EF of 0.5 with increasing clay amount. The initial EF of 0.5 represents the racemic mixture of the two acephate enantiomers found in an aqueous solution with no sorbent present. EF values above 0.5 indicate greater proportions of the first eluting enantiomer (in the case of acephate, this is the (+) enantiomer) over the second (the (−) enantiomer) whereas with values below 0.5 the abundance of the second eluting enantiomer is higher than the first. Increasing additions of clay result in a linear increase of the EF. Since these values are for the acephate enantiomers present in the supernatant they indicate preferential sorption of the (−) enantiomer to the K10 surface. Increasing clay additions result in further deviation from the racemic state in a linear fashion.

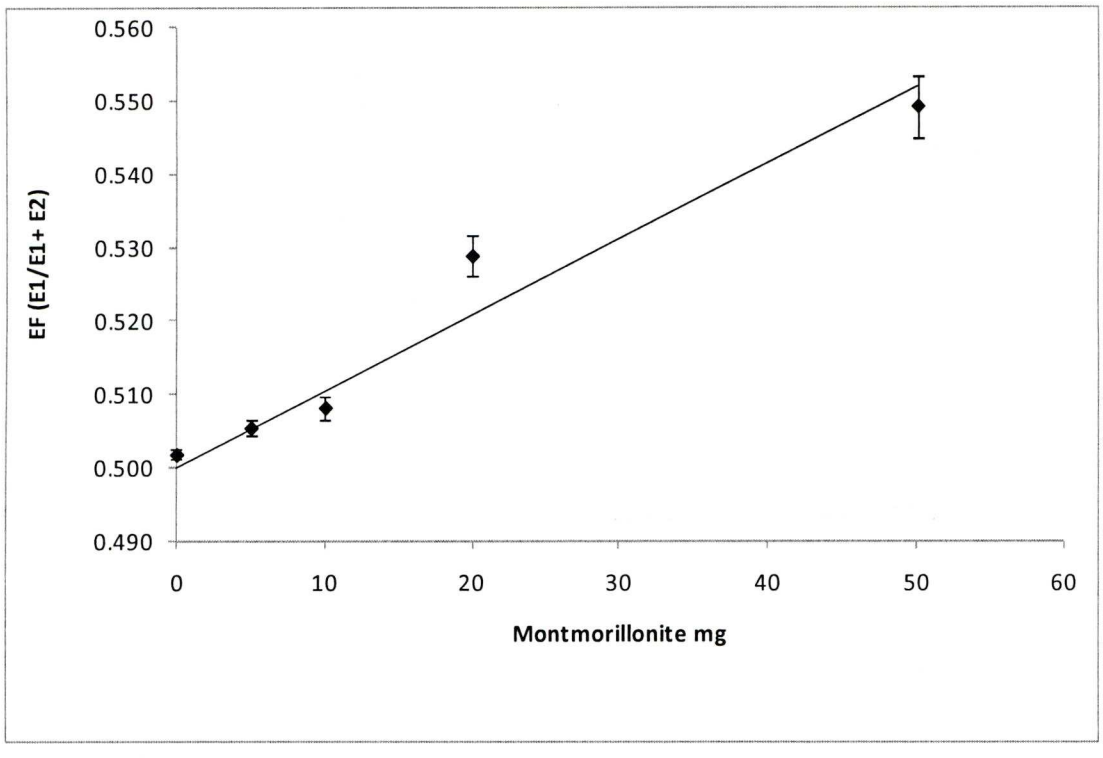

Figure 3.6 Enantiomeric fraction (EF) for acephate enantiomers in the supernatant after adsorption at the surfaces of K10 clay. Error bars represent the standard error calculated for each data point.

By plotting the amount of acephate sorbed to the surface of the sorbent against the enantiomeric fraction calculated from the same experiment it becomes easier to deduce the extent, pattern and consistency of the enantioselective nature of the sorbent. Furthermore, insight into the way the sorbate molecules bind to a substrate surface may be gained. Such deductions can be made by identifying any apparent trends and assessing the extent of such trends' conformity to the data points. Figure 3.7 shows a trend in the data points whereby steadily increasing adsorption results in an apparent (although not calculated) exponential increase in enantiomeric fraction, or deviation from a racemic state. It appears that the more the acephate molecules bind at the sorbate surface, the more enantiomer selective the sorption processes become. This suggests that the presence of the acephate molecules at adsorption sites affects the extent of enantioselectivity in the continuing adsorption process. In other words interaction between acephate enantiomers must be enantioselective. The molecular dipole interaction may be an independent binding mechanism for acephate or it may simply *affect* the adsorption of acephate by other means. In any case, it is probable that this interaction enables enantiomer specific adsorption as a chiral environment is provided by the presence of asymmetric enantiomers of acephate in

uneven proportions. This is acceptable in the latter stages of equilibration once enantioselective adsorption has already begun and would explain how the preference increases as more acephate is adsorbed. However, while the initial coverage of acephate is racemic it should not be possible for acephate-acephate interactions to begin showing an overall enantiomer specific preference. Perhaps the required initial chiral environment could be provided by the interaction of acephate enantiomers and adsorption sites on the clay surfaces. (See Pályi et al. 2004 and others).

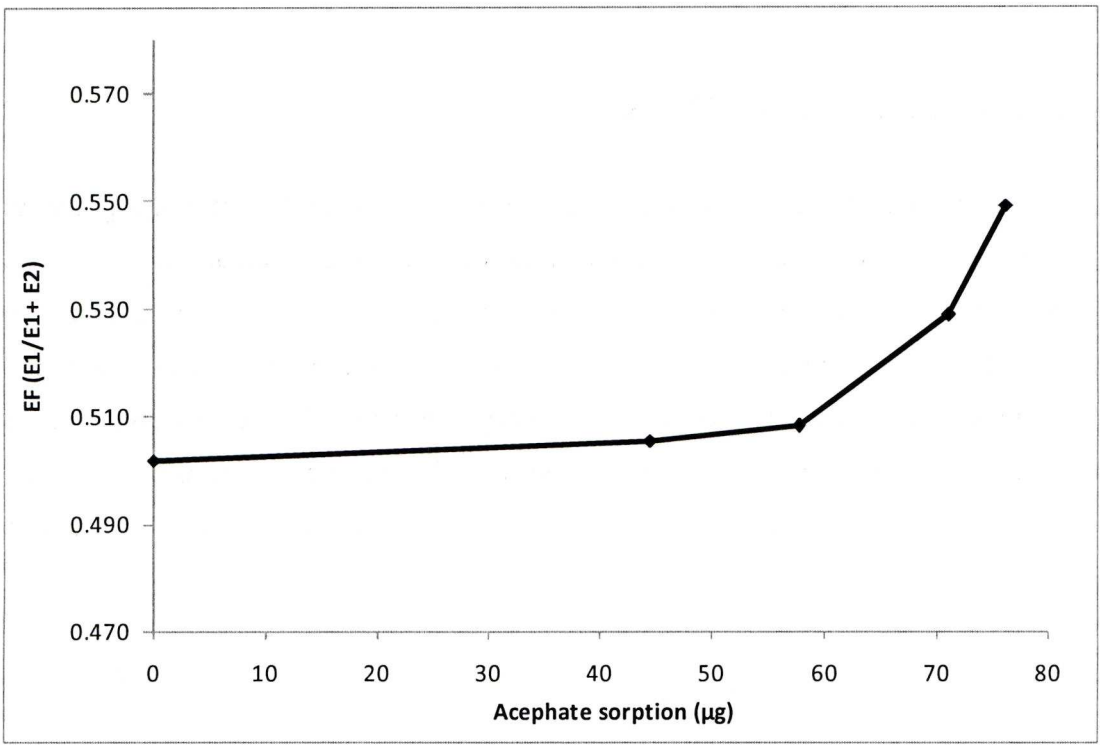

Figure 3.7 EF values plotted against Acephate sorption (µg) on K10

3.2 Acephate Adsorption on Kaolinite

Kaolinite was substituted for K10 in a similar batch sorption experiment. The structure is shown in Figure 3.8.

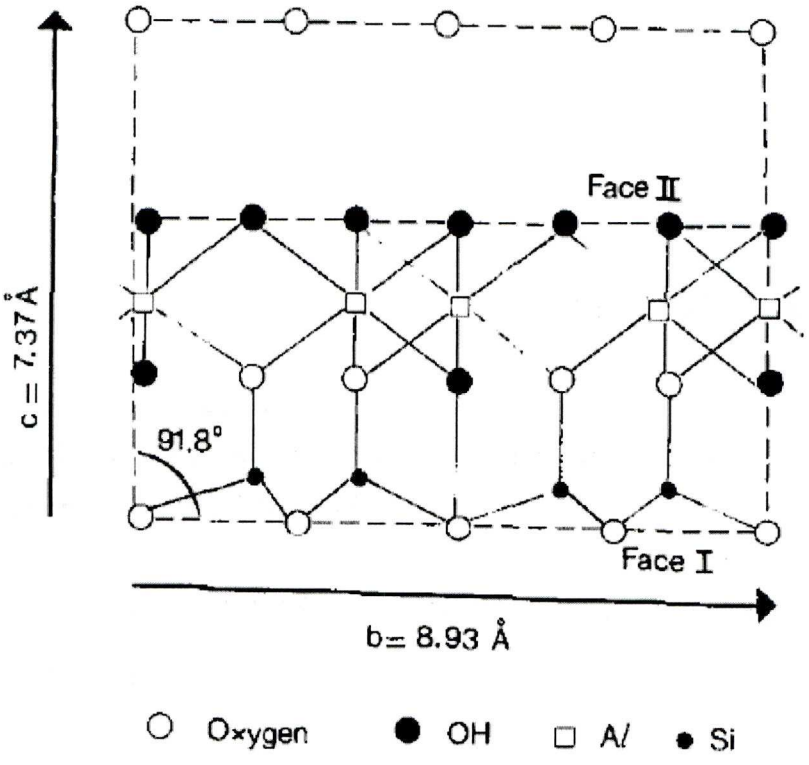

Figure 3.8 The structure of Kaolinite, as depicted by Julg & Ozias (1988)

In batches of 5 and 10 mg of kaolinite, adsorption of acephate was undetectable (Figure 3.9). However, with increasing quantity of sorbent 20 mg and above, we see an increase in the acephate sorption. Between 10 and 100 mg, the amount of adsorption increases in a similar fashion to the montmorillonite K10 whereby the adsorption increases by smaller increments as more sorbent becomes available. Between 50 and 100 mg, however, the increase appears to be linear. Overall the extent of adsorption does not conform to the Langmuir equation with no trend being observed when the equilibrium concentration divided by the amount sorbed per unit mass of clay is plotted against the equilibrium concentration alone (Figure 3.10). This suggests that the mechanism for adsorption is different from that on K10 where competition for sorption at active sites is present and retards further sorption. Perhaps the properties or structure of kaolinite provide an environment where sorbate molecules can bind with less competition for active sites. Adsorption in multiple

layers may occur more easily in kaolinite's interlayer spaces than in that of K10 and perhaps the edge sites provide a more accessible environment for adsorption.

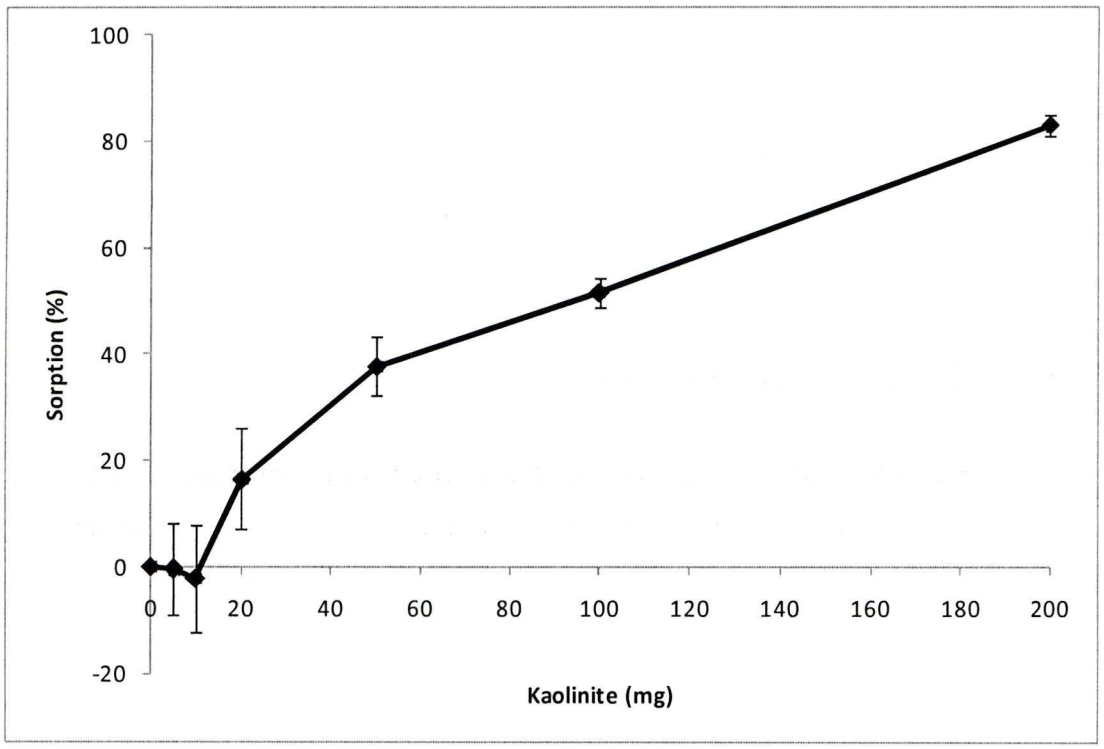

Figure 3.9 Acephate sorption (%) on the surfaces of kaolinite. Error bars represent the standard error calculated for each data point.

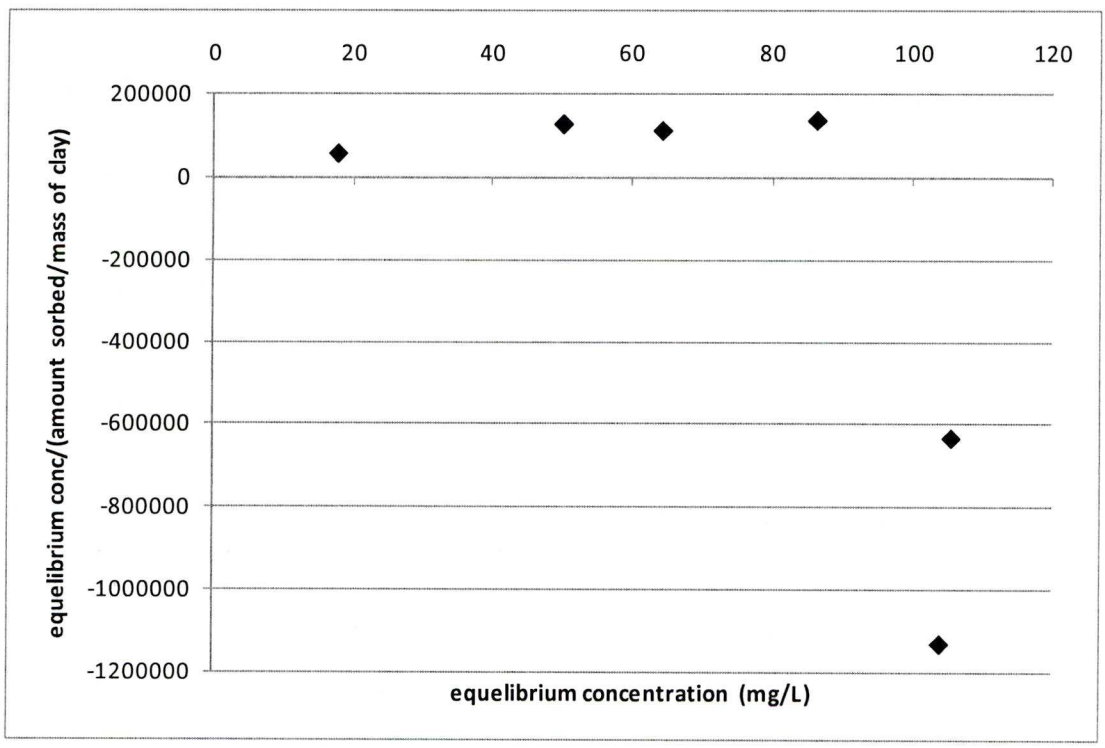

Figure 3.10 Langmuir conformity plot for acephate sorption on kaolinite surfaces

On the other hand, it is of note that in comparison with K10 significantly more kaolinite was required in the experiments in order to achieve a similar extent of acephate removal from the supernatant. This is presumably due to the difference in surface area of the two sorbents used. Figure 3.11 presents the % sorption plotted against the available surface area of sorbent for each batch. Presenting the data in this way enables better comparison of the sorptive capabilities of K10 and Kaolinite and in this case reveals that although the sorption on kaolinite appears to be closer to being linear (Figure 3.9) there are not enough data to confirm this. In fact, sorption on kaolinite is in keeping with that on K10 and may have continued in such a way if more surface area had been available.

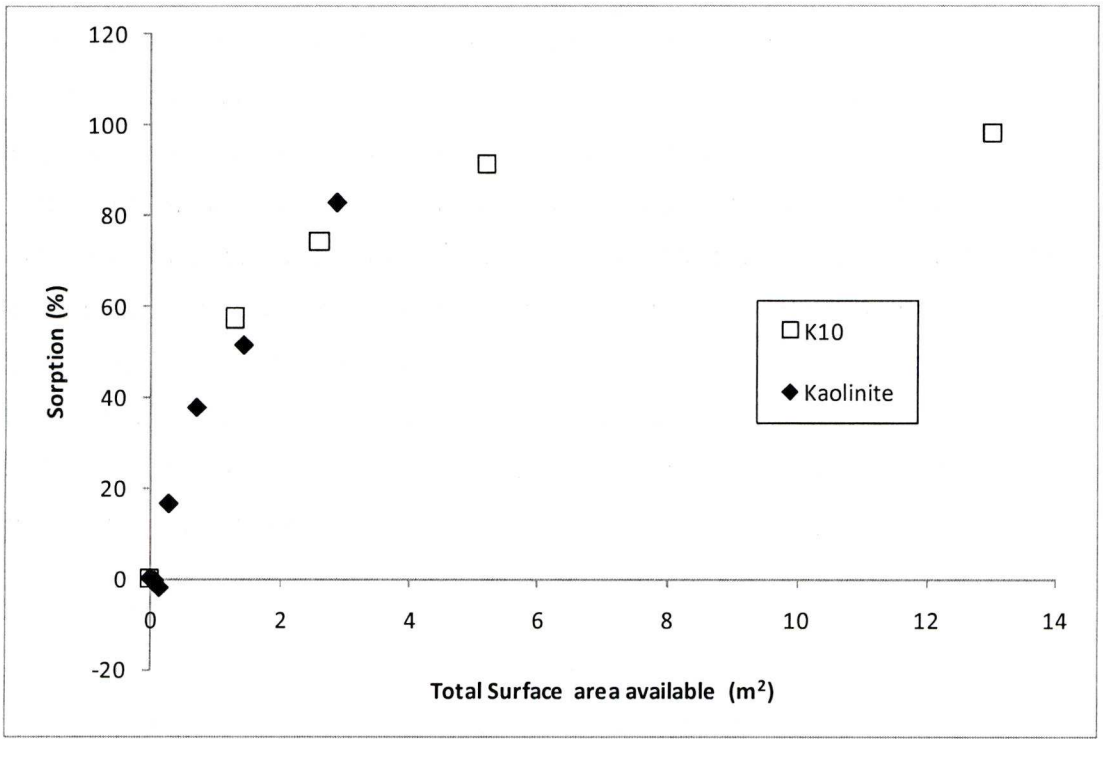

Figure 3.11 The percentage sorption of acephate on the surface of montmorillonite K10 and kaolinite clay plotted against the total available surface area for a given batch. Each point represents the result of an individual batch within the sorption experiment.

It is apparent from the EF plot for acephate on the kaolinite surface (Figure 3.12) that no preferential adsorption of either enantiomer occurs in any of the batch sorption experiments with less than or equal to 100 mg clay additions. There is some variation in EF but it occurs within the range of the error. It is not until 200 mg of sorbent is present that significant preferential adsorption of the (−) enantiomer can be observed on the clay surface. It is important to note the difference in scale in comparison to the

EF plot for K10; so while significant, the maximum preference obtained through the current experiments is much weaker.

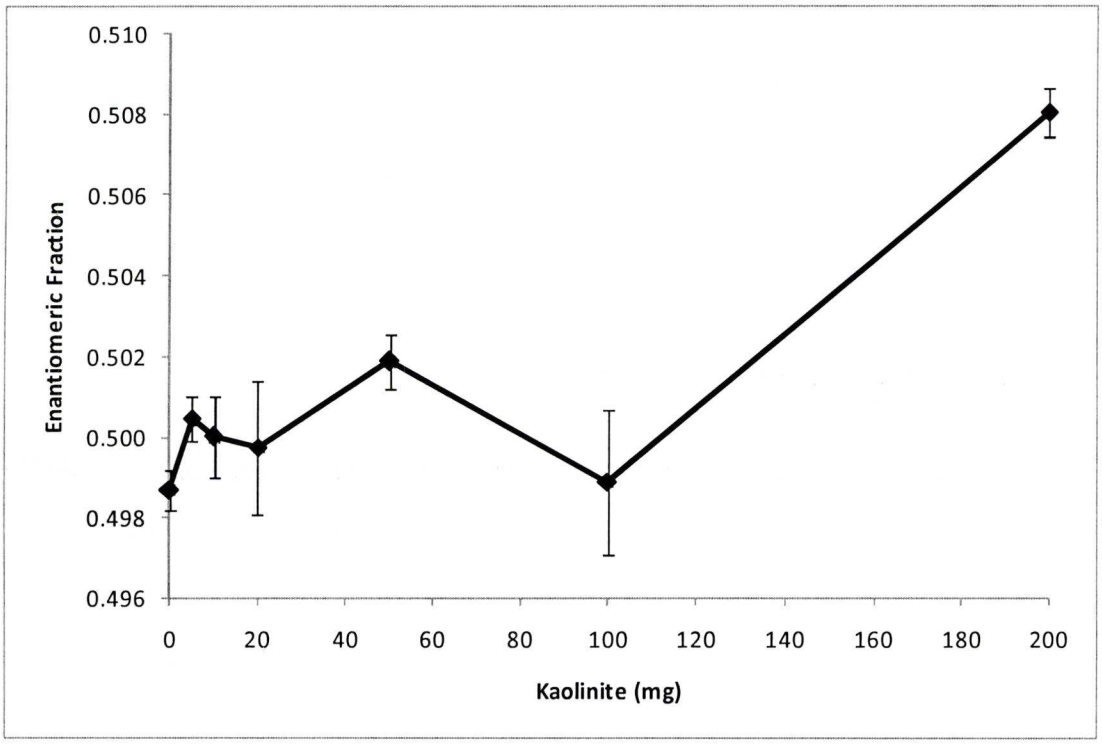

Figure 3.12 EF values for acephate enantiomers in the supernatant after adsorption at the surfaces of kaolinite clay. Error bars represent the standard error calculated for each data point.

However, by plotting the EF for acephate enantiomers on kaolinite and K10 against the total available surface area in each batch (Figure 3.13) it can be seen that the two clays do, in fact, show similar enantiomer selective preferences and, thus, adherence to similar adsorption mechanism should not be ruled out. Furthermore, it is possible to project the trendlines forward for each data set in order to predict the EF as surface areas increase beyond those used in this experiment. In this case, it is valuable to project the kaolinite trendline forward so that EF can be predicted for surface areas as high as those of K10 and thus make the full sets of data comparable. A similar trend to that of K10 is observed, although the magnitude of the maximum enantiomer selective preference shown by K10 is ~35 % larger than that of the forecasted maximum for kaolinite.

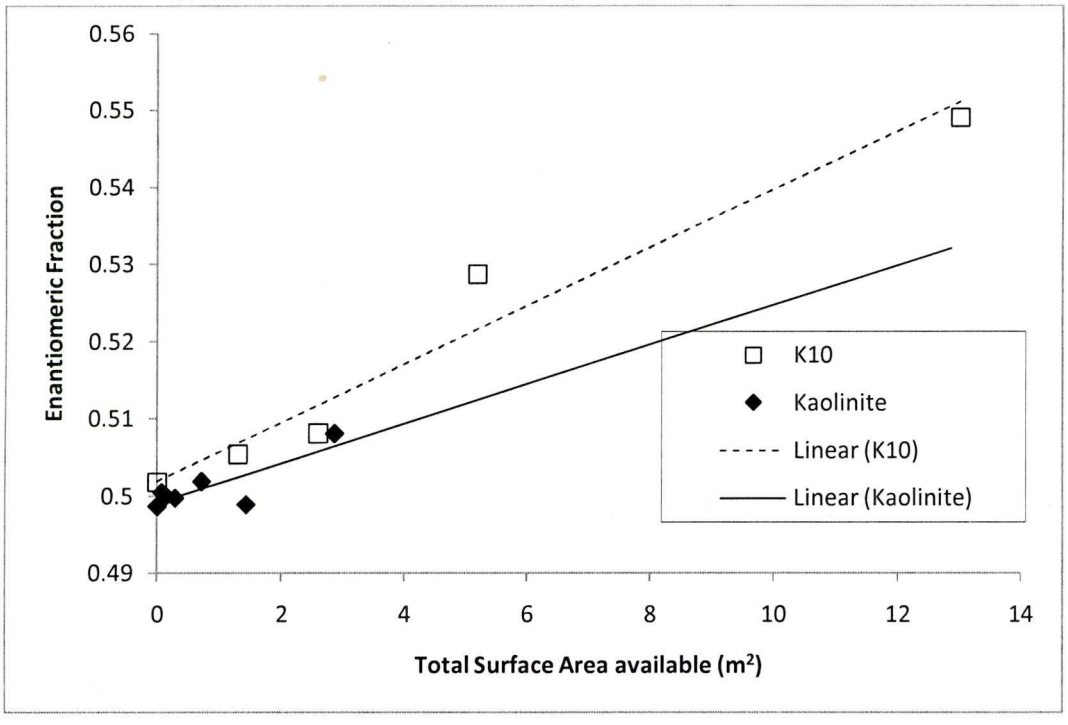

Figure 3.13 The EF calculated for enantiomers of acephate adsorbed on the surface of montmorillonite K10 and kaolinite clay plotted against the total available surface area for a given batch. Each point represents the result of an individual batch within the sorption experiment.

Some insight into the mechanism of preferential enantiomer selection by kaolinite towards acephate can be taken from the result of plotting acephate sorption on kaolinite against the subsequent EF values (Figure 3.14). There appears to be no rapid acceleration in deviation from the racemic state (EF of 0.5) with increased sorption as was seen in the case of K10 (Figure 3.7). This implies that the presence of acephate molecules already bound to kaolinite by whatever means has no effect on the extent of enantiomer selectivity shown by kaolinite throughout the adsorption process. Hence, a chiral environment is not provided by the interaction of initial non-racemically adsorbed acephate molecules and the kaolinite surface, or if there is such an environment, it has no affect on further enantioselective processes.

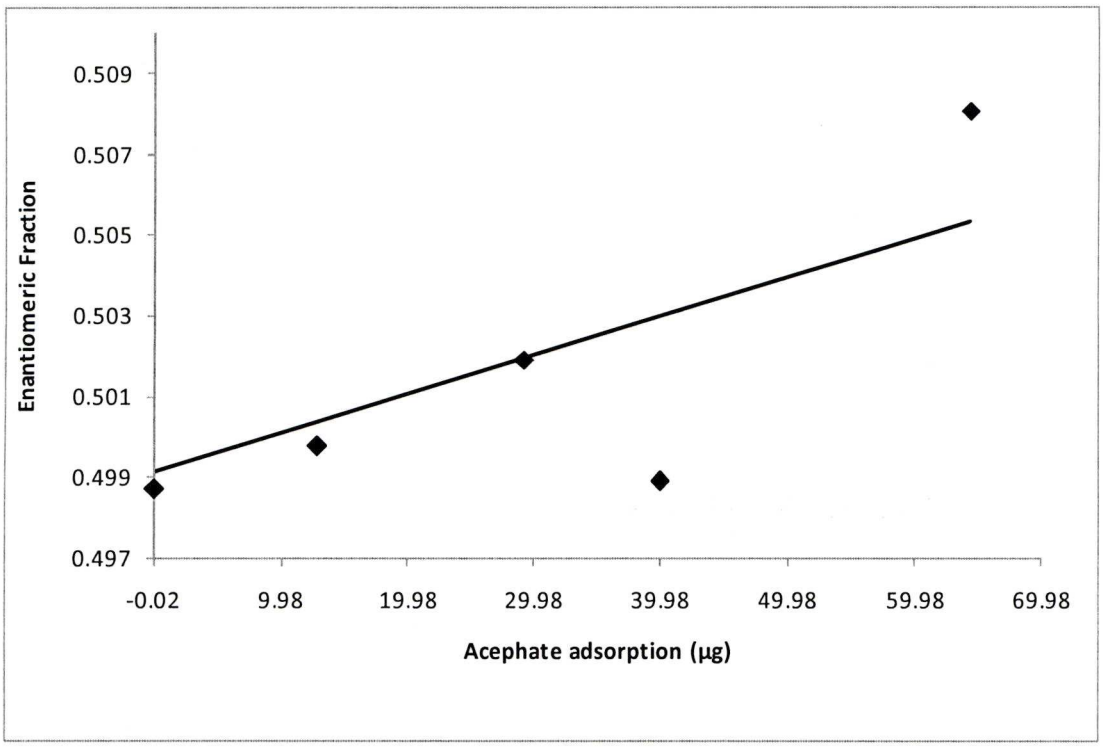

Figure 3.14 Acephate sorption (µg) on kaolinite plotted against the subsequent EF values

3.3 Acephate Adsorption on Aluminium Oxide Powder

In sorption batches involving acephate and aluminium oxide significant sorption is only observed in the presence of 100 and 200 mg of sorbent. Only a relatively small amount of acephate is adsorbed from the supernatant solution. Also, less adsorption appears to occur in the 200 mg sorbate batch than in the 100 mg batch. This is unlikely to be a real occurrence as the relatively large error bars indicate the likely lack of statistical difference between the two points.

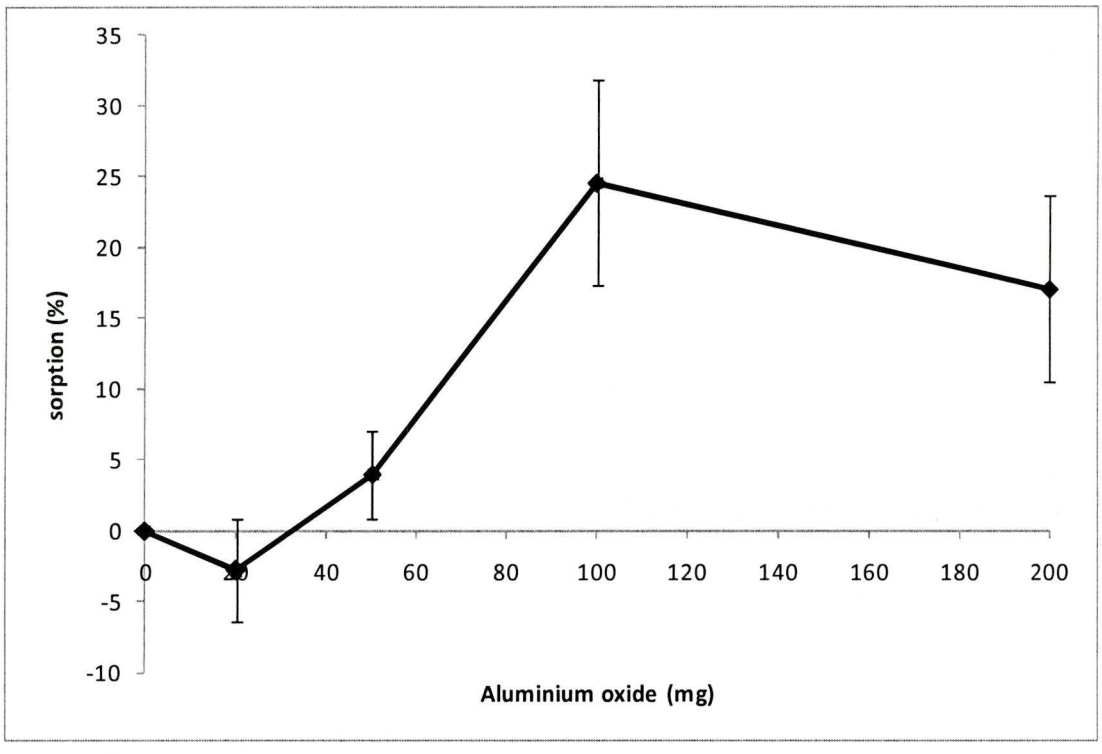

Figure 3.15 Acephate sorption (%) on the surfaces of aluminium oxide. Error bars represent the standard error calculated for each data point.

The plot of EF for sorption on the aluminium oxide surface shows very little evidence of enantioselective adsorption. Only in the 50 mg batch is there any significant deviation from the racemic state of acephate enantiomers. However, considering the extremely low level of adsorption of acephate in this batch it is unlikely that this is a reliable result.

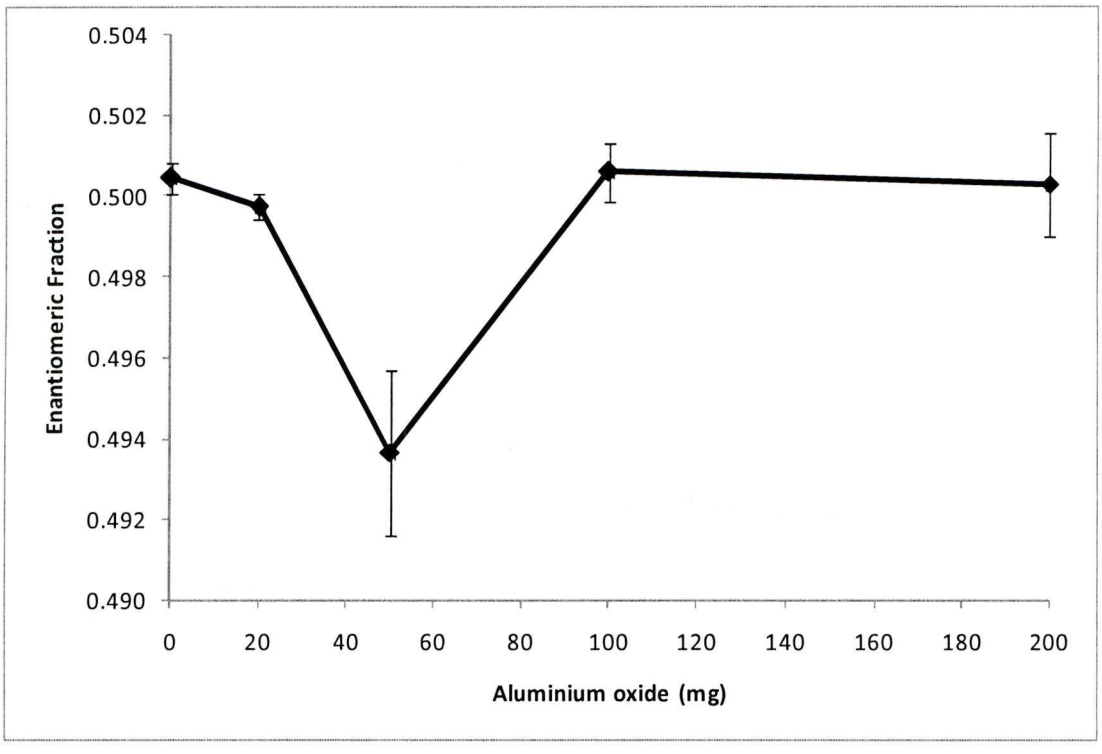

Figure 3.16 EF values for acephate enantiomers in the supernatant after adsorption at the surfaces of aluminium oxide. Error bars represent the standard error calculated for each data point.

From the results so far, it can be inferred that some of the sorbents, namely K10 and kaolinite, have an inherent ability to distinguish between enantiomers of acephate. Such a distinction is thought by many to be impossible due to the lack of chirality in the sorbents' crystal structures. Some argue that kaolinite does actually have some chirality (Jackson 1971) whereby catalytically active faces of the crystals act as specific templates which preferentially adsorb and polymerize particular amino acids with the L-configuration.They hypothesise that this is possibly due to an electrical dipole creating asymmetry within the structure. On one side of the structure there is a negatively charged $[Si_2O_5]^{-2}$ layer, while on the other there is positively charged $[Al_2OH_4]^{+2}$ which results in linear asymmetry. However, Jackson (1971) admits that it is difficult to ascertain whether this is the cause of the observed specific enantiomer selection as the chirality of the sorbate enantiomers exhibit three-dimensional asymmetry. On the other hand, it is generally agreed that montmorillonite has no chirality associated with its crystal structure (Bonner 1991). Despite this, there has also been reported a preference by bentonite clay (montmorillonite) towards the adsorption of some L-amino acid enantiomers over the corresponding D- enantiomer (Bondy & Harrington 1979).

The results detailed above raise several questions about why and how such observations might come about. How can a clay mineral, widely accepted to be of achiral crystal structure show a preference to a specific enantiomer of a chiral compound? What are the chemical mechanisms involved in the binding process? Where do such interactions occur within the sorbent structure? Assuming that the enantiomer selective preference by both clays is real, then such a distinction must presumably occur at a limited number of positions associated with the sorbent. This could be through interaction by either reaction with, or replacement of, any interlayer species. It may also occur at a surface of the clay's tetrahedral silicate or octahedral aluminosilicate layers either within the interlayer space or at the layers' edge sites. Additionally, the effects of initially adsorbed sorbate on the way any further adsorption occurs should not be ignored. Further experimentation in this work aims to shed light on the different aspects of adsorption questioned here.

CHAPTER 4 ADSORPTION ON MODIFIED MINERAL SURFACES

The strong sorption of acephate to the surface of K10 with its large adsorption capacity and, in particular, the enantioselective nature of such sorption encouraged further investigation of the relationship. By pre-treating the K10 and making small modifications to the interlayer components it was hoped that insight could be gained into the enantioselective mechanisms at the sorbate–sorbent interface. This chapter documents a series of batch sorption experiments involving K10 subjected a number of such pre-treatments and surface modifications. The implications of the results are discussed where relevant. Figure 4.1 provides a summary of experiments in this chapter while emphasising the sequential nature of their development.

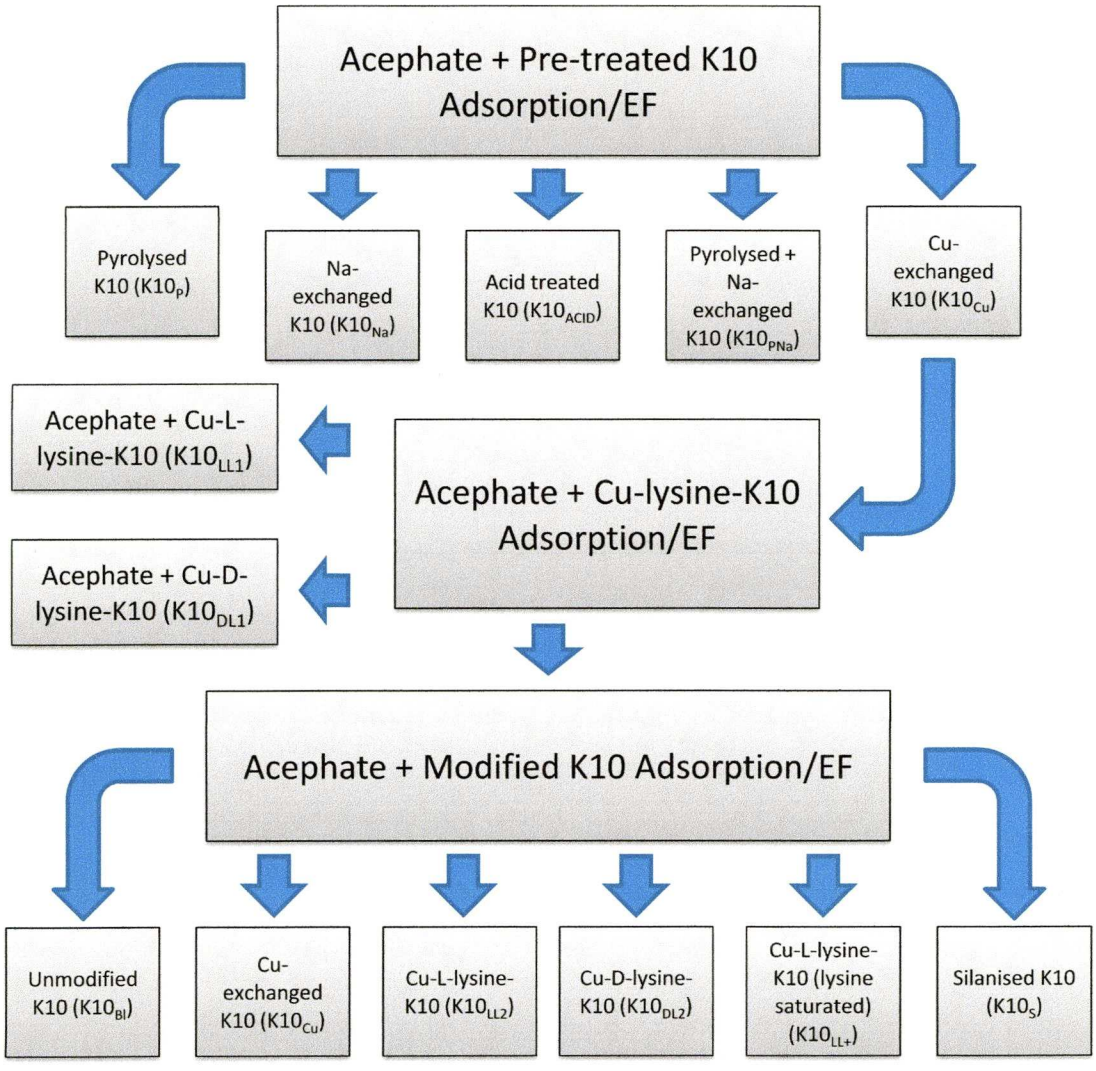

Figure 4.1 Schematic representation of the order of key experiments throughout this chapter. See respective sections within the chapter for definitions of abbreviations.

4.1 Batch sorption experiments with acephate (100.9mg/L) and montmorillonite K10 with various pre-treatment methods

Five K10 modifications were prepared for batch sorption experiments with acephate. Two modifications were prepared by interlayer cation exchange processes resulting in a mono-cationic interlayer environment of Na^+ ($K10_{Na}$) cations and one of Cu^{2+} ($K10_{Cu}$) anions. These particular modifications would hopefully give an idea of the influence of different interlayer ionic cations on the adsorptive and enantioselective capabilities of the sorbent as a whole. A further treatment was applied by pyrolysing some of the Na-exchanged K10 ($K10_{PNa}$). This meant that a direct comparison between a pyrolysed and non-pyrolysed sorbent with a single, known interlayer exchangeable cation could be made. This is one way of looking at the effect of pyrolysation on the sorptive and enantioselective capabilities of the sorbent and

whether any effect is due to the removal of biotic contamination or from structural changes caused by the high temperatures. An additional application to raw montmorillonite K10 involved acid treatment ($K10_{ACID}$) so as to improve control over the pH of the sorbent environment and to assess the effect on adsorption and enantioselectivity. The unmodified K10 ($K10_P$), acting loosely as a blank for this set of experiments, was pyrolysed for the purpose of removing organic contamination. A quick reference table of abbreviations for section 4.1 is included below:

Table 4.1 Abbreviations for K10 pre-treatments and modifications in section 4.1

Abbreviation	Pre-treatment/Modification
$K10_P$	Pyrolysed K10 clay
$K10_{Na}$	Na-exchanged K10 clay
$K10_{PNa}$	Na-exchanged and pyrolysed K10 clay
$K10_{ACID}$	Acid treated K10 clay (pH 4)
$K10_{Cu}$	Cu exchanged K10

All the modifications strongly adsorbed acephate from the solution (Figure 4.2) in a similar pattern to that previously seen with K10 batch sorption experiments. The similarity between adsorption for the different modifications is notable with most differences falling within the bounds of statistical error. However, it does seem that $K10_P$ was able to adsorb the most acephate in most of the batches. $K10_{ACID}$ provided the least adsorption in the batch with the largest mineral content but only by a very small margin.

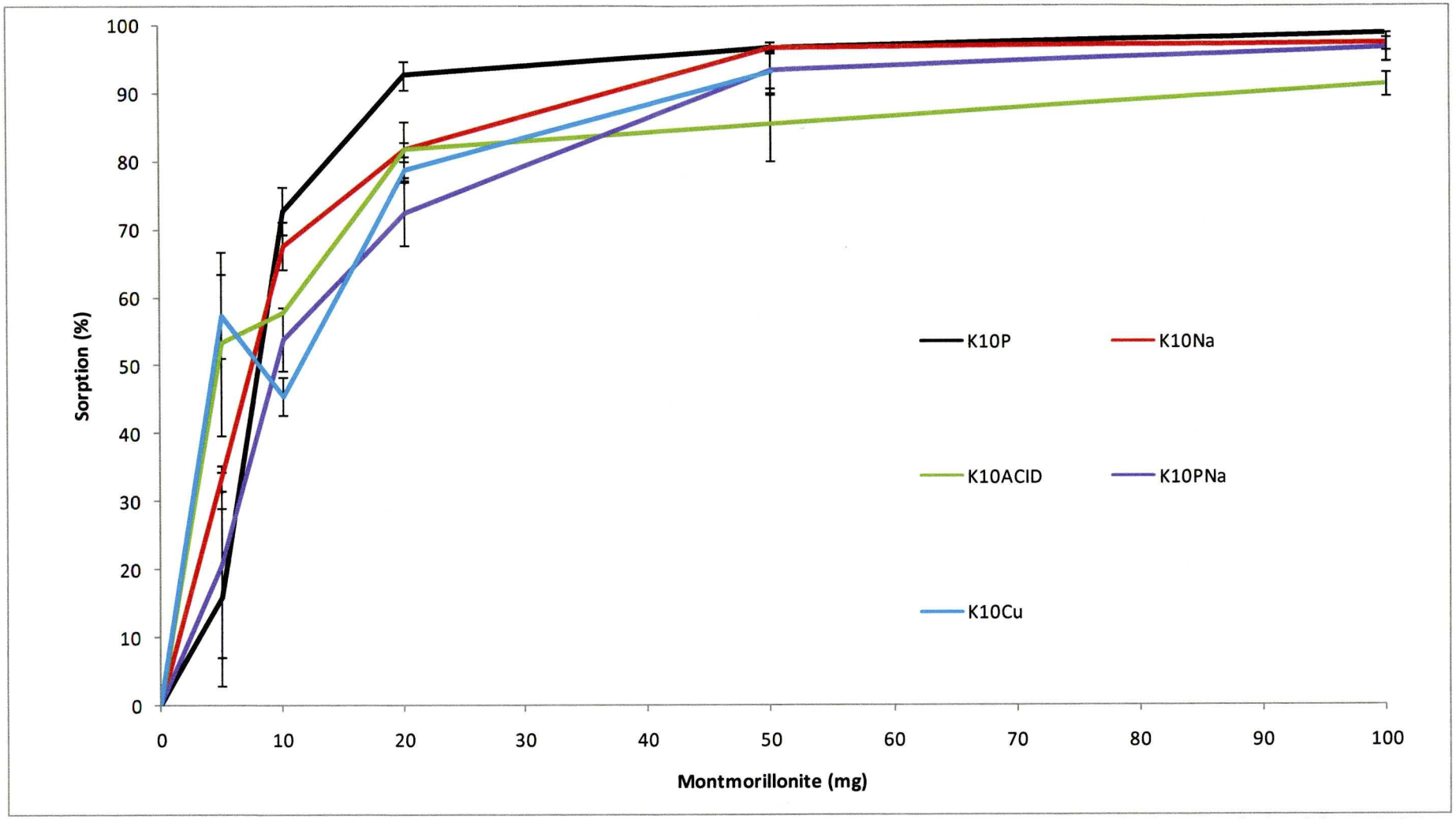

Figure 4.2 Average acephate sorption (%) at the surface of various pre-treated K10 surfaces. Error bars represent the standard error calculated for each data point.

There are also signs of a step in the sorption plot for $K10_{Cu}$. The step occurs in the 10 mg batch and could result from a number of causes and could give insight into the mode of adsorption at the clay surface. A perfect Langmuir isotherm or conformity to the linear form of the Langmuir equation assumes that the adsorption must occur as a monolayer in the interlamellar spaces of the sorbent. However, variation in the form of a stepped isotherm means that adsorption energies must be changing en route to equilibrium. The sorbate is certainly capable of forming a bilayer within the sorbent's interlayer space and thus, there must be a point at which the adsorption mode changes from being a solely sorbate-sorbent interaction, to one where the sorbate can also interact with already bound molecules. Such actions are greatly dependent on layer charge. An increase in the layer charge means a greater amount of cations are needed to neutralize the structure and the more likely they are to interact with each other during the equilibration process. For example an ion that forms a monolayer in bentonite SWy-2 will probably form a bilayer in vermiculite because of the latter's higher surface charge density. As well as the formation of a bilayer, increasing amounts of sorbate in the interlayer can result, depending on the size and shape of the sorbate, in the formation of a paraffinic layer (described in Figure 4.3).

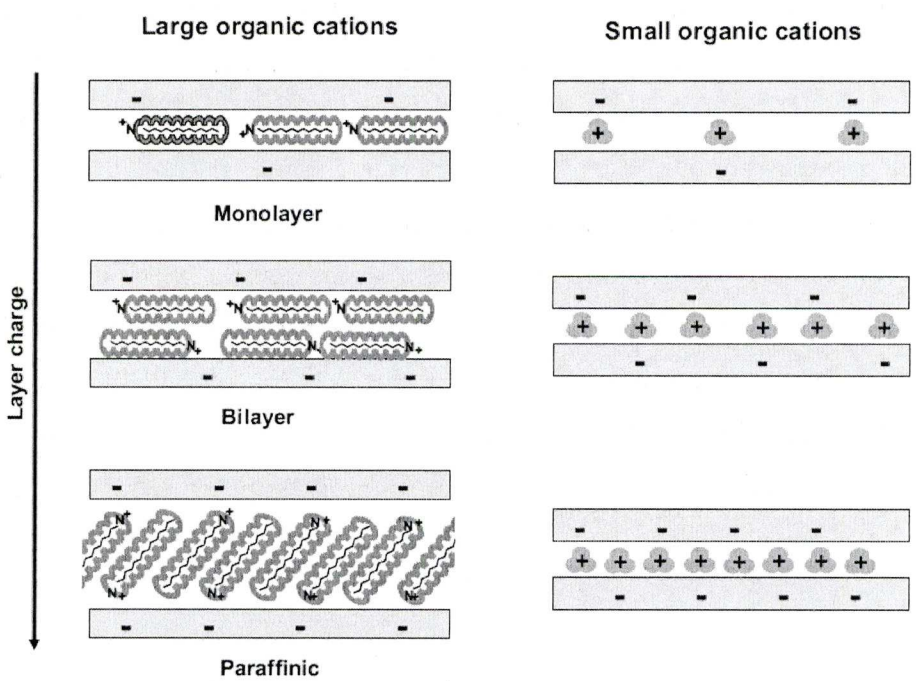

Figure 4.3 Examples for possible arrangements of large and small organic cations in clay mineral interlayers as a function of the layer charge of the clay mineral (Cornejo et al. 2008)

The overall affinity of the sorbate for the clay depends on the nature of both the sorbate and the sorbent. For example a hydrophobic sorbate will have a higher affinity to bentonite SAz-1 (higher charge) than bentonite SWy-2 (lower charge) because the increase in the number of modifier molecules in the interlayer space, present as layers or in a paraffinic structure, means there is less space for water molecules (Cornejo et al. 2008). The same may apply for smaller modifier molecules where an increase in layer charge of the clay will not necessarily mean doubling up of the layers but will mean a decrease in the free space in the interlayer. Presumably polar, hydrophilic sorbates will have a greater affinity for lower charge clays. Either way, a stepped isotherm can indicate cooperative interactions among the adsorbed molecules (Konda et al. 2002). Such interactions, perhaps in the form of surface polymerization, multilayer sorption, or stereochemical interactions, cause the adsorbing molecule to become stabilized on the clay surface within the interlayer space and thus they produce an enhanced affinity of the surface for the sorbate as its surface excess increases (Sposito 2008). At this point stereochemistry can become important and enantioselective adsorption viable as small chiral environments may form stochastically. It is then conceivable that an enantiomeric dissymmetry might then propagate across the whole surface due to steric interference from the already adsorbed species. Nakamura et al. (1988) describe an analogous process involving active $Ru(phen)_3^{2+}$ and Na-montmorillonite. Briefly, they explain that a surface loaded with an enantiomeric excess should exhibit strong enantioselectivity towards further adsorption of a chiral molecule. This is because unoccupied spaces on the partially loaded surface will only accept enantiomers of opposite form into adjacent spaces as a result of steric interference. Fundamentally, the enantiomeric form of the initial molecules adsorbed and the way they orient themselves at the mineral surface appears to be vital in determining the overall selectivity and adsorption capability of the surface.

In general, the pre-treatments and modifications had very little overall effect on the sorption of acephate to the montmorillonite surface (Figure 4.2). It is interesting to note here that SEM micrograph images taken of dried samples for each K10 modification in this section show very little visual variation between batches. Furthermore, the chemical compositions observed in the respective SEM spectra were very similar in each case. The SEM micrograph images and spectra are

presented in the appendix in Figures A1.1 – A1.5. Nonetheless, Figure 4.4, showing the Langmuir conformity plots for the five pre-treated K10 surfaces, can be interpreted to support the idea that two of the pre-treatments cause a change in the sorption mechanism. Batches with $K10_P$, $K10_{Na}$ and $K10_{PNa}$ all yield R^2 values above 0.9. This indicates conformity to the linear form of the Langmuir equation. However, the $K10_{Cu}$batch resulted in a low R^2 value of 0.48 while the $K10_{ACID}$ batch reveals no sign of a proportional relationship at all. Results such as these indicate that the mode of sorption does not conform to the linear form of the Langmuir equation but they do not give any clue as to what the actual mechanism may be.

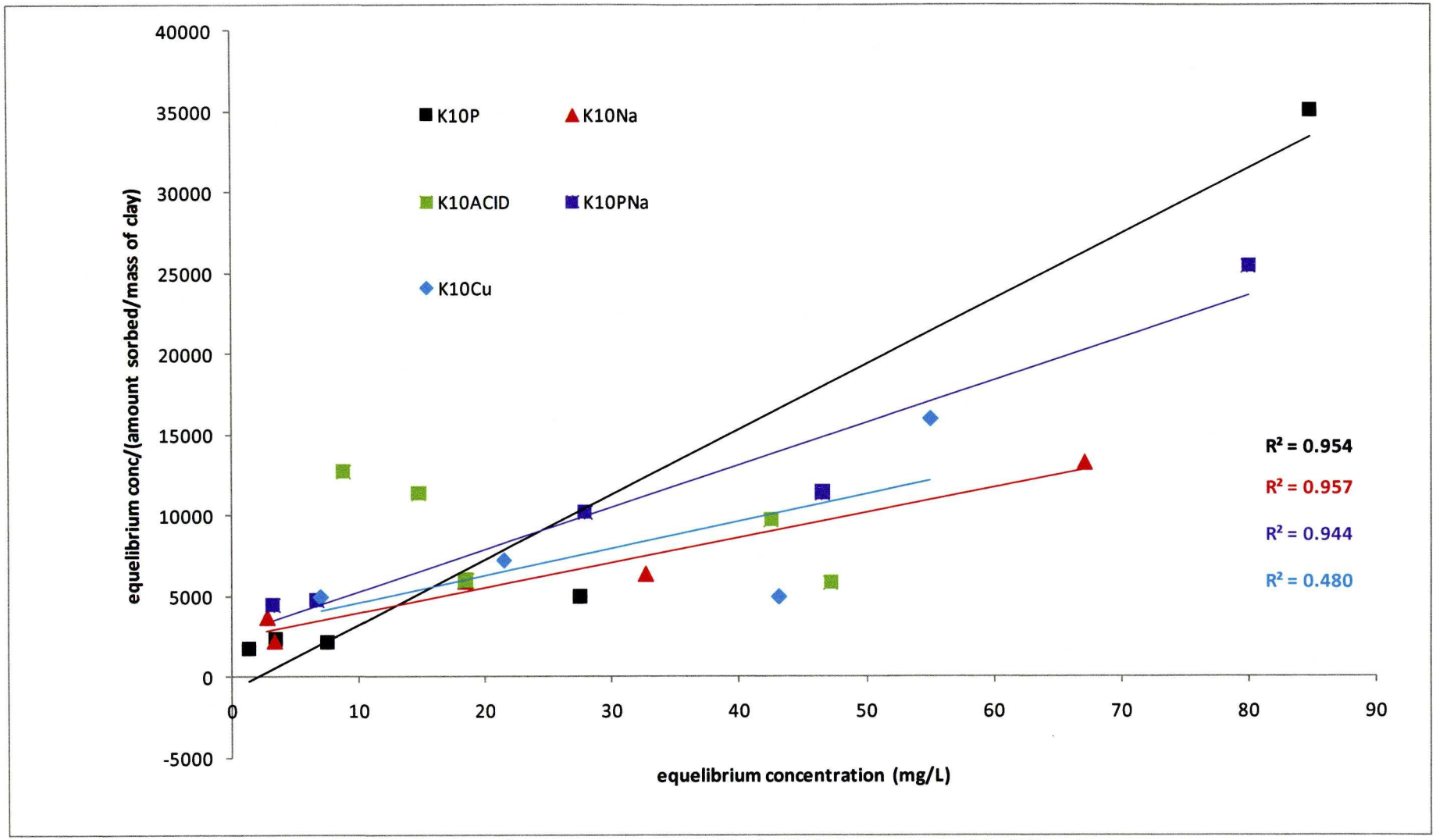

Figure 4.4 Langmuir conformity plot for acephate sorption on several montmorillonite K10 clays pre-treated in different ways.

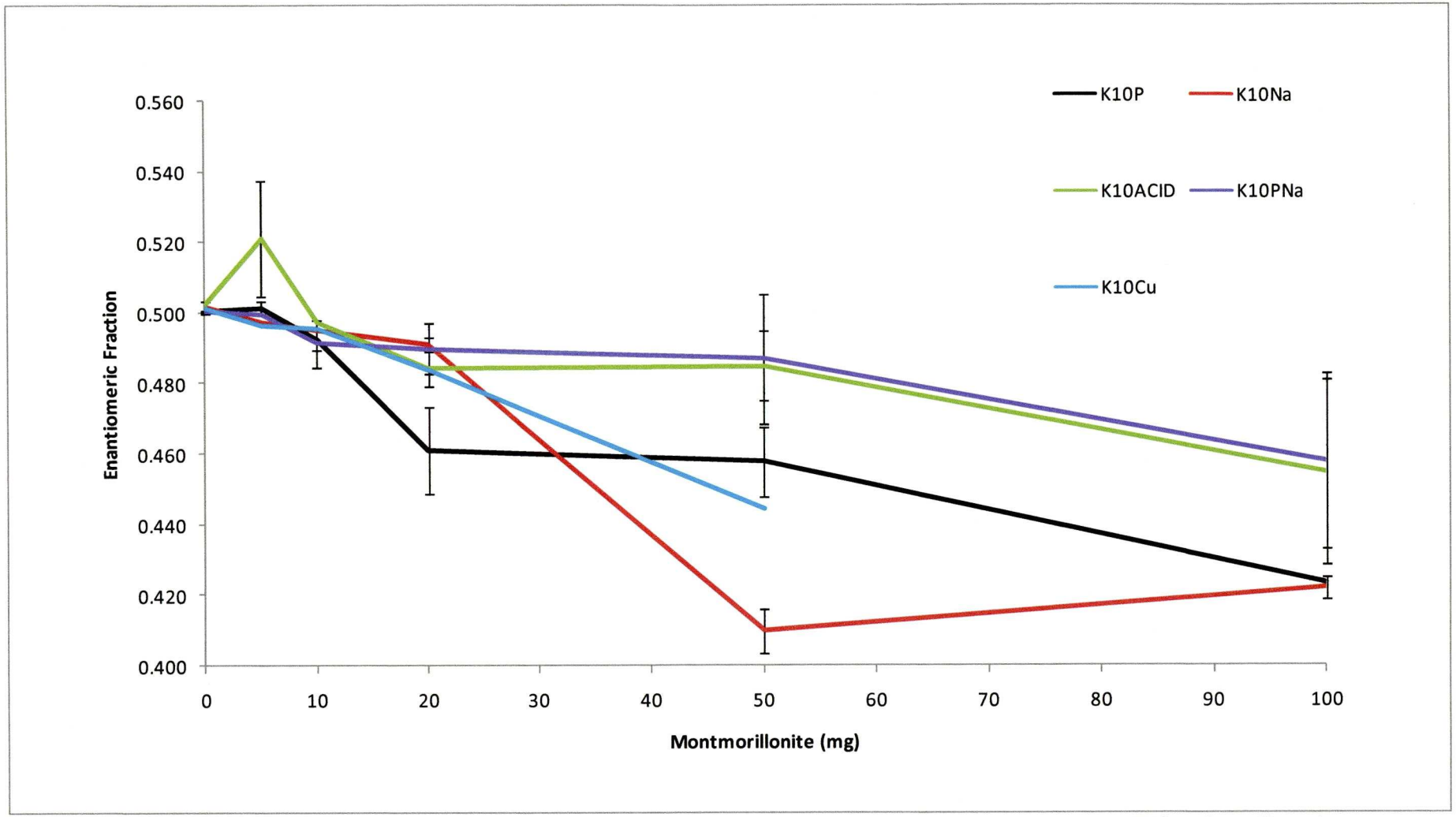

Figure 4.5 EF values for acephate enantiomers in the supernatant after adsorption at the surfaces of a variety of pre-treated K10 surfaces. Error bars represent the standard error calculated for each data point.

The plots of EF variations for different pre-treatments and modifications of K10 (Figure 4.5) yield some interesting results. $K10_P$ shows significant enantiomer selective adsorption of acephate and of a similar order to that seen in Section 3.1. However, in this case, the preference is towards the (+) enantiomer despite the conditions for experiments being essentially identical. All the pre-treated and modified clays display some enantiomer specific selection and all towards the same enantiomer. $K10_{ACID}$ and $K10_{PNa}$ displayed the least preference to the (+) enantiomer overall and had the largest error with the significance of the preference being relatively small. On the other hand, $K10_{Na}$ showed a very strong preference to the (+) enantiomer in the batch with 50 mg of the clay. The selectivity did not increase further in the 100 mg batch. $K10_{Cu}$ also enantioselectively adsorbed acephate in batches up to 50 mg but the 100mg clay batch was unavailable for analysis.

It is clear that enantiomer selective sorption has occurred in at least some of the pre-treated batches. However, the remaining three batches show significant selective adsorption, at least once the sorbate is present at 50 mg or more. The $K10_{PNa}$ and $K10_{ACID}$ exhibit weaker enantioselectivity that is only significant (i.e. greater than the range of the standard error for the data) in the 50 mg batch. This is enough to suggest the specific enantiomer preference is a real observation. Several questions are raised by these observations, in particular:

(1) Why does the observed enantioselective adsorption hold a preference for the (+) enantiomer when in previous experiments under similar conditions K10 has shown a preference to the (−) enantiomer?

(2) Why is there such a marked difference between the enantioselective capacities of Na–exchanged K10 with and without pyrolysis?

In the initial set of K10 sorption experiments where the (−) enantiomer was preferentially adsorbed, it was suggested that the reason for any enantioselective adsorption at all was simply through chance, resulting in a number of neighbouring sorbate enantiomers being of the same sign. A chiral environment would arise and may result in further adsorption being enantioselective. Such unichiral domains resulting in achiral surfaces becoming chiral have been documented (Haq et al. 2009) and are discussed towards the end of the chapter. This coincidental initiation of a chiral environment and subsequent enantioselective adsorption might explain the

difference in sign of the enantioselectivity between experiments and perhaps answer the first question posed above. However, the set of experiments involving pre-treated K10 involved five separate experiments, all of which exhibited some level of preferential adsorption of the same enantiomer. This is unlikely to have occurred by chance. Furthermore, the data for each individual experiment is obtained by at least three repeat runs, which makes the idea that chance alone could determine the enantiomer preference of the sorbent in a given experiment unlikely.

Other work has shown that soils of the same mineral composition, which have displayed enantioselective adsorption of certain organic pesticides, can switch their enantiomer preference to the opposite sign as a result of changes in environmental conditions (Lewis et al. 1999). Hence, adsorption of ruelene and dichlorprop on Brazilian soils resulted in the switch of the sign of enantiomer selective degradation depending on whether or not deforestation had occurred at the sample collection point. Lewis et al. (1999) do not speculate about what property of the soil or the soil environment may have changed due to the differing environmental conditions resulting in such observations. It is worth noting though that the pH of soil in deforested areas is normally significantly lower than in nearby forested areas (e.g. Cavelier et al. 1999). As with the majority of studies of this kind, the authors assume uneven proportions of enantiomers to be due to enantiomer selective breakdown as a result of microbial action. Nonetheless, their work does show non-racemic adsorption at mineral surfaces and highlights the strong effect of environmental conditions on the extent of such enantioselectivity. Another study reported that peat amendment to calcareous soils could reverse the enantioselectivity of the degradation of dichlorprop and mecoprop (Romero et al. 2000). More probingly, however, Buerge et al. (2003) investigated the effect of pH on the enantioselective degradation rates of the fungicide metalaxyl. They found that in soil residues where pH values were > 5 the [S] enantiomer of metalaxyl was larger than the [R] enantiomer. However, when the pH was reduced to < 4, the preference switched and [R] > [S]. They also re-evaluated published kinetic data and found that the herbicides dichlorprop and mecoprop showed similar correlations. It is probable that the primary mode of adsorption in such experiments was biodegradation but such a critical dependence on pH might still apply to experiments carried out in this work. The reversal of enantiomer preference could occur in a sterile environment, provided

the mechanism for the switch comes from the effect of pH on the clay rather than on any biological enzymes present.

With respect to the effect of the solvent on enantioselectivity, one fundamental difference not yet addressed between the two experiments involving acephate and K10 only is the medium in which the sorbate is dissolved. In Section 3.1 the acephate-K10 experiment employed acetonitrile as a solvent whereas water is used when the same experiment is repeated in this section as part of the first set of modified K10 experiments. Table 4.2 displays the solvents used for each experiment discussed so far in this chapter and the sign of the enantioselective preference observed. The table also provides a useful summary of the extent of deviation from the racemic state given as percentages.

Table 4.2 Reference table displaying the minerals used, how they were modified and the solvent in which they were suspended for each batch sorption experiment discussed up to this point in the chapter. The maximum deviation from the racemic state, as a percentage, for acephate enantiomers is also displayed.

Mineral	Modification	Solvent	Maximum Deviation from Racemic (%)
Montmorillonite K10	None	Acetonitrile	9.8
Kaolinite	None	Acetonitrile	1.6
Aluminium oxide	None	Acetonitrile	–
Montmorillonite K10	None	Water	−15.6
Montmorillonite K10	Na+ exchange	Water	−18
Montmorillonite K10	Acid treatment	Water	−9
Montmorillonite K10	Na+ exchange	Water	−8.4
Montmorillonite K10	Cu+ exchange	Water	−11

The effect of the solvent on the enantioselective behaviour of a sorbent towards adsorbing chiral molecules has been reasonably well studied (Tawaki & Klibanov 1992; Hirose et al. 1992; Ueji et al. 1992; Wescott & Klibanov 1994; Carrea et al. 1995; Egri et al. 1996; Fernández et al. 2001; Berglund 2001; Klibanov 2001) and perhaps provides the most likely answer to question (1) above. Fitzpatrick and Klibanov (1991), although not observing the full switch in sign, reported that the enantioselectivity of the substrate was directly affected by certain physicochemical properties of the solvents such as hydrophobicity, dipole moment and dielectric constant. Tawaki & Klibanov (1992) were the first workers to observe a complete reversal in the enantiomer preference of a sorbent due entirely to the solvent used. They found that toluene and acetonitrile as solvents caused a protease enzyme to react strongly with opposite enantiomers of an ester during transesterification. Meanwhile, Hirose et al. (1992) found that different enantiomers of certain esters could be produced with an *ee* as high as 89% simply by changing the solvent from diisopropyl ether to cyclohexane. In this case both solvents were saturated with water. The work of Ueji et al. (1992) showed similar outcomes but with the switch coming as a direct consequence of the polarity of the solvent. They cite specific interactions between the solvent and the substrate resulting in conformational change. It was proposed that changing the solvent caused disruption of the intramolecular hydrogen bonds through the formation of intermolecular hydrogen bonds between the solvent and the substrate. Subsequently, the (R) enantiomer of the sorbate cannot bind correctly to the deformed active site resulting in significant reduction in reactivity of that enantiomer. However, the corresponding (S) enantiomers were less affected by the deformed active site because they did not accommodate well, even before the solvent was changed. So, in this case, the reversal in enantioselectivity of the substrate is due to the ability of the (R) enantiomer to bind to the deformed active site becoming lower than that of the (S) enantiomer. This could apply to the experiments here, whereby the active sites of the clay surface are disrupted with the change of solvent from acetonitrile to water. This might also explain the reduction in overall sorption observed in some later experiments using water as the solvent.

More recently, Fernández et al.(2001) provided a relevant example of solvent induced enantioselectivity reversal on a complexed clay catalyst and subsequent

mechanistic explanation. They argue that a decrease in the dielectric constant of the solvent will increase the electrostatic attraction between the cationic intermediate and the anionic clay sheet resulting in the intermediate being physically closer to the clay surface. The proximity of the clay sheet affects the symmetry of the intermediate complex involving it in the steric environment of the active sites potentially responsible for enantioselective adsorption. Thus the relative energies of the transition states and the stereochemical course of the reactions are modified. The reversal of enantioselectivity observed in experiments in this work could be due to a similar mechanism and, in addition, it could then be inferred that the cationic intermediate remains involved in the adsorption process rather than being removed through an exchange process.

Resolution of the second question is likely to come from determination of what special properties emerge in clay that has been pre-pyrolysed. There are surprisingly few papers that outline the effects of high temperature pre-treatment of aluminosilicate clays (Yilmaz 2003; Miller et al. 1982; Bradley & Grim 1950). It is clear that the heating of a clay mineral can cause a change in the way cations are sorbed in the interlayer spacing. Under standard conditions in an aqueous, colloidal suspension the cations would normally be hydrated. This means they are surrounded by polar water molecules. Since 2:1 silicate clays such as montmorillonite can be viewed as having a layered oxygen structure with sites of localized negativity they are therefore weak electron donors. As such, the dissolved cations can interact with the clay surface through hydrogen bonding. This is possible due to their primary and secondary spheres of hydration, which can act as dielectric links between two point charges (the cations and the clay surface oxygen atoms)(Miller et al. 1982). Even at normal temperatures the clay will not always be fully hydrated and thus some cations will reside directly on the interlayer surface within the hexagonal holes created by the tetrahedral silicate layers. In fact cations with low hydration energies (< 100 kcal/mol) will tend to prefer this form of interlayer sorption (Miller et al. 1982). Na^+, the main cation component of the K10 interlayer, has a hydration energy of ~ 97 kcal/mole (Wulfsberg 1991). It will, therefore, most likely adsorb at the interlayer surfaces via a combination of both mechanisms but require heating in order to cause further dehydration of the cations and more cases of direct residence at the interlayer surface. Furthermore, subjection to high temperature pre-treatment may also allow a

third mechanism for the clay to neutralise its charge. In some cases the dehydrated cation may pass through the base of the hexagonal hole where it resides and fill the vacant octahedral site in the central aluminosilicate layer. This mechanism is only possible in the case where certain criteria are satisfied. At room temperature the radius of the cation should optimally be 0.74 - 0.87 Å (McBride 1976) and since Na^+ has a radius of 1.16 Å, this is an unlikely mechanism. However, if a large enough energy input is applied charge neutralisation by this method can be achieved and, furthermore, it becomes possible for cations of larger radii to interact in this manner. Octahedral migration generally results in more effective charge neutralization and preferential collapse of the interlayer. Reddy et al. (2009) also noted that high temperature (400 °C) pre-treatment of K10 caused layer collapse although it is unclear whether the process is reversible on rehydration in deionised water. Brindley & Ertem (1971) suggest that for clays having interlayer cations with large hydration energies, re-expansion can occur even when extensive charge neutralization has taken place. Presumably this is not the case when Na+, with its low hydration energy, is the predominant interlayer cation. In many cases, with high temperature pre-treatment, hydrolysis may occur as a means of charge neutralization. However, the relatively low hydration energy of Na^+ means that hydrolysis is unlikely to occur in a predominantly Na-montmorillonite such as K10 (Miller et al. 1982). In general, it seems likely that the pre-heating (400 °C) of Na-exchanged K10 will have caused some level of irreversible interlayer collapse. This does not necessarily mean a reduction in adsorption capabilities towards an organic sorbate but does mean the mechanism of such adsorption may partially change.

4.1.1 Temperature Pre-treatment of Montmorillonite K10

As previously discussed, temperature can have a significant effect on the interlayer structure of clay minerals and, thus, on the adsorption of organic species. Three sets of batch sorption experiments were conducted with the same K10 clays pre-heated at different temperatures. The aim was to determine the effect of temperature on the sorptive and enantioselective capabilities of K10. The equilibration period was reduced to 18 h to prevent excessive sorption and subsequent difficulties with detection in the supernatant. The three batches involved K10 that had previously been unheated ($K10_{RT}$), heated to 105 °C ($K10_{105}$) or heated to 400 °C ($K10_{400}$). $K10_{RT}$ exhibited the strongest sorptive capacity of the three batches with ~77%of the

acephate left in the supernatant after equilibration. The amount of sorption then decreased by a small amount in the $K10_{105}$ batch and further in the $K10_{400}$batch indicating that temperature pre-treatment may have a detrimental effect on the sorptive capabilities of K10.

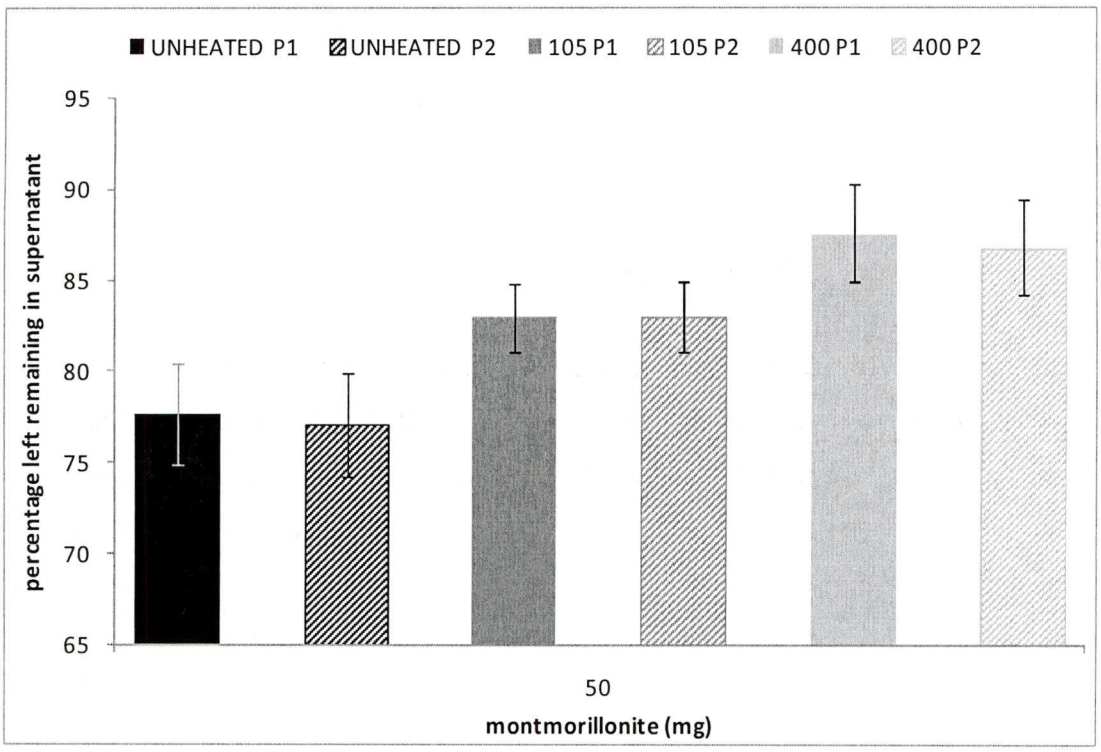

Figure 4.6 Effect of temperature on acephate sorption at the surfaces of K10 clay; each batch involves 50 mg of sorbent. P1 refers to the enantiomer eluted from the column first and P2 second. Error bars represent the standard error calculated for each data point.

The subsequent calculation of EFs (Figure 4.7) provides no indication of significant deviation from the racemic state of acephate enantiomers. These observations indicate that despite having a small but significant reducing effect on K10's sorptive capabilities, high temperature pre-treatment does not impact on any enantioselective properties the clay might possess or have adopted.

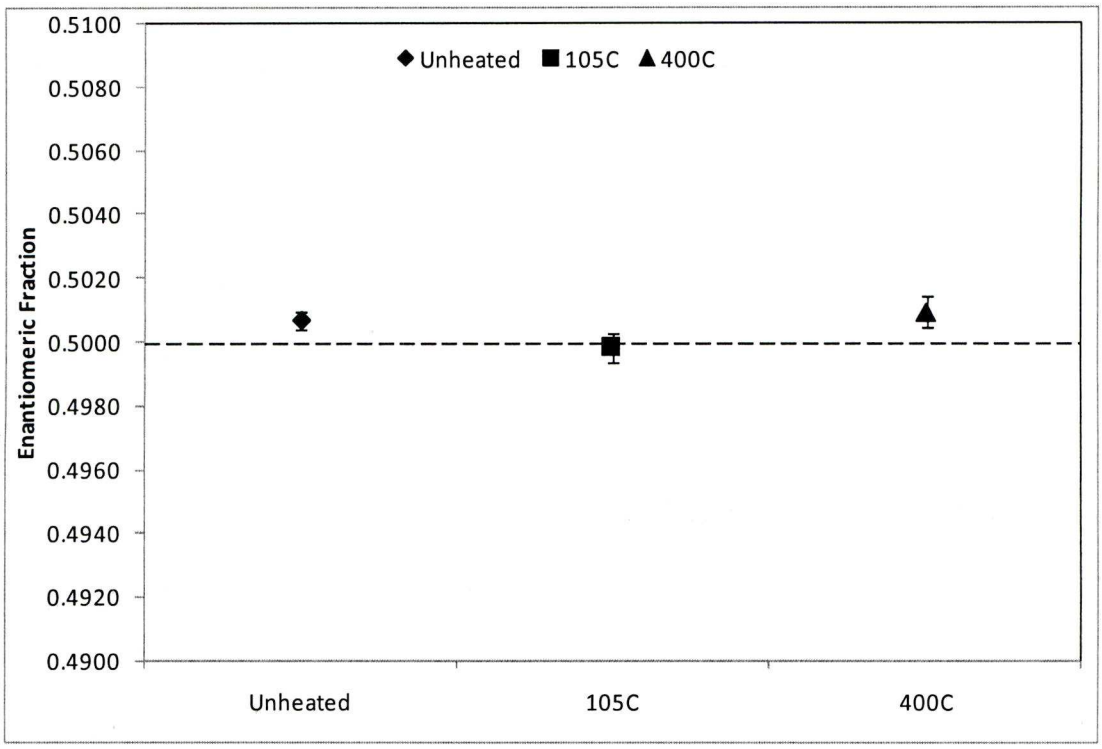

Figure 4.7 EF values for a variety of temperature pre-treatments to K10 after acephate sorption. Error bars represent the standard error calculated for each data point while the black dotted line represents a racemic mixture of the two enantiomers.

This simple batch sorption experiment deals only with a K10 clay that, despite pre-heating, is otherwise untreated. The identity of one or more cations that might be present in the interlayer space has not been confirmed in this work or by the supplier, Sigma Aldridge. However, it is likely that a variety of cations, including Na^+, K^+, Ca^{2+} and Mg^{2+} are present (Shanbhag & Halligudi 2004). Shanbhag & Halligudi also suggest that trivalent cations such as Al^{3+} are likely to be present and contribute to the Brønsted acidity of K10. This is significant because it means that by Na-exchange K10 is transformed from having a multitude of cations occupying the interlayer space to having solely Na^+.

So under normal circumstances the pre-pyrolysis of K10 should have a small impact on the adsorption of acephate but negligible effect on any enantioselective activity. However, once Na-exchanged, the pre-pyrolysis of K10 results in a very small reduction in sorption *but* significantly reduces the observed enantioselective behaviour. As previously discussed, it appears that high temperature pre-treatment has a profound effect on how Na^+, but not necessarily other cations, is bonded to surfaces within the K10 structure. It seems, therefore, that the mechanism for enantioselective adsorption involves interaction with the interlayer cation and that

this mechanism is hindered by net movement of the cation from its state as a hydrated ligand towards positions within hexagonal holes on the interlayer surface or even in vacant octahedral sites within the aluminosilicate layer. Alternatively, it may be the organic sorbate's interaction with the hexagonal holes that is hindered by the change in the way Na^+ is bound causing a reduction in the enantioselective adsorption of the sorbate. The mechanism of enantioselective adsorption remains unclear.

4.2 Batch Sorption Experiments Involving Acephate (100.5mg/L) and Montmorillonite-Cu-L-Lysine Complex

The interesting results of the batch sorption experiments involving different montmorillonite K10 clays with modified interlayer environments, led to modifications. The hypothesis tested was that inclusion of a chiral organic species in the interlayer space, as a complex with the exchangeable cation, would yield information about the adsorption capabilities of such a complexed clay and its ability to preferentially adsorb enantiomers of acephate. Furthermore, insight into the adsorptive mechanisms at work and the whereabouts of their occurrence might be inferred. Lysine was chosen as it is a common amino acid, one of life's essential building blocks. Complexes were prepared with both the biologically active L- form of lysine and the inactive D- form. Cu^{2+} was also exchanged into the interlayer in the preparation process to form part of the complex thereby removing the unknown element of the ionic contents of the interlayer space. Furthermore, copper is known to interact strongly with amino acids and hence should be a good choice for attaching amino acids to a clay surface. Additionally, the guaranteed removal of Na^+ cations from the interlayer meant the potential for reduction in enantiomeric activity, caused by the binding mechanism of said cation (Section 4.1), was eliminated from the experiments.

Batch sorption experiments involving acephate and the K10-Cu-L-lysine complex ($K10_{LL1}$) yielded a sorption plot (4.8) similar to that in previous K10 sorption studies in this work. Increasing amounts of sorbent in the batches resulted in increased sorption of acephate. Again, the increase in the amount of acephate adsorbed decreased with greater sorbent amounts in the batches giving the familiar curved plot line. The 100 mg sorbent batch has a very small standard error indicated by the error bars (Figure 4.8) and shows the sorption of over 90 % of the acephate from the

supernatant solution. The EF correlates very strongly with sorption and despite exhibiting relatively large errors, shows very significant preferential adsorption of acephate's (+) enantiomer. This is a preference for the same enantiomer of acephate as observed in the pre-treated batch experiments but, of course does not correspond to the preferential adsorption of the opposite enantiomer in the initial experiments with K10 alone.

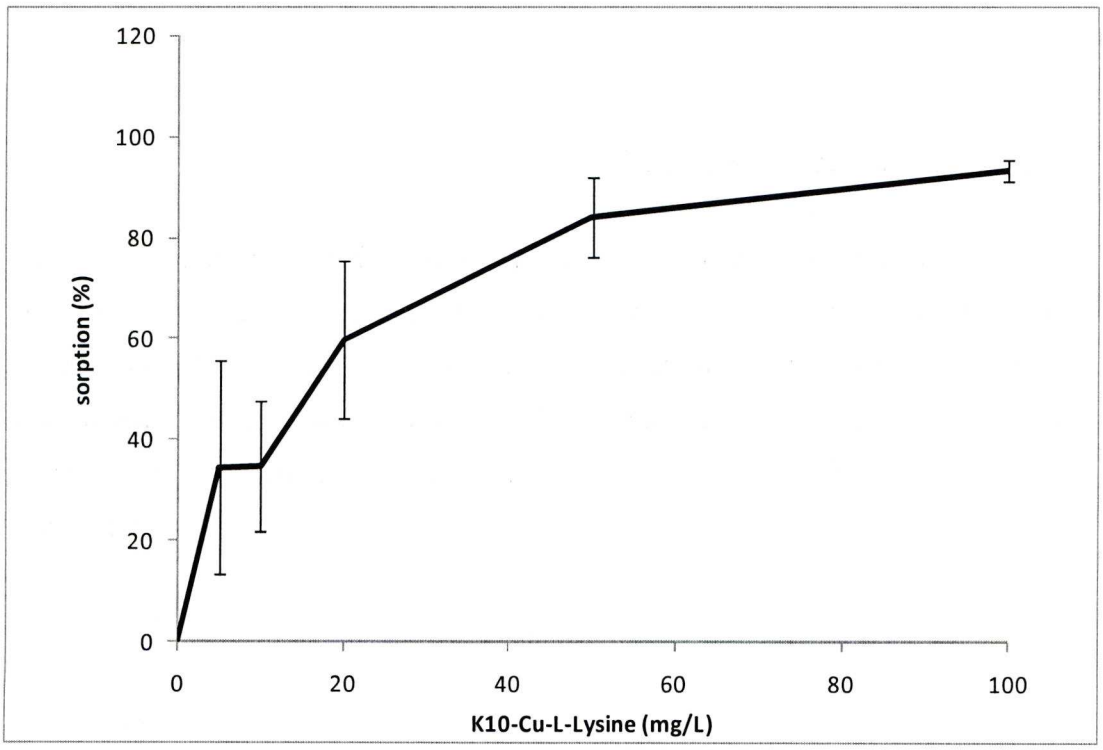

Figure 4.8 The amount of acephate sorption (%) at the surfaces of Cu-L-lysine modified K10. Error bars represent the standard error calculated for each data point.

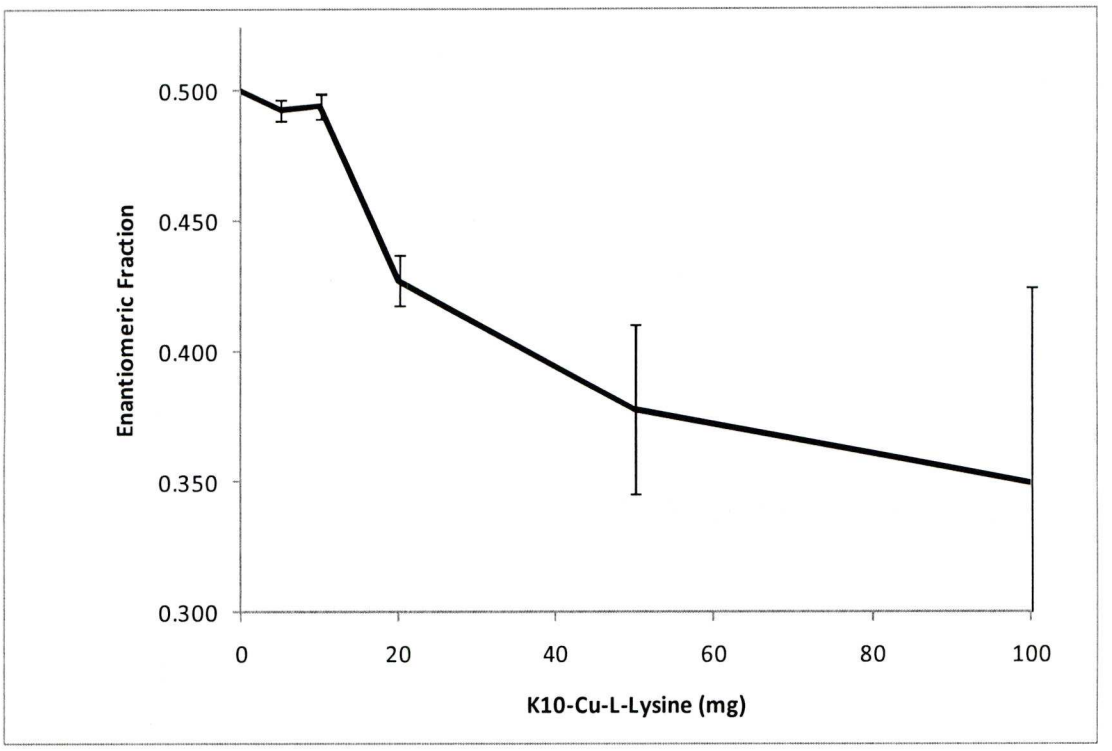

Figure 4.9 The EF of acephate remaining in the supernatant solution after adsorption at the surface of Cu-L-lysine modified K10. Error bars represent the standard error calculated for each data point.

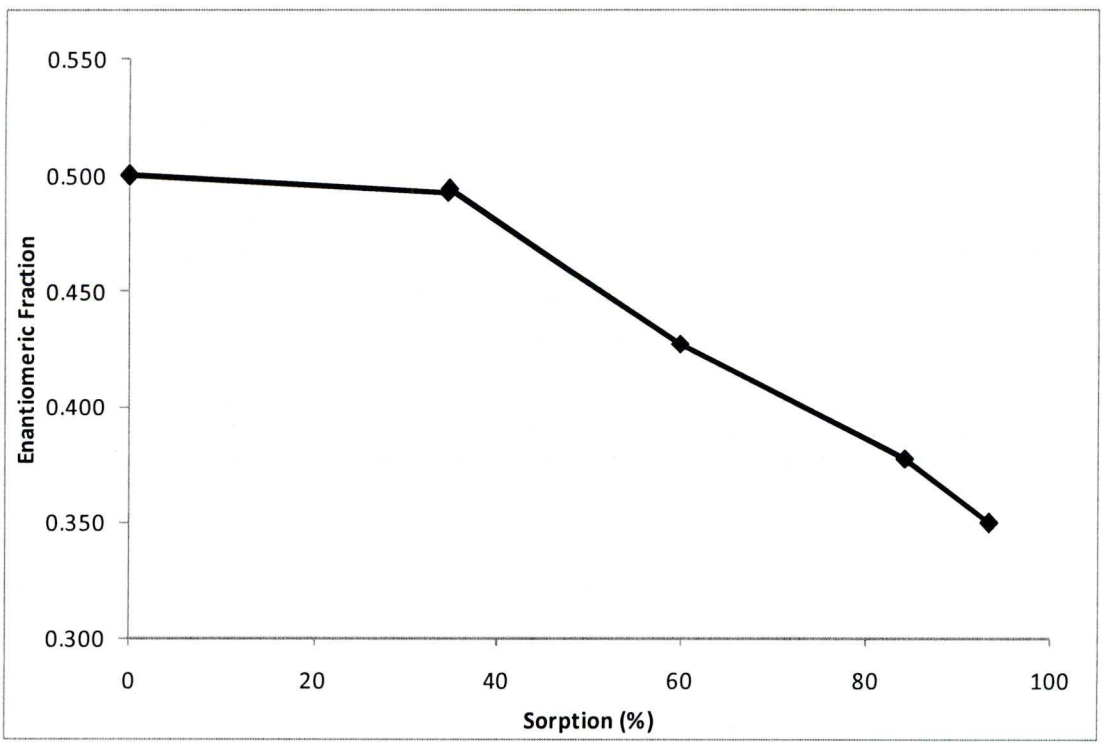

Figure 4.10 Sorption of acephate (%) on the surface of Cu-L-lysine modified K10 plotted against the subsequent EF values for the enantiomers of acephate.

An interesting feature of the sorption plot for acephate on $K10_{LLI}$ (Figure 4.8) is the slight sign of a step feature in the 10 mg batch. Between the 5 and 10 mg batches there is no increase in the amount of acephate sorbed following a very similar path to that of acephate on $K10_{Cu}$ discussed above. In this case the observation is not necessarily significant as any deviation from the suspected pattern lies well within the standard error of the data points indicated by the error bars and is, thus, unlikely to be a real result. Considering, however, that in both cases this feature has occurred involving a K10 sorbent with a Cu-exchanged interlayer, it is an observation worth noting. Again, the idea that the sorbate molecules are interacting as they adsorb and affecting adsorption energies must be considered. In this case, there is also a link to the enantioselectivity; no significant deviation from the racemic state is observed in the EF plot until after the 10 mg batch (Figure 4.9). Since this is the point at which the step occurs, it seems indicative that the interaction between adsorbing molecules and those already adsorbed is required for enantioselectivity to occur. Perhaps a chiral environment formed by adsorbed molecules of acephate is a key factor in further enantiomer selective adsorption. This point is reiterated in Figure 4.10 independently of any step feature: initially as adsorption increases, enantioselectivity (derived from deviation from the racemic state) is negligible but after ~35% sorption it increases rapidly and steadily, suggesting that a certain level of acephate coverage must be achieved for the extent of enantioselectivity to become significant.

The preferential adsorption of the (+) enantiomer to $K10_{LLI}$ is extremely pronounced. However, given the range of the standard error for the 50 and 100 mg batches (Figure 4.9), the enantioselectivity may not be as large as implied. Nonetheless, even taking the error range into account, the deviation still appears to be larger than in any other experiment conducted throughout this work. A comparison to the previous $K10_{Cu}$ batch sorption experiment gives an indication that inclusion of a single-enantiomer amino acid to the K10 interlayer has a significant positive effect on the strength of its enantioselective capacity. It is likely that the formation of such a chiral complex provides a secondary mechanism for enantiomer specific adsorption thus enhancing the overall enantioselectivity of the clay towards molecules of acephate. Tsvetkov & Mingelgrin(1987b) prepared a montmorillonite-Cu-L-lysine complex very similar to the one used here and showed that such modified clay could provide an adsorption system that displayed a stronger affinity for a particular enantiomer of

some α-amino. Theng (1974) explains, from the work of Bodenheimer & Heller(1967), that the strong adsorption of lysine by copper-montmorillonite was attributed to the presence in the lysine zwitterion of a basic (amino) group which could coordinate to copper. Further work (Jang & Condrate 1972) indicated that the species coordinated to interlayer Cu ions in montmorillonite has the zwitterionic configuration (Figure 4.11):

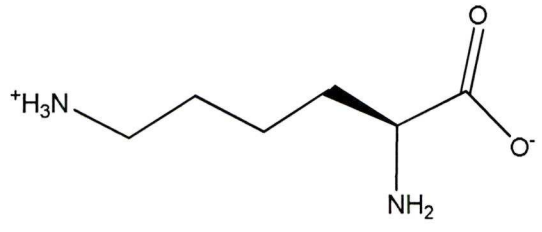

Figure 4.11 Zwitterionic configuration of lysine coordinated to interlayer Cu ions in montmorillonite (structure confirmed by Jang & Condrate 1972)

The pH of the equilibrated suspension lies at between 8.5 and 9. Since the pKa values for the α-amino and ε-amino groups are 8.95 and 10.53 respectively, the ε-amino is certain to be protonated while there may be a mixture of both protonated and un-protonated α-amino groups. The carboxylic group with a pKa of 2.18 will remain un-protonated and negatively charged. As such, this is a reasonable configuration for the lysine molecule in the experiments carried out here. Tsvetkov & Mingelgrin (1987b) suggest that a double ligand is formed between two molecules of lysine and a single Cu^{2+} cation. The binding process involves a biligand complex formation utilising the zwitterionic configuration above where the α-amino group and the carboxylate oxygen of lysine are bound to Cu^{2+} while the ε-amino group is protonated. This gives the complex a positive charge and allows strong adsorption on the negatively charged clay surface. In this respect, lysine is an excellent choice for the formation of a clay-Cu complex, as it is one of the few α-amino acids that is capable of forming the biligand complex which is responsible for its strong clay binding ability. The resulting complex is depicted in the following schematic (Figure 4.12).

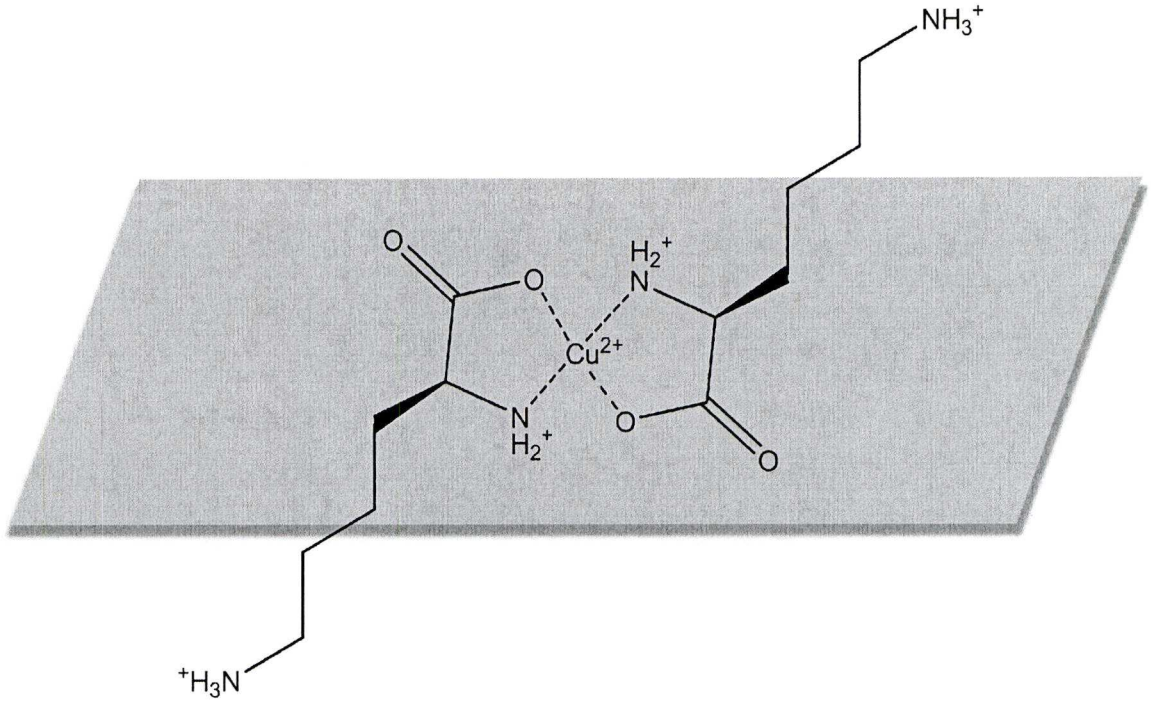

Figure 4.12 Schematic representation of the probable formation of Cu-lysine complex at the surface of K10 clay (grey box)

Tsvetkov & Mingelgrin (1987b) proposed that the mechanism of optical resolution involved ligand exchange. They argued that exchange was most probably between at least one of the lysine molecules in the Cu-lysine complex and the molecule being adsorbed. Furthermore, this could have been followed by cation exchange between the adsorbed Cu-lysine complex and both the released lysine and the complex formed by the ligand exchange. The data they presented suggest that a mixed ligand involving the Cu^{2+} cation binding with one of the original lysine molecules as well as the newly adsorbed amino acid was formed by ligand exchange. This ligand exchange was responsible for the optical resolution. This could apply to the experiments here with the acephate molecule forming part of the mixed ligand instead of Tsvetkov & Mingelgrin's newly adsorbed amino acid. Furthermore, the addition of this mechanism as an extra source of acephate adsorption might explain the increased enantioselectivity observed in the K10-Cu-L-lysine experiment (Figure 4.9).

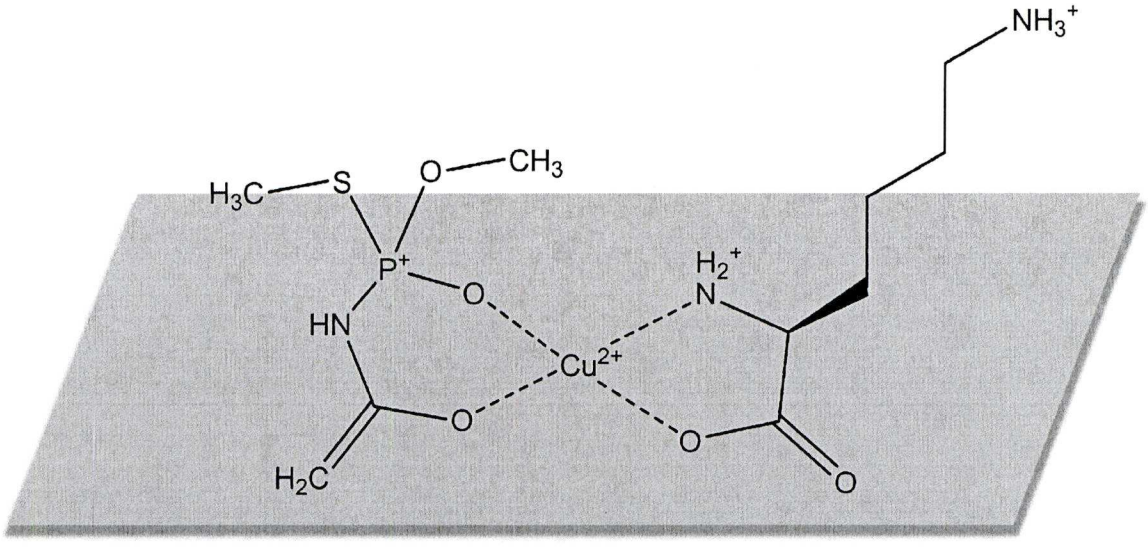

Figure 4.13 Schematic representation of ligand exchange where one of the bound lysine molecules is replaced by an acephate molecule resulting in a Cu-L-lysine complex bound at the surface of K10 (grey box) (complex adapted from Tsvetkov & Mingelgrin 1987b)

4.3 Batch Sorption Experiments Involving Acephate (100.5mg/L) and Montmorillonite-Cu-D-Lysine Complex

Montmorillonite-Cu-D-Lysine ($K10_{DL1}$) also strongly adsorbed acephate from its aqueous solution. However, Figure 4.14 suggests sorption in a linear fashion indicating the mechanism for sorption may have been different and thus subject to different sorptive properties. It must be noted that the errors allow for substantial deviation from the shape of the graph. As such the linear nature of the relationship between acephate and $K10_{DL1}$ is not assured. Again, the EF is well correlated to the amount of sorption and displays strong preferential adsorption of the (+) enantiomer of acephate in the 50 mg sorbent batch. Overall, however, the enantiomer specific sorption is more pronounced for $K10_{LL1}$ than $K10_{DL1}$. This was somewhat surprising as the same mechanism of sorption was expected for complexes containing either enantiomer of the amino acid.

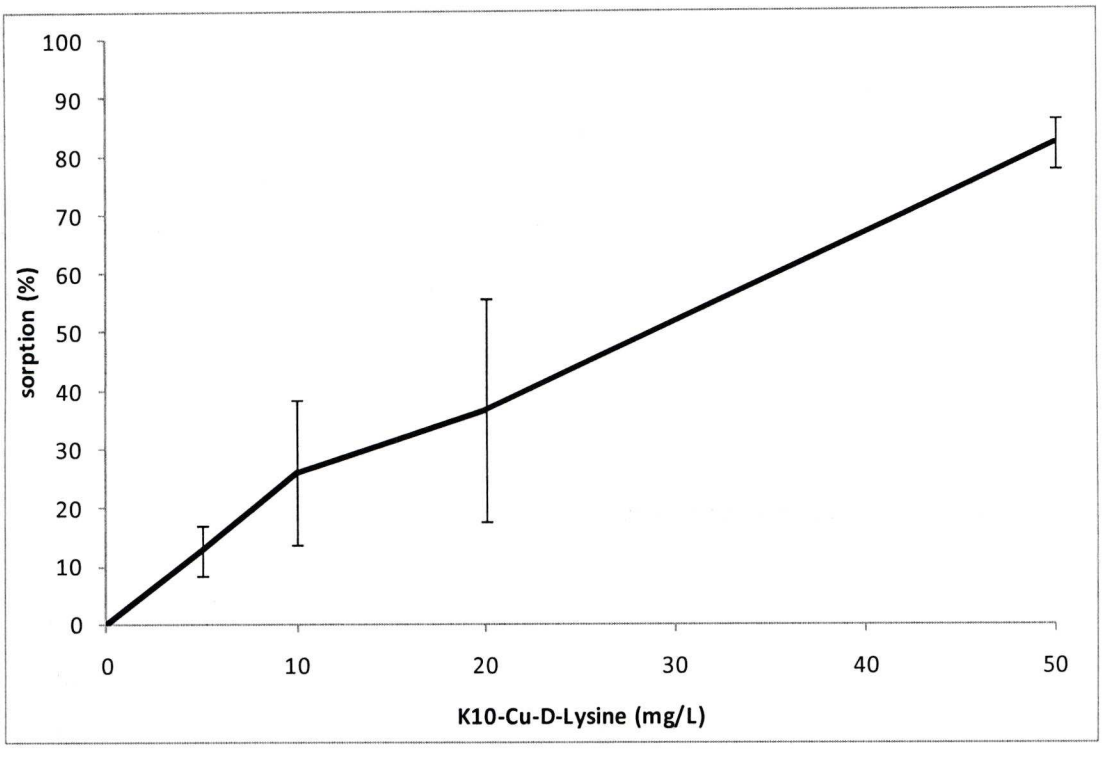

Figure 4.14 The amount of acephate sorption (%) at the surfaces of Cu-D-lysine modified K10. Error bars represent the standard error calculated for each data point.

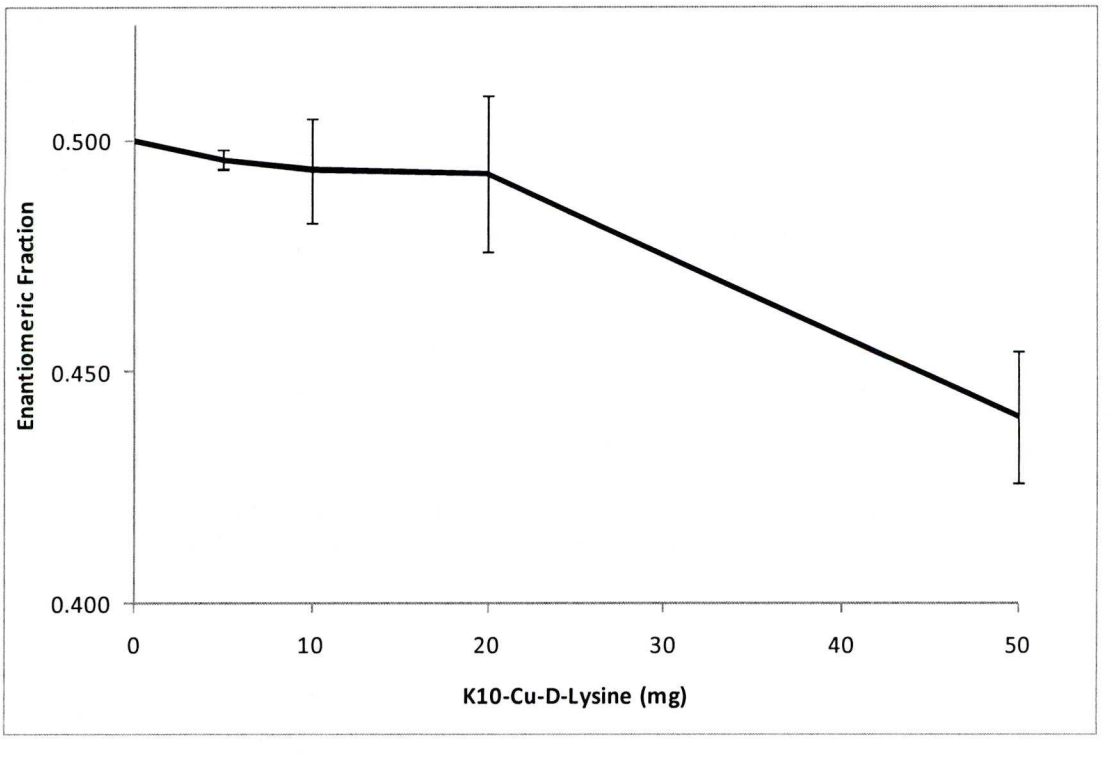

Figure 4.15 The EF of acephate remaining in the supernatant solution after adsorption at the surface of Cu-D-lysine modified K10. Error bars represent the standard error calculated for ach data point.

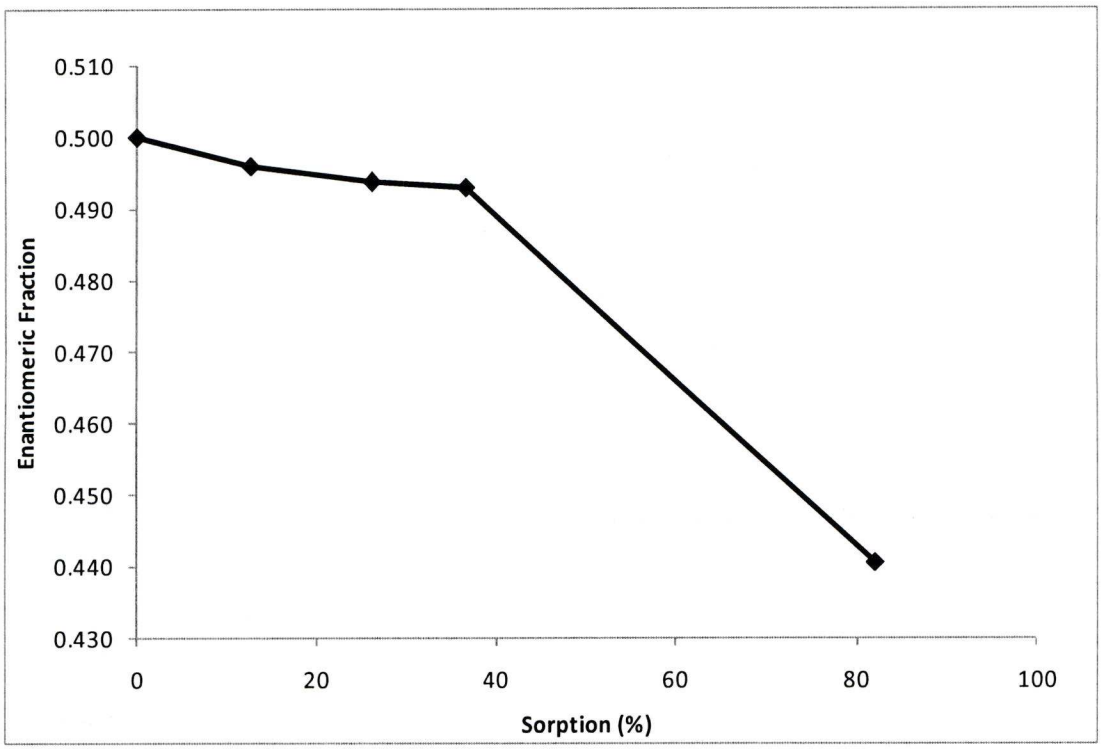

Figure 4.16 Sorption of acephate (%) on the surface of Cu-D-lysine modified K10 plotted against the subsequent EF values for the enantiomers of acephate.

Despite the lower enantioselectivity seen in the $K10_{DL1}$ batch (Figure 4.15) and the slower adsorption rate (seen from the difference in shape of the plots in Figure 4.8 and Figure 4.14) the plot comparing sorption and enantioselectivity is very similar to that observed in the $K10_{LL1}$ batch. Enantioselectivity remains relatively small until after ~40% of the acephate is adsorbed reinforcing the idea that there must be a significant amount of acephate adsorbed at the clay surface before any enantioselective adsorption can be achieved.

A particularly interesting feature of these results is the fact that $K10_{LL1}$ (Figure 4.9) and $K10_{DL1}$ (Figure 4.15) do not show preference to the opposite enantiomers of acephate. This observation contradicts that of Tsvetkov & Mingelgrin (1987b) who demonstrated that switching the sign of the lysine molecule in the clay-Cu complex resulted in preferential adsorption of the opposite enantiomer for a variety of amino acids. This might have been expected as the sign of the overall asymmetric centre of the clay-Cu-amino acid complex would be reversed. The contradiction also applies to the binding process discussed earlier in this chapter (Section 4.3) that leads to the enhanced enantiomer specific resolution of acephate on $K10_{LL1}$. However, there may be a very specific characteristic of the clay surface that causes the geometry of the

complex adsorption to be different between the two systems (containing either the (+) or (-) enantiomer). As the complex resides at the clay surface within the interlayer space, the way it interacts, and more specifically, the way the complexed acephate interacts with the clay surface will be vital to the enantioselective nature of the continuing adsorption. If one option is to bond in a way that hides the chiral centre of the complexed acephate, for example, then enantioselectivity may be significantly reduced as further adsorption occurs throughout the equilibration process. If this is the case then it provides further evidence for the idea that enantioselective adsorption relies on a stereoselective interaction between the newly arriving sorbate and those already bound in the early stages of equilibration. Furthermore, it provides an alternative to the idea that the montmorillonite itself shows a preference to one enantiomer over the other. At least in the early stages of adsorption montmorillonite need not adsorb more of one enantiomer than the other, it simply needs to interact with them in different ways in terms of the geometry of adsorption.

4.4 Batch Sorption Experiments Involving Acephate (100.4mg/L) and Montmorillonite modifications

The previous batch sorption experiments yielded interesting results but were based on quite a small data set. Here, the same modifications were repeated and the experiments run with more replicates and therefore improved reliability. The predominant difference in the method was that the only batches prepared contained the maximum mineral amount from the previous set of experiments (50 mg). Since averaging the batches produces only one value for the sorption of each enantiomer, the results are presented in the form of a histogram (Figure 4.17). Additionally, with a set amount of sorbent in each batch, the sorption can be displayed in mg/g of clay. The total amount of acephate available in each sample equates to 1.51 mg/g of clay. Overlaid on the plot are the EF results for each modified batch. A quick reference table of abbreviations for section 4.4 is included in Table 4.3:

Table 4.3 Reference table of abbreviations for further K10 modifications in Section 4.4

Abbreviation	Pre-treatment/Modification
$K10_{BL}$	Unmodified K10 clay
$K10_{Cu}$	Cu-exchanged K10 clay
$K10_{LL}$	L-lysine-exchanged Cu-K10 clay
$K10_{DL}$	D-lysine-exchanged Cu-K10 clay
$K10_{LL+}$	L-lysine-exchanged Cu-K10 clay (fully saturated L-lysine due to higher concentration additions)
$K10_{S}$	Derivatised K10 clay through silanisation

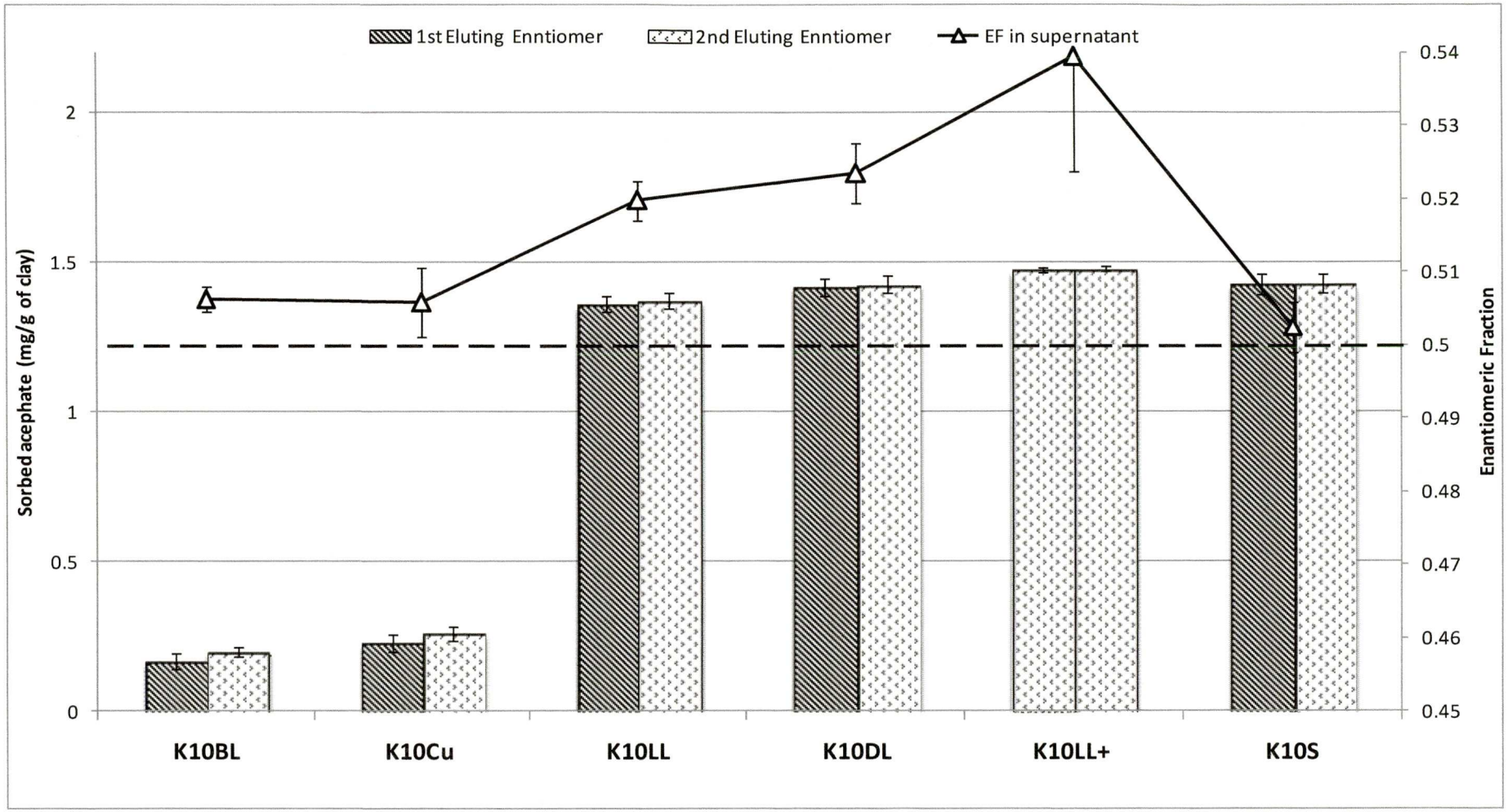

Figure 4.17 (Column plot) the amount of acephate sorbed (mg/g) at a variety of modified K10 surfaces and (line plot) the subsequent EF values for each modification. The total amount of acephate available in each sample equates to 1.51 mg/g of clay. Error bars represent the standard error calculated for each data point while the black dotted line represents a racemic mixture of the two enantiomers.

Comparing the $K10_{LL2}$ and $K10_{DL2}$ batches with the $K10_{LL+}$ batch showed high levels of sorption in each case while a significantly larger preference for the (−) acephate enantiomer was observed in the latter. The $K10_{LL+}$ batch was prepared with greatly increased amounts of L-lysine as there was no guarantee that the ratio of clay to complex being used in the preparation of the standard K10-Cu-lysine batches was sufficient to ensure total saturation of the interlayer with the prepared complex. The sole difference – if the standard batch is not considered fully saturated – is that there would be more occurrences of the biligand structure between the Cu^{2+} cation and the lysine molecule and thus greater capacity for ligand exchange with acephate molecules. If the mechanism proposed above was dominant in enantioselectivity, it would explain the greater deviation from the racemic state of the $K10_{LL+}$ complex. However, the lysine concentration was not measured in the supernatant making it difficult to confirm the existence of an exchange mechanism. Also, it must be noted, that the standard error of the data point for EF in the $K10_{LL+}$ batch is particularly large. Nonetheless, there is still a strong possibility that the mechanism is correct and the results of the two Cu-lysine batch experiments here can be seen as evidence if not proof.

The silanised K10, on the other hand, despite strongly adsorbing acephate shows no preference for one enantiomer over the other. Such a notable absence of any enantioselectivity after silanisation is evidence that the hydroxyl groups, while not playing a significant role in the retention of acephate as an adsorbed species, do have a considerable affect on the clay's enantioselective properties. This is an important observation that requires explanation.

The standard structure for K10, shows hydroxyl groups situated predominantly at severed edge sites of the aluminate layer (see structures in Theng 1974). Since the only mechanism for adsorption at the edge sites would involve the hydroxyl groups and their removal does not affect overall adsorption it can be assumed that adsorption is not occurring at the edge sites. There are, however, further hydroxyl groups situated within the aluminosilicate structure of the clay. Two oxygens out of the three on each side of the octahedral aluminate layer are bound to silicates forming the tetrahedral layer sandwiching the octahedral layer. The third oxygen, facing in towards the interlayer space, exists as a hydroxyl group (see Figure 3.3 in the previous chapter for the general structure of montmorillonite). As it appears that

adsorption probably occurs within the interlayer rather than at edge sites, there must be an interaction with these hydroxyl groups that is not require for adsorption but that is essential for enantioselectivity. Ligand exchange within the interlayer space is unlikely to be affected in any way by the hydroxyl groups effectively shielded by the tetrahedral silicate layer. One situation may be that adsorption occurs at sites where at least some of the adsorbed enantiomers can be affected by the hydroxyl groups in such a way as to be able to provide an environment where one enantiomer of acephate is preferred over the other. This might involve forces of attraction but should not be the principal mode of adsorption. For this to be possible, the adsorption sites must occur at the layer surface, within the hexagonal holes of the tetrahedral layer or, as discussed previously, within the vacant octahedral space after penetration of the tetrahedral layer. Another situation might exist where a small number of acephate molecules do, in fact, bind with the hydroxyl groups. They would be too few to significantly affect the overall adsorption if the hydroxyl groups were removed but in their presence they could provide a unique alteration to the surface that would affect further adsorption of acephate molecules.

On the discussion of hydroxyl groups within the K10 structure, it is worth noting the alternative structure for montmorillonite proposed by Endelman and Favejee (1940). The structure is explained by Theng (1974) and used in the work of some others (Laszlo 1990) and illustrated in Figure 4.18.

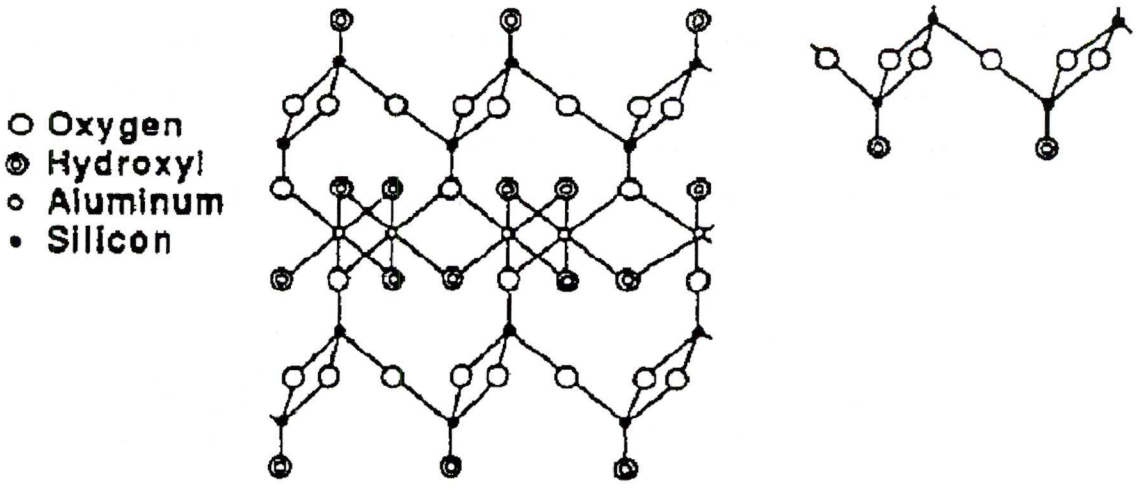

Figure 4.18 An alternative structure for montmorillonite first proposed by Edelman & Favejee(1940) with the apical oxygen atoms facing in towards the interlayer spaces. The drawing is from Laszlo (1990)

They suggest that every other SiO_4 in the tetrahedral sheet is inverted. The apical oxygens on each inverted tetrahedral, now pointing towards the interlayer space, is replaced by hydroxyl groups which also fill the gaps left by in the octahedral sheet. If the Edelman-Favejee structure exists then hydroxyl groups will be much more readily available for interactions with the sorbate. The possibilities already suggested as explanation to the observations above might still be applicable if the alternative structure was in place but the acephate molecules would no longer have to penetrate the tetrahedral sheet in order to interact with the hydroxyl groups.

Theng et al. (1974) suggests that both structures can exist depending on the type of clay in question. *Wyoming* type clay takes on the standard structure and *Cheto* type the Edelman-Favejee structure. Surprisingly, the parent material of K10 is not obviously apparent. Both Loh and Li (1999) and Clark et al. (1994) state that Montmorillonite Tonsil 13 is the source clay for K10 but no further information is provided. However, the chemical composition of K10, determined by Dr. Steve Crowley of the University of Liverpool (unpublished data; Table 4.4), appears quite different to that of Tonsil 13 found in the literature (Adams et al. 1986). Laszlo (1990) depicts montmorillonite in the form of the Edelman-Favejee structure and refers to it in discussion of the catalytic uses of K10. Again, however, no further information or sources for why this structure was assumed correct, was provided.

Table 4.4 The percentage composition of unmodified K10 including the three predominant mineral elements attained from XRD analysis.

Predominant Minerals	Composition (%)
Smectite	56.01
Quartz	29.03
Muscovite	14.97

A particularly notable observation in Figure 4.17 is that the $K10_{BI}$ and $K10_{Cu2}$ batches show an extremely low capacity for adsorption, relative to that of the other batches in this experiment but also to that of previous experiments. The reason for such low levels of adsorption is unclear but one of the outcomes is that a smaller amount of adsorption will probably be mirrored by EFs denoting smaller deviation from the racemic state (which is the case here). This is because it would be assumed

that each adsorbing molecule involves a tiny amount of selective adsorption and therefore selectivity would be directly linked to the amount of acephate sorbed. This might not be entirely accurate in all cases as there may be situations where either (1) all the selectivity occurs in the initial part of adsorption as the first molecules begin binding to the clay surface – this should result in an EF plot in which deviation rapidly occurs in the early stages of adsorption and then plateaus as adsorption continues to increase – or (2) all the selectivity occurs in the later stages of adsorption, perhaps as the adsorbing molecules begin to interact with each other – this should result in an EF plot that only begins to deviate at a late stage in the adsorption process as sorption continues to increase. It is worth noting that scenario (1) is observed in the batch sorption experiments involving kaolinite. This could be expected as kaolinite is known to have some level of inherent structural chirality (as discussed earlier in the chapter) and thus potential for enantioselective adsorption of a chiral sorbate directly at its surface in the early stages of the equilibration process. Conversely, scenario (2) is observed to some extent in the batch sorption experiments involving K10. Likewise this could be expected as K10 lacks structural chirality and would require some level of sorbate coverage before enantioselectivity could become possible.

For the case here (Figure 4.17), however, the EF appears closely correlated with the amount of adsorption thus supporting the initial assumption that selectivity occurs consistently throughout the adsorption process. A difficulty arises, therefore, in comparing the EF data points for $K10_{BL}$ and $K10_{Cu}$ to those of the K10-Cu-lysine batches, for example, where adsorption of acephate is much greater and, in turn, more selective in their adsorption towards the (−) enantiomer. In an attempt to account for this, the mass of the bound sorbate could be incorporated in to the equation for EF. Since the values for EF can only lie between 0.5 and 1.0 it would be appropriate to use an assessment of enantioselectivity that can be increased linearly as the mass of adsorbed acephate is taken in to account in each case. Equation 3.3 below represents the percentage deviation of the EF from the racemic state for acephate enantiomers per average mass of sorbed acephate for each batch of the experiment (E_{Rel}).

$$E_{Rel} = \frac{\left[\frac{EF_R - EF}{EF_R}\right] 100}{m_{sorb}} \qquad \text{(Equation 3.3)}$$

Where EF_R is the EF value for a racemic mixture, EF is the experimentally obtained value of EF for the enantiomers of acephate present in the supernatant and m_{sorb} is the amount of acephate sorbed at the surface of the clay measured in mg. The equation has been used to calculate values for E_{Rel} in each batch of the experiment, the results for which are presented in Figure 4.19 below:

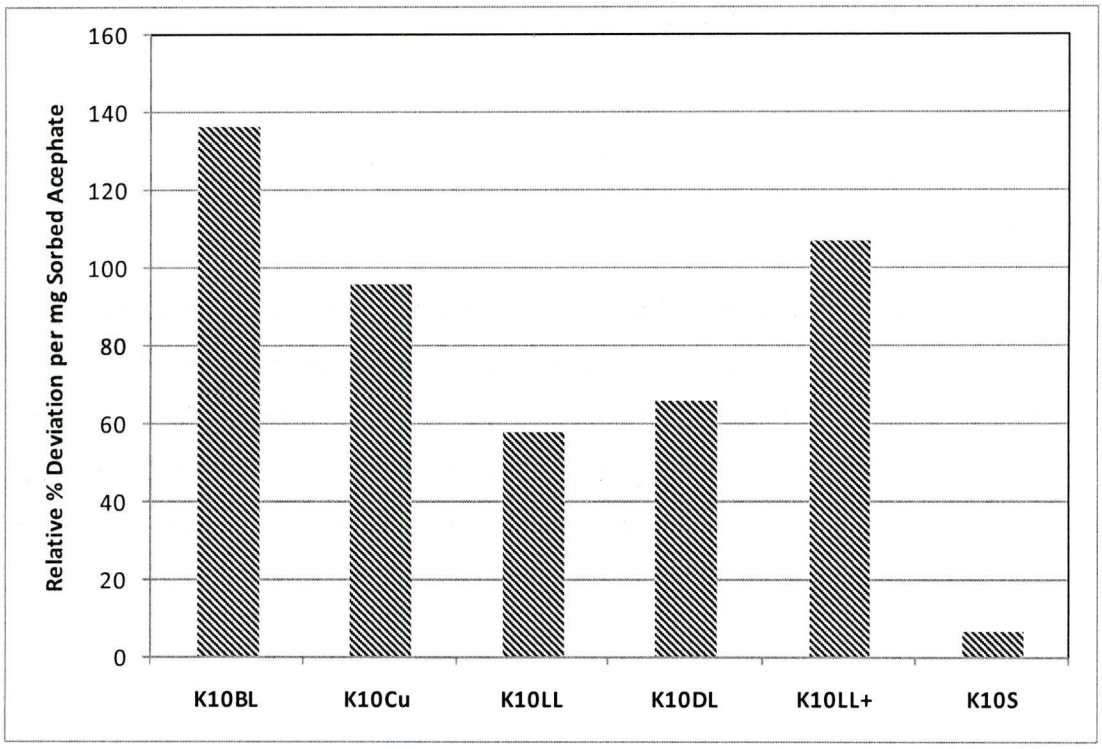

Figure 4.19 Column plot showing relative percentage deviation from racemic per mass of sorbed acephate in each batch labelled in the x-axis. The larger the column, the greater the extent of enantioselective adsorption shown by the clay modification in question towards acephate enantiomers. The sign of the preferred enantiomer cannot be construed from this plot.

This plot gives an interesting view of how the enantioselectivity of each batch might look if adsorption was relatively consistent throughout. The extent of enantioselectivity for the lysine modified K10 batches and the silanised batch remain similar to that observed in Figure 4.17 due to the consistent level of sorption. However, in the $K10_{BL}$ and $K10_{Cu}$ batches it can be seen that, had there been a similar level of adsorption then the enantioselectivity exhibited by the batches might have actually been larger than that for the other batches. The implication is that

although it can be associated with a greater extent of acephate adsorption, the modification of K10 with lysine does not necessarily induce greater enantioselectivity. This is of course a very simplified way of taking into account the effect of adsorption on enantioselectivity as there are many factors that are not considered, such as increasing competition for active sites. Furthermore it is remains unclear why the percentage sorption of acephate in the $K10_{BL}$ and $K10_{Cu}$ batches is uncharacteristically low relative to earlier experiments in this work.

One additional observation of note is that, once more, the complexes separately containing L- and D-lysine appear to show preference to the same enantiomer. Again, this can be construed to mean that any enantioselectivity observed is not due to exchange or interaction with lysine in the Cu-lysine complex. This does not necessarily mean that ligand exchange is not the mechanism for adsorption, and even enantioselectivity, but does suggest that an enantiomer preference arises as a result of an interaction to which the chirality of lysine is irrelevant.

CHAPTER 5 ADSORPTION ON MINERAL SURFACES UNDER NOVEL CONDITIONS

This chapter documents the next stage in the sequential development of the experiments throughout this work. With some exceptions, focus shifts from investigating the impact of sorbent surface modifications on enantioselectivity, towards the control of experimental conditions in basic batch sorption experiments. This approach aims to give insight from a new perspective into the mechanisms that control enantiospecific adsorption processes at the sorbate-sorbent interface. Furthermore, the results of the experiments in this chapter may give some indication of how the components studied might behave in conditions found in the environment.

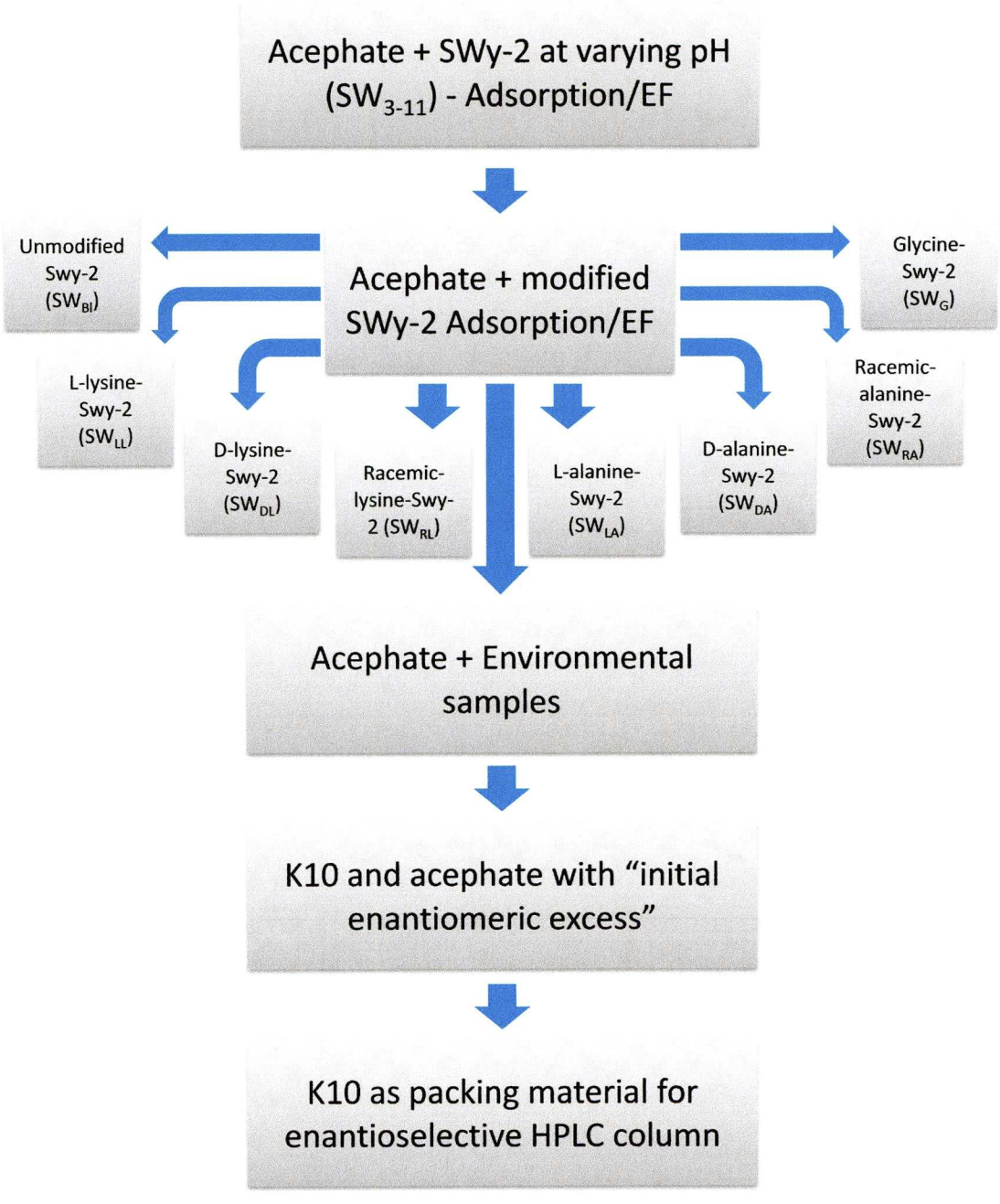

Figure 5.1 Schematic representation of the order of key experiments throughout this chapter. See respective sections within the chapter for definitions of abbreviations.

5.1 Acephate (100mg/L) and bentonite [SWy-2] at varying pH

The importance of pH to the sorptive capability of clay minerals is well known and discussed in Chapter 1 of this work. A simple batch sorption experiment was carried out to investigate the effects of pH on the sorption of acephate to the surface of montmorillonite clay and more specifically to assess its effects on enantioselectivity. The clay used was bentonite SWy-2 (SW), a natural clay mineral consisting predominantly of montmorillonite and sourced from deposits in Wyoming, USA. The switch from montmorillonite K10 was made so as to better replicate

environmental conditions as the K10 form is an acid-treated smectite developed for catalysis and quite removed from its natural condition. Furthermore, the structure of the aluminosilicate layers for SW is accepted as the Hofmann-Endell-Wilm-Marshall-Maegdefrau-Hendricks structure (Theng 1974). Proposed by Hofmann et al. (1933), this is the standard structure for the majority of known montmorillonite clays. Five clays were adjusted to different pH values ($SW_{3\text{-}11}$) with the subscript value indicative the pH of the clay suspension.

The maximum adsorption of acephate seemed to occur at neutral pH whilst the least adsorption was observed with SW_3. The maximum sorption possible, based on the amount of acephate in the sample, was ~5.0 mg/g of clay, while the maximum observed was ~1.6 mg/g of clay. Intriguingly, the sorption of acephate does not correlate directly to the EF as had been seen in most batch sorption experiments conducted up to this point. SW_{11}shows no significant chiral preference for either form of acephate but with decreasing pH an escalating preferential sorption of the (+) enantiomer can be seen.

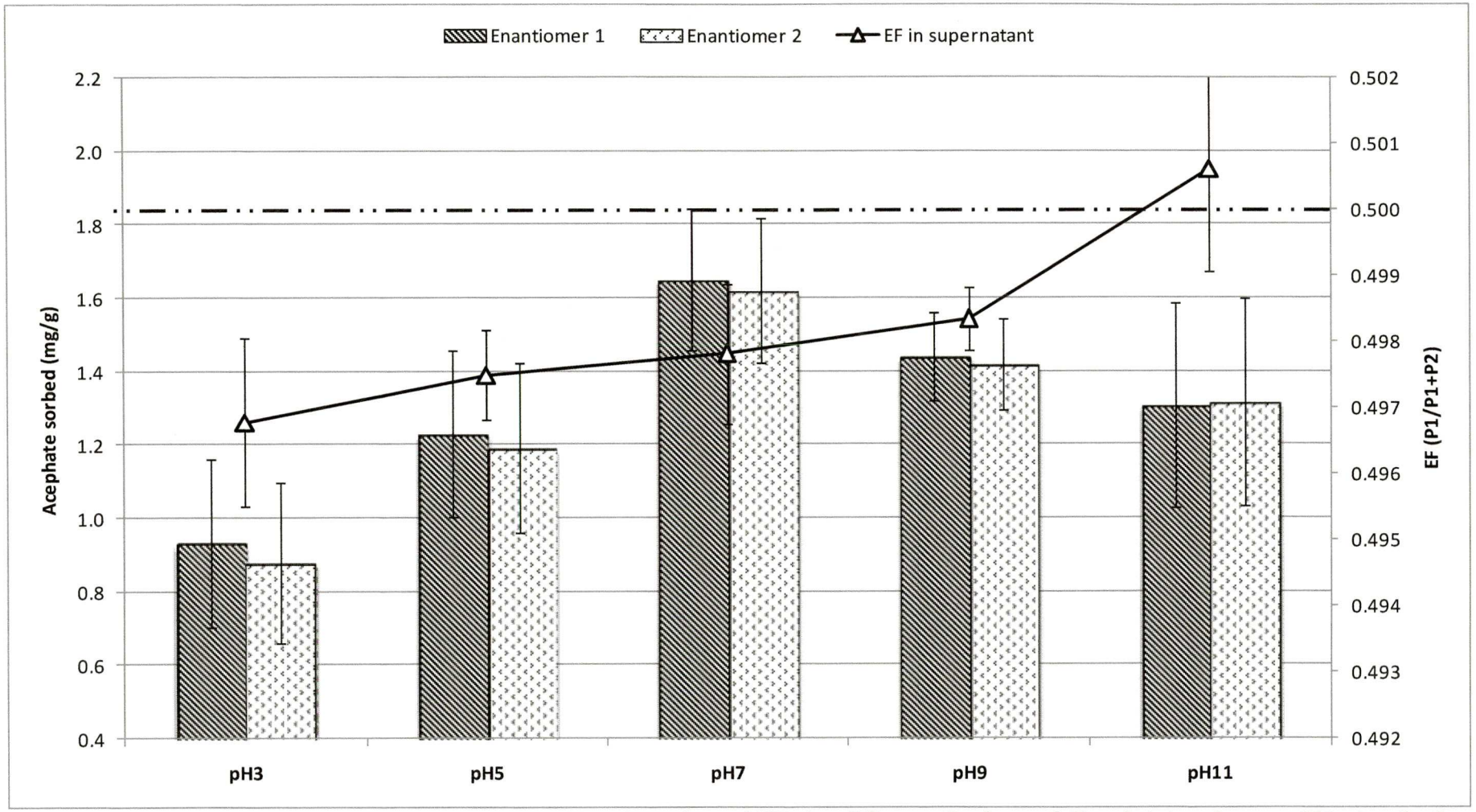

Figure 5.2 (Column plot) the amount of acephate sorbed (mg/g) at the surfaces of SWy-2 at different pH values and (line plot) the subsequent EF values for the batches at each pH. The maximum sorption possible, based on the amount of acephate in the sample, was ~5.0 mg/g of clay. Error bars represent the standard error calculated for each data point while the black dotted line represents a racemic mixture of the two enantiomers.

The adsorption of a molecule on a clay surface often depends on the pH of the mixture (Weber 1966; Banat et al. 2000). This is normally as a result of the effect of pH on the solubility of the molecule. Acephate is unusual in that its solubility is not affected by pH (Singh et al. 1998). Acephate can become ionised at pH below its pK_a (8.5) forming protonated cations, while at pH values above its pK_a it will not. As such, it would be expected that it is soluble in water at a pH lower than its pK_a but insoluble in water at higher pH. This is not the case with acephate as the relatively high electronegativity of the S, O and N atoms results in the P atom acquiring a positive charge and the S, O and N atoms a negative charge. Acephate is a polar molecule, and even under non-ionising conditions and because of the presence of negative P=O and C=O bond domains, it also acquires a potent electron-rich domain (Singh et al. 1998). Therefore, acephate may remain in solution at high pH values due to dipole-dipole interactions in polar solvents such as water. The sorption of acephate to SWy-2 peaks at pH 7, the nearest value to its pK_a without exceeding it. It seems likely, therefore, that the inability of acephate to ionise above pH 8.5 has a negative effect on its ability to adsorb to the clay. This supports the idea that acephate may bind through ligand formation with the exchangeable cation or ligand exchange with an already bound lysine molecule, as acephate would need to be ionised in order for such mechanisms to function. The adsorption does not cease completely at pH above the pK_a of acephate as there are likely to be other binding mechanisms, such as hydrogen bonding, at work. Below the pH value for the pK_a of acephate there is a steady decrease in adsorption to SWy-2 (Figure 5.2). This may be explained by an increase in competition with H^+ ions for active binding sites on the clay surface as pH decreases (McLaren et al. 1958; Weber 1966). At lower pH, more surface silanol groups will be protonated making it increasingly difficult for acephate to bind directly to the clay surface. It is possible that the extent of ligand exchange or formation is unaffected at lower pH levels and the observed fall in adsorption is due entirely to the reduction in direct binding at the clay surface. However, if the surface silanols are fully protonated, at low enough pH there will be an excess of protons in the interlayer space potentially taking on the role of an exchangeable cation. This is likely to affect the ligand formation process but whether acephate molecules would exchange with the H+ ions or adsorb by direct association with them is unclear.

5.2 Acephate (100mg/L) and bentonite [SWy-2] with various modifications

Another phase of modifications was carried out based on results from the bentonite SWy-2 system. Eight SWy-2 batches with modified surfaces were prepared, including an unmodified batch (SW_{Bl}) to act as a control. The L- and D- forms of lysine were used again to form individual complexes with the clay (SW_{LL} and SW_{DL} respectively) following the same method as in previous experiments. Further modifications were prepared using both enantiomeric forms of the amino acid, alanine (SW_{LA} and SW_{DA}). Batch sorption experiments involving the incorporation of an amino acid that is smaller in size than lysine, such as this would potentially provide more information about the arrangement of molecules in the interlayer space. In the case of both chiral amino acids, a modification constituting a racemic mixture of both enantiomers was prepared (SW_{RL} and SW_{RA} respectively) and is described in detail in Chapter 2. The clay was also modified with the achiral amino acid, glycine (SW_G) in an attempt to further understand the effects of chiral and achiral complexation on the sorption of chiral species in the interlayer. A reference table of abbreviations for Section 5.2 is included below:

Table 5.1 Table of abbreviations for Bentonite (SWy-2) modifications in section 5.2

Abbreviation	Pre-treatment/Modification
SWBL	Unmodified SWy-2 bentonite
SWLL	L-lysine-exchanged SWy-2 bentonite
SWDL	D-lysine-exchanged SWy-2 bentonite
SWRL	Racemic lysine-exchanged SWy-2 bentonite
SWLA	L-alanine-exchanged SWy-2 bentonite
SWDA	D-alanine-exchanged SWy-2 bentonite
SWRA	Racemic alanine-exchanged SWy-2 bentonite
SWG	Glycine-exchanged SWy-2 bentonite

The results (Figure 5.3) show that sorption of acephate at the surface of SW_{Bl} was only ~30% of the total adsorbable material (~4.0 mg/g of sorbent). SW_{RL}, however, sorbed almost three times more acephate, as did SW_{DL}. This was not the case for SW_{LL} which sorbed more that SW_{Bl} but significantly less than SW_{DL}. All modifications with alanine as well as SW_G led to minor amounts of sorption of ~15 – 30%. The EFs for each batch provided evidence for a small degree of preferential

sorption of the (+) enantiomer of acephate. SW_{RA} and SW_G showed the least enantiomeric preference being almost insignificant, although intriguingly, SW_{DA} appeared to be the most enantioselective of the bentonite modifications.

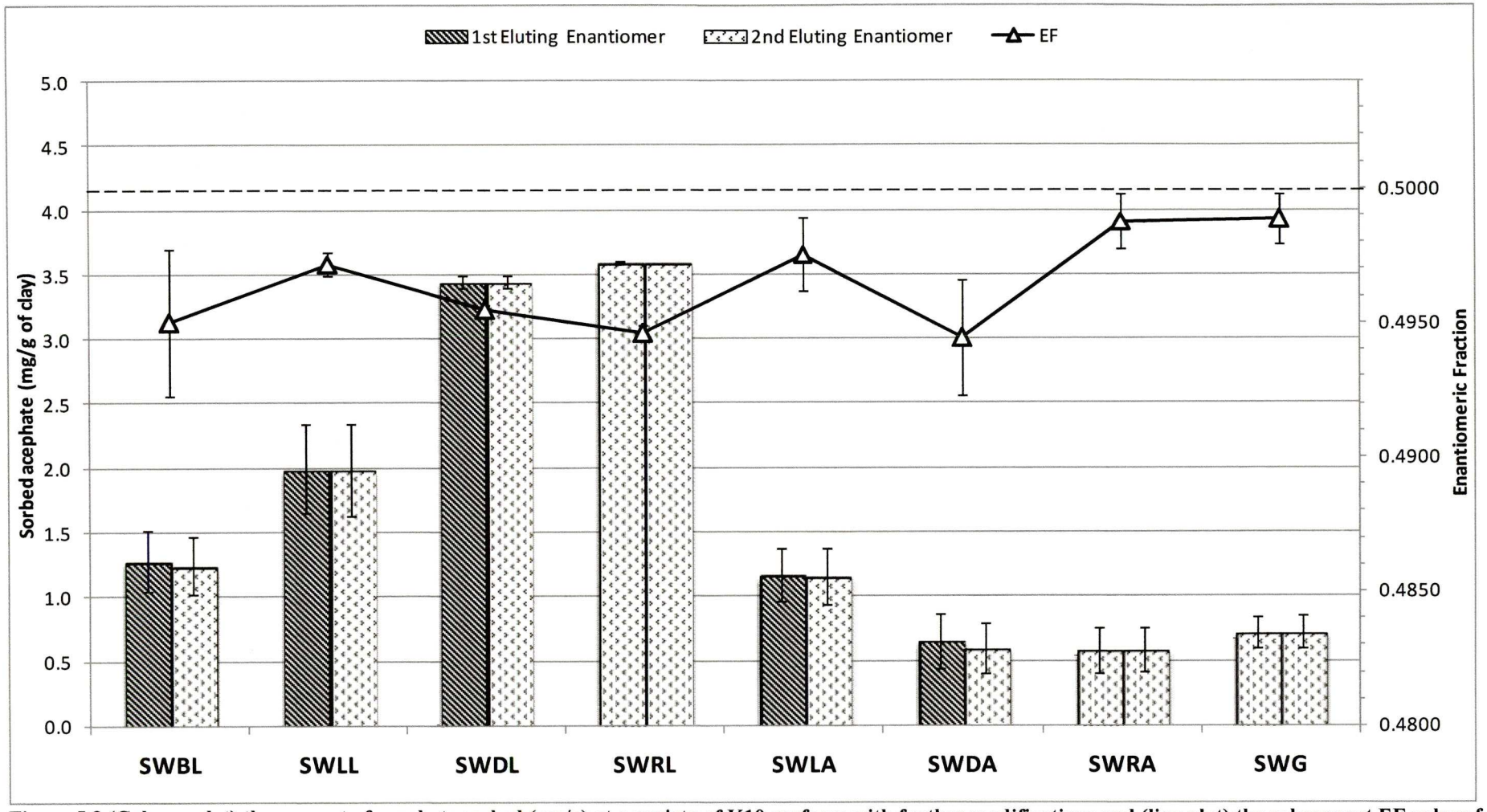

Figure 5.3 (Column plot) the amount of acephate sorbed (mg/g) at a variety of K10 surfaces with further modifications and (line plot) the subsequent EF values for the each modification. The maximum sorption possible, based on the amount of acephate in the sample, was ~4.0 mg/g of clay. Error bars represent the standard error calculated for each data point while the black dotted line represents a racemic mixture of the two enantiomers.

In this set of experiments, the pH was adjusted to 8 for each batch and so, given the pK_a of acephate, it is likely to have been ionisation in each case.

Stronger sorption of acephate on lysine modifications than the SW_{Bl} might be explained by the additional ligand exchange mechanism for adsorption available with the presence of a Cu-lysine complex. However, this would not support the idea that acephate forms ligands with the interlayer cation without the presence of a Cu-lysine complex as suggested previously. Nonetheless, involvement of acephate in a ligand may simply be more likely if lysine has already formed a ligand with the interlayer cation. Of course, none of the batches here have been exchanged with Cu or any other cation so the clay will include several cations in the interlayer. Na^+ and Ca^{2+} are the most prominent interlayer cations but there is likely to be a wide range of other cations. The double positive charge of the Ca^{2+} cation means it should be able to form a biligand in the same way as the Cu^{2+} cation can. However, the singly charged Na cation, presumably, will only be able to support the formation of a single ligand. As discussed previously (with reference to Tsvetkov & Mingelgrin 1987b), ligand exchange has been proposed as a mechanism leading to enantioselectivity, particularly with the involvement of a biligand formation. If this were the case, a reduction in enantioselectivity would generally be expected over batches involving a doubly charged cation as the sole exchangeable cation in the interlayer. A reduction in the deviation from the racemic state *is* observed between this experiment and that involving copper exchanged K10 batches and so it might be concluded that the charge on the interlayer cation and thus the extent of the ligand and biligand formation has a significant effect on enantioselective adsorption of acephate.

One unexpected observation is that the L-lysine modified batch adsorbs significantly less acephate than the D-lysine and racemic batches. The cause for this is unclear but is likely to have something to do with the way the lysine molecule, complexed or not, interacts with the clay surface. There may be something specific about the clay surface or the spatial orientation of the opposing lysine enantiomers that encourages such antipodes to bind in a different orientation. This is not to say that a preference will be observed, simply that the orientation of the interaction might be different. Subsequently, the sorption of acephate by the clay-lysine complex may be enhanced or reduced depending on its compatibility with the different shapes of the active adsorption sites created by the opposite lysine enantiomers. Thus, SW_{DL} might

coincidently provide a more convenient environment for adsorption of acephate than SW_{LL} does. This occurs independently of any enantiomer specific adsorption of the acephate molecules, but by assessing at the EF for each lysine modified batch it is clear that, in addition to its reduced sorptive capabilities, the enantioselectivity of SW_{LL} is significantly lower than that of SW_{DL}. The above idea could be extended to account for preferential adsorption of acephate. For example, the difference in orientation of the D-lysine complex at the surface of the clay may provide a slightly more favourable environment for enantioselectivity. This does not necessarily have to affect the sign of the preferential adsorption (i.e. cause a reversal) but simply enhance the overall deviation of EF from the racemic state.

The low levels of adsorption by the alanine and glycine modified batches might be explained by their reduced ability to form a biligand with the interlayer cation. Lysine is effective in this manner as its α-amino group can bind, along with the carboxylic oxygen, to the cation while the ε-amino group is protonated and forms the positive charge required to form a complex with its clay substrate. The lack of a ε-amino group in the alanine and glycine structures means this mechanism cannot occur.

At pH 8 the carboxyl group and amino group of both alanine and glycine will most probably be ionised, i.e. in their zwitterionic form. This would mean a complex may be formed with an interlayer cation but with a neutral overall charge and therefore an inability to form a complex with the clay. If this occurs, perhaps the freed protons are taken on by the clay as interchangeable cations. The acephate would then essentially be adsorbing to H-montmorillonite.

Another interesting point is that, according to Bodenheimer & Heller (1967), lysine (but not glycine or alanine), while complexed with the montmorillonite, causes the basal spacing to increase. If the occurrence of Cu-lysine complexes is increased there would duly be greater opportunity for acephate to be involved in ligand exchange. However, the increased basal spacing is probably due purely to the larger size of the lysine molecule and, thus, more space should be available for acephate to reside and be adsorbed by other means. Enantioselectivity is no stronger, on the whole, in the lysine modified batches than in the SW_{BI} batch providing another indication that any enantiomer preference is not occurring as a result of acephate interaction with lysine.

Furthermore, the SW_{RA} batch shows little enantioselectivity whereas the SW_{RL} batch shows a relatively strong preference to acephate's (+) enantiomer. This indicates that a chiral environment and subsequent enantioselective sorption is not provided by the chirality of the complexed amino acid, as both alanine and lysine are chiral, but that the involvement of lysine in the complex does have an overall effect on enantioselectivity. So, the lack of significant enantioselectivity in the SW_G batch, suggesting its presence has a detrimental effect on enantiomer specific sorption, is not necessarily due to its lack of chirality.

However, the above observations and the fact that, again, opposite enantiomer preference is not observed between the batches of L- and D-enantiomer complexes of either chiral amino-acid does not necessarily mean that zero enantioselectivity arises due to the chirality of lysine. If the effects of lysine provide only a small proportion of the enantioselectivity occurring then one would not expect the involvement of opposite lysine enantiomers to cause the enantiomer preference to completely switch, but to be somewhat altered. Here, and in previous experiments, the batch involving the D-lysine modification has shown a greater deviation from the racemic state than that involving the L-lysine. It might, therefore, be that L-lysine does cause an opposite enantiomeric preference but that it is also opposite to the dominant, unknown, enantiomer preference and, thus, only reduce deviation, as observed, from the racemic state.

5.3 Effect of acephate concentration on SWy-2 basal spacing

The distance between the base of an aluminosilicate unit sheet and the base of the adjacent unit is known as the basal spacing. This includes the interlayer space and varies depending, predominantly, on how much water it has taken on. Various reports have suggested that the size of the basal spacing can vary depending on how much of a sorbate species has been adsorbed (Banat et al. 2000; Cornejo et al. 2008). In this study XRD techniques were used to determine the basal spacing of bentonite SWy-2 with varying amounts of acephate adsorbed at its surface (see Chapter 2 for procedure). Such information should provide understanding of where and how the acephate is adsorbing to the clay surfaces. An increase in basal spacing with acephate concentration will confirm the residence of acephate in the interlamellar space. Figure 5.4, showing °2θ for the different concentrations of acephate in the initial supernatant, appears to indicate a small increase in basal spacing with increasing

acephate sorption. However, it is important to note that the downward slope of the plots show almost no variation in °2θ whereas the upward slopes display significantly more. This implies that it is the shape of the peak that is changing and giving the impression of increasing °2θ, while in fact very little increase is actually present (Dr. S. Crowley, personal communication).

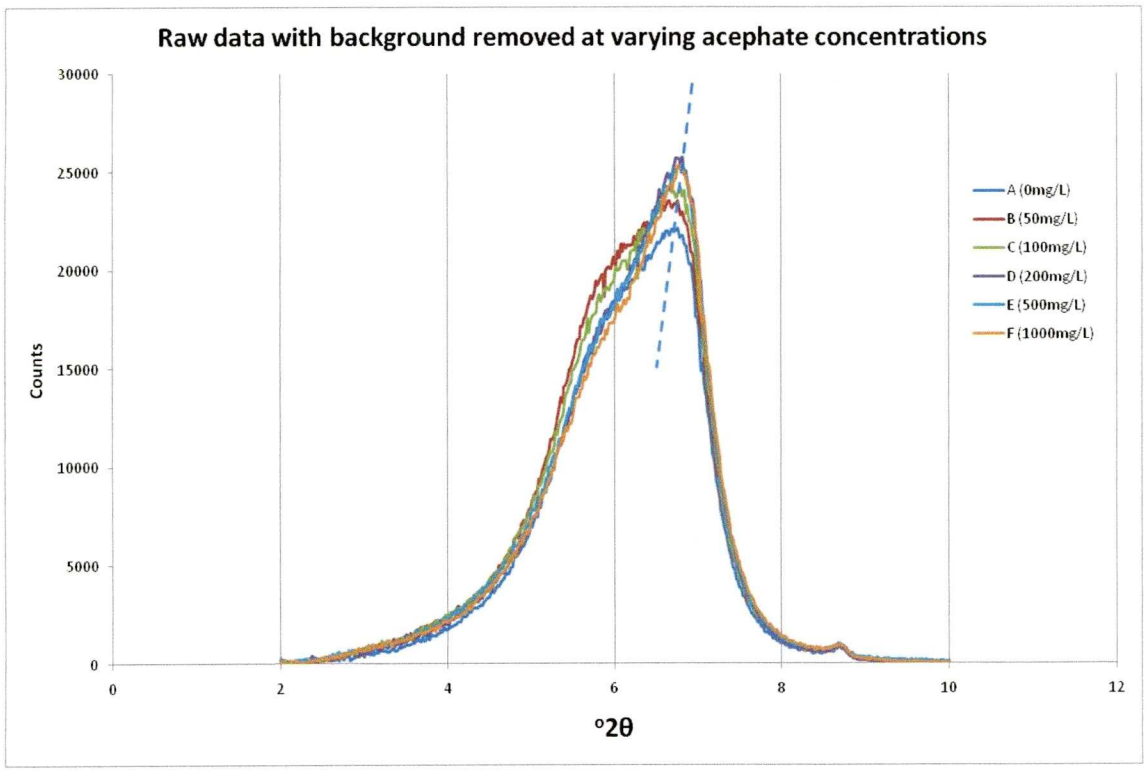

Figure 5.4 Raw XRD data for SWy-2 in aqueous suspension with background removed at increasing acephate concentrations

The two following XRD plots (Figure 5.5 and Figure 5.6) show how variation in the water content of the interlayer space can result in a different shape to the overall plot. Water in the interlayer is present in the form of layers. The more water becomes incorporated the more likely it will exist as two layers rather than one and the proportion of clay units with one layer to those with two layers will change. Increasing additions of acephate make the plot appear more like Figure 5.6 where clay particles with double layer water molecules dominate. A small increase in humidity was observed over the course of the experiment. This could well be responsible for the shift in shape of the XRD plots, essentially meaning that the effect of acephate adsorption on basal spacing is negligible. Such results do not prove or disprove the presence of acephate in the interlamellar space.

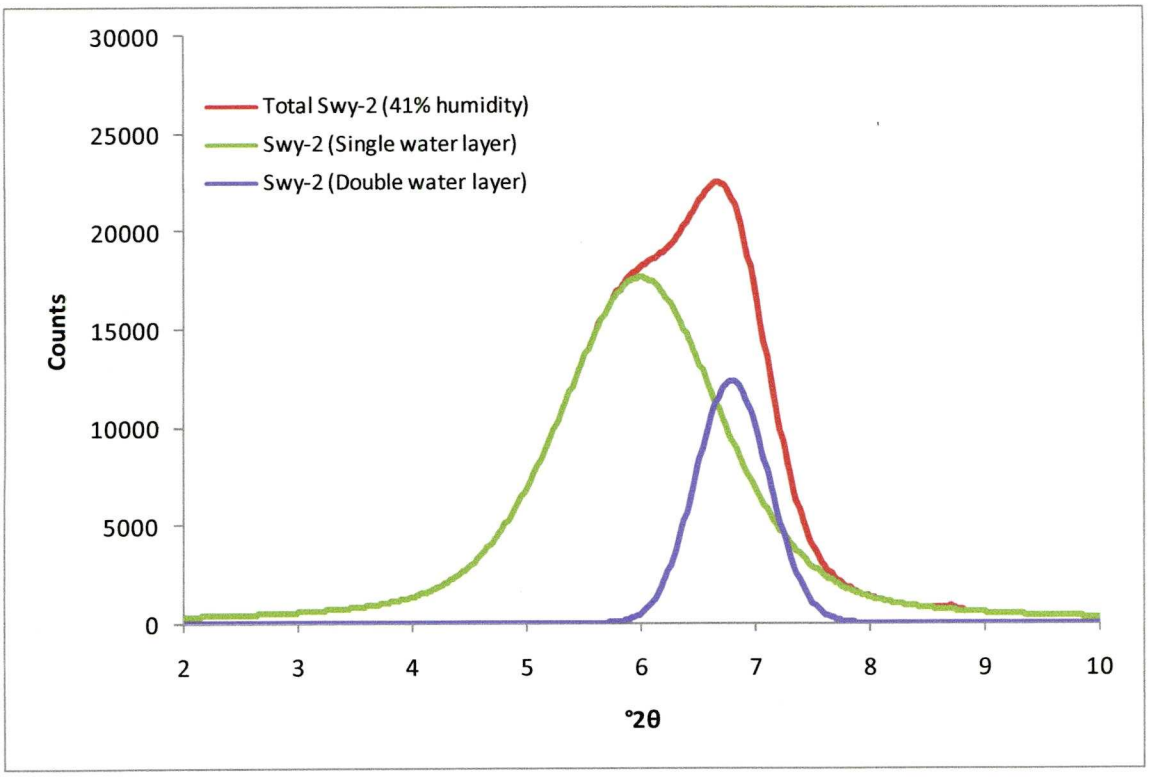

Figure 5.5 XRD data for total SWy-2 in aqueous suspension with background removed at 41 % humidity. The SWy-2 containing a single water layer can be seen in green while the SWy-2 containing a double water layer is in purple

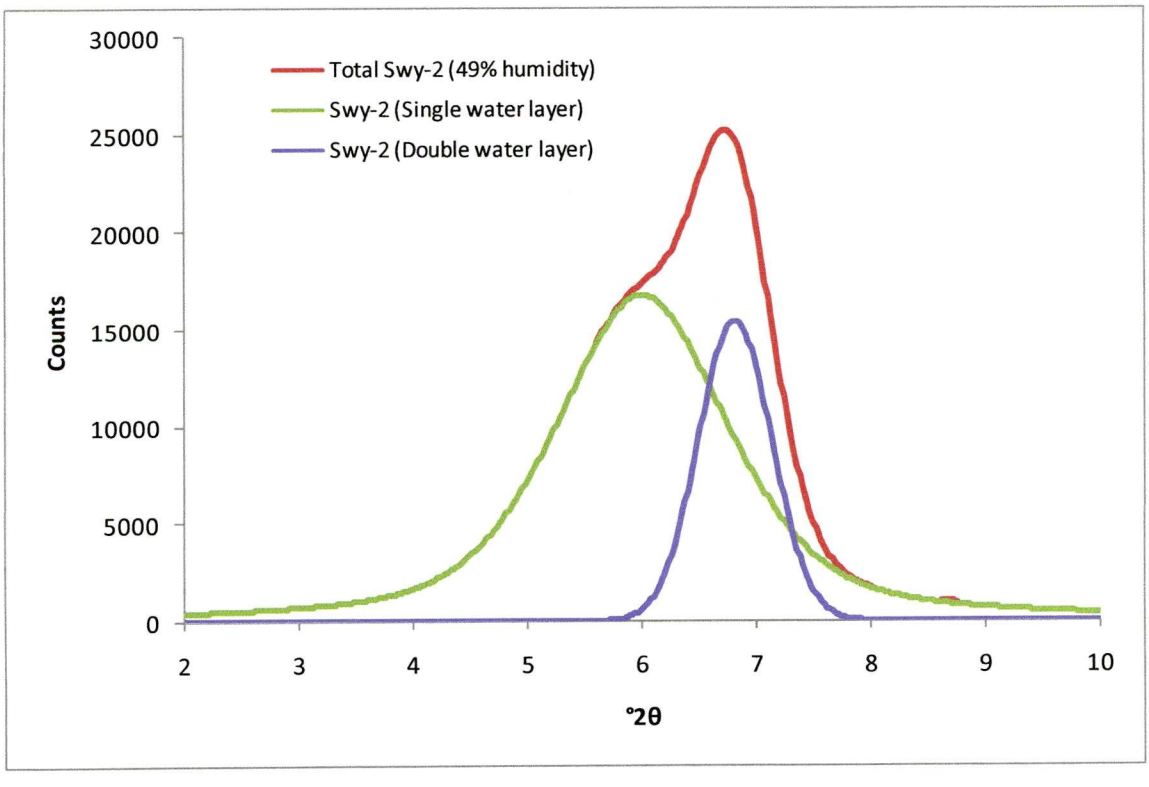

Figure 5.6 XRD data for total SWy-2 in aqueous suspension with background removed at 49 % humidity. The SWy-2 containing a single water layer can be seen in green while the SWy-2 containing a double water layer is in purple

5.4 Acephate (100mg/L) sorption on SWy-2 bentonite (raw material and 0.5 – 2.0 μm fraction)

Experimentally, bentonite SWy-2 proved to be more difficult to work with than montmorillonite K10 because is made up of a wide range of particle sizes. This was noted in the preparation of batch sorption experiments as its tendency to coagulate made it difficult to suspend the bentonite in water. To try and resolve this issue a bentonite batch was prepared consisting of particles with diameters in the range of 0.5 – 2.0 μm (SW_2) (see Chapter 2 for full procedure). Its sorption capabilities were compared to the unseparated, or 'raw', bentonite (SW_R). The SW_R batch sorbed acephate in a linear fashion (Figure 5.7), with a maximum sorption of ~53 % of the sorbate being removed from the supernatant in the batch with the most clay. The EF values indicate fairly strong preferential selection of the (−) enantiomer which peaked immediately in the batch with the smallest addition of clay (Figure 5.8). For all further batches with increased amounts of clay, a similar level of preference is observed with no further increase.

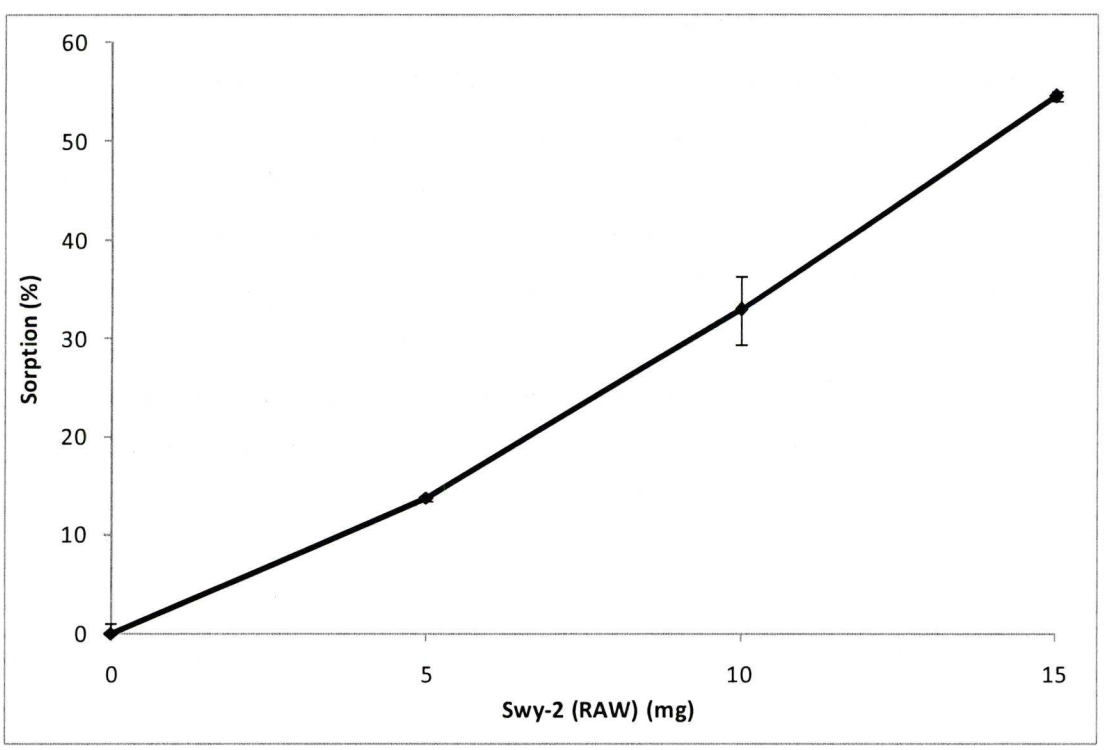

Figure 5.7 Thepercentage of acephate sorbed at the surface of raw untreated Swy-2 bentonite (SW_R). Error bars represent the standard error calculated for each data point.

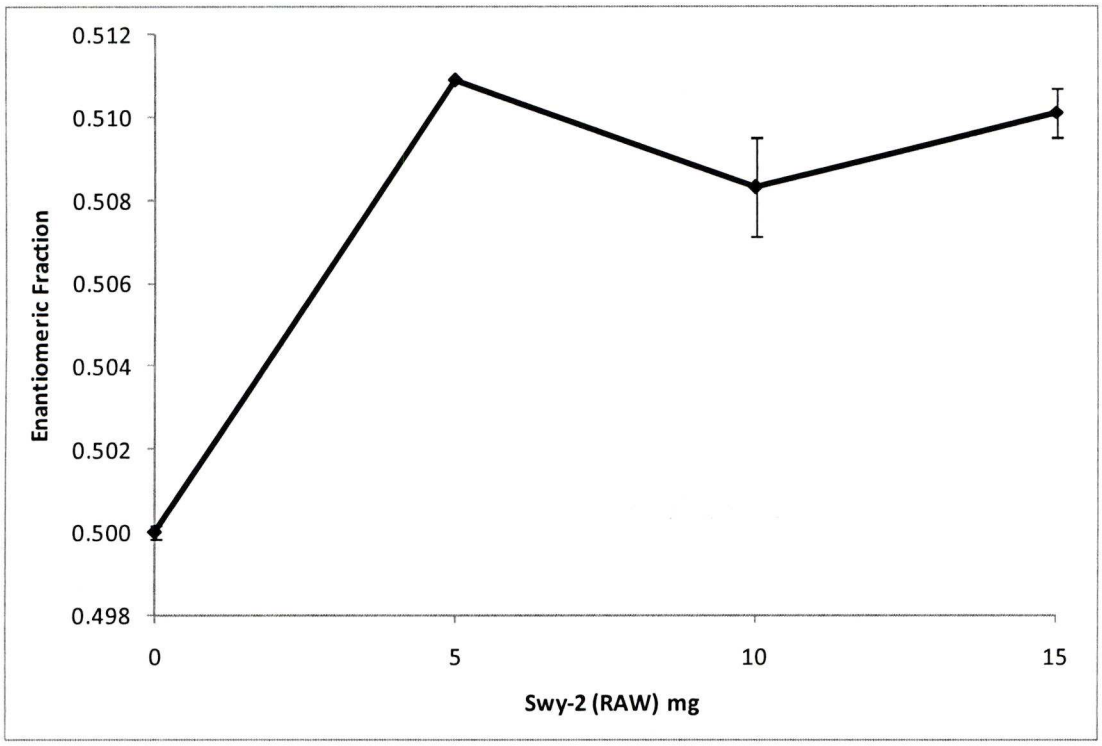

Figure 5.8 EF values for acephate enantiomers in the supernatant after adsorption at the surfaces of raw untreated Swy-2 bentonite (SW_R). Error bars represent the standard error calculated for each data point.

The linear increase in acephate adsorption with rising amounts of SW_R suggests that the active sites are saturated in each batch. In other words, the amount of adsorption is limited by the extent of surface area available on which to bind. This observation is unusual for this work as most sorption plots have show rapid initial increase in sorption before a steady reduction in growth resulting in a distinctly curved plot line. The observation is reasonable, however, as SW_R has been subjected to very little refinement since removal from its terrestrial source. As such, it is likely to contain a large variation in grain size and probably a significantly reduced surface area.

The deviation from the racemic state observed in Figure 5.8 does not correlate closely to the sorption described above but increases sharply before plateauing after the 5 mg batch. The cause for this is likely to be due to the kinetic properties of the adsorption process as discussed earlier in the chapter. In this case it might be inferred that the majority of the enantioselective activity happens in the early stages of the equilibration process. This might indicate non-reliance on interaction with other acephate molecules for enantiomer specific adsorption and more specifically the selective nature of the direct bond between acephate and the clay surface.

The 0.5 – 2.0 μm bentonite fraction exhibited significantly less adsorption (Figure 5.9). Initially, between 0 and 10 mg additions, acephate was linearly sorbed up to ~30 % but in the final batch containing 15 mg of clay the increase was less pronounced and the plot showed signs of levelling off and an overall maximum sorption of ~33.5 %. The subsequent EF (Figure 5.10), again, showed preference for the (−) enantiomer but not to the same extent as with the raw bentonite.

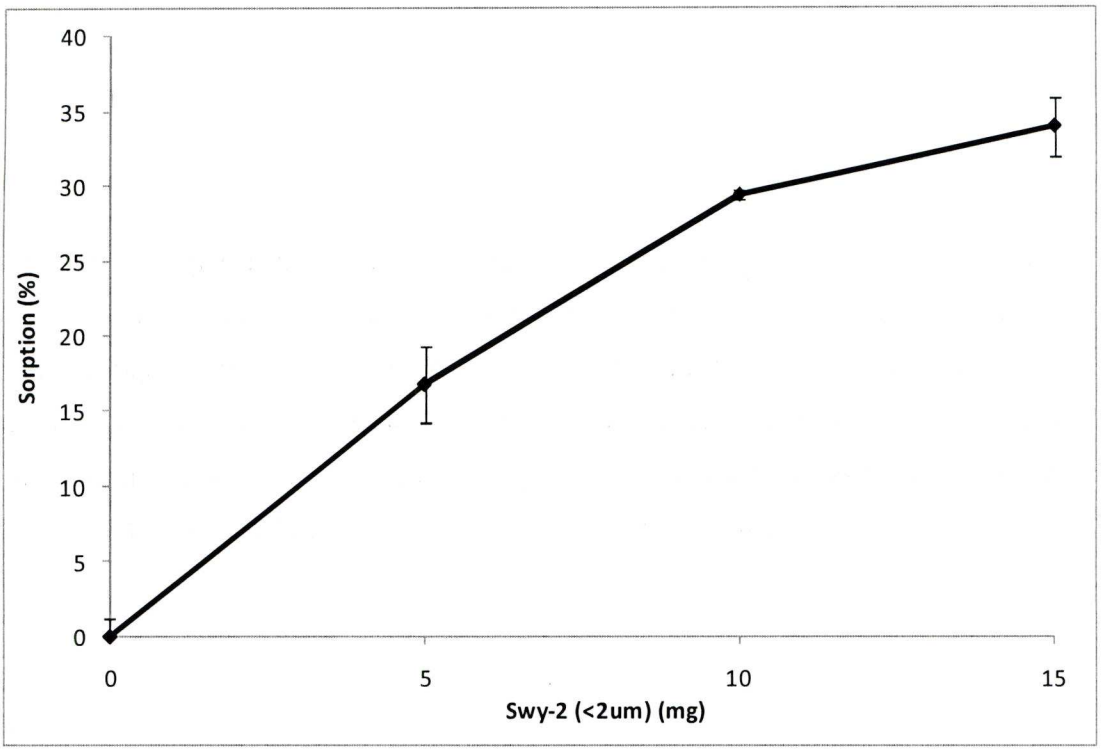

Figure 5.9 The percentage of acephate sorbed at the surface of size fractionated (0.5 – 2.0 μm) Swy-2 bentonite (SW_F). Error bars represent the standard error calculated for each data point.

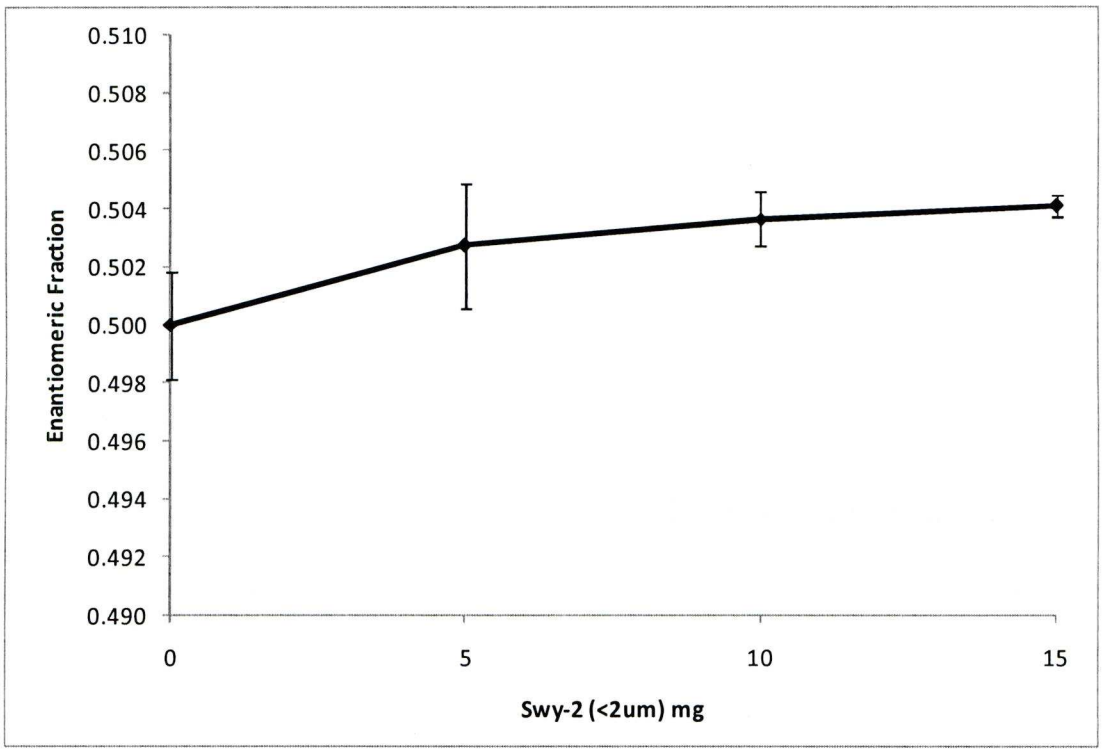

Figure 5.10 EF values for acephate enantiomers in the supernatant after adsorption at the surfaces of size fractionated (0.5 – 2.0 μm) Swy-2 bentonite (SW_F). Error bars represent the standard error calculated for each data point.

Once more, the non-linearity observed in Figure 5.9 is likely to be linked to the surface area of the clay. Since the bentonite in this case has been size fractionated in order to remove the larger particles and some of the extremely small particles it is probable that the surface area has increased significantly. As a result the larger the mineral addition in the batch the less likely the active sites are to be saturated with acephate. In which case, competition for the sites will play more of a part and overall sorption will increase at a lower rate resulting in the observed curved plot. However, it is also of note that the overall sorption in the SW_F batches is somewhat smaller than those in the SW_R batches. This is contrary to what would be expected if the surface area is indeed larger in the SW_R batches. As such, perhaps the more likely conclusion is that the bulk of the surface area is found in the extremely small fraction (< 0.5 μm) which has been removed in the SW_F batches and that the surface area of SW_R, therefore, is significantly greater. This would account for the greater level of sorption observed and, therefore, would also begin to explain why the deviation from the racemic state displayed in Figure 5.10 is smaller than that for the SW_R batches. The reduction in enantioselectivity, however, is actually even greater than the reduction in sorption should account for and thus suggests that the majority of

enantiomer specific sorption occurs at particle surfaces present in the < 0.5 μm fraction and such an observation could give insight in to the location of the enantioselective adsorption mechanism. One could speculate the indication is that the selective component of the adsorption occurs in greater proportion at the edge sites of the clay particles of which there will be more in the smaller size fraction only present in SW_R.

5.5 Acephate with SWy-2 (20 mg) bentonite: variation of pesticide concentration: 10-500mg/L Acephate (H_2O)

Another way of obtaining information on the sorptive mechanisms of clays is to set up a series of batch sorption experiments in which the amount of mineral remains constant while the concentration of the sorbate in the initial supernatant is varied. In the present experiments acephate in aqueous solution was combined with a constant amount of the raw bentonite SWy-2. The amount of adsorption in a set of experiments such as this is best presented as an adsorption isotherm by plotting the equilibrium concentration against the amount sorbed (Figure 5.11). The initial increase in sorbate resulted in the expected sharp increase in sorption to the clay. However, two further increases in initial sorbate concentration resulted in a rapid decrease in sorption until the final addition of the maximum concentration of acephate saw the highest level of sorption.

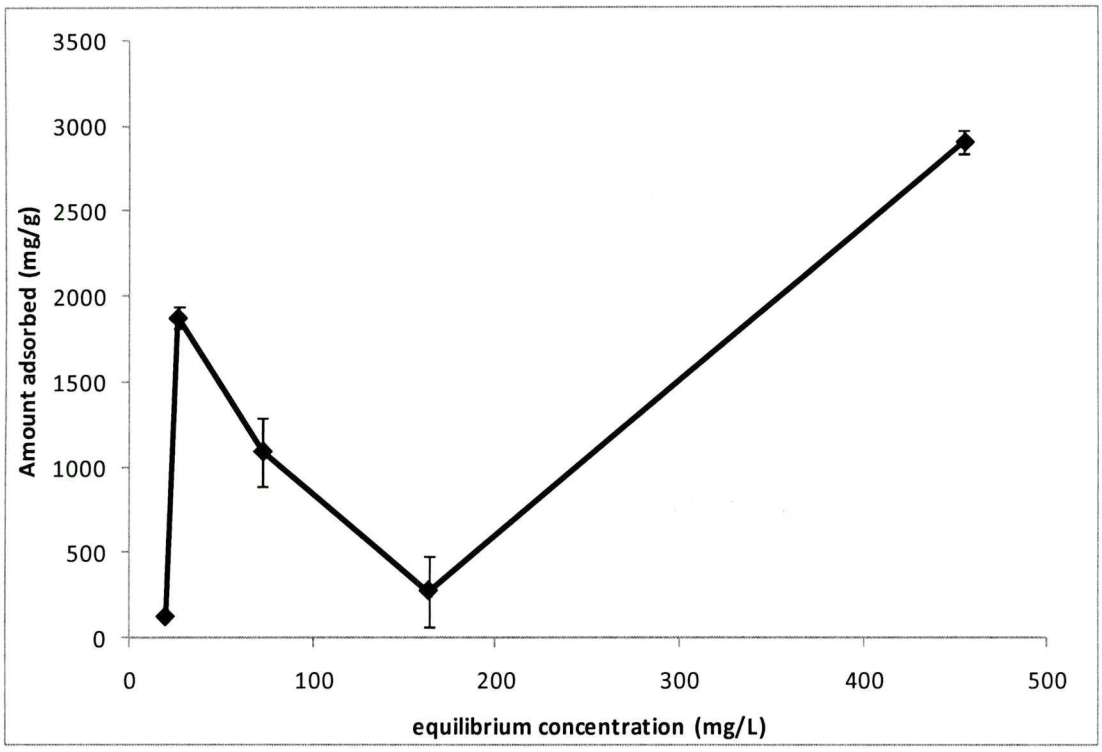

Figure 5.11 Acephate sorption (mg/g) at the surfaces of Swy-2

The occurrence of a step feature in an adsorption isotherm is not uncommon and can come about for numerous reasons including the initiation of a second sorbate layer in the interlamellar space. However, the plot in Figure 5.11 does not fit any known isotherm models and the cause of the decrease in sorbed material while equilibrium concentration continues to increase remains unclear.

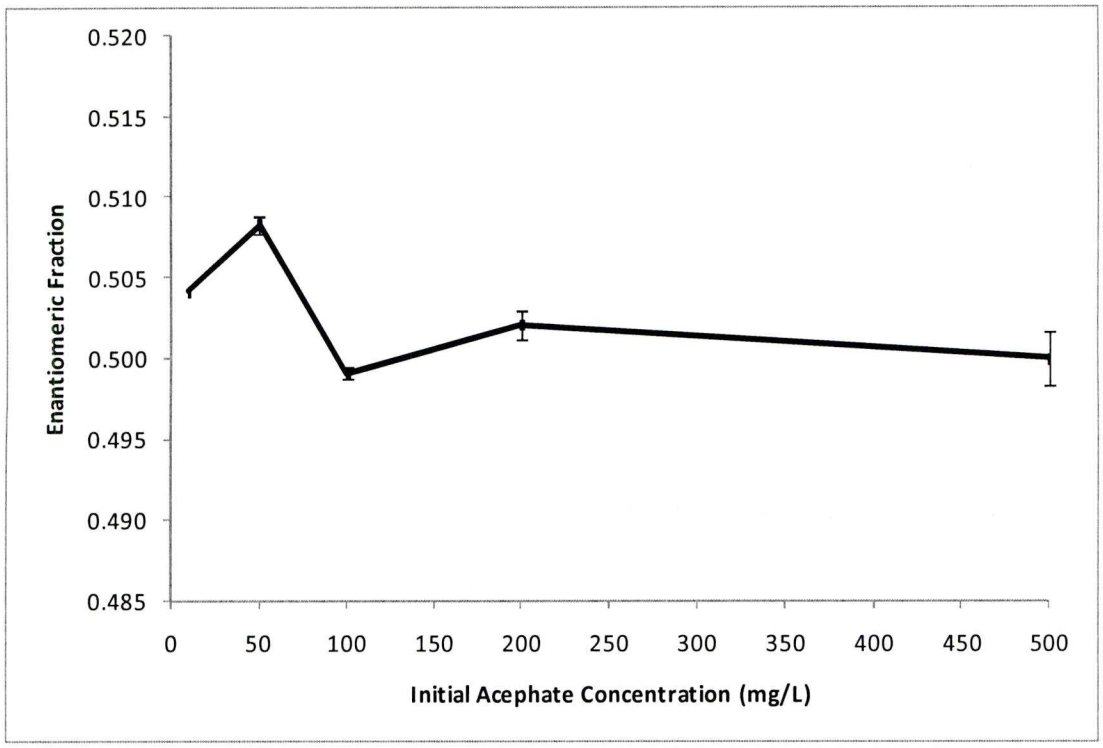

Figure 5.12 EF values for acephate in the supernatant after sorption of increasing concentrations of acephate by SWy-2. Error bars represent the standard error calculated for each data point.

Subsequent EFs did not correlate with the adsorption isotherm and, in fact, showed almost no preference for a specific enantiomer. The batch including the lowest concentration of acephate gave elevated EF values both in the bentonite batch and in the control batch involving no sorbent. Such anomalous results are likely to be due to the distortion of peak shape and size at low concentrations of acephate leading to greater uncertainties in the measured EF values. One batch (50 mg/L initial supernatant concentration) did show different EF values for the experimental and control batches indicating a statistically significant selective preference of the (−) enantiomer. Why, however, this would have occurred in the batch with the smallest initial concentration of acephate is unclear.

5.6 Acephate sorption on environmental samples

The results of batch sorption experiments involving acephate and varying amounts of homogenised deep-sea sediments from the north east Atlantic Ocean are presented below. The sediments in each batch were either untreated (labelled E) or pyrolysed prior to use (labelled EP). In the case of the untreated mineral batches we see the highest level of sorption, at 1.5 mg/g of sorbent, in the batch containing 100 mg of material with slightly reduced sorption in the 50 and 200 mg mineral batches. The

reason for this is unclear as increased mineral content of the mixture should result in greater numbers of active sites, less chance of competition between sorbate molecules and, thus, a general increase in adsorption. However, given the unrefined nature of the samples and despite attempted homogenisation, it is quite possible that any given batch will contain a significantly different mineral make-up. On the whole, similar levels of sorption are seen between the EP mineral batches but with a slight increase in sorption from the smallest mineral addition to the largest. Overall, though, it was surprising to see that the amount of adsorption does not increase in proportion to the increase of available mineral in the batch.

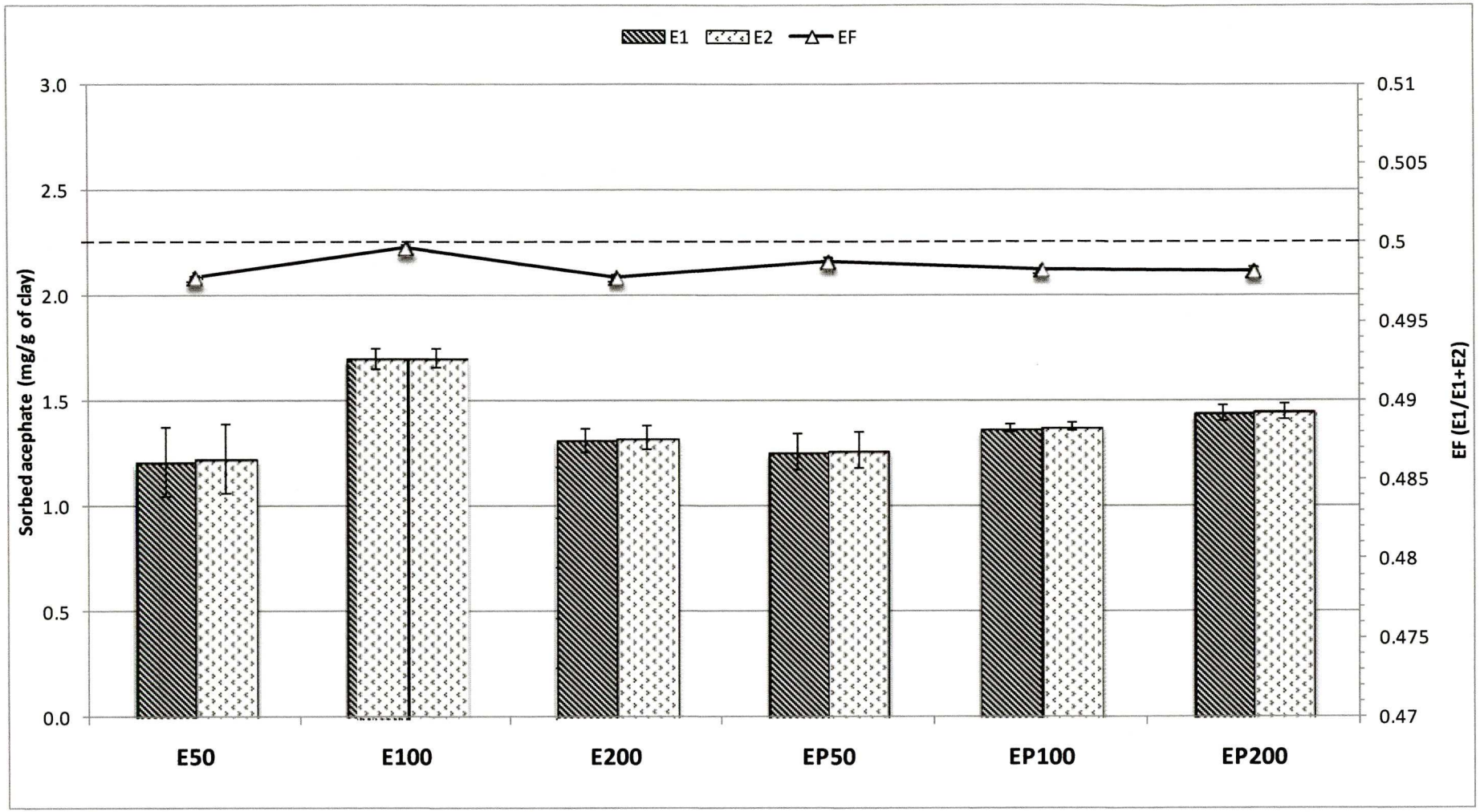

Figure 5.13 (Column plot) the amount of acephate sorbed (mg/g) at the surfaces of varying amounts of environmental samples after pyrolysation (EP) or no pyrolysation (E) and (line plot) the subsequent EF values for the each batch. Error bars represent the standard error calculated for each data point while the black dotted line represents a racemic mixture of the two enantiomers.

The EF values for all batches indicate a small level of preferential sorption of the (+) enantiomer of acephate equating to less than 0.5 %. The variation in EF between batches is almost non-existent, perhaps with the exception of the E100, where the EF is extremely close to 0.5 indicating a lack of enantiomer preference. Interestingly, it is this batch which shows the greatest amount of adsorption. It is seems that something is contained in the mineral of this sample not present in the other samples that is capable of stronger non-enantioselective, adsorption of acephate.

5.7 Initial enantiomeric excess experiment with acephate and montmorillonite K10

Recent work by Green et al. (1989) and, in particular, Haq et al. (2009) has found that enantiomeric imbalances can lead to nonlinear symmetry breaking in the organisation of adsorbate structure on the surface of an adsorbent. Their work prompted a set of batch sorption experiments to try to assess the impact of an initial enrichment of one enantiomer on subsequent enantiomer specific sorption of a chiral species at the surface of an achiral substrate. This involved varying initial EF values for known initial acephate concentration and constant mineral content. As access was not available to the individual enantiomers of acephate, a slightly different approach was taken. A straightforward sorption experiment was carried out between K10 and acephate which in the past had yielded enantiomer specific preferential adsorption. The supernatant was then removed and used as the initial supernatant for the following cycle of batch sorption experiments. Six such cycles were carried out. One drawback to conducting the initial enantiomeric excess experiment in this manner was that in each cycle the initial acephate concentration was smaller than in the previous cycle. As such, the cycles could no longer be repeated once the initial concentration dropped below the point where EF values can be reliably determined.

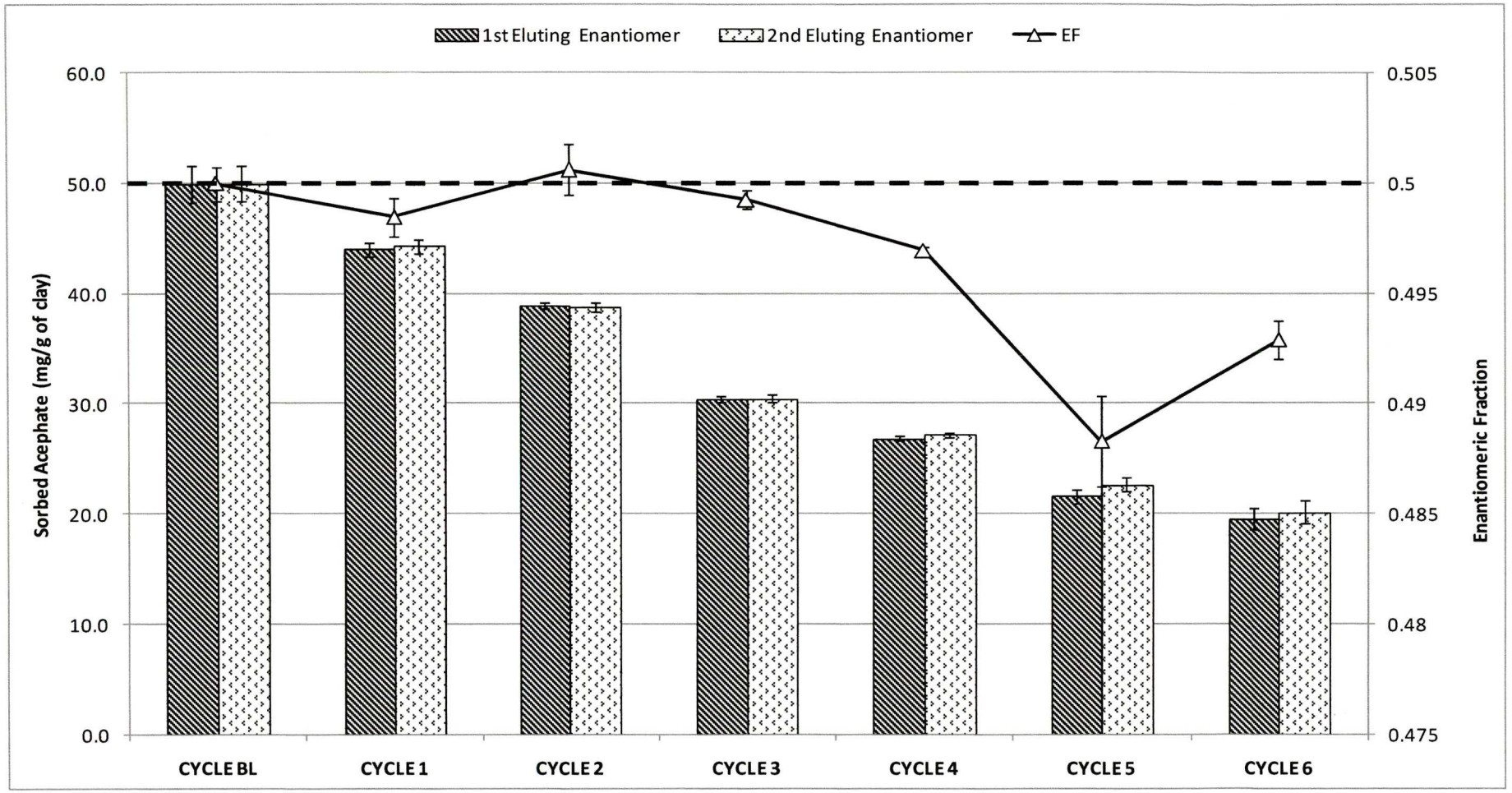

Figure 5.14 (Column plot) the amount of acephate in supernatant (mg/g) after sorption at the surfaces of K10 clay after repeated sorption cycles and (line plot) the subsequent EF values for the each cycle. Error bars represent the standard error calculated for each data point while the black dotted line represents a racemic mixture of the two enantiomers.

The cycles showed a near linear decrease in acephate concentration in the supernatant after each sorption experiment (Figure 5.14). It was determined through analysis of variance (ANOVA) that the sample means for EF of each cycle differ significantly. Nonetheless, in the first three cycles very little deviation from the racemic state of acephate was observed. However, significant enantiomer specific preferential adsorption could be inferred from the remaining cycles with the strongest preference being observed in the fifth cycle. Furthermore, Cycle 4, 5 and 6 were all shown to be significantly different from each other based on a 5% LSD value of 0.003[4].

Overall it can be inferred that an initial enantiomeric enrichment (e.e.) in the sorbate of a simple batch sorption experiment has a significant effect on the extent of enantioselective adsorption occurring at the surface of the sorbent. In general, the larger the e.e. in the initial supernatant solution the greater the deviation was from the racemic state after equilibration. Looking further into the findings of Haq et al. (2009) may give insight into the results seen here. Their experiments involved the exposure of enantiopure and racemic tartaric acid (TA) to the surface of clean Cu (110) via sublimation into an ultra-high vacuum chamber. STM and LEED techniques showed an equal distribution of tartaric acid (TA) enantiomers when the initial e.e. of TA in the supernatant was zero. However, clearly visible in the STM images (Figure 5.15 a), domains of single enantiomer adsorption were observed providing a strong indication that the sorbate molecules interact with each other as they adsorb to the surface.

The introduction of TA with a slight e.e. excess saw the domains of adsorption of the majority enantiomer dominate nonlinearly (the percentage deviation from the racemic state was much larger for the adsorbed species compared to that in the initial supernatant) (Figure 5.15 b). Meanwhile, the minority enantiomers exhibited a striking inability to form homochiral conglomerate domains of significant size. For example, an e.e. of 0.2 resulted in 75% coverage of the majority enantiomer. Overall, therefore, the observations demonstrated drastic symmetry breaking as a consequence of small enantiomeric excesses in the initial sorbate solution.

[4] The least significant difference (LSD) was calculated, based on a P value of 0.05, from the ANOVA of the data (Appendix 1.4).

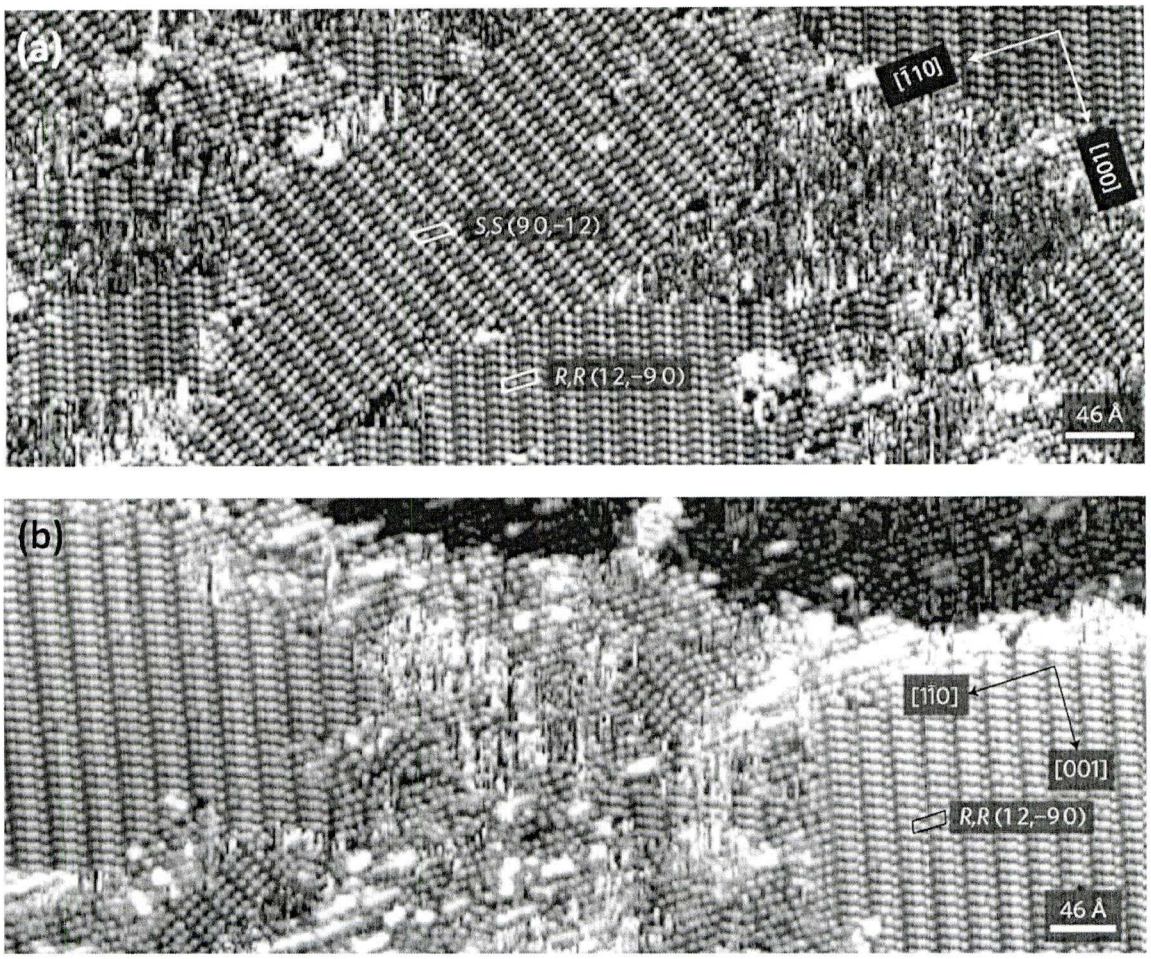

Figure 5.15 The formation of (a) racemic tartaric acid (TA) and (b) enantiomerically unbalanced tartaric acid (R,R TA in large domains and S,S TA in small disorganised domains) on the surface of Cu (110).

The formation of homochiral conglomerate domains, even when overall coverage is racemic, occurs because an energy preference drives each enantiomer to occupy its preferred chiral organisation. Thus, an energy penalty prevents an already adsorbed enantiomer from taking on its opposite enantiomorph. This reasoning can presumably be applied to the experiment here, although it is still not clear whether the acephate molecules are adsorbed through direct interaction with the interlayer surface or through ion exchange or ligand formation with the interlayer cation. In the case where ligand exchange or formation is the dominant form of adsorption then the formation of a superstructure, as explored above, will become less of a viable occurrence. However, if the ligand formations are close enough together for the incorporated acephate molecules to interact then the overall effect may be that of a superstructure.

A final observation of note is that at low coverage of the sorbent surface, the whole system remains disorganised whereas higher coverage forces a more organised system due to greater density of the organised structure. If this applies to experiments throughout this work then it can be presumed that, where a set amount of mineral has been used, the extent of coverage is sufficient to cause enantioselectivity if, indeed, it is observed. Additionally, in experiments where a variety of mineral amounts have been used, this idea could explain the initial peak followed by a levelling off of enantioselectivity as seen in the raw SWy-2 batch experiment in Section 5.5.

5.8 Montmorillonite K10 as a packing material for an HPLC column

An experiment was developed to determine whether the apparent selective behaviour observed between acephate and K10 could be harnessed in an attempt to provide some groundwork for the development of a new enantiopurification technique. The fundamental hypothesis was that an HPLC column packed with montmorillonite K10 serving as the stationary phase would retard or prevent the progress of one of the enantiomers of acephate in solution more than the other. Attempts were made in vain to quantify the resulting peaks provided as an output from the DAD UV-detector employed. Consequently, the eluting solution was collected as a fraction and prepared for GC analysis. This made it possible to assess whether any of the sorbate had remained in the column and, if so, whether it had been retained enantioselectively. Figure 5.16 shows the concentration of the acephate enantiomers remaining in the eluent after being passed through the K10 packed column. Less than 40 mg/L remains of the 100.4 mg/L of acephate present in the initial aqueous solution injected onto the column. This suggests that at least 60 % of the acephate molecules are retained by the stationary phase.

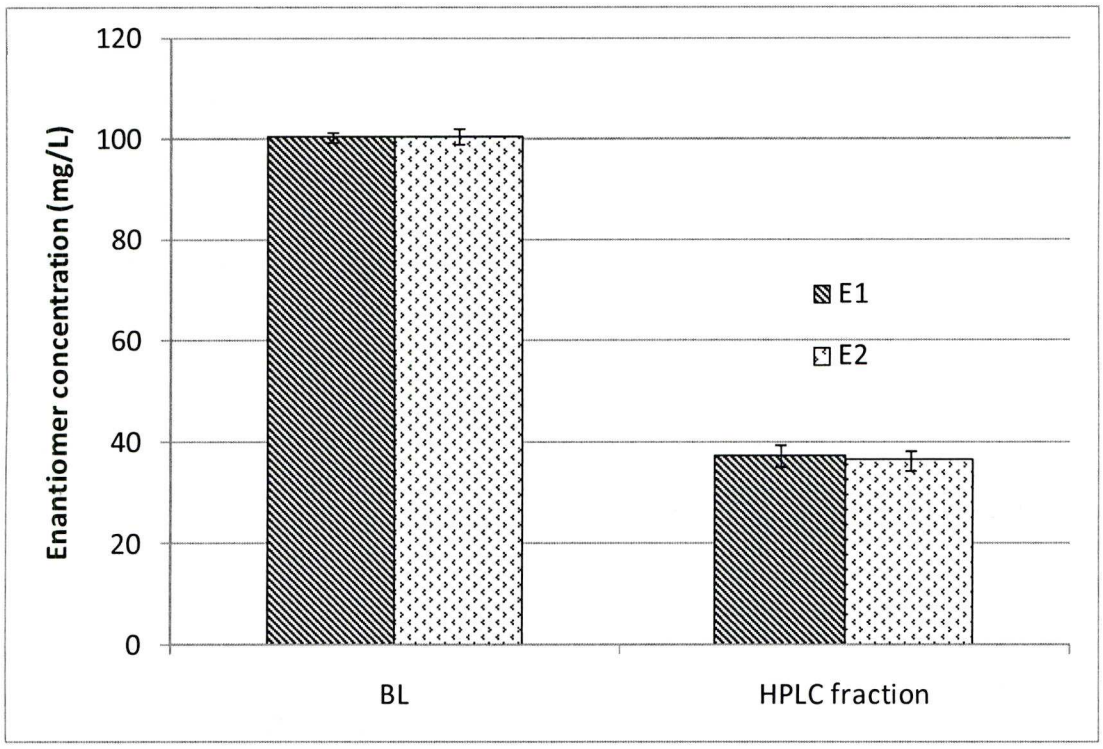

Figure 5.16 Column plot displaying the concentration of acephate enantiomers in an aqueous solution (BL) compared to the concentration of acephate enantiomers remaining in the eluent after being passed through a K10 packed column (HPLC fraction); analysis conducted on an Agilent 1100 HPLC system.

The enantiomeric fraction was calculated for enantiomers of acephate remaining in the eluent after being passed through the K10 packed column (Figure 5.17). A small but significant deviation from the racemic state is observed, indicated by an EF of 0.506 which equates to an imbalance of just over 1 %. It is apparent, therefore, that K10 used as a stationary phase in a customised HPLC column is indeed capable of chirally selective retention resulting in elution of a non-racemic mixture of acephate enantiomers.

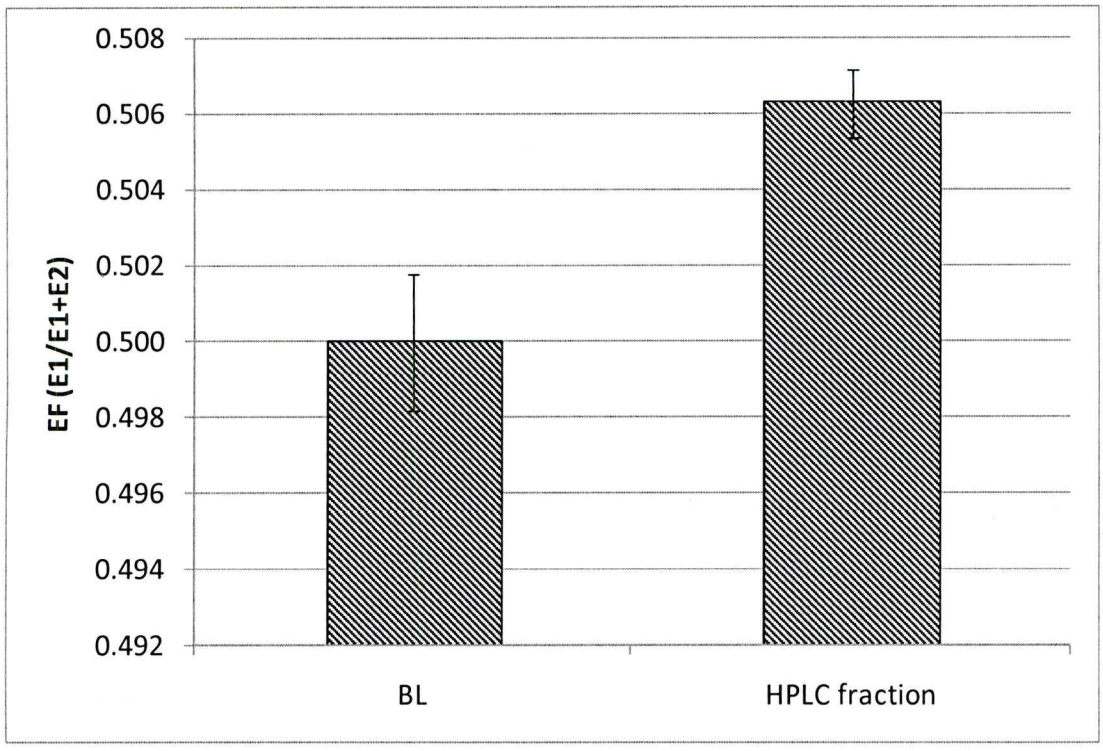

Figure 5.17 Column plot displaying the enantiomeric fraction (EF) calculated for acephate enantiomers in an aqueous solution (BL) and for acephate enantiomers remaining in the eluent after being passed through a K10 packed column (HPLC fraction)

The results provide foundations for a chiral resolution technique that is extremely inexpensive in relation to commercially produced, current chiral stationary phases such as cyclodextrin based capillary columns for GC and macrocyclic glycoprotein based columns for HPLC (Sigma-Aldrich ®). Of course, method development is very much in its infancy and significant problems must be overcome before larger scale separations become viable. For example, presently, quantification of the eluting enantiomers is not possible on HPLC with a DAD UV-detector. Further experimentation is required in order find the correct conditions on the column as well as the right choice of detector. Additionally, a large proportion of the sorbate remains on the column meaning that repeat runs of the same solution in order to increase the enantiomeric imbalance on route to enantiopurification becomes difficult and the efficiency poor. Furthermore, the present inability to quantify using the HPLC system alone means it is unclear whether the eluent is being subjected to multiple adsorption/desorption cycles within the column resulting in greater retardation of a particular enantiomer; or whether both enantiomers are eluted at exactly the same time but after enantioselective adsorption and equilibration has occurred. Another unknown factor is whether all the eluent is removed from the column before the next

acephate injection. It is understood that a significant proportion remains for the period that the fraction is being removed for GC analysis but it is unclear whether this is then eluted during the blank injection between sample runs. The retained acephate may remain bound indefinitely while not interfering with adsorption in subsequent runs. This might be possible for a limited number of runs while the large surface area of K10 provides a sufficient number of active sites for uncompetitive adsorption. Such queries could be resolved quite simply if quantification of acephate passed through the K10 column could be achieved on the HPLC system alone.

The pre-adsorption of acephate on the surface of K10 as a complex sorbent has not been addressed in this work. There is significant scope for further work involving simple batch sorption experiments consisting of acephate and a K10- acephate complex. Assuming that the complex involved a non-racemic presence of acephate, it is possible that enantioselectivity in the following batch sorption experiment would be greatly enhanced. This would be in keeping with many results from the work in this project where the extent of enantioselectivity is dependent on interactions with already bound enantiomers of the sorbate. In a specific example, Nakamura et al. (1988) explain that while a racemic mixture of a chiral sorbate will cover the whole surface of a sorbent, an enantiopure sorbate will leave half of the surface unoccupied because of steric interference among the adsorbed species. Furthermore, subsequent adsorption on a surface loaded with pure enantiomers should display strong enantioselectivity towards further adsorption of a chiral molecule. This should also apply, to some extent, to a system where the initial coverage is enantiomerically unbalanced rather than enantiopure. Again, this could be tested with simple batch sorption experiments.

5.9 Some implications for the origin of homochirality of life theories

Many of the experiments throughout this work can be interpreted to provide insight into, or support of current theories on the origin of the homochirality of life reviewed in Chapter 1 of this work. Briefly, however, the homochirality of life must have come about from either deterministic or stochastic processes. The deterministic approach essentially states that homochirality emerged as a result of the intrinsic homochirality of the universe; either through chiral electroweak forces causing the L-form of amino acids to be more stable than the D- form or, alternatively, through the inherent ability of circularly polarised light, existing throughout the universe, to

induce enantioselective photo-resolution of racemates (Weissbuch et al. 2005). A stochastic approach suggests that spontaneous mirror symmetry breaking could have occurred in systems not yet at equilibrium in a pre-biotic world. Since the work here provides evidence of enantiomer selective adsorption at the surfaces of achiral minerals, such as montmorillonite, the suggestion that clay surfaces could act as a substrate for the adsorption and unbalancing of racemic amino acid mixtures as well as a catalyst for the amplification of the small enantiomeric excess, is worth considering. Normally, a major drawback to theories considering clay minerals as playing a part in the origin of homochirality is that those minerals considered are chiral. This allows a logical explanation for enantiomer specific selection but falls short when it is accepted that there is a globally racemic distribution of the mineral enantiomorphs and that there is no reason therefore to expect a global imbalance in amino acid enantiomer adsorption. Enantioselective adsorption at the surface of montmorillonite, however, is not due to an inherent chirality of the mineral and thus does not have an equal distribution of left and right hand adsorbing enantiomorphs. Instead it must derive its selectivity from other conditions and prerequisites involved in the adsorption process. Assuming that such conditions were met in a prebiotic earth, the enantioselective adsorption of amino acids for example would have shown a specific preference for one of the enantiomers provided the conditions remained the same. Such a process coupled with possible mechanisms for further enantiomeric enrichment of adsorbed species provides a feasible basis for the explanation of the homochirality of life. Furthermore, some clay minerals, such as kaolinite, are thought to act as a template, catalysing the polymerisation of amino acids into peptides (Degens 1989). It is conceivable, therefore, that a prebiotic clay mineral which preferentially adsorbed L-amino acids would catalyse the formation of like-oriented peptides and proteins leading to a life system modelled around, and dependent on the L-form of amino acids.

5.10 Some implications for environmental impact of chiral OP pesticides

It is clear from the results of many of the experiments conducted in this project that preferential, enantiomer selective adsorption of acephate is possible by some achiral mineral surfaces. Given the fairly typical properties of acephate as an OP pesticide it can be assumed that it is not the only member of its class capable of being subjected to such asymmetric adsorption. Thus, it is important to assess the effect of such a

phenomenon on the impact of chiral OP pesticides in the environment. Most chiral OPs are assumed to remain in a racemic mixture of enantiomers as they are distributed and dispersed. However, enantiomeric imbalances are observed in samples of OP pesticides in the environment (for example Valenzuela Díaz & P. D. S. Santos 2001) and are normally presumed to be due to biotic degradation (Hegeman & Laane 2002). If, as discussed in Chapter 1, the relative toxicological effect of the enantiomers are different then a deviation from the racemic state of enantiomers found in the environment will have an effect on the overall toxicity of the chemical. The assumed toxicity, therefore, and the subsequent impact on non-target species might be entirely incorrect. As such, it is important to assess and understand all possible causes for the enantiomeric imbalances observed. In this work we see a wide range of enantiomeric deviations from the racemic state caused by adsorption onto mineral surfaces. Some of the large deviations of up to ~ 30% observed after a 48 h equilibration period would have an immediate and significant effect on the overall toxicity of the pesticide. However, significant deviations of less than 2% from a racemic mixture of enantiomers are also observed and will thus have a limited effect on the toxicity of the molecule. Furthermore, it might be assumed that after equilibration, the process of enantiomer selective adsorption will cease. In environmental conditions, however, a single and final equilibration is unlikely, especially given the semi-volatile nature of most OP pesticides. Multiple adsorption-desorption cycles occurring due spatial temperature changes or day/night cycles might cause significant amplification of the deviation from the racemic state, particularly given the apparent significance of an initial enantiomeric imbalance. Figure 5.18 below shows how a small enrichment of one of the enantiomers of a chiral compound can be amplified over a number of fractionation cycles.

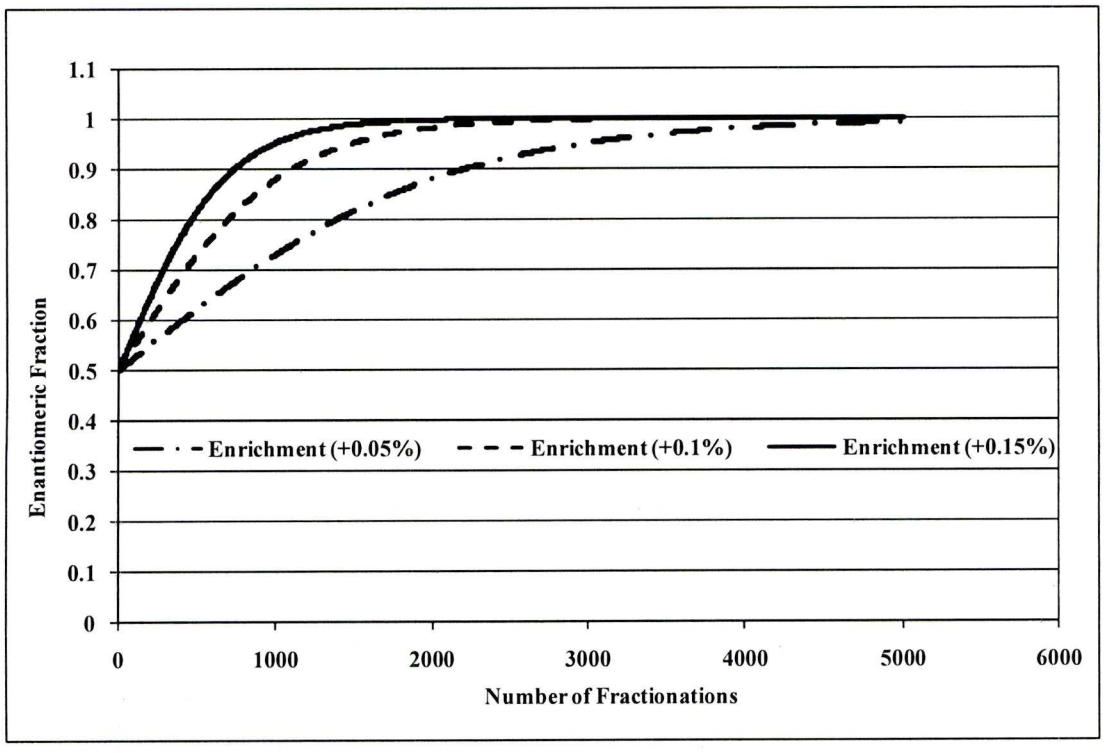

Figure 5.18 Model illustrating the rate of increase in enantiomeric fraction (EF) over a number of fractionation cycles where in each of which an enrichment of 0.05 % (dots and dashes), 0.1 % (dashed line) and 0.15 % (solid line) occurs.

The model assumes that each fractionation causes a further enrichment of the percentage stated in the legend. In fact, in light of the results presented in Section 5.7 above, this model is a particularly conservative one given that an initial enantiomeric imbalance appears to give rise to a disproportionately larger deviation in subsequent adsorption cycles. The model also makes the assumption that the deviation of EF from the racemic state will always be in the same direction. Results obtained throughout this project suggest this is not the case. However, Figure 5.18 is simply an example of how deviation of EF may escalate in the environment. The fractionations typically represent day/night cycles as the SVOC is evaporated into the atmosphere during the heat of the day before cooling and condensing at night. Such repeated deposition is likely to involve adsorption and desorption at mineral surfaces. The model provides a stark image of how quickly EFs can deviate from their racemic state and thus, differ dramatically from their perceived toxicity.

Chapter 4 provides a brief summary of the important results discussed throughout this chapter and provide concluding remarks relating to significant findings and further work and recommendations.

CHAPTER 6 SUMMARY AND CONCLUSIONS

This project has focussed in detail on the identification of enantiomer selective adsorption of the chiral organophosphorus insecticide, acephate, on a variety of mineral surfaces, some chiral, some achiral, in predominantly aqueous systems. Acephate was chosen for its chiral nature and as a typical current-use pesticide while the mineral sorbents were chosen due to their sorptive capabilities, large global prevalence and prebiotic relevance.

Gas chromatography has been the apparatus of choice for the majority of the analyses and used to assess the potential of selective adsorption of one enantiomer over the other on the mineral surfaces. Such enantioselectivity was assessed by the calculation of the enantiomeric fraction based on repeated quantitative determination of the mean concentration of the sorbate in the supernatant liquid.

Initial batch sorption experiments involving acephate adsorption at the surface of montmorillonite K10 (K10) revealed that the rate of adsorption showed conformity with the Langmuir equation while a seemingly exponential increase in preference for the (–) enantiomer of acephate was observed with increasing adsorption. Given the asymmetric nature of K10, this is a significant finding comparable to that of Bondy and Harrington (1979) who found that bentonite showed an enantiomer specific affinity for the L-form of some amino acids. The results here, however, are the first to be reported showing such enantioselectivity for a current-use chiral pesticide. Furthermore, the observed relationship between sorption and EF has implied that some level of interaction between newly adsorbing acephate molecules and those already bound is required for enantioselectivity to occur. This is in contrast to the experiments involving kaolinite, which show a preference for the same enantiomer of acephate but indicate that enantioselectivity occurs without the need for acephate-acephate interactions. Given the asymmetry of the kaolinite crystal, discussed in depth by Jackson (1971), such contrasting sorptive properties between K10 and kaolinite might have been expected.

In a subsequent experiment, there was a step feature in the adsorption plot for a Cu-exchanged K10. This gave an indication that multilayer sorption or stereochemical interactions were involved, causing the adsorbing molecule to become stabilized on

the clay surface and thus producing an enhanced affinity of the surface for the sorbate as its surface excess increases. Since significant enantioselectivity was also observed in this batch sorption experiment, support was provided for the idea that acephate molecules need to interact with each other as well as the clay surface in order for an enantiomeric imbalance to emerge.

A marked and unexpected observation was made when comparing enantioselectivity in the initial unmodified K10 batch sorption experiments and the unmodified K10 batch making up part of the pre-treated K10 experiments. Both displayed significant enantiomer specific adsorption but with a preference towards the enantiomers of opposite sign. It was concluded that the choice of solvent was responsible for the switch in preference. Batches with an acetonitrile solvent gave rise to a preference for the (–) enantiomer of acephate while the use of aqueous solution resulted in a complete switch to the (+) enantiomer. The finding appears to be unique to unmodified, abiotic 2:1 clay substrates. It is suggested here, based on work by Fernandez et al. (2001), that the observation may be due to a difference in the dielectric constant of the solvent causing the distance between clay surface and exchangeable cation to be altered thus affecting the extent to which the sorbate is involved in the steric environment of the active sites. Further work is strongly recommended in this area; a variety of solvents might be used in a series of batch sorption experiment to investigate the sign of enantioselectivity with changing dielectric constant and polarity.

The individual enantiomers of lysine were introduced to K10 to form ligands with the exchangeable cation in order to provide a chiral complex within the interlayer. Both enantiomeric forms of the prepared complex showed significant enantiomer specific adsorption, again for the (+) enantiomer of acephate. A mechanism for the adsorption is proposed whereby one of two lysine zwitterions attached to the doubly charged interlayer cation of the sorbent complex is replaced by the acephate enantiomer in a ligand exchange process. It is important to note, however, that the opposite enantiomeric forms of the clay-lysine complex did not display an enantiomer specific preference for opposite enantiomers of acephate (although significant variation in the extent enantioselectivity was observed). It was concluded, therefore, that the enantiomer specific preference observed arises as a result of an interaction to which the chirality of the clay-lysine complex is irrelevant. The exact

cause of the enantioselectivity remains unclear but it seems likely that there is a very specific characteristic of the clay surface that causes the geometry of the complex adsorption to be different between the two systems (containing either the (+) or (–) enantiomer). As the complex resides at the clay surface within the interlayer space, the way it interacts, and more specifically, the way the complexed acephate interacts with the clay surface will be vital to the enantioselective nature of the continuing adsorption. For example, if the molecule binds in a way that hides the chiral centre of the complexed acephate, then enantioselectivity may be significantly reduced as further adsorption occurs throughout the equilibration process.

Some further insight into the mechanism for adsorption was provided through batch sorption experiments involving derivatised K10. The removal of hydroxyl groups through silanisation had no effect on the overall adsorption of acephate but calculated EFs revealed that an enantiomer specific preference had not occurred. It can be concluded, therefore, that hydroxyl groups present in the clay structure, whilst not playing a significant role in the retention of acephate as an adsorbed species, do have a considerable effect on the clay's enantioselective properties. Adsorption must occur at sites where at least some of the adsorbed enantiomers can be affected by the hydroxyl groups in such a way as to be able to provide an environment where one enantiomer of acephate is preferred. The conclusion is, therefore, that the proximity of hydroxyl groups is a critical factor in determining the enantioselectivity of an adjacent adsorption site.

Experiments involving adsorption onto clay surfaces set at variety of pH values provided further support for ligand formation as a mechanism for adsorption. In order for acephate to form a ligand with the exchangeable cation it must be ionised. This could only occur at pH values below its pKa of 8.5 and is reflected in the adsorption results that show a peak at pH 7 with reduced adsorption at pH 9 and 11. Lower levels of adsorption observed for batches at pH 5 and 3 could be explained by an increase in competition with H^+ ions for active binding sites on the clay surface as acidity of the suspension increases. Furthermore, an increase in enantioselectivity is observed at low pH, which supports the involvement of hydroxyl groups in the enantiomer selective process as it coincides with an increasing number of protonated silanol groups.

Finally, the experiment involving initial enantiomeric enrichments of acephate in a solution set to adsorb to an unmodified K10 surface was designed to complement the work of Haq et al. (2009) and yielded interesting results. In general, it was shown that an enantiomer imbalance at the beginning of the equilibration process enhances the enantioselectivity for acephate enantiomers by the clay surface. The importance of acephate-acephate interactions throughout the adsorption process is clear insomuch that an uneven coverage of adsorbing enantiomers in the early stages of equilibration will cause further enantioselectivity to an extent beyond that provided by the initial imbalance of enantiomers.

There is significant scope for further research to be conducted on several aspects of the work completed in this project. Detailed investigations into enantioselective adsorption at abiotic mineral surfaces have been carried out through controlled modelling of fundamental processes at work in the environment. However, application to the real world would be enhanced by extensive monitoring of EFs in a large number of environmental samples from different compartments and from a range of locations. This would provide further insight into how the ratio of enantiomers varies over time and distance from source in different mediums across the globe. Analogous research has been conducted extensively for organochlorine pesticides but due to their perceived low persistence, organophosphorus pesticides have received little attention. In the light of results from this work it is recommended that care be taken when assuming biotic degradation to be the sole cause of enantiomeric imbalances observed in some environmental samples. Furthermore, it is clear that not enough is known about the mechanisms by which the enantiomers of chiral organophosphorus pesticides adsorb to minerals in the environment and to what extent the ratios of enantiomers vary as they are transported by whatever means. As such, given the differing toxicities between enantiomers, it is suggested that future compilation of lists detailing the threat of organophosphorus pesticides in the environment take into account the potential for non-racemic enantiomeric mixtures. Indeed, the classification of organophosphorus pesticides, in this scenario, as separate entities would be preferred.

REFERENCES

Abid, S., 2008. *Chiral Processes in the Natural Environment.* Liverpool, UK: University of Liverpool.

Adams, J.M., Martin, K., McCabe, R.W. & Murray, S., 1986. Methyl t-butyl ether (MTBE) production: a comparison of montmorillonite-derived catalysts with an ion-exchange resin. *Clays Clay Minerals*, 34, 597–603.

Ali, I. & Aboul-Enein, H.Y., 2004. *Chiral Pollutants: Distribution, Toxicity and Analysis by Chromatography and Capillary Electrophoresis*, John Wiley & Sons.

Altaner, S., Hower, J., Whitney, G. & Aronson, J., 1984. Model for K-bentonite formation: evidence from zoned K-bentonites in the disturbed belt, Montana. *Geology*, 12(7), 412-415.

Bada, J., 1995. Origins of homochirality. *Nature*, 374(6523), 594-595.

Banat, F.A., Al-Bashir, B., Al-Asheh, S. & Hayajneh, O., 2000. Adsorption of phenol by bentonite. *Environmental Pollution*, 107(3), 391-398.

Barrie, L.A., Gregor, D., Hargrave, B., Lake, R., Muir, D., Shearer, R., Tracey, B. & Bidleman, T.F., 1992. Arctic Contaminants - Sources, Occurrence And Pathways. *Science Of The Total Environment*, 122(1-2), 1-74.

Barron, L.D., 2008. Chirality and life. *Space Science Reviews*, 135(1), 187–201.

Bennett, C.E., Dal Nogare, S., Safranski, L.W. & Lewis, C.D., 1958. Trace Analyses by Gas Chromatography. *Analytical Chemistry*, 30(5), 898-902.

Bentley, R., 1995. From optical activity in quartz to chiral drugs: Molecular handedness in biology and medicine. *Perspectives in Biology and Medicine*, 38(2), 188-229.

Bergaya, F. & Vayer, M., 1997. CEC of clays: Measurement by adsorption of a copper ethylenediamine complex. *Applied Clay Science*, 12(3), 275-280.

Bergaya, F., Theng, B.K.G. & Lagaly, G., 2006. *Handbook of clay science*, Elsevier.

Berglund, P., 2001. Controlling lipase enantioselectivity for organic synthesis. *Biomolecular engineering*, 18(1), 13–22.

Bidleman, T.F., Jantunen, L., Helm, P.A., Brorstrom-Lunden, E. & Juntto, S., 2002. Chlordane enantiomers and temporal trends of chlordane isomers in arctic air. *Environ. Sci. Technol*, 36(4), 539-544.

Biot, J.B., 1844. Communication d'une note de M. Mitscherlich. *Comptes Rendus de l'Académie des Sciences*, 19, 720.

Blumer, M., 1957. Removal of Elemental Sulfur from Hydrocarbon Fractions. *Analytical Chemistry*, 29(7), 1039-1041.

Bodenheimer, W. & Heller, L., 1967. Sorption of aamino-acids by copper montmorillonite. *Clay Minerals*, 7, 167-176.

Bondy, S. & Harrington, M., 1979. L Amino acids and D-glucose bind stereospecifically to a colloidal clay. *Science*, 203(4386), 1243-1244.

Bonner, W.A., 1995. Chirality and life. *Origins of Life and Evolution of Biospheres*, 25(1), 175–190.

Bonner, W.A., 1994. Enantioselective autocatalysis. Spontaneous resolution and the prebiotic generation of chirality. *Origins of Life and Evolution of the Biosphere*, 24(1), 63-78.

Bonner, W.A., 1991. The origin and amplification of biomolecular chirality. *Origins of Life and Evolution of the Biosphere*, 21(2), 59-111.

Bonner, W.A. & Flores, J.J., 1973. On the asymmetric adsorption of phenylalanine enantiomers by kaolin. *Currents in modern biology*, 5(2), 103-113.

Bonner, W.A. & Flores, J.J., 1975. Experiments on the origins of optical activity. *Origins of Life*, 6(1-2), 187-194.

Bonner, W.A., Kavasmaneck, P., Martin, F. & Flores, J.J., 1974. Asymmetric adsorption of alanine by quartz. *Science*, 186(4159), 143-144.

Bonner, W.A., Kavasmaneck, P., Martin, F. & Flores, J.J., 1975. Asymmetric adsorption by quartz: A model for the prebiotic origin of optical activity. *Origins of Life*, 6(3), 367-376.

Borden, D. & Giese, R.F., 2001. Baseline studies of the clay minerals society source clays: cation exchange capacity measurements by the ammonia-electrode method. *Clays and Clay Minerals*, 49(5), 444-445.

Bradley, W.F. & Grim, R.E., 1950. *High temperature thermal effects of clay and related materials*, Urbana, Illinois.

Brigatti, M.F., Galan, E. & Theng, B.K.G., 2006. Structures and minerology of clay minerals. In *Handbook of clay science*. Elsevier Ltd, pp. 19-86.

Brindley, G. & Ertem, G., 1971. Preparation and solvation properties of some variable charge montmorillonites. *Clays and Clay Minerals*, 19(6), 399-404.

Buerge, I., Poiger, T., Müller, M. & Buser, H., 2003. Enantioselective degradation of metalaxyl in soils: Chiral preference changes with soil pH. *Environmental Science and Technology*, 37(12), 2668-2674.

Burkow, I.C. & Kallenborn, R., 2000. Sources and transport of persistent pollutants to the Arctic. *Toxicology Letters*, 112-113, 87-92.

Buser, H.R. & Mueller, M.D., 1994. Isomer- and enantiomer-selective analyses of toxaphene components using chiral high-resolution gas chromatography and detection by mass spectrometry/mass spectrometry. *Environmental Science & Technology*, 28(1), 119-128.

Buser, H. & Mueller, M.D., 1995. Isomer and Enantioselective Degradation of Hexachlorocyclohexane Isomers in Sewage Sludge under Anaerobic Conditions. *Environmental Science & Technology*, 29(3), 664-672.

Cahn, R., Ingold, C. & Prelog, V., 1956. The specification of asymmetric configuration in organic chemistry. *Experientia*, 12(3), 81-94.

Cairns Smith, A., 1975. A case for an alien ancestry. *Proceedings of the Royal Society of London - Biological Sciences*, 189(1095), 249-274.

Calvin, M., 1969. Chemical evolution. *Chemistry in Britain*, 5(1), 22-28.

Carrea, G., Ottolina, G. & Riva, S., 1995. Role of solvents in the control of enzyme selectivity in organic media. *Trends in Biotechnology*, 13(2), 63–70.

Castro-Puyana, M., Salgado, A., Hazen, R.M., Crego, A. & Alegre, M., 2008. The first contribution of capillary electrophoresis to the study of abiotic origins of homochirality: Investigation of the enantioselective adsorption of 3-carboxy adipic acid on minerals. *Electrophoresis*, 29(7), 1548-1555.

Cavelier, J., Aide, T.M., Dupuy, J.M., Eusse, A.M. & Santos, C., 1999. Long-term effects of deforestation on soil propertions and vegetation in a tropical lowland forest in Colombia. *Ecotropicos*, 12(2), 57–68.

Chambers, H.W., Boone, J.S., Carr, R.L. & Chambers, J.E., 2001. Chemistry of Organophosphorus Insecticides. In *Handbook of Pesticide Toxicology*. San Diego: Academic Press, pp. 913-917.

Chambers, J.E., Carr, R.L., Boone, J.S. & Chambers, H.W., 2001. The Metabolism of Organophosphorus Insecticides. In *Handbook of Pesticide Toxicology*. San Diego: Academic Press, pp. 919-927.

Christidis, G.E. & Huff, W.D., 2009. Geological Aspects and Genesis of Bentonites. *ELEMENTS*, 5(2), 93-98.

Clark, J., Cullen, S., Barlow, S. & Bastock, T., 1994. Environmentally friendly chemistry using supported reagent catalysts: Structure-property relationships for clayzic. *Journal of the Chemical Society, Perkin Transactions 2*, (6), 1117-1130.

Cornejo, J., Celis, R., Pavlovic, I. & Ulibarri, M.A., 2008. Interactions of pesticides with clays and layered double hydroxides: a review. *Clay Minerals*, 43(2), 155-175.

Costa, L., 2006. Current issues in organophosphate toxicology. *Clinica Chimica Acta*, 366(1-2), 1-13.

Coulombe, C.E., Wilding, L.P. & Dixon, J.B., 1996. Overview of Vertisols: Characteristics and Impacts on Society. In Academic Press, pp. 289-375.

Cronin, J. & Reisse, J., 2005. Chirality and the Origin of Homochirality. In *Lectures in Astrobilogy*. Berlin/Heidelberg: Springer-Verlag.

Cronin, J.R. & Pizzarello, S., 1997. Enantiomeric excesses in meteoritic amino acids. *Science*, 275(5302), 951.

Dalgliesh, C., 1952. The optical resolution of aromatic amino-acids on paper chromatograms. *Journal of the Chemical Society (Resumed)*, 3916-3922.

Davankov, V.A. & Kurganov, A., 1983. The role of achiral sorbent matrix in chiral recognition of amino acid enantiomers in ligand-exchange chromatography. *Chromatographia*, 17(12), 686-690.

Davankov, V.A., Meyer, V.R. & Rais, M., 1990. A vivid model illustrating chiral recognition induced by achiral structures. *Chirality*, 2(4), 208-210.

De Lange, H., Lahr, J., Van Der Pol, J., Wessels, Y. & Faber, J., 2009. Ecological vulnerability in wildlife: An expert judgment and multicriteria analysis tool using ecological traits to assess relative impact of pollutants. *Environmental Toxicology and Chemistry*, 28(10), 2233-2240.

Degens, E.T., 1989. Clay Minerals-Blueprints of Early Life. *Haematology and blood transfusion*, 32, 500.

Degens, E.T., Matheja, J. & Jackson, T.A., 1970. Template catalysis: asymmetric polymerization of amino acids on clay minerals. *Nature*, 227(5257), 492-493.

Didymus, J., Young, J. & Mann, S., 1994. Construction and morphogenesis of the chiral ultrastructure of coccoliths from the marine alga Emiliania huxleyi. *Proceedings of the Royal Society B: Biological Sciences*, 258(1353), 237-245.

Downing, E., 2002. *Environmental fate of Acephate*, Sacramento, CA: Department of Pesticide Regulation.

Drayer, D.E., 2001. The Early History of Stereochemistry: from the discovery of molecular asymmetry and the first resolution of a racemate by Pasteur to the asymmetrical chiral carbon of Van't Hoff and Le Bel. *Clinical Research and Regulatory Affairs*, 18(3), 181–203.

Druzina, B. & Stegu, M., 2007. Degradation study of selected organophosphorus insecticides in natural waters. , 1079-1093.

Edelman, C.H. & Favejee, J.C.L., 1940. On the crystal structure of montmorillonite and halloysite. *Z. Krist*, 102, 417–431.

Egri, G., Baitz-Gács, E. & Poppe, L., 1996. Kinetic resolution of 2-acylated-1, 2-diols by lipase-catalyzed enantiomer selective acylation. *Tetrahedron: Asymmetry*, 7(5), 1437–1448.

Ehrich, M. & Jortner, B., 2001. Organophosphorus-Induced Delayed Neuropathy. In *Handbook of Pesticide Toxicology*. San Diego: Academic Press, pp. 987-1012.

Engel, M.H. & Nagy, B., 1982. Distribution and enantiomeric composition of amino acids in the Murchison meteorite. *Nature*, 296(5860), 837-840.

Faller, J., Hühnerfuss, H., Konig, W.A., Krebber, R. & Ludwig, P., 1991. Do marine bacteria degrade α-hexachlorocyclohexane stereoselectively. *Environmental Science and Technology*, 25(4), 676-678.

Faller, J., Hühnerfuss, H., Konig, W.A. & Ludwig, P., 1991. Gas chromatographic separation of the enantiomers of marine organic pollutants. Distribution of α-HCH enantiomers in the North Sea. *Marine Pollution Bulletin*, 22(2), 82-86.

Fan, S. & Walters, J., 2002. *Use information and air monitoring recommendations for the pesticide active ingredients acephate, chlorothanonil and methamidophos*, Sacramento, California: California Department of Pesticide Regulation (DPR).

Fernández, A.I., Fraile, J.M., García, J.I., Herrerías, C.I., Mayoral, J.A. & Salvatella, L., 2001. Reversal of enantioselectivity by change of solvent with clay-immobilized bis (oxazoline)-copper catalysts. *Catalysis Communications*, 2(5), 165–170.

Fischer, E., 1894. Influence of Configuration on the Action of Enzymes. *Ber. Dtsch. Chem. Ges*, 27, 2985–2993.

Fitzpatrick, P. & Klibanov, A.M., 1991. How can the solvent affect enzyme enantioselectivity? *Journal of the American Chemical Society*, 113(8), 3166-3171.

Frank, F., 1953. On spontaneous asymmetric synthesis. *BBA - Biochimica et Biophysica Acta*, 11(C), 459-463.

Freed, V., Schmedding, D., Kohnert, R. & Haque, R., 1979. Physical chemical properties of several organophosphates: some implication in environmental and biological behavior. *Pesticide Biochemistry and Physiology*, 10(2), 203-211.

Friebele, E., Shimoyama, A., Hare, P. & Ponnamperuma, C., 1981. Adsorption of amino acid entantiomers by Na-montmorillonite. *Origins of Life*, 11(1-2), 173-184.

Garay, A. & Ahlgren-Beckendorf, J., 1990. Differential interaction of chiral β-particles with enantiomers. *Nature*, 346(6283), 451-453.

Garrido Frenich, A., Mart\'ınez Vidal, J.L., Moreno Fr\'ıas, M., Olea-Serrano, F., Olea, N. & Cuadros Rodriguez, L., 2003. Determination of organochlorine pesticides by GC-ECD and GC-MS-MS techniques including an evaluation of the uncertainty associated with the results. *Chromatographia*, 57(3), 213–220.

Garrison, A.W., 2006. Probing the enantioselectivity of chiral pesticides. *Environmental Science & Technology*, 40(1), 16-23.

Garrison, A.W., Schmitt, P., Martens, D. & Kettrup, A., 1996. Enantiomeric Selectivity in the Environmental Degradation of Dichlorprop As Determined by High-Performance Capillary Electrophoresis. *Environmental Science & Technology*, 30(8), 2449-2455.

Gassmann, G., 1981. Chromatographic separation of diasteriomeric isoprenoids for the identification of fossil oil contamination. *Marine Pollution Bulletin*, 12(3), 78-84.

Gil-Av, E., Feibush, B. & Charles-Sigler, R., 1966. Separation of enantiomers by gas liquid chromatography with an optically active stationary phase. *Tetrahedron Letters*, 7(10), 1009-1015.

Goldberg, E.D. & Griffin, J.J., 1964. Sedimentation Rates and Mineralogy in the South Atlantic. *Journal of Geophysical Research*, 69(20).

Green, M., Reidy, M., Johnson, R., Darling, G., O'Leary, D. & Willson, G., 1989. Macromolecular stereochemistry: The out-of-proportion influence of optically active comonomers on the conformational characteristics of polyisocyanates. The sergeants and soldiers experiment. *Journal of the American Chemical Society*, 111(16), 6452-6454.

Griffin, J., Windom, H. & Goldberg, E., 1968. The distribution of clay minerals in the World Ocean. *Deep-Sea Research and Oceanographic Abstracts*, 15(4), 433-459.

Grim, R.E., 1968. *Clay Mineralogy* 2nd ed., McGraw-Hill Inc.,US.

Hageman, K.J., Simonich, S.L., Campbell, D.H., Wilson, G.R. & Landers, D.H., 2006. Atmospheric deposition of current-use and historic-use pesticides in snow at national parks in the western United States. *Environ. Sci. Technol*, 40(10), 3174–3180.

Haq, S., Liu, N., Humblot, V., Jansen, A. & Raval, R., 2009. Drastic symmetry breaking in supramolecular organization of enantiomerically unbalanced monolayers at surfaces. *Nature Chemistry*, 1(5), 409-414.

Harner, T., Wiberg, K. & Norstrom, R., 2000. Enantiomer fractions are preferred to enantiomer ratios for describing chiral signatures in environmental analysis. *Environmental Science & Technology*, 34(1), 218-220.

Hashizume, H., Theng, B.K.G. & Yamagishi, A., 2002. Adsorption and discrimination of alanine and alanyl-alanine enantiomers by allophane. *Clay Minerals*, 37(3), 551-557.

Haüy, R.J., 1809. *Tableau comparatif des resultats de la cristallographie et de l'analyse chimique, relativement a la classification des mineraux / Par M. l'abbe Hauy*, Paris : Bruxelles :: chez Courcier, Culture et civilisation.

Havinga, E., 1954. Spontaneous formation of optically active substances. *BBA - Biochimica et Biophysica Acta*, 13(C), 171-174.

Hazen, R.M., 2004. Chiral crystal faces of common rock-forming minerals. In *Progress in Biological Chiralty*. Oxford: Elsevier Ltd, p. 429.

Hazen, R.M., 2006. Mineral surfaces and the prebiotic selection and organization of biomolecules. *American Mineralogist*, 91(11-12), 1715-1729.

Hazen, R.M., Filley, T. & Goodfriend, G., 2001. Selective adsorption of L- and D-amino acids on calcite: Implications for biochemical homochirality. *Proceedings of the National Academy of Sciences of the United States of America*, 98(10), 5487-5490.

Hegeman, W.J.M. & Laane, R., 2002. Enantiomeric enrichment of chiral pesticides in the environment. In *Reviews of Environmental Contamination and Toxicology, Vol 173*. Reviews of Environmental Contamination and Toxicology. pp. 85-116.

Held, G. & Gladys, M., 2008. The Chemistry of Intrinsically Chiral Surfaces.

Hermanson, M.H., Isaksson, E.H., Teixeira, C., Muir, D.C.G., Compher, K.M., Li, Y.F., Igarashi, I. & Kamiyama, K., 2005. Current-use and legacy pesticide history in the Austfonna ice cap, Svalbard, Norway. *Environmental Science & Technology*, 39(21), 8163-8169.

Hirose, Y., Kariya, K., Sasaki, I., Kurono, Y., Ebiike, H. & Achiwa, K., 1992. Drastic solvent effect on lipase-catalyzed enantioselective hydrolysis of prochiral 1,4-dihydropyridines. *Tetrahedron Letters*, 33(47), 7157-7160.

Hobbs, J., Cygan, R., Nagy, K., Schultz, P. & Sears, M., 1997. All-atom ab initio energy minimization of the kaolinite crystal structure. *American Mineralogist*, 82(7-8), 657-662.

Hofmann, U., Endell, K. & Wilm, D., 1933. Kristalstruktur und Quellung yon Montmorillonit. *Z. Krist*, 86, 340–348.

Horvath, J.D. & Gellman, A.J., 2003. Naturally chiral surfaces. *Topics in Catalysis*, 25(1), 9–15.

Hühnerfuss, H., Faller, J., R. Kallenborn, König, W.A., Ludwig, P., Pfaffenberger, B., Oehme, M. & Rimkus, G., 1993. Enantioselective and nonenantioselective degradation of organic pollutants in the marine ecosystem. *Chirality*, 5(5), 393–399.

Hühnerfuss, H. & Kallenborn, R., 1992. Chromatographic separation of marine organic pollutants. *Journal of Chromatography*, 580(1-2), 191-214.

Hühnerfuss, H., Kallenborn, R., Konig, W.A. & Rimkus, G., 1992. Preferential enrichment of the (-t-)-a-hexachlorocyclohexane in cerebral matter of harbour seals. *Organohalogen Compd*, 10, 97–100.

Hunt, J., Anderson, B., Phillips, B., Nicely, P., Tjeerdema, R., Puckett, H., Stephenson, M., Worcester, K. & de Vlaming, V., 2003. Ambient toxicity due to chlorpyrifos and diazinon in a central California coastal watershed. *Environmental Monitoring and Assessment*, 82(1), 83-112.

Jackson, T.A., 1971. Preferential polymerization and adsorption of L-optical isomers of amino acids relative to D-optical isomers on kaolinite templates. *Chemical Geology*, 7(4), 295-306.

Jang, S. & Condrate, R.A., 1972. The IR spectra of lysine adsorbed on several cation-substituted montmorillonites. *Clays and Clay Minerals*, 20, 79–82.

Jantunen, L. & Bidleman, T.F., 1998. Organochlorine Pesticides and Enantiomers of Chiral Pesticides in Arctic Ocean Water. *Archives of Environmental Contamination and Toxicology*, 35(2), 218-228.

Jantunen, L. & Bidleman, T.F., 1997. Air-water gas exchange of hexachlorocyclohexanes (HCHs) and the enantiomers of alpha-HCN in arctic regions (vol 101, pg 28837, 1996). *Journal Of Geophysical Research-Atmospheres*, 102(D15), 19279-19282.

Jiang, J.Q., Cooper, C. & Ouki, S., 2002. Comparison of modified montmorillonite adsorbents - Part I: preparation, characterization and phenol adsorption. *Chemosphere*, 47(7), 711-716.

Joyce, G., Visser, G. & Van Boeckel, C., 1984. Chiral selection in poly(C)-directed synthesis of oligo(G). *Nature*, 310(5978), 602-604.

Julg, A., 1990. Asymmetrical adsorption on kaolinite and origin of the L-homochirality of the amino acids in the proteins of living organisms. *Sciences Geologiques - Memoire*, 85, 25-34.

Julg, A., Favier, A. & Ozias, Y., 1990. A theoretical study of the difference in the behavior ofl- andd-alanine toward the two inverse forms of kaolinite. *Structural Chemistry*, 1(1), 137-141.

Julg, A. & Ozias, Y., 1988. Asymmetric adsorption of ethyliminium cation on kaolinite and -homochirality of amino acids in proteins. *Journal of Molecular Structure*, 179(1), 17-25.

Kallenborn, R. & Hühnerfuss, H., 2001. *Chiral environmental pollutants: trace analysis and ecotoxicology*,

Kallenborn, R., Hühnerfuss, H. & Konig, W.A., 1991. Enantioselective metabolism of (±)-α-1,2,3,4,5,6-hexachlorocyclohexane in organs of the eider duck. *Angewandte Chemie - International Edition in English*, 30(3), 320-321.

Kanekar, P.P., Bhadbhade, B., Deshpande, N.M. & Sarnaik, S.S., 2004. Biodegradation of Organophosphorus Pesticides. *Proc. Indian natn Sci Acad. B70 No*, 1, 57–70.

Karagunis, G. & Coumoulos, G., 1938. A New Method of Resolving a Racemic Compound. *Nature*, 142, 162.

Kemp, J.C., Henson, G.D., Steiner, C.T. & Powell, E.R., 1987. The optical polarization of the Sun measured at a sensitivity of parts in ten million. *Nature*, 326(6110), 270–273.

Klabunovskii, E.I., 2001. Can enantiomorphic crystals like quartz play a role in the origin of homochirality on earth? *Astrobiology*, 1(2), 127-131.

Klabunovskii, E.I. & Thieman, W., 2000. The role of quartz in the origin of optical activity on earth. *Origins of Life and Evolution of the Biosphere*, 30(5), 431-434.

Klecka, G.M., 2000. *Evaluation of Persistence and Long-Range Transport of Organic Chemicals in the Environment: Guidelines and Criteria for Evaluation and Assessment*, S E T a C Foundation.

Klibanov, A.M., 2001. Improving enzymes by using them in organic solvents. *Nature*, 409(6817), 241-246.

Konda, L.N., Czinkota, I., Fuleky, G. & Morovjan, G., 2002. Modeling of Single-Step and Multistep Adsorption Isotherms of Organic Pesticides on Soil. *Journal of Agricultural and Food Chemistry*, 50(25), 7326-7331.

Kondepudi, D., Kaufman, R. & Singh, N., 1990. Chiral symmetry breaking in sodium chlorate crystallization. *Science*, 250(4983), 975-976.

König, W.A., Icheln, D., Runge, T., Pfaffenberger, B., Ludwig, P. & Hühnerfuss, H., 1991. Gas chromatographic enantiomer separation of agrochemicals using modified cyclodextrins. *Journal of High Resolution Chromatography*, 14(8),

530-536.

König, W.A., Lutz, S. & Wenz, G., 1988. Modified Cyclodextrins - Novel, Highly Enantioselective Stationary Phases for Gas Chromatography. *Angewandte Chemie International Edition in English*, 27(7), 979-980.

Kozawa, K., Aoyama, Y., Mashimo, S. & Kimura, H., 2009. Toxicity and actual regulation of organophosphate pesticides. *Toxin Reviews*, 28(4), 245-254.

Kulp, E. & Switzer, J., 2007. Electrochemical biomineralization: The deposition of calcite with chiral morphologies. *Journal of the American Chemical Society*, 129(49), 15120-15121.

Lambert, O., Pouliquen, H. & Clergeau, P., 2005. Impact of cholinesterase-inhibitor insecticides on non-target wildlife: A review of studies relative to terrestrial vertebrates. *Revue d'Ecologie (La Terre et la Vie)*, 60(1), 3-20.

Laszlo, P., 1990. Catalysis of organic reactions by inorganic solids. *Pure and Applied Chemistry*, 62(10), 2027-2030.

Le Bel, J.A., 1874. Sur les relations qui existent entre les formules atomiques des corps organiques, et le pouvoir rotatoire de leurs dissolutions. *Bull. Soc. Chim. Paris*, 22, 337.

Levadie, B. & Harwood, J.F., 1960. An Application of Gas Chromatography to Analysis of Solvent Vapors in Industrial Air. *American Industrial Hygiene Association Journal*, 21(1), 20.

Lewis, D.L., Garrison, A.W., Wommack, K.E., Whittemore, A., Steudler, P. & Melillo, J., 1999. Influence of environmental changes on degradation of chiral pollutants in soils. *Nature*, 401(6756), 898-901.

Lin, K., Zhou, S.S., Xu, C. & Liu, W.P., 2006. Enantiomeric resolution and biotoxicity of methamidophos. *Journal of Agricultural and Food Chemistry*, 54(21), 8134-8138.

Liu, W., Gan, J., Schlenk, D. & Jury, W., 2005. Enantioselectivity in environmental safety of current chiral insecticides. *Proceedings of the National Academy of Sciences of the United States of America*, 102(3), 701-706.

Lochmüller, C. & Souter, R., 1975. Chromatographic resolution of enantiomers. Selective review. *Journal of Chromatography A*, 113(3), 283-302.

Loh, T. & Li, X., 1999. Clay montmorillonite K10 catalyzed aldol-type reaction of aldehydes with silyl enol ethers in water. *Tetrahedron*, 55(35), 10789-10802.

Lotti, M. & Moretto, A., 2005. Organophosphate-induced delayed polyneuropathy. *Toxicological Reviews*, 24(1), 37-49.

Luckham, P.F. & Rossi, S., 1999. The colloidal and rheological properties of

bentonite suspensions. *Advances in Colloid and Interface Science*, 82(1-3), 43-92.

Ludwig, P., Hühnerfuss, H., König, W.A. & Gunkel, W., 1992. Gas chromatographic separation of the enantiomers of marine pollutants. Part 3. Enantioselective degradation of α-hexachlorocyclohexane and γ-hexachlorocyclohexane by marine microorganisms. *Marine Chemistry*, 38(1-2), 13-23.

Mackay, D., Di Guardo, A., Paterson, S., Kicsi, G., Cowan, C. & Kane, D., 1996. Assessment of chemical fate in the environment using evaluative, regional and local-scale models: Illustrative application to chlorobenzene and linear alkylbenzene sulfonates. *Environmental Toxicology and Chemistry*, 15(9), 1638-1648.

Mahajna, M., Quistad, G. & Casida, J., 1997. Acephate insecticide toxicity: Safety conferred by inhibition of the bioactivating carboxyamidase by the metabolite methamidophos. *Chemical Research in Toxicology*, 10(1), 64-69.

Mannschreck, A., Kiesswetter, R. & von Angerer, E., 2007. Unequal activities of enantiomers via biological receptors: Examples of chiral drug, pesticide, and fragrance molecules. *Journal of Chemical Education*, 84(12), 2012-2017.

Maruyama, M., Tsukamoto, K., Sazaki, G., Nishimura, Y. & Vekilov, P., 2009. Chiral and achiral mechanisms of regulation of calcite crystallization. *Crystal Growth and Design*, 9(1), 127-135.

Mason, S., 1988. Biomolecular homochirality. *Chemical Society Reviews*, 17, 347-359.

Matthies, M., Klasmeier, J., Beyer, A. & Ehling, C., 2009. Assessing persistence and long-range transport potential of current-use pesticides. *Environmental Science and Technology*, 43(24), 9223-9229.

McBride, M., 1976. Hydration structure of exchangeable $Cu2^{+}$ in vermiculite and smectite. *Clays and Clay Minerals*, 24(4), 211-212.

McCullough, J. & Lemmon, R., 1974. The question of the possible asymmetric polymerization of aspartic acid on kaolinite. *Journal of Molecular Evolution*, 3(1), 57-61.

McLaren, A.D., Peterson, G.H. & Barshad, I., 1958. The adsorption and reactions of enzymes and proteins on clay minerals: IV. Kaolinite and montmorillonite. *Soil Science Society of America Journal*, 22(3), 239.

McLean, J., Sims, R., Doucette, W., Caupp, C. & Grenney, W., 1988. Evaluation of mobility of pesticides in soil using U.S. EPA methodology. *Journal of Environmental Engineering*, 114(3).

McNaught, A.D. & Wilkinson, A., 1997. *IUPAC compendium of chemical terminology*, IUPAC.

Meier, L. & Nüesch, R., 1999. The lower cation exchange capacity limit of montmorillonite. *Journal of Colloid and Interface Science*, 217(1), 77-85.

Meierhenrich, U., 2008. *Amino acids and the asymmetry of life: caught in the act of formation*, Berlin: Springer-Verlag.

Mermut, A.R. & Lagaly, G., 2001. Baseline studies of The Clay Minerals Society Source Clays: Layer-charge determination and characteristics of those minerals containing 2: 1 layers. *Clays and Clay Minerals*, 49(5), 393–397.

Mermut, A.R. & Cano, A.F., 2001. Baseline studies of the clay minerals society source clays: Chemical analyses of major elements. *Clays and Clay Minerals*, 49(5), 381-386.

Meyer, V.R. & Rais, M., 1989. A vivid model of chiral recognition. *Chirality*, 1(2), 167-169.

Miller, S.E., Heath, G.R. & Gonzalez, R.D., 1982. Effects of temperature on the sorption of lanthanides by montmorillonite. *Clays and Clay Minerals*, 30(2), 111–122.

Mills, W.H., 1932. Some aspects of stereochemistry. *Journal of the Society of Chemical Industry*, 51(37), 750–759.

Miyazaki, A., Nakamura, T., Kawaradani, M. & Marumo, S., 1988. Resolution and Biological-Activity of Both Enantiomers of Methamidophos and Acephate. *Journal of Agricultural and Food Chemistry*, 36(4), 835-837.

Muir, D.C.G., Teixeira, C. & Wania, F., 2004. Empirical and modeling evidence of regional atmospheric transport of current-use pesticides. *Environmental Toxicology and Chemistry*, 23(10), 2421-2432.

Nakamura, Y., Yamagishi, A., Iwamoto, T. & Koga, M., 1988. Adsorption properties of montmorillonite and synthetic saponite as packing materials in liquid-column chromatography. *Clays & Clay Minerals*, 36(6), 530-536.

Norrish, K., 1954. The swelling of montmorillonite. *Discussions of the Faraday Society*, 18, 120-134.

Oravec, M., Simek, Z. & Holoubek, I., 2010. The effect of humic acid and ash on enantiomeric fraction change of chiral pollutants. *Colloids and Surfaces A: Physicochemical and Engineering Aspects*, 359(1-3), 60-65.

Orme, C.A., Noy, A., Wierzbicki, A., McBride, M.T., Grantham, M., Teng, H.H., Dove, P.M. & DeYoreo, J.J., 2001. Formation of chiral morphologies through selective binding of amino acids to calcite surface steps. *Nature*, 411(6839), 775-779.

Pályi, G., Zucchi, C. & Caglioti, L., 2004. *Progress in biological chirality*, Elsevier.

Pasteur, L., 1948. *Researches on the Molecular Asymmetry of natural organic products...(1860)*, E. & S. Livingstone, Ltd.

Pirkle, W.H., House, D.W. & Finn, J.M., 1980. Broad spectrum resolution of optical isomers using chiral high-performance liquid chromatographic bonded phases. *Journal of Chromatography A*, 192(1), 143-158.

Ponnamperuma, C., Shimoyama, A. & Friebele, E., 1982. Clay and the origin of life. *Origins of Life and Evolution of Biospheres*, 12(1), 9-40.

Qin, S., Budd, R., BONDARENKO, S., Liu, W. & Gan, J., 2006. Enantioselective degradation and chiral stability of pyrethroids in soil and sediment. *Journal of Agricultural and Food Chemistry*, 54(14), 5040-5045.

Reddy, C.R., Bhat, Y., Nagendrappa, G. & Jai Prakash, B., 2009. Brønsted and Lewis acidity of modified montmorillonite clay catalysts determined by FT-IR spectroscopy. *Catalysis Today*, 141(1-2), 157-160.

Reigart, J.R. & Roberts, J.R., 1999. *Recognition and management of pesticide poisonings*, Environmental Protection Agency Washington DC.

Ridal, J.J., Bidleman, T.F., Kerman, B.R., Fox, M.E. & Strachan, W.M.J., 1997. Enantiomers of α-Hexachlorocyclohexane as Tracers of Air−Water Gas Exchange in Lake Ontario. *Environmental Science & Technology*, 31(7), 1940-1945.

Romero, E., Matallo, M., Peña, A., Sánchez-Rasero, F., Schmitt-Kopplin, P. & Dios, G., 2000. Dissipation of racemic mecoprop and dichlorprop and their pure R-enantiomers in three calcareous soils with and without peat addition. *Environmental Pollution*, 111(2), 209-215.

Ruch, E., 1968. Homochirality, a principle for the classification of molecules belonging to special classes. *Theoretica Chimica Acta*, 11(3), 183-192.

Rushing, D.E., 1958. Gas Chromatography in Industrial Hygiene and Air Pollution Problems. *American Industrial Hygiene Association Journal*, 19(3), 238.

Shanbhag, G. & Halligudi, S., 2004. Intermolecular hydroamination of alkynes catalyzed by zinc-exchanged montmorillonite clay. *Journal of Molecular Catalysis A: Chemical*, 222(1-2), 223-228.

Shoonheydt, R.A. & Johnston, C., 2006. Surface and interface chemistry of clay minerals. In *BERGAYA, F. et al, Handbook of Clay Science. Amsterdam: Elsevier Ltd.* Elsevier Ltd, pp. 87-113.

Siffert, B. & Naidja, A., 1992. Stereoselectivity of montmorillonite in the adsorption and deamination of some amino acids. *Clay Minerals*, 27(1), 109-118.

Singh, A.K., White, T., Spassova, D. & Jiang, Y., 1998. Physicochemical, molecular-

orbital and electronic properties of acephate and methamidophos. *Comparative Biochemistry and Physiology - C Pharmacology Toxicology and Endocrinology*, 119(1), 107-117.

Sposito, G., 2008. *The chemistry of soils*, Oxford University Press US.

Suh, I., Park, K.H., Jensen, W.P. & Lewis, D.E., 1997. Molecules, Crystals, and Chirality. *Journal of Chemical Education*, 74(7), 800.

Sumner, D., 1997. Carbonate precipitation and oxygen stratification in late Archean seawater as deduced from facies and stratigraphy of the gamohaan and frisco formations, transvaal supergroup, South Africa. *American Journal of Science*, 297(5), 455-487.

Szeto, S.Y., Maccarthy, H.R., Oloffs, P.C. & Shepherd, R.F., 1979. Fate of Acephate and Carbaryl in Water. *Journal of Environmental Science and Health Part B-Pesticides Food Contaminants and Agricultural Wastes*, 14(6), 635-654.

Támara, M., 2009. *Factors Controlling Enantiomer-Selective Amino Acid Adsorption on Mineral and Metal Surfaces*. Liverpool, UK: University of Liverpool.

Tawaki, S. & Klibanov, A.M., 1992. Inversion of enzyme enantioselectivity mediated by the solvent. *Journal of the American Chemical Society*, 114(5), 1882–1884.

Teng, H.H., Dove, P., Orme, C.A. & De Yoreo, J., 1998. Thermodynamics of calcite growth: Baseline for understanding biomineral formation. *Science*, 282(5389), 724-727.

Theng, B.K.G., 1974. *The chemistry of clay-organic reactions*, Hilger London.

Tsvetkov, F. & Mingelgrin, U., 1987a. Optically selective adsorption of alpha -amino acids on montmorillonite-Cu-l-lysine complexes in high-pressure liquid chromatography. *Clays & Clay Minerals*, 35(5), 391-399.

Tsvetkov, F. & Mingelgrin, U., 1987b. Optically selective adsorption of α-amino acids on montmorillonite-Cu-L-lysine complexes in high pressure liquid chromatography. *Clays and Clay Minerals*, 35(5,391-399).

Ueji, S., Fujino, R., Ōkubo, N., Miyazawa, T., Kurita, S., Kitadani, M. & Muromatsu, A., 1992. Solvent-induced inversion of enantiosflectivity in lipase-catalyzed esterification of 2-phenoxypropionic acids. *Biotechnology Letters*, 14(3), 163–168.

US EPA, O.O.P.P., 2009. Reregistration Status for Organophosphates | Pesticides | US EPA.

USDA-SCS, 1994. "Global Soil Regions." World Soil Resources, Soil Survey Division of the Soil, Conservation Service.

Valenzuela Díaz, F.R. & Santos, P.D.S., 2001. Studies on the acid activation of Brazilian smectitic clays. *Química Nova*, 24(3).

Valverde, J.L., Sanchez, P., Dorado, F., Asencio, I. & Romero, A., 2003. Preparation and characterization of Ti-pillared clays using Ti alkoxides. influence of the synthesis parameters. *Clays and Clay Minerals*, 51(1), 41-51.

Van't Hoff, J.H., 1874. Sur les formules de structure dans l'espace. *Arch. Neerl. Sci. Exactes Nat*, 9, 445–454.

Wang, P., Jiang, S.R., Liu, D.H., Zhang, H.J. & Zhou, Z.Q., 2006. Enantiomeric resolution of chiral pesticides by high-performance liquid chromatography. *Journal of Agricultural and Food Chemistry*, 54(5), 1577-1583.

Wania, F., 2003. Assessing the potential of persistent organic chemicals for long-range transport and accumulation in polar regions. *Environmental Science & Technology*, 37(7), 1344-1351.

Wania, F., Axelman, J. & Broman, D., 1998. A review of processes involved in the exchange of persistent organic pollutants across the air-sea interface. *Environmental Pollution*, 102(1), 3-23.

Wania, F. & Mackay, D., 1996. Tracking the distribution of persistent organic pollutants. *Environmental Science & Technology*, 30(9), A390-A396.

Weber, J.B., 1966. Molecular structure and pH effects on the adsorption of 13 s-triazine compounds on montmorillonite clay. *Am. Mineral*, 51, 1657–1670.

Wedyan, M. & Preston, M.R., 2005. Isomer-selective adsorption of amino acids by components of natural sediments. *Environmental Science & Technology*, 39(7), 2115-2119.

Weissbuch, I., Leiserowitz, L. & Lahav, M., 2005. *Stochastic "mirror symmetry breaking" via self-assembly, reactivity and amplification of chirality: Relevance to abiotic conditions.*

Wescott, C.R. & Klibanov, A.M., 1994. The solvent dependence of enzyme specificity. *Biochimica et Biophysica Acta (BBA)-Protein Structure and Molecular Enzymology*, 1206(1), 1–9.

West, P.W., Sen, B. & Sant, B.R., 1959. Determination of Total Gaseous Pollutants in Atmosphere. *Analytical Chemistry*, 31(3), 399-401.

Wiberg, K., Oehme, M., Haglund, P., Karlsson, H., Olsson, M. & Rappe, C., 1998. Enantioselective analysis of organochlorine pesticides in herring and seal from the Swedish marine environment. *Marine Pollution Bulletin*, 36(5), 345-353.

Williams, A., 1996. Opportunities for chiral agrochemicals. *Pesticide Science*, 46(1), 3-9.

Wong, C.S., 2006. Environmental fate processes and biochemical transformations of chiral emerging organic pollutants. *Analytical and Bioanalytical Chemistry*, 386(3), 544-558.

Wulfsberg, G., 1991. *Principles of descriptive inorganic chemistry*, University Science Books.

Yamagishi, A., 1981. Stereoselective adsorption on a clay surface modified by an optically active nickel(II) tris(1,10-phenanthroline) chelate. *Journal of the Chemical Society, Chemical Communications*, (21), 1128-1129.

Yamagishi, A., 1982. Racemic adsorption of dicyanobis(1,10-phenanthroline)iron(II) on colloidally dispersed sodium montmorillonite. *Inorganic Chemistry*, 21(5), 1778-1782.

Yamagishi, A., 1983. Chirality recognition of a clay surface modified by an optically active metal chelate. *Journal of the Chemical Society, Dalton Transactions*, (4), 679-681.

Yamagishi, A., 1985. Chromatographic resolution of enantiomers having aromatic groups by an optically active clay-chelate adduct. *Journal of the American Chemical Society*, 107(3), 732-734.

Yamagishi, A., 1987. Optical resolution and asymmetric syntheses by use of adsorption on clay minerals. *Journal of Coordination Chemistry*, 16(2), 131–211.

Yen, J.H., Lin, K.H. & Wang, Y.S., 2000. Potential of the insecticides acephate and methamidophos to contaminate groundwater. *Ecotoxicology and Environmental Safety*, 45(1), 79-86.

Yilmaz, G., 2003. Temperature effects and shrinkage properties of clay. *American Ceramic Society Bulletin*, 82(12).

Youatt, J.B. & Brown, R.D., 1981. Origins of Chirality in Nature: A Reassessment of the Postulated Role of Bentonite. *Science*, 212(4499), 1145-1146.

Zhang, J., Gupta, R.K. & Wilkie, C.A., 2006. Controlled silylation of montmorillonite and its polyethylene nanocomposites. *Polymer*, 47(13), 4537-4543.

Zhou, Kunde Lin, Ling Li, Meiqing Jin, Jing Ye & Weiping Liu, 2009. Separation and toxicity of salithion enantiomers. *Chirality*, 9999(9999), NA.

Zhou, J.L., Rowland, S. & Mantoura, R.F.C., 1995. Partition of synthetic pyrethroid insecticides between dissolved and particulate phases. *Water Research*, 29(4), 1023-1031.

Zipper, C., Suter, M., Haderlein, S., Gruhl, M. & Kohler, H., 1998. Changes in the

enantiomeric ratio of (R)- to (S)-mecoprop indicate in situ biodegradation of this chiral herbicide in a polluted aquifer. *Environmental Science and Technology*, 32(14), 2070-2076.

APPENDIX

1.1 Analysis of mineral structures using a scanning electron microscope (SEM)

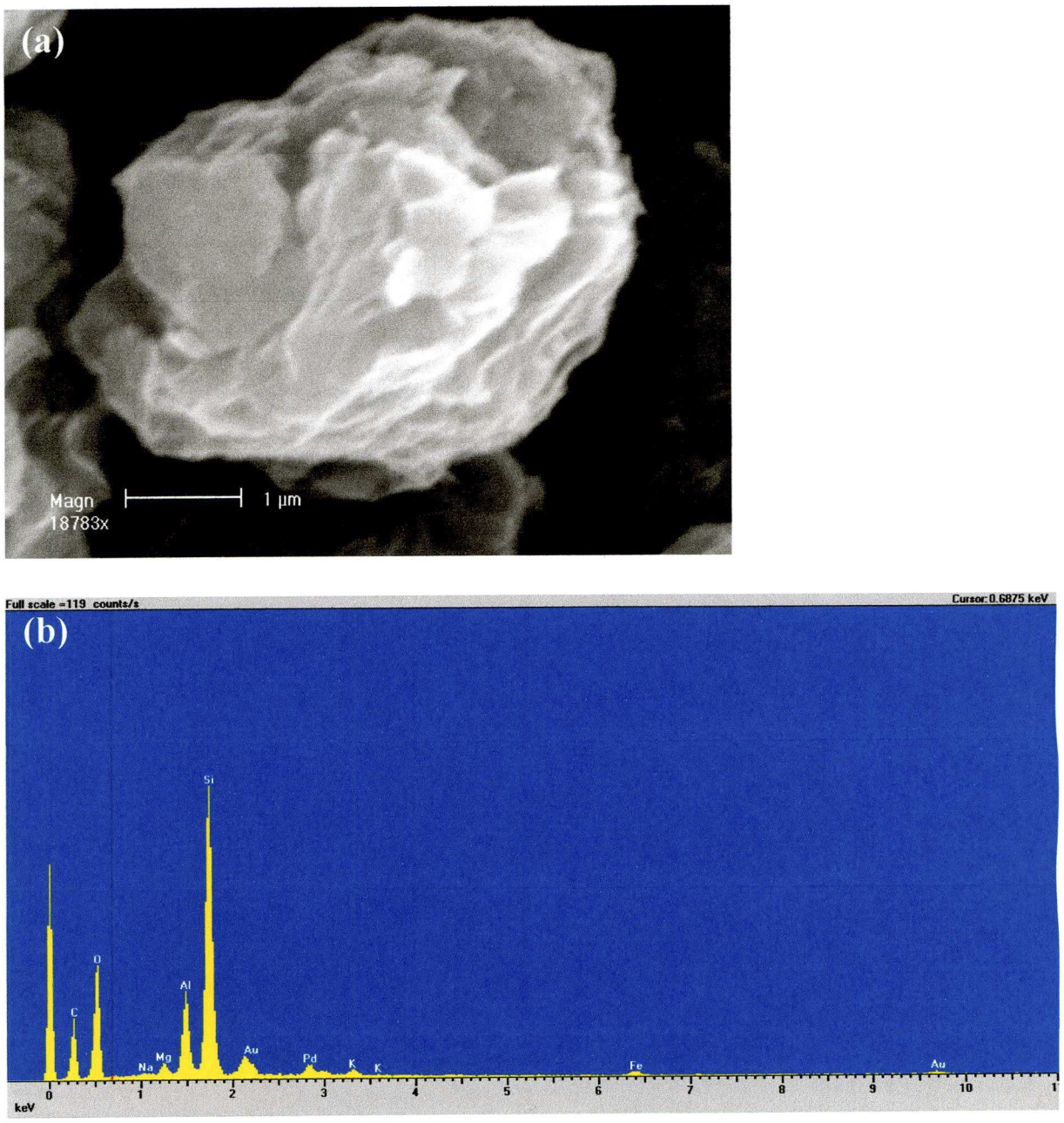

Figure A1.1 Pyrolysed raw K10: a) SEM image; b) spectra

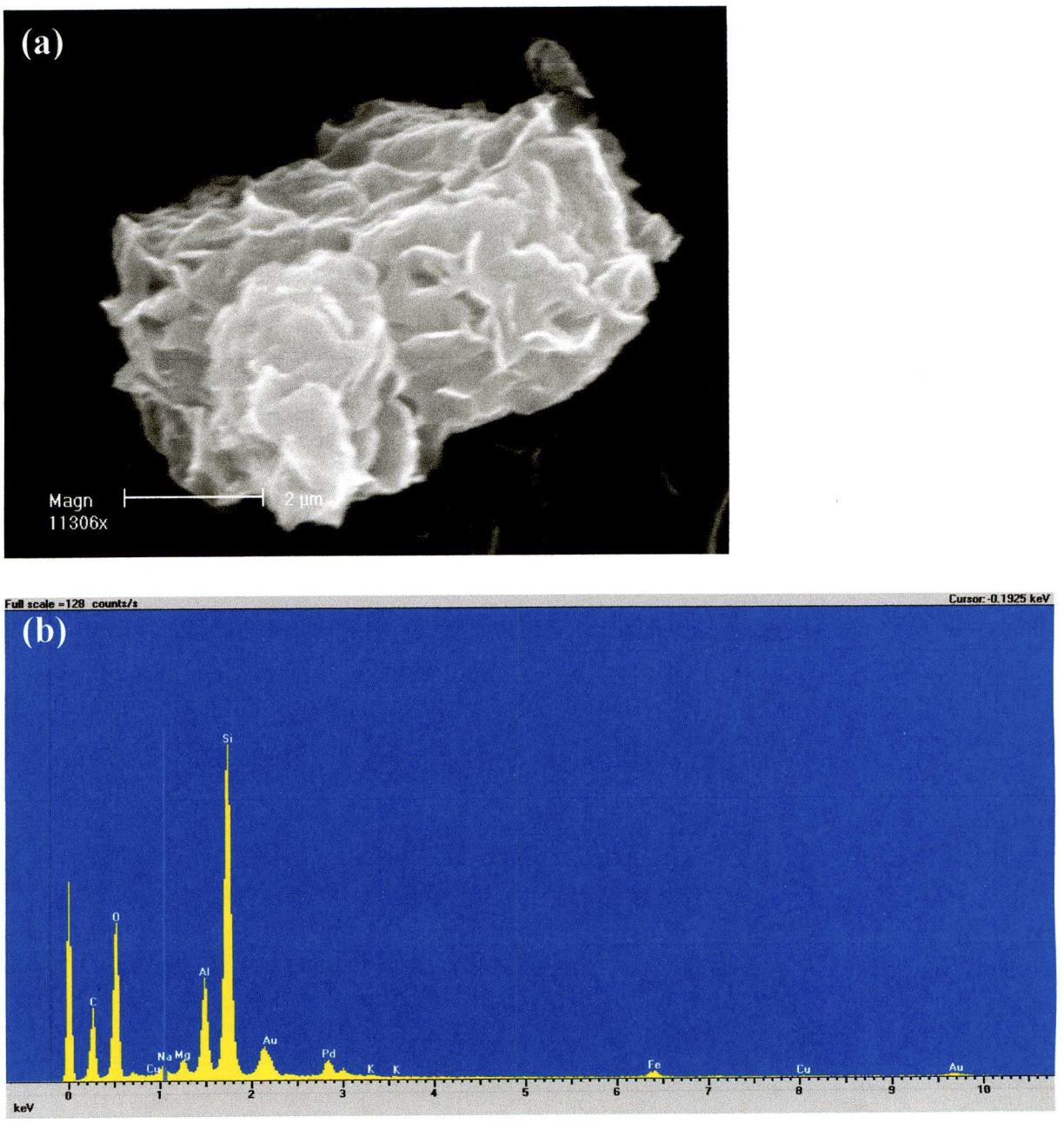

Figure A1.2 Na-exchanged K10 without pyrolysis: a) SEM image; b) spectra

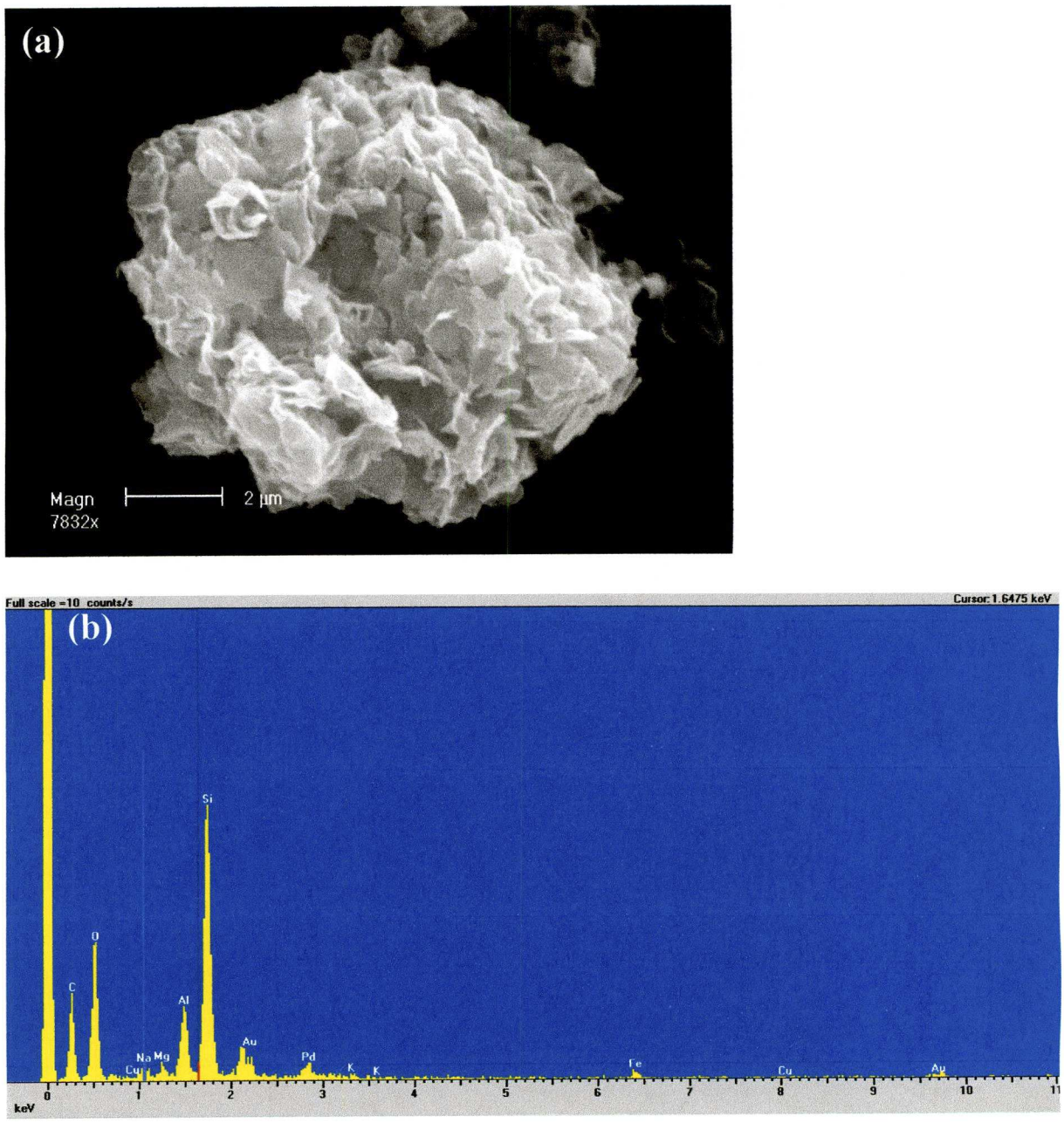

Figure A1.3 Na-exchanged K10 with pyrolysis: a) SEM image; b) spectra

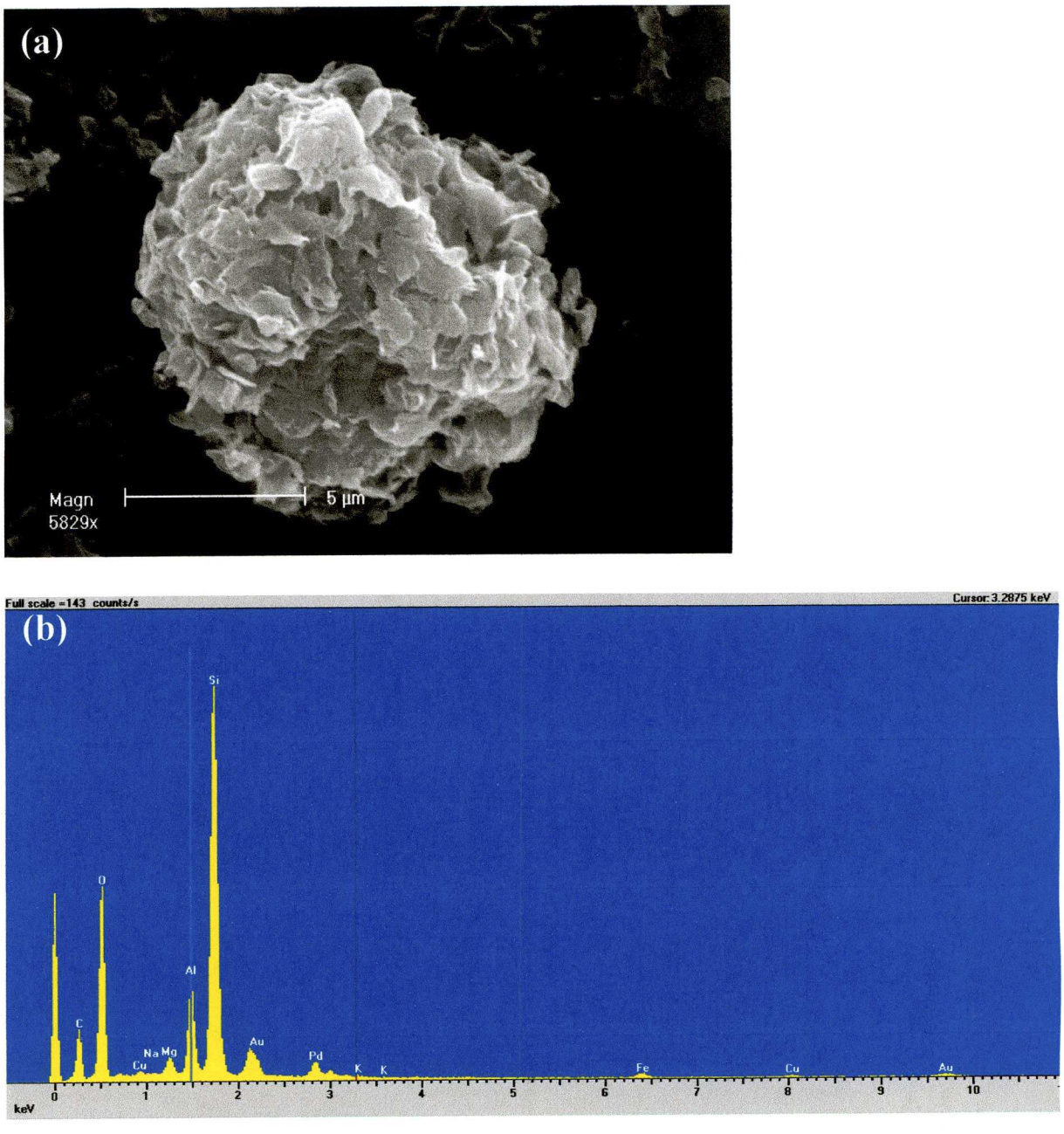

Figure A1.4 Cu-exchanged K10: a) SEM image; b) spectra

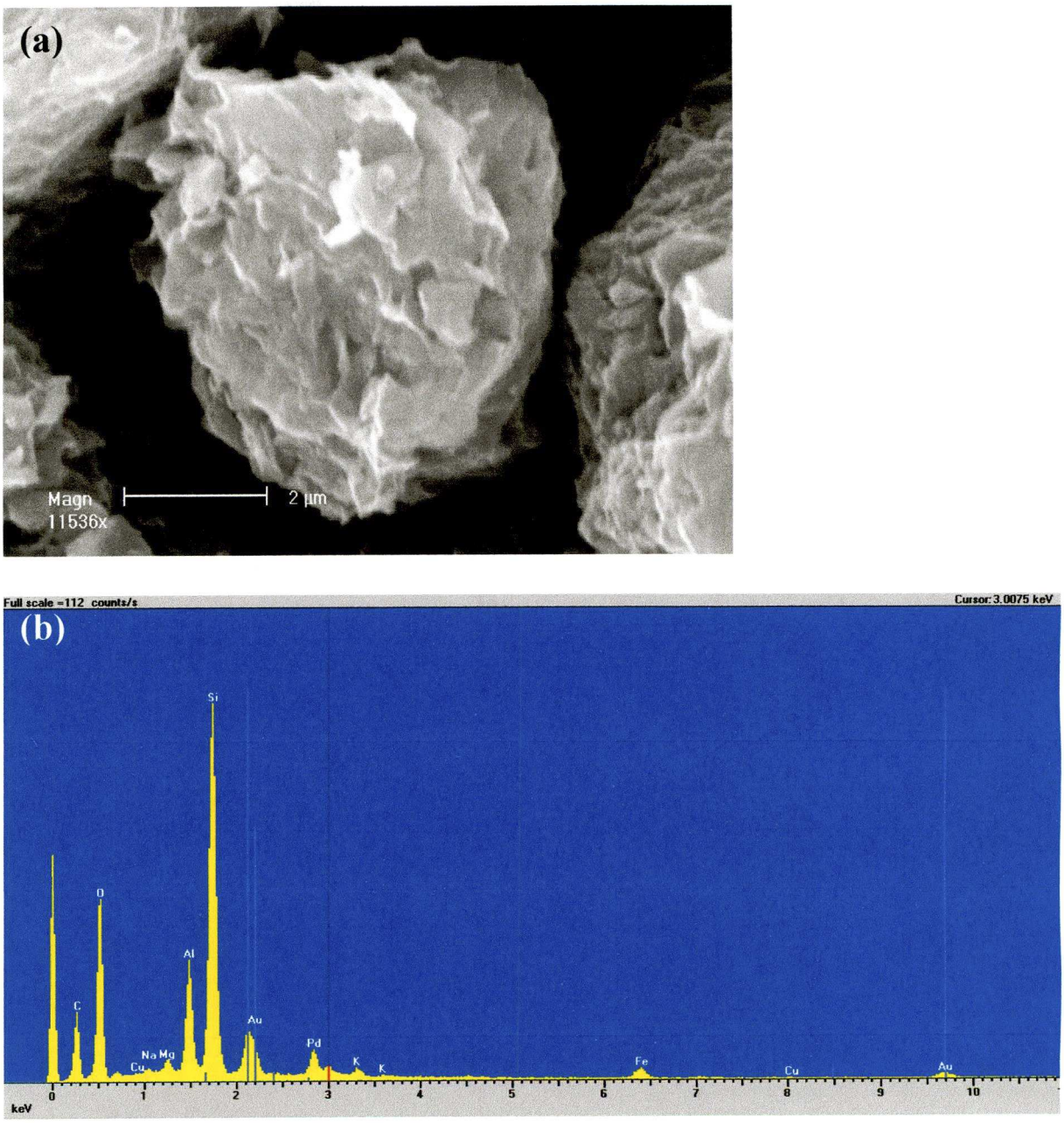

Figure A1.5 Acid treated K10: a) SEM image; b) spectra

1.2 Sorption of acephate with activated copper

Copper has been included as an interchangeable cation in the interlayer space of the sorbents used in many of the batch sorption experiments carried out to date. To examine the direct effect of copper on the sorption of acephate by clay minerals a different approact was required. One way of achieving this was to assess the sorptive capabilities of copper alone. To maintain consistency with previous experiments it was preferable that the experiment be of a batch sorption type with the sorbent suspended in aqueous solution. Activated copper was prepared as the sorbent as it

fitted such criteria. Furthermore it was supposed that some of the activated copper could be combined with L-lysine in solutions to form a Cu-L-lysine complex. This could provide more information on the sorptive and enantioselective capabilities of the Cu-lysine modified clays used in previous experiments. In batch sorption experiments both forms of activated copper strongly sorbed the acephate present in solution. The difference between the two forms of activate copper were also significantly different with the copper alone removing ~83 % of the acephate from the solution while the Cu-lysine complex removed only ~54 %. In terms of EF, deviation from 0.5 is small but, in some cases, significant. Initially, with 500 mg of the sorbent, the activated copper alone appears to preferentially adsorb the (−) enantiomer of acephate while the copper-lysine complex prefers to select the (+) enantiomer. The variation is only small and when the addition of sorbent is increased to 1000 mg significant preferential selection of either enantiomer is no longer seen.

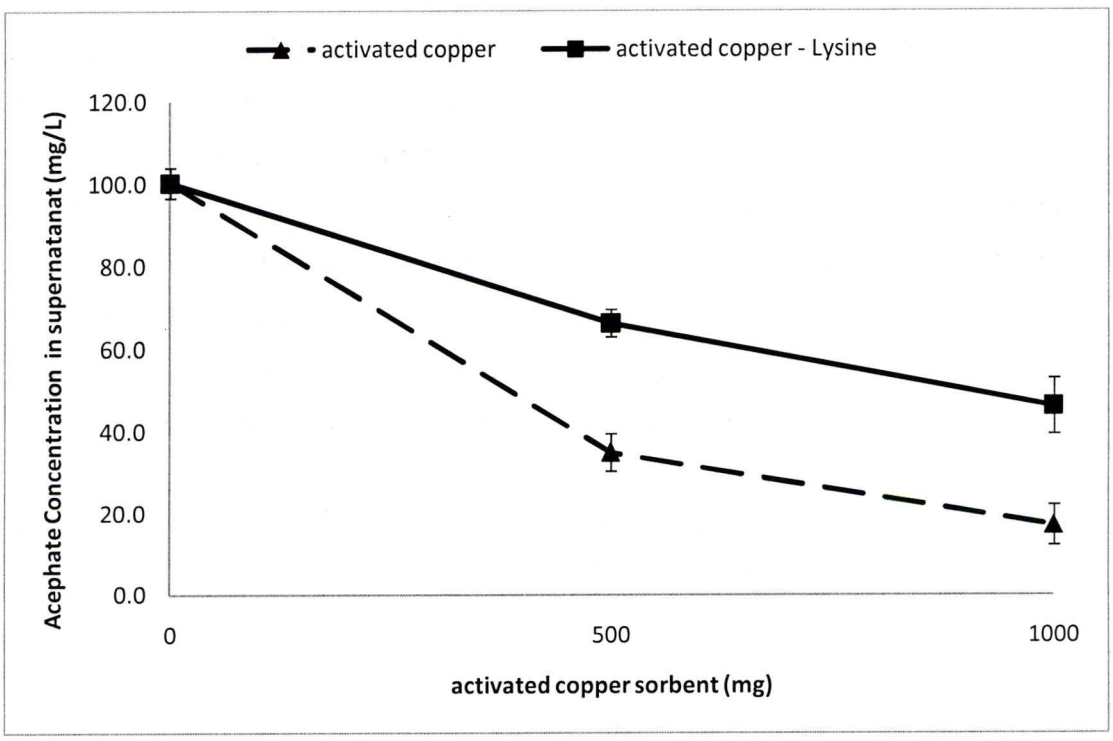

Figure A1.6 The amount of acephate in supernatant (mg/g) after sorption at the surfaces of increasing amounts of activated copper. Error bars represent the standard error calculated for each data point.

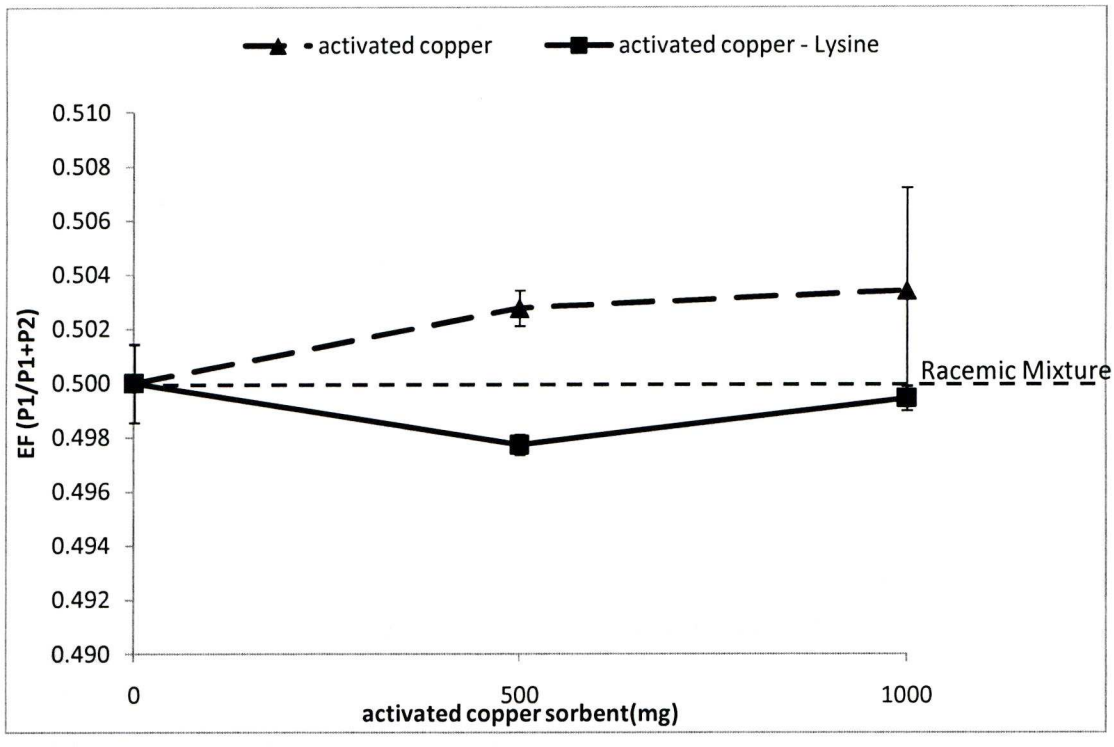

Figure A1.7 EF values for acephate in the supernatant after sorption at the surfaces of activated copper. Error bars represent the standard error calculated for each data point.

1.3 Langmuir Conformity manipulations

Isotherms for the sorption of organophosphorus pesticides on clay minerals can normally be explained by the linear form of the Langmuir equation (got ref for this somewhere) given below:

$$\frac{C}{\frac{x}{m}} = \frac{1}{kV_m} + \frac{C}{V_m}$$

Where C is the equilibrium concentration, x is the amount adsorbed per unit weight m of clay while k and V_m are constants; the latter being identifiable with the monolayer capacity of the adsorbent (Theng 1974). Adsorption can be said to conform to the Langmuir equation if a straight line is observed when *C/(x/m)* is plotted against C. Given the parameters, this equation and the test for conformity can apply to the results of batch sorption experiments where the amount of clay is the variable and the initial sorbate concentration a constant. In the figures below, such conformity tests have been applied to several of the experimental results obtained in this work. The nearer the R^2 value for a data set is to 1.0 the more closely the adsorption conforms to the Langmuir equation.

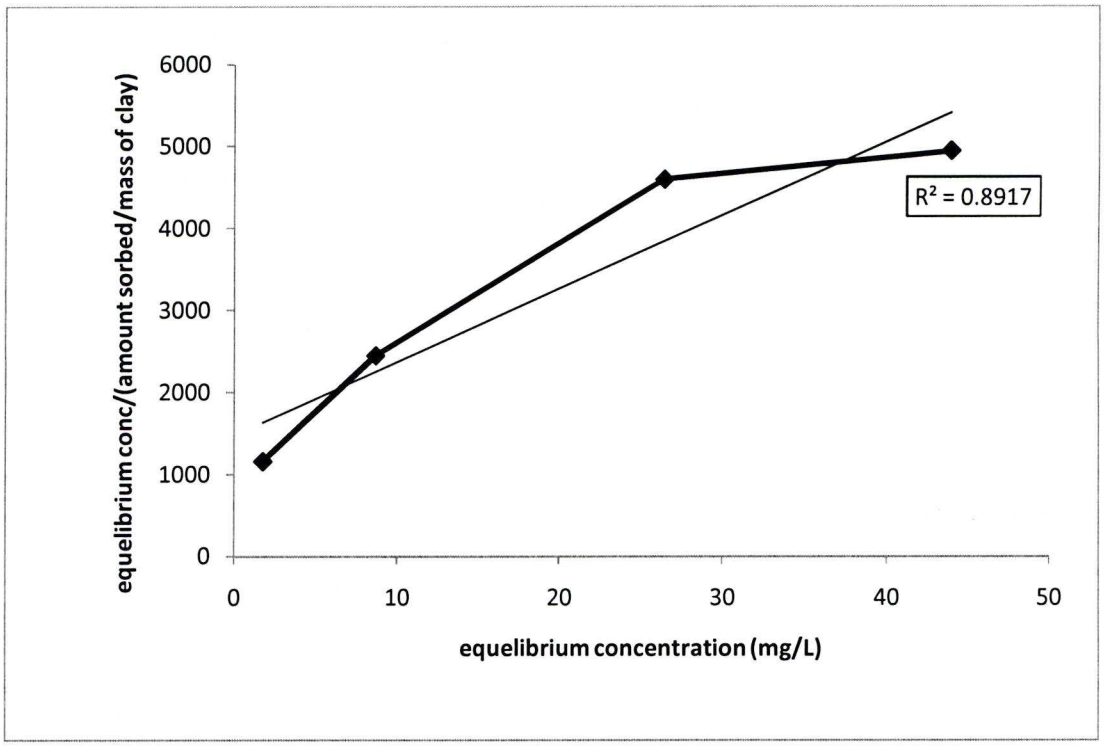

Figure A1.8 Langmuir conformity plot for acephate sorption on montmorillonite K10 surfaces

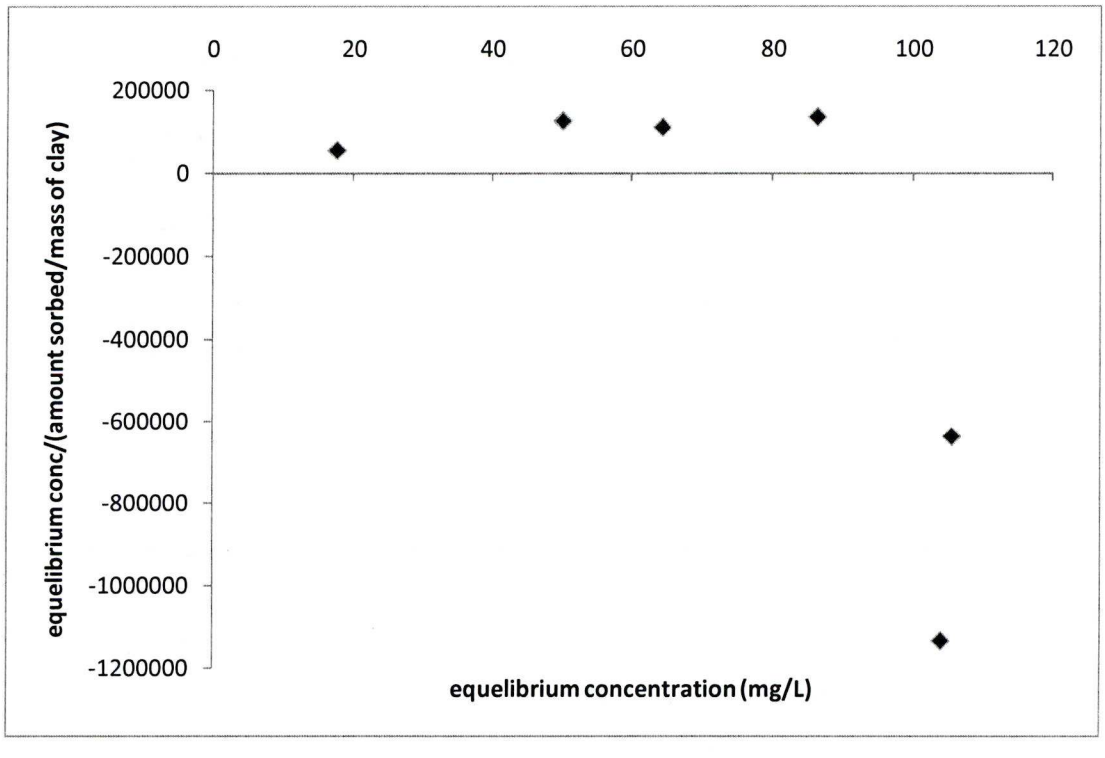

Figure A1.9 Langmuir conformity plot for acephate sorption on kaolinite surfaces

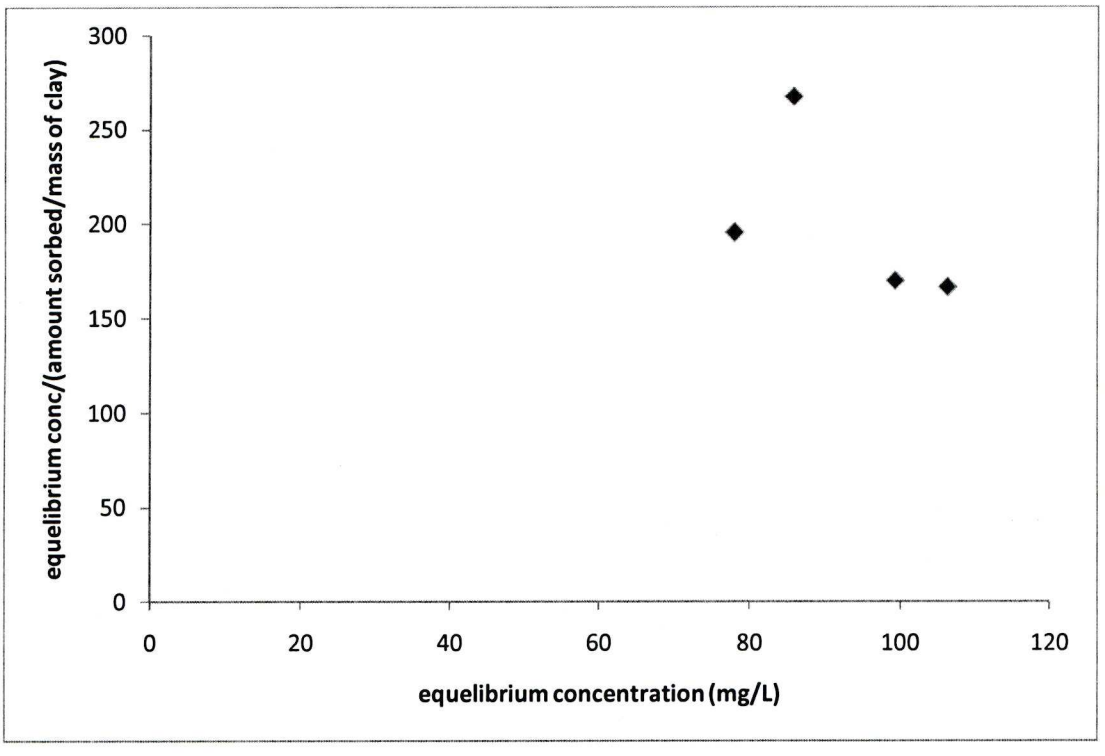

Figure A1.10 Langmuir conformity plot for acephate sorption on aluminium oxide surfaces

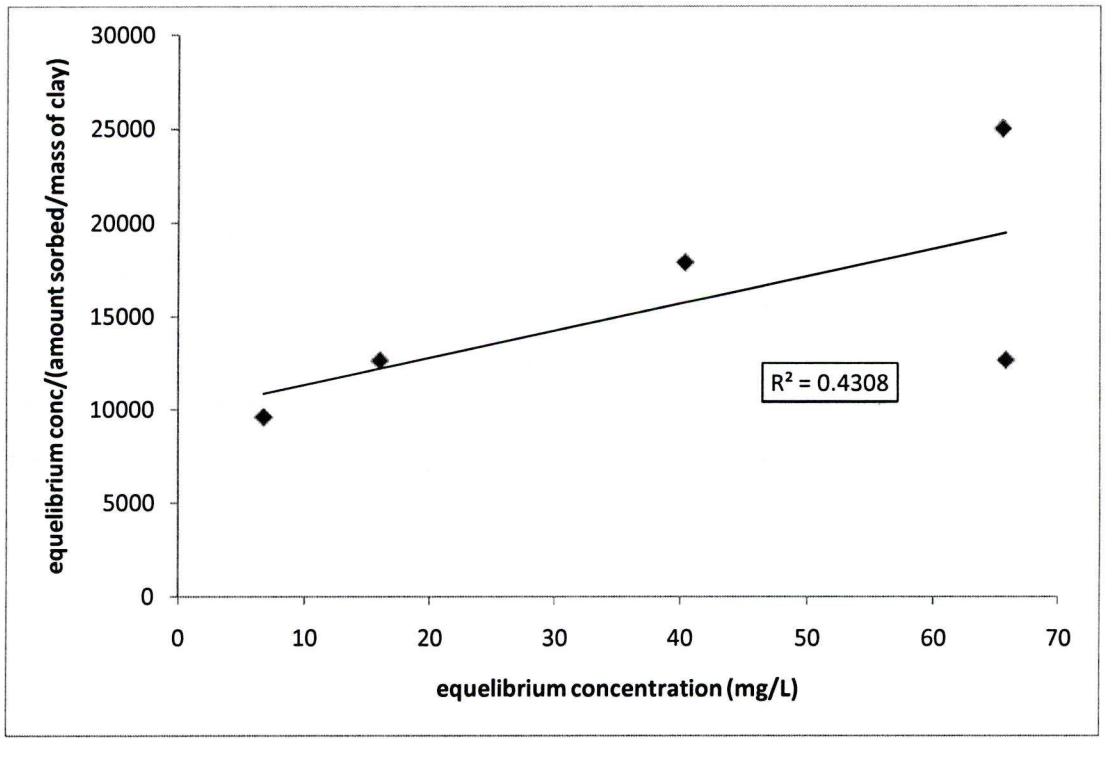

Figure A1.11 Langmuir conformity plot for acephate sorption on K10-Cu-L-lysinesurfaces

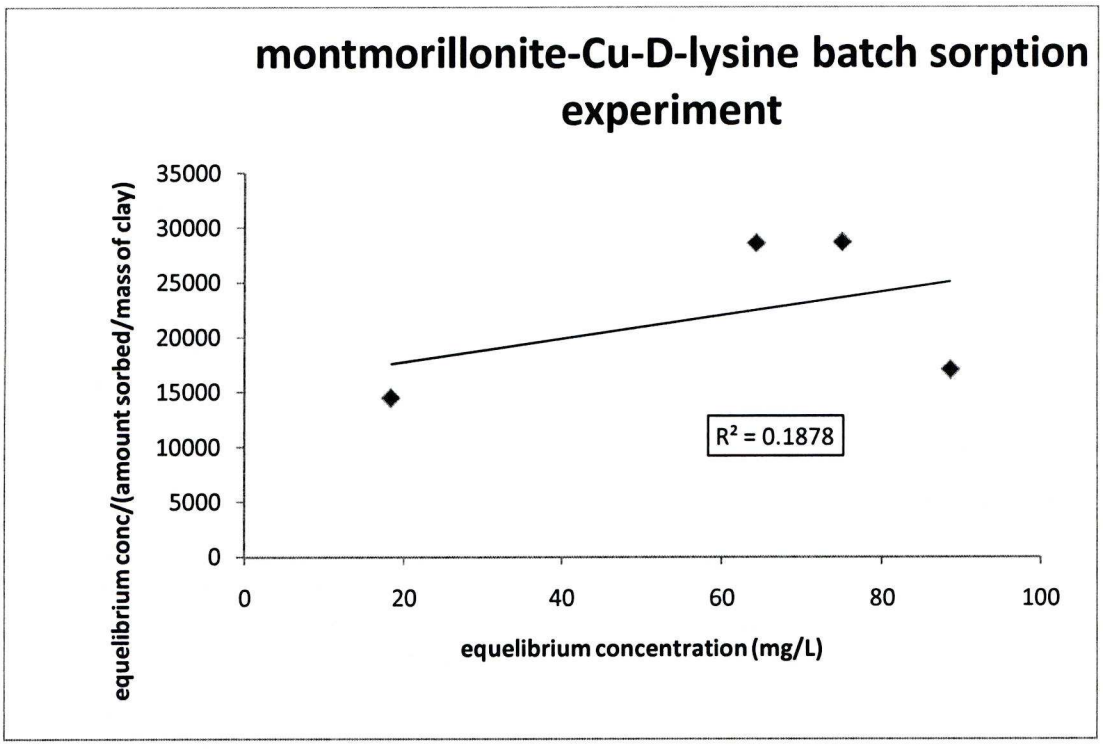

Figure A1.12 Langmuir conformity plot for acephate sorption on K10-Cu-D-lysinesurfaces

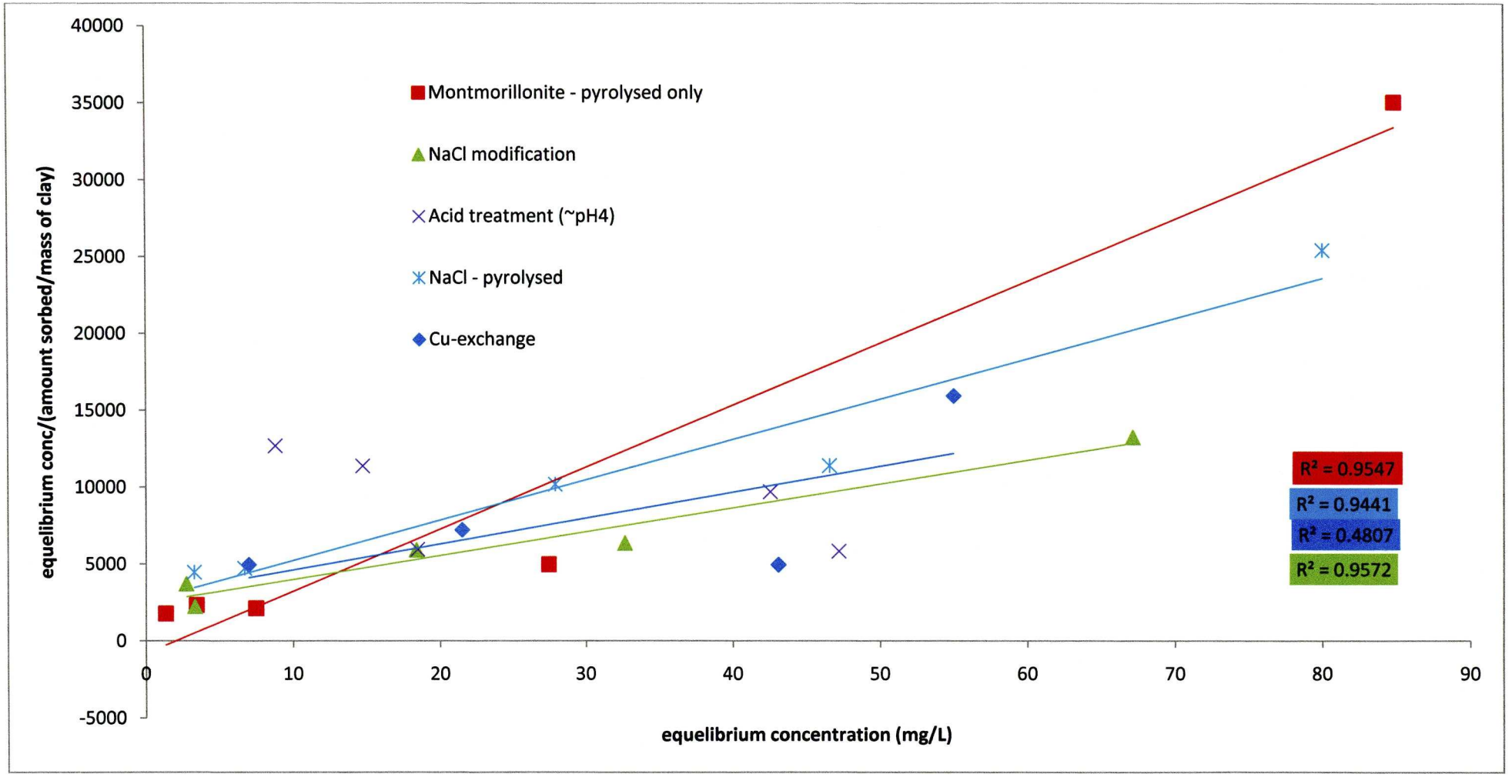

Figure A1.13 Langmuir conformity plot for acephate sorption on of a variety of pre-treated and modified K10 surfaces

The R^2 values for each set of data where the calculation was possible are presented in Table A1.1.

Table A1.1 R^2 values for Langmuir conformity plots and their corresponding sorbates and sorbents

Sorbate	Sorbent	R^2 value
Acephate	K10	0.891
Acephate	Kaolinite	N/A
Acephate	Aluminium oxide	N/A
Acephate	K10-Cu-L-lysine	0.430
Acephate	K10-Cu-D-lysine	0.187
Acephate	K10 – pyrolysed only	0.954
Acephate	K10 – NaCl treated only	0.957
Acephate	K10 – acid treatment (pH4)	N/A
Acephate	K10 – NaCl treated – pyroly	0.944
Acephate	K10 – Cu exchanged	0.480

1.4 Analysis of Variance (ANOVA)

ANOVA was performed for the results of the enantiomeric excess experiment (Section 5.7) on the data for both sorption and EF. A summary of the outcome is provided in Table A1.2 and A1.3 respectively. The value for the least significant difference, based on a P value of 0.05, (5% LSD) is also included in the summary.

Table A1.2 ANOVA output for the sorption of acephate at the surface of K10 in the "enantiomeric excess experiment".

SUMMARY

Groups	*Count*	*Sum*	*Average*	*Variance*
CYCLE BL	3	150.0	50.0	32.1
CYCLE 1	3	132.6	44.2	4.7
CYCLE 2	3	116.6	38.9	1.4
CYCLE 3	3	91.4	30.5	1.2
CYCLE 4	3	81.2	27.1	0.5
CYCLE 5	3	66.4	22.1	4.8
CYCLE 6	3	59.8	19.9	11.7

ANOVA

Source of Variation	*SS*	*df*	*MS*	*F*	*P-value*	*F crit*	*5% LSD*
Between Groups	2336.9	6	389.5	48.3	1.5E-08	2.85	4.96
Within Groups	112.8	14	8.1				
Total	2449.7	20					

Table A1.3 ANOVA output for the EF of acephate at the surface of K10 in the "enantiomeric excess experiment".

SUMMARY

Groups	*Count*	*Sum*	*Average*	*Variance*
CYCLE BL	3	1.500	0.500	1.7E-06
CYCLE 1	3	1.496	0.499	2.3E-06
CYCLE 2	3	1.502	0.501	4.0E-06
CYCLE 3	3	1.498	0.499	6.0E-07
CYCLE 4	3	1.491	0.497	8.5E-08
CYCLE 5	3	1.465	0.488	1.2E-05
CYCLE 6	3	1.478	0.493	2.2E-06

ANOVA

Source of Variation	*SS*	*df*	*MS*	*F*	*P-value*	*F crit*	*5% LSD*
Between Groups	0.00037	6	6.2E-05	18.6	6.36E-06	2.85	0.003
Within Groups	4.7E-05	14	3.3E-06				
Total	0.00042	20					